



Virginia Commonwealth University  
VCU Scholars Compass

---

Theses and Dissertations

Graduate School

---

2014

## Synthetic, Sulfated, Lignin-Based Anticoagulants

Akul Mehta

*Virginia Commonwealth University*

Follow this and additional works at: <https://scholarscompass.vcu.edu/etd>

 Part of the [Pharmacy and Pharmaceutical Sciences Commons](#)

© The Author

---

Downloaded from

<https://scholarscompass.vcu.edu/etd/598>

This Dissertation is brought to you for free and open access by the Graduate School at VCU Scholars Compass. It has been accepted for inclusion in Theses and Dissertations by an authorized administrator of VCU Scholars Compass. For more information, please contact [libcompass@vcu.edu](mailto:libcompass@vcu.edu).

© Akul Yugesh Mehta

All Rights Reserved

# **SYNTHETIC, SULFATED, LIGNIN-BASED ANTICOAGULANTS**

A dissertation submitted in partial fulfillment of the requirements for the degree of  
Doctor of Philosophy at Virginia Commonwealth University

by

**AKUL YUGESH MEHTA**

B. Pharm. University of Mumbai, India.

Supervisor: DR. UMESH R. DESAI

Professor, Department of Medicinal Chemistry

Virginia Commonwealth University

Richmond, Virginia

April 2014

## Acknowledgements

Over the years, I have met number of people, who have been key figures in my PhD. and for shaping me into who I am today. I would like to thank some of these people in specific for their support and influence on me.

Firstly, I am thankful to my parents Mr. Yugesh S. Mehta and Mrs. Jayendra Y. Mehta, for all their support and sacrifice, to help me get the best of everything in the world possible. I will always be grateful to them for their endless love, care and support. I would also like to thank my grandparents – Dada, Dadi, Nana and Nani; I hope I make them proud as they look down upon me from the heavens. I am thankful to my sister, Sunali and brother-in-law Paresh, who have always been there for me when I needed them.

To my PhD. advisor, Dr. Umesh Desai; I am thankful for taking me under his wing and helping me excel in my career. Dr. Desai has always let me express my creativity and understanding, while giving useful feedback and ideas. He has always believed in me, even when I was down. Without him, the work in this thesis would not have been possible. He is an excellent teacher and mentor.

I would like to thank our collaborators who have been influential in the work presented here:

1. Dr. Donald Brophy's laboratory, especially Erika J. Martin and Bassem M. Mohammed from the Department of Pharmacotherapy and Outcome Sciences, Virginia Commonwealth University – for their help in the ex vivo studies in chapter 4.
2. Dr. David Gailani at the Vanderbilt University – for help with the in vivo mouse studies described in chapter 4.

3. Dr. Alireza Rezaei at the Saint Louis University – for providing the recombinant thrombin mutants and recombinant factor XIa (catalytic domain and wild type).
4. Dr. Paul Bock at Vanderbilt University – for providing the hirugen peptide.
5. Dr. Takao Kishimoto at Toyama Prefectural University – for providing authentic  $\beta$ -O4 lignin polymer for comparison.
6. Ms. Malaika Argade in the Desai Lab – For help with the introductory results reported in chapter 5, which constituted her thesis work.
7. Dr. Aurijit Sarkar in the Desai Lab – For technical assistance in the modeling studies performed in chapter 5 and always having time to help others.

I appreciate the time and effort taken by my committee members- Dr. Umesh Desai, Dr. Martin Safo, Dr. Rong Huang, Dr. Tonie Wright and Dr. Donald Brophy; to provide their inputs with first my oral proposal and also my final dissertation.

I am thankful to all Desai Lab members (past and present) who have been always helpful and supportive. They have been more of friends than colleagues. These include fellow synthetic chemists Dr. Preetpal Sidhu, Dr. Rami Al-Horani and Dr. Rajesh Karuturi, who have been helpful in my training in synthesis; Dr. Jay Thakkar, Dr. Joseph Timothy King and Dr. Aiye Liang for training in biochemistry and analytical techniques. Other lab members who have provided a great working environment and help include Mr. Rio Boothello, Mr. Shrenik Mehta, Ms. Pooja Ponnusamy, Ms. Yingzi Jin, Dr. May Abdel-Aziz, Dr. Philip Mosier, Dr. Qibing Zhou, Dr. Nehru Viji Sankaranarayanan, Dr. Balaji Nagarajan.

I would like to thank the Department of Medicinal Chemistry, the School of Pharmacy and the Graduate School at Virginia Commonwealth University, for the opportunity to complete my

doctoral studies and their support. I would also like to thank the National Institutes of Health for the funding provided, which supported the work (grants HL090586 and HL107152).

Some important family members also need to be thanked, who have made coming to the USA for my education possible: especially, Dr. Jagdish Sheth and Mrs. Madhu Sheth for their help in supporting my first year of my PhD. Also I would like to thank Mr. Bipin Shah, Mrs. Vaishakhi Shah, Mr. Pravin Parekh and Mrs. Pallavi Parekh, who have helped me get used to life in the USA.

A big thank you to all my foodie friends in Richmond, who have made living here a fun time and grocery a hobby- Harsh, Hardik, Atul, Rio, Shrenik, Pratik (Agni), Pratik (James), Aravind (Reddy), Vijay Bhai, Jigar, Ronak, Dharik, Harshad, Shankar, Aditya, Dipen, Jayul, Vishwadeep, Rakesh, Soumya, Shilpa, Sayali, Priyanka, Suditi, Khushboo, Soundarya, Farhana, Tanvi, Della, Batul, Divya, Anisha, and Shrinal. And another big thank you for my other tolerant friends, who have been forgiving for the lack of time I give them due to my PhD- Harshit, Shweta, Vivek (Vicky G), Sambhav, Sahil, Anand, Varun, Nupur, Janice, Abhishekh, Romil, Parshva, Amit, Tanvi M., Tanvi P., Melroy, Shazia, Sharan, Priyanka J., Priyanka G. and Malvi.

I would like to thank some key educators in my life. The teachers at MET's Institute of Pharmacy for giving me the strong foundation in my B. Pharm., which is required for understanding key principles in my PhD. In particular I would especially like to thank Mrs. Bhagwati Raheja and Mrs. Poonam Advani for inducing the interest in medicinal chemistry within me. I would also like to thank Mr. Amit D. Shah (Sensei), who has taught me how to be disciplined and strong in the face of hurdles.

Lastly, and most importantly, I would like to thank my wife, Sweety Mehta. She is an angel who has blessed me with all her time, patience, sacrifice, love and care, throughout my PhD and even before. I hope someday I can give her all that she desires in lieu of whatever she has given me.

## Table of Contents

	Page
Acknowledgements.....	ii
List of Tables .....	xiii
List of Figures.....	xiv
Abstract.....	xviii
Chapter	
1 Introduction.....	1
1.1 Blood, Coagulation and Hemostasis .....	1
1.2 The Coagulation Cascade.....	2
1.3 The Platelets .....	4
1.4 Structure of Thrombin.....	7
Catalytic Triad and Mechanism .....	9
Active Site Structure .....	11
The Sodium Binding Site .....	13
Exosite 1 .....	15
Exosite 2.....	15



1.5	Thrombin Allostery .....	18
	Sodium Binding Site and Thrombin Allostery.....	18
	Exosite 1 and Thrombin Allostery .....	19
	Exosite 2 and Thrombin Allostery .....	19
	Link between Allosteric Sites.....	21
1.6	Sulfated Tyrosine Containing Proteins Involved in Hemostasis.....	22
1.7	Structure and Functions of GPIb $\alpha$ .....	24
1.8	Interaction Between Thrombin and GPIb $\alpha$ – Structure and Function.....	27
1.9	Structure and Function of Factor XIa – An Emerging Target for Prophylactic Anticoagulation .....	32
1.10	Current Thrombin, GPIb $\alpha$ and Factor XIa Inhibitors.....	35
2	Rationale .....	40
	2.1 Background .....	40
	2.2 Structural Resemblance to Direct Exosite 2 Binding Inhibitors .....	41
	2.3 Mechanistic Resemblance Inspired from STRAP found in GPIb $\alpha$ .....	44
	2.4 Questions to be Answered.....	45
3	Synthesis and Biochemical Analysis of Sulfated $\beta$ -O4 Lignin (SbO4L) Polymer...47	
	3.1 Introduction .....	47

3.2 Experimental .....	48
Materials.....	48
Synthesis of SbO <sub>4</sub> L.....	49
Size Exclusion Chromatography of SbO <sub>4</sub> L .....	54
Reversed-Phase Ion-Pairing (RPIP) UPLC-MS.....	55
Direct Inhibition of Enzymes of the Coagulation Cascade .....	56
Inhibition of Other Heparin-Binding Serine Proteases .....	58
Effect of SbO <sub>4</sub> L on Antithrombin III Inhibition.....	59
Inhibition of Activation of Protein C by Thrombin-Thrombomodulin Complex in the presence of SbO <sub>4</sub> L .....	59
Variation of SbO <sub>4</sub> L Inhibition on Various Types of Thrombins.....	60
Fibrinogen Assay.....	61
Michaelis Menten Kinetics.....	61
Competition with Heparin, Hirugen Peptide and recombinant GPIIb $\alpha$ .....	62
Mutagenesis Studies .....	63
Probing Allosteric Change in Active Site using Quenching .....	63
Quantitating Number of Ionic Interactions Involved by Salt Dependence Studies on Affinity .....	64

Reversal of SbO4L Mediated Thrombin Inhibition by Protamine.....	65
3.3 Results .....	66
Synthesis of SbO4L.....	66
SbO4L is a Sulfated Polymeric Species which can be Reproducibly Synthesized.....	70
SbO4L is a Selective and Potent Inhibitor of Thrombin and Plasmin among the Coagulation Enzymes .....	72
SbO4L does not Inhibit Other Heparin Binding Serine Proteases .....	75
Antithrombin III does not Potentiate SbO4L Mediated Thrombin Inhibition .....	77
SbO4L Inhibits Thrombomodulin-Bound Thrombin Less Potently .....	78
SbO4L Inhibits Different Types of Thrombin in Equivalent Manner.....	80
SbO4L Shows Similar Potency Against Thrombin for Fibrinogen Substrate .....	81
SbO4L is a Non-Competitive Inhibitor of Thrombin.....	82
SbO4L does not Compete with Exosite 1 Ligand Hirugen Peptide, but Competes with Exosite 2 Ligands Heparin and GPIIb $\alpha$ .....	83
SbO4L Mediates Thrombin Inhibition via Binding to Arg233, Lys235 and Lys236 residues on Exosite 2.....	89

	SbO4L Causes Allosteric Changes in Active Site that Restricts Quenching by Acrylamide .....	92
	SbO4L binds Exosite 2 with Approximately Five Ionic Interactions .....	94
	Thrombin Inhibition by SbO4L can be Reversed by Protamine .....	97
	3.4 Discussion .....	98
4	Advanced Level Characterization of Antithrombotic Potential of SbO4L.....	105
	4.1 Introduction .....	105
	4.2 Experimental Procedures.....	107
	Materials .....	107
	Plasma APTT/PT Assays .....	108
	Effect of Serum Albumin on the Inhibition Efficacy of SbO4L .....	108
	Preparation of Platelet Rich and Platelet Poor Plasma .....	109
	Platelet Aggregation Assay .....	109
	ATP Secretion Assay .....	109
	Haemostatic Analysis System .....	110
	Thromboelastography TEG Analysis of Clot Formation .....	110
	In Vivo FeCl <sub>3</sub> Carotid Artery Thrombosis Model.....	111
	In Vivo Rose-Bengal Laser Thrombosis Model .....	111

Tail Bleeding Time .....	112
4.3 Results .....	112
SbO4L Prolongs Clot Formation in Plasma APTT/PT Assays .....	112
SbO4L Inhibition of Thrombin is Abrogated in the Presence of Albumin .....	113
SbO4L Potently Inhibits Platelet Aggregation in Platelet Rich Plasma (PRP) .....	114
SbO4L Potently Prevents ATP Secretion by Platelets in PRP .....	117
SbO4L Inhibits Platelet Prothrombotic Function in Whole Blood when Analyzed using Hemostasis Analysis System (HAS) .....	118
SbO4L Inhibits Thrombus Formation in Whole Blood when Analyzed using Thromboelastography (TEG).....	120
SbO4L shows potent Antithrombotic Action in FeCl <sub>3</sub> Thrombosis Model, Rose Bengal Laser Injury Model and Tail-Bleeding Time In Vivo in Mice .....	122
4.4 Discussion .....	125
5 Identifying Novel Lignin Based Inhibitors and Mechanisms for Factor XIa.....	129
5.1 Introduction .....	129

5.2 Experimental Procedures.....	136
Materials.....	136
fXIa Structure Model Generation.....	136
Docking of Compound 24 .....	137
Inhibition of Catalytic Domain of Factor XIa .....	137
Effect on Protein Anisotropy in Presence of 24 using Perrin Plot .....	138
5.3 Results .....	139
Preparation of a Knowledge-Based Model for Full-Length Factor XIa	139
Docking Suggests Probably Binding Pose for Benzofuran Trimers .....	139
Inhibition of Factor XIa by 24 is Apple-Domain Driven.....	142
Inhibition of Factor XIa by 24 Causes a Dramatic Conformational Change in Protein Structure.....	143
5.4 Discussion .....	145
References.....	149
Appendix A. Abbreviations .....	180

## List of Tables

	Page
Table 1: Cross reactivity of chemoenzymatically synthesized lignins CDSO3, FDSO3 and SDSO3 against heparin binding serine proteases shows potent IC <sub>50</sub> .....	44
Table 2: Parameters for sulfated $\beta$ -O4 lignin (SbO4L) inhibition of coagulation proteases.....	75
Table 3: The Michaelis-Menten Kinetic Parameters of SbO4L Inhibition of Thrombin .....	83
Table 4: Inhibition parameters of human $\alpha$ -thrombin by SbO4L in the presence of exosite 1 (HirP) and exosite 2 (UFH and GPIb $\alpha$ ) ligands.....	88
Table 5: Inhibition parameters of SbO4L for different thrombin exosite 2 mutants in comparison to wild type recombinant protein.. ..	90
Table 6: Dissociation Constant of SbO4L at various concentrations of NaCl. ....	96
Table 7: A comparison of the $\Gamma$ salt values of SbO4L to various thrombin binding ligands from literature .....	96
Table 8: Hemostasis Analysis System Parameters for SbO4L Anticoagulation in Comparison to Enoxaparin .....	120
Table 9: Thromboelastography Parameters for SbO4L Anticoagulation in Comparison to Enoxaparin. ....	122
Table 10: Inhibition Parameters of Sulfated Small Molecules (SSMs) against factor XIa.. ..	133

## List of Figures

	Page
Figure 1: The coagulation cascade of blood. ....	2
Figure 2: The role of platelets during injury. ....	6
Figure 3: The structure of human thrombin. ....	8
Figure 4: Serine Protease Catalysis. ....	10
Figure 5: The active site of thrombin. ....	12
Figure 6: Structural difference due to sodium binding relays into the catalytic triad. ....	14
Figure 7: Structure of human thrombin showing all electropositive residues (arginines and lysines) present on the exosite 1 .....	16
Figure 8: Structure of human thrombin showing all electropositive residues (arginines and lysines) present on the exosite 2 .....	17
Figure 9: Tyrosine sulfation reaction as catalyzed by tyrosylprotein sulfo transferase (TPST) enzymes in the presence of 3'-phosphoadenosine 5'-phosphosulfate (PAPS). ....	23
Figure 10: The GPIb-IX-V complex. ....	25
Figure 11: Comparison of two reported crystal structures of GPIb $\alpha$ and thrombin. ....	29
Figure 12: GPIb $\alpha$ interaction with thrombin exosite 2. ....	30
Figure 13: Structure of Factor XI and XIa. ....	33
Figure 14: Structures of anticoagulants that have been introduced to the clinic .....	37



Figure 15: Rationale behind the creation of synthetic sulfated $\beta$ -O4 lignin (SbO4L) polymer ....	41
Figure 16: Synthetic scheme for production of SbO4L .....	69
Figure 17: Characterizing molecular size of SbO4L .....	71
Figure 18: Comparison of three different batches of SbO4L using RPIP-UPLC-MS and Thrombin Inhibition.....	72
Figure 19: Direct inhibition of serine proteases of the coagulation cascade by SbO4L.....	74
Figure 20: SbO4L inhibition of other heparin-binding serine proteases .....	76
Figure 21: Effect of antithrombin III on SbO4L inhibition of thrombin .....	78
Figure 22: SbO4L inhibition of thrombin-thrombomodulin complex.....	79
Figure 23: Inhibition of different types of thrombin by SbO4L.....	80
Figure 24: Inhibition of thrombin mediated conversion of fibrinogen to fibrin by SbO4L.....	81
Figure 25: Michaelis-Menten kinetics of Spectrozyme TH hydrolysis by thrombin in the presence of SbO4L.....	82
Figure 26: Effect of exosite 1 binding competitor hirudin-based peptide (HirP) on the inhibition of thrombin by SbO4L.....	84
Figure 27: Effect of exosite-2 binding competitor unfractionated heparin (UFH) on the inhibition of thrombin by SbO4L.....	85
Figure 28: Effect of exosite-2 binding ligand GPIIb $\alpha$ on the inhibition of thrombin by SbO4L. ...	87

Figure 29: Effect of SbO4L on Thrombin Mutants .....	91
Figure 30: Active site fluorescence quenching in presence of SbO4L.....	93
Figure 31: Effect of salt on SbO4L binding to thrombin.....	95
Figure 32: Protamine-mediated reversal of SbO4L inhibition of thrombin. ....	98
Figure 33: Dual mechanism of antithrombotic action by SbO4L in advanced assays. ....	106
Figure 34: Prolongation of clotting time as a function of SbO4L concentration in either the prothrombin time (PT) or the activated partial thromboplastin time (APTT) assay.....	113
Figure 35: The effect of serum albumin on the thrombin inhibition potential of SbO4L. ....	114
Figure 36: A comparison of $\alpha$ -thrombin and $\gamma$ -thrombin as platelet aggregation initiators. $\alpha$ - thrombin causes the formation of a fibrin mesh which traps the platelet aggregates. ....	115
Figure 37: Variation in the level of platelet aggregation as a function of the concentration of SbO4L .....	116
Figure 38: Reduction in the level of ATP released by platelets in the presence of varying levels of SbO4L.....	117
Figure 39: Comparison of the effect of SbO4L on platelet function in whole blood using hemostasis analysis system (HAS <sup>TM</sup> ). ....	119
Figure 40: Effect of SbO4L on whole blood hemostasis using Thromboelastography (TEG). ..	121
Figure 41: In vivo anticoagulant effect of SbO4L as observed in C57BL/6 mice. ....	124

Figure 42: Rationale for screening sulfated small molecule library to identify factor XIa selective inhibitor.....	130
Figure 43: Library of sulfated small molecules (SSMs).....	132
Figure 44: Compound 24 inhibits factor XIa by allosteric mechanism. ....	135
Figure 45: Modeling studies for inhibitor 24.....	141
Figure 46: Loss in inhibition potency of 24 upon removal of the Apple domains containing the putative site of binding.....	143
Figure 47: Binding of 24 to factor XIa induces a large conformational change.....	145

## Abstract

### SYNTHETIC, SULFATED, LIGNIN-BASED ANTICOAGULANTS

by Akul Yugesh Mehta, Ph.D.

A dissertation submitted in partial fulfillment of the requirements for the degree of Doctor of Philosophy at Virginia Commonwealth University.

Virginia Commonwealth University, 2014.

Supervisor: Umesh R Desai

Chemoenzymatically synthesized low molecular weight lignin polymers have been previously found to be potent inhibitors of a number of serine proteases via allosteric mechanisms targeting heparin binding sites. Herein, we describe the creation of synthetic sulfated  $\beta$ -O4 lignin (SbO4L) polymer, which is more homogenous compared to previous lignins with respect to its inter-monomeric linkage. SbO4L is a selective inhibitor of thrombin and plasmin. SbO4L was found to act via a unique mechanism targeting thrombin exosite 2 in a manner similar to platelet glycoprotein Iba (GPIba). Advanced hemostasis and thrombosis assays demonstrated that SbO4L acts via a dual mechanism: as an anticoagulant, by allosteric inhibition of thrombin catalysis; and as an antiplatelet agent, by competing with platelet GPIba. These mechanisms are comparable in potency to low molecular weight heparins currently used in the market, indicating that targeting exosite 2 may yield clinically useful drugs in the future. Since the  $\beta$ -O4 type lignin was found to be selective for thrombin and plasmin, we hypothesized that other scaffolds from lignins could be potent inhibitors of other serine proteases. In particular, we screened a library of

synthetic sulfated small molecules against factor XIa – an emerging target for prophylactic anticoagulation. Our search identified a sulfated benzofuran trimer (a mimic of  $\beta$ -5 type linkage found in lignins) as a potent inhibitor of factor XIa. Surprisingly, this inhibitor did not compete with heparin. A plausible binding site in the A3 domain of factor XIa was proposed by using molecular modeling techniques. The binding pose demonstrated good correlation with the structure activity data from in vitro studies. Further confirmation that the apple domains were required was proved by testing the trimer against recombinant catalytic domain. A 40-fold decrease in activity was observed. A temperature-dependant perrin plot demonstrated that factor XIa undergoes a large conformational change in the presence of the trimer, which is possibly converting the enzyme back into the zymogen-like shape. In general, the synthetic sulfated lignins can act as a useful foundation to develop anticoagulant, antiplatelet, and anti-inflammatory molecules in the future.

## **Chapter 1: Introduction**

### **1.1 Blood, Coagulation and Hemostasis**

Blood is an essential body fluid that helps transport nutrients to all cells of the body, while simultaneously transporting metabolic waste products away from the cells for excretion.<sup>1</sup> An average human being contains almost 4 liters of blood within the body. Part of this is made up of proteins, which float in the liquid fraction of blood called plasma and are essential for coagulation and transportation of nutrients. The other part of blood is composed of cells. Three major types of cells make up the cellular composition of blood, namely: (a) Red blood cells (erythrocytes) – essential for carrying oxygen to various tissues of the body. (b) White blood cells (leucocytes) – essential for fighting infections and performing various protective functions. (c) Platelets (thrombocytes) – essential for prevention of blood loss.<sup>1</sup>

In toto, these components of blood help perform a variety of functions such as supplying nutrients and oxygen to various parts of the body; transporting waste products from various tissues to the kidneys; lungs and liver for metabolism and excretion; protecting the body from various infections; maintaining body pH, hydration and temperature; and coagulation in case of injury. Thus, proper blood flow within the body is essential to maintain the homeostatic balance of the body.<sup>1</sup>

To maintain appropriate blood flow conditions, procoagulant and anticoagulant factors are present within the blood.<sup>2</sup> In case of injury, excessive blood loss is prevented by the

procoagulant factors, which result in hemostasis. Simultaneously, anticoagulant factors help maintain proper blood flow within the rest of the body. This balance of procoagulant and anticoagulant factors is maintained by certain proteins and regulatory factors present in the blood by a process known as the coagulation cascade, along with the platelet cells of the blood.<sup>2</sup>

## 1.2 The Coagulation Cascade

The coagulation cascade is composed of several proteins which are freely floating within the blood in their inactive state or zymogen form (Figure 1). Upon injury or under pathological conditions, these zymogens are activated in a sequential step by step manner via either the intrinsic pathway (contact activation pathway) or the extrinsic pathway (tissue factor pathway).

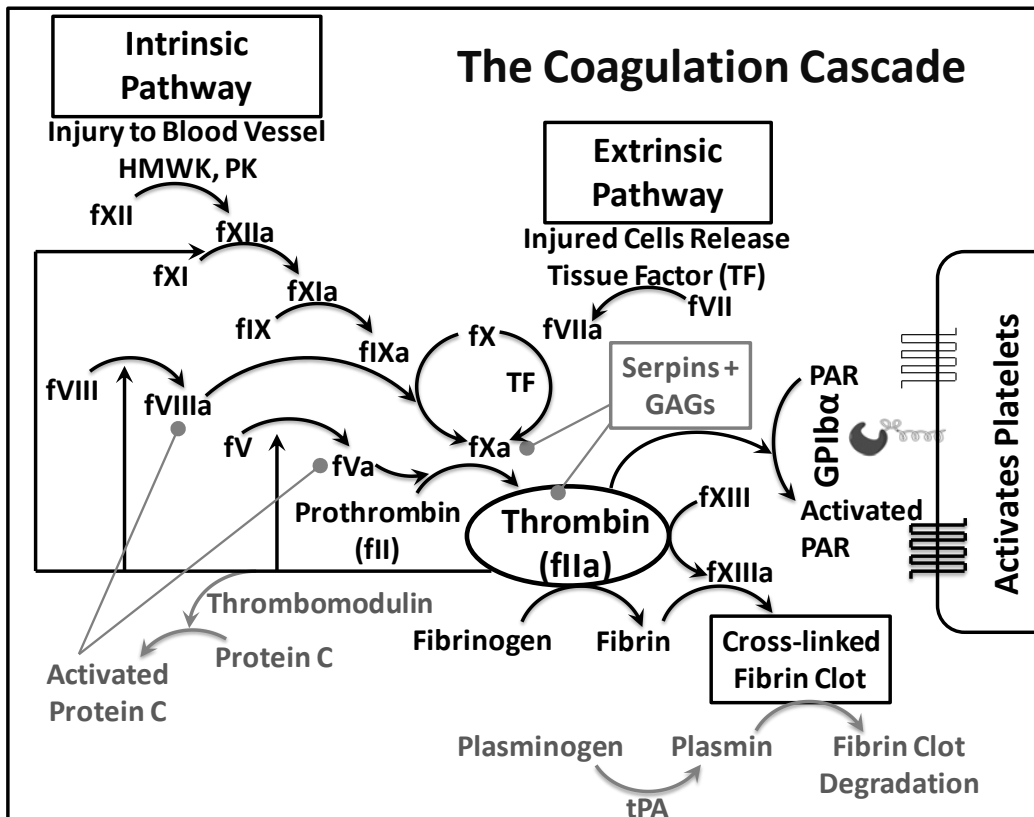


**Figure 1.** The coagulation cascade of blood. In black are the procoagulant factors, while in grey are the anticoagulant pathways. Thrombin (factor IIa) plays a key role in the cascade. It

*catalyzes the conversion of soluble fibrinogen to insoluble fibrin which eventually leads to clot formation by thrombin activated fXIIIa. It acts as a link between the cascade and platelets for aggregation via binding to glycoprotein Iba (GPIba). It provides positive feedback to the cascade by activating fXI, fVIII and fV, while also providing negative feedback in presence of thrombomodulin via protein C pathway. Thrombin activity can be regulated by serpin-GAG complexes. Image adapted from reference 3.*<sup>3</sup>

In case of injury, there is damage to the endothelium which exposes the subendothelial tissues (mainly composed of smooth muscle cells). These subendothelial cells express tissue factor (TF) on their surface, which acts as a receptor for factor VII in turn activating it to form factor VIIa.<sup>4,5</sup> The TF-VIIa complex forms the extrinsic tenase complex which is capable of activating factor X of the common pathway.<sup>6</sup> On the other hand, the intrinsic pathway of coagulation is a means of amplification of clot formation. It is activated when collagen (or other anionic substances such as dextran sulfate) is exposed and forms a complex with high-molecular weight kininogen (HMWK), prekallikrein and factor XII.<sup>7</sup> Upon formation of this complex, prekallikrein is activated to kallikrein and factor XII gets activated to form factor XIIa. Factor XIIa in turn catalyzes the activation of factor XI to factor XIa, which subsequently activates factor IX to factor IXa. Factor IXa is then capable of activating factor X of the common pathway.<sup>8</sup>

The sequential activation via either of the pathways leads to the activation of factor X to factor Xa from where the final common pathway initiates. Factor Xa catalyzes the conversion of prothrombin (factor II) to thrombin (factor IIa). Thrombin has a large array of functions within the cascade (Figure 1): (a) its primary role is to catalyze the conversion of soluble fibrinogen to



insoluble fibrin which ultimately leads to a “clot” that can plug the site of bleeding or damage;<sup>9</sup> (b) it also activates factor XIII to factor XIIIa, which helps in cross-linking of the fibrin and hence strengthens the clot;<sup>9</sup> (c) it provides positive feedback to the coagulation cascade by activating factors VIII,<sup>10</sup> and factor V,<sup>11</sup> which can dramatically propagate the clot formation by forming the tenase and prothrombinase complexes with factor IXa and factor Xa, respectively; (d) it can itself activate factor XI to factor XIa further providing positive feedback to the cascade;<sup>12</sup> (e) it can even activate platelets by binding to platelet glycoprotein Iba (GPIba) which can help in platelet plug formation via activation and aggregation;<sup>13</sup> (f) and lastly, thrombin also plays a subtle anticoagulant role in the presence of thrombomodulin by activation of protein C, which is capable of degrading factor VIIIa and factor Va, and has anti-inflammatory actions.<sup>14,15</sup>

The fibrin clot thus formed, along with the aggregated platelets forms a thrombus, which helps in checking the blood loss and begin the wound healing process. Anticoagulant factors such as heparin along with the serine protease inhibitors (serpins), antithrombin and heparin co-factor II, help maintain proper blood flow within the circulatory system away from the site of thrombus formation.<sup>16</sup> Furthermore, fibrinolytic pathways involving plasmin can help break down already present clots within the body to restore normal blood flow once healing has completed.<sup>17</sup>

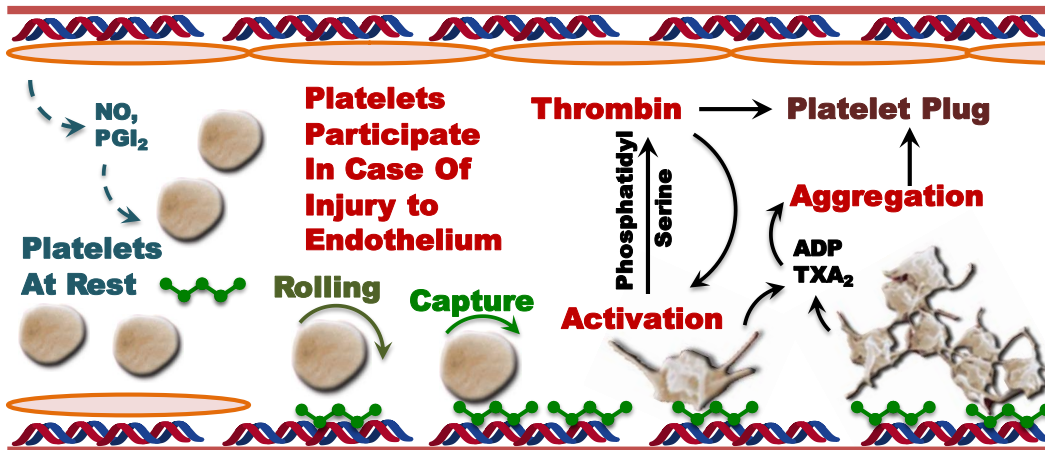
### **1.3 The Platelets**

Hematopoietic stem cells present within the bone marrow form the highly specialized megakaryocyte cells, which function to produce and release platelets into the circulation.<sup>18</sup> Platelets are anuclear, discoid shaped cells, which range from 1-3  $\mu\text{m}$  in diameter and 0.5  $\mu\text{m}$  in





thickness and are the smallest cells found in the circulation.<sup>19,20</sup> Blood vessel walls are lined with a layer of endothelial cells, which play important physiological roles and participate directly in hemostasis by interaction with blood components (Figure 2). They are also believed to be the building blocks of vessels.<sup>21</sup> The endothelial cells release nitric oxide and prostacyclin, which help keep the platelets in their inactive state.

Underlying the layer of endothelial cells is a basement membrane. Below the membrane is a layer of collagen matrix and smooth muscle cells. The basement membrane (subendothelium) underlying the endothelium produces collagen on the surface. Platelets bind to the collagen via a cell adhesion protein called the von Willebrand factor (vWF), which is present in the blood (Figure 2). Thus, under physiological conditions collagen is not exposed to the blood stream where platelets are present. However, upon injury, collagen is exposed to the blood stream and can activate the platelets with the help of vWF present in the blood.<sup>22</sup>

Upon activation, platelets release alpha granules and dense granules which in turn activate other platelets generating a chain reaction (Figure 2). The components from these granules, such as ADP and thromboxane-2 (TXA-2) help in adhesion and aggregation of platelets, and are also procoagulant and repairing in nature.<sup>23</sup> Aspirin, which is an antiplatelet drug, targets the biosynthesis of TXA-2 to provide antiplatelet effects. Activation of platelets also exposes phosphatidylserine on the platelet surface, which activates factor Xa to enhance thrombin generation and propagate the coagulation cascade to form a fibrin mesh.<sup>24</sup> The unique character demonstrated by activated platelets is that they undergo a dramatic shape-change, producing pseudopods from their surface and obtaining a more stellate shape. Platelet shape change is a complex process, which is controlled by proteins that regulate actin architecture.<sup>25</sup> Such a platelet is then able to clump with other platelets to form the platelet plug.



**Key:**

	= Endothelial Cells		= Von Willebrand factor
	= Inactive Platelets		= Collagen

*Figure 2. The role of platelets during injury. From left to right: During normal blood flow, endothelial cells keep the platelets at rest by releasing nitric oxide (NO) and prostacyclin (PGI<sub>2</sub>). The endothelial cells also act as a barrier preventing von Willebrand factor from interacting with collagen. During injury, the endothelial layer is disrupted exposing the collagen to the Von Willebrand factor. Binding of VWF to collagen provides a surface for interaction of platelet surface integrins and glycoprotein Iba. This causes the platelets to roll on the vessel wall and be captured via stable adhesion even under flow. Interaction of collagen with GPVI stimulates the spreading of the platelet and activation, which in turn releases feedback agonists ADP and thromboxane-2 (TXA-2) causing recruitment of more platelets for activation. Furthermore, activation of platelets exposes phosphatidylserine on platelet surface which provides a procoagulant surface for thrombin activation. Together, aggregation of activated platelets and thrombin mediated fibrin mesh formation lead to formation of platelet plug.*

Platelets mediate a number of vascular and cellular responses via a number of receptors.<sup>26,27</sup> Since both coagulant factors and platelets assist in hemostasis, there is significant cross-talk between the two systems via platelet receptors. The platelet receptors mainly involved in such inter-play include:

1. Glycoprotein Ib $\alpha$  (GPIb $\alpha$ ) - which is known to interact with thrombin, vWF and other coagulation factors such as factor XI, XII, VIIa and kininogen.
2. Protease activated receptors PAR1, PAR3 and PAR4 – which are known receptors for thrombin and are activated by thrombin.
3. Integrins like  $\alpha$ Ib $\beta$ 3 – which are known to bind with fibrinogen and vWF for adhesion.

Of these reactions, the GPIb $\alpha$ -thrombin reaction is critical for platelet-coagulation inter-play. GPIb $\alpha$  is one of the most abundant surface receptors on platelets and thrombin is a versatile catalytic enzyme. In fact, thrombin bound to GPIb $\alpha$  shows an increased catalytic ability towards PAR activation suggesting that physiologically this complex might play a crucial role in recruiting platelets during hemostasis induced by the coagulation system.

#### **1.4 Structure of Thrombin**

Thrombin is a ~36,000 Da globular enzyme which is formed from its precursor prothrombin via cleavage of two peptide bonds, i.e., R320-I321 and R272-T273 (prothrombin numbering).<sup>28-32</sup> Upon activation thrombin is composed of an amino terminal light chain (“A” chain ~6,000 Da) and a carboxy terminal heavy chain (“B” chain ~31,000 Da).<sup>30</sup> The two chains are covalently linked via single disulfide bond.<sup>32</sup> Structurally, thrombin contains an active site

with a catalytic triad, a sodium binding site and two allosteric electropositive sites called exosite 1 and exosite 2 (Figure 3).

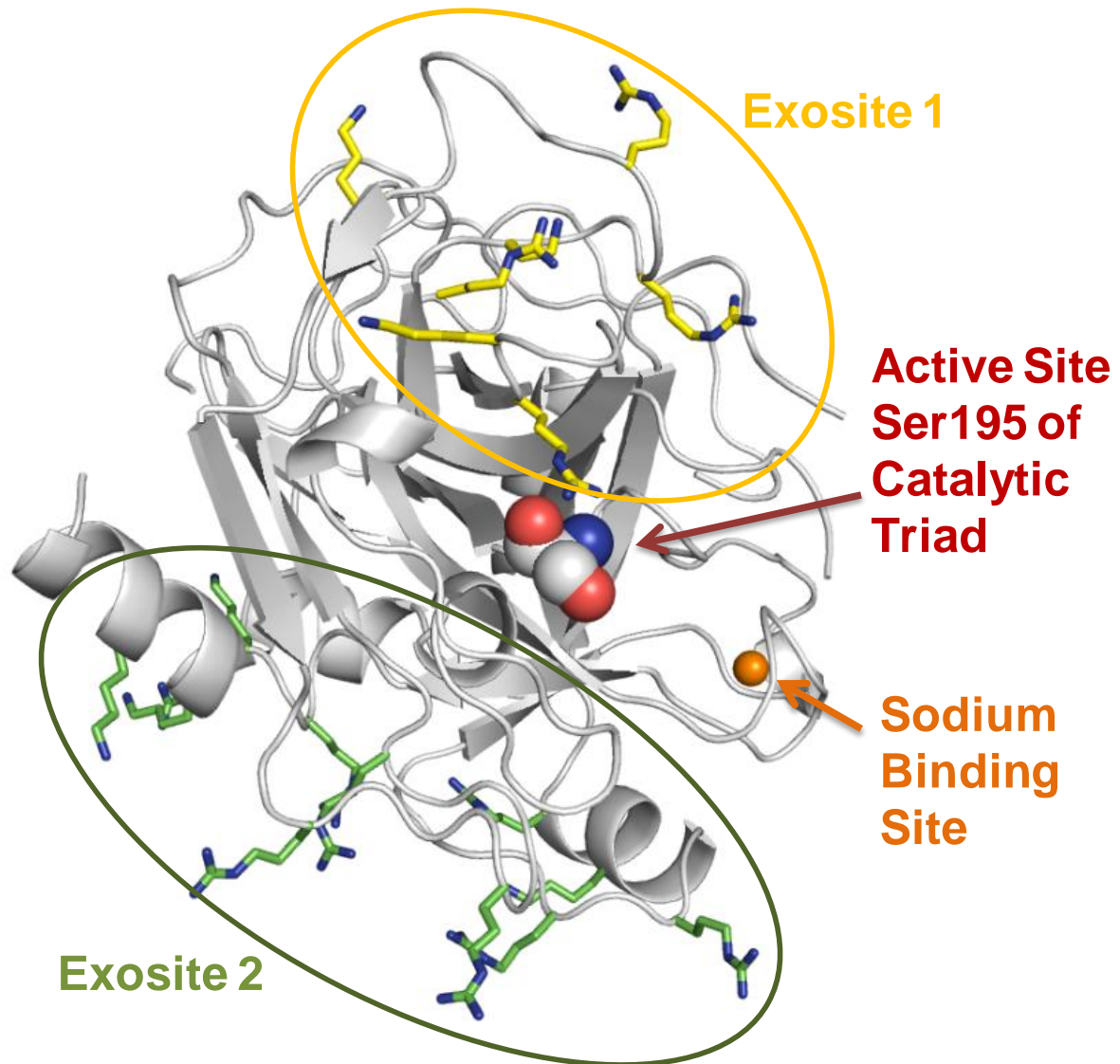


**Figure 3.** The structure of human thrombin, showing the presence of a Ser195 at the active site catalytic triad, a sodium binding site located close by, and two electropositive allosteric sites called exosite 1 and exosite 2.

### *Catalytic Triad and Mechanism*

Thrombin is a serine protease. A specific serine residue (Ser195) within the active site is essential for its protein cleaving catalytic activity (Figure 4A).<sup>33</sup> This serine residue is a part of a catalytic triad composed of Ser195, His57 and Asp102 (chymotrypsin numbering), which is involved in a “ping-pong” catalysis involving the substrate and water (Figure 4B).<sup>34</sup> The hydroxyl group on the serine (seroxide) acts as a nucleophile and attacks the carbonyl carbon of the peptide substrate to form a tetrahedral intermediate. To enhance this nucleophilicity of the Ser195, the His57 lone pair on N<sub>3</sub> or N $\epsilon$  of the imidazole ring is capable of accepting the hydrogen of the hydroxyl of the Ser195. The Asp102 carboxylate hydrogen bonds with the other imino group (N<sub>1</sub> or N $\delta$ ) on the histidine imidazole to further catalyze the formation of the tetrahedral intermediate. The nitrogen-carbon bond within the substrate finally breaks as the peptide nitrogen accepts the hydrogen from the histidine to release the amine fragment of the substrate (C-terminus). The carbonyl part of the substrate in turn forms a covalently linked acyl-enzyme intermediate. At this moment, water comes into the reaction to re-protonate the His57, while the hydroxyl moiety attacks the carbonyl carbon of the acyl-enzyme intermediate to form another tetrahedral intermediate. In the final step, the protonated His57 is capable of regenerating the Ser195 hydroxyl while the tetrahedral intermediate structure breaks down to release the carboxylate part of the substrate (N-terminus).

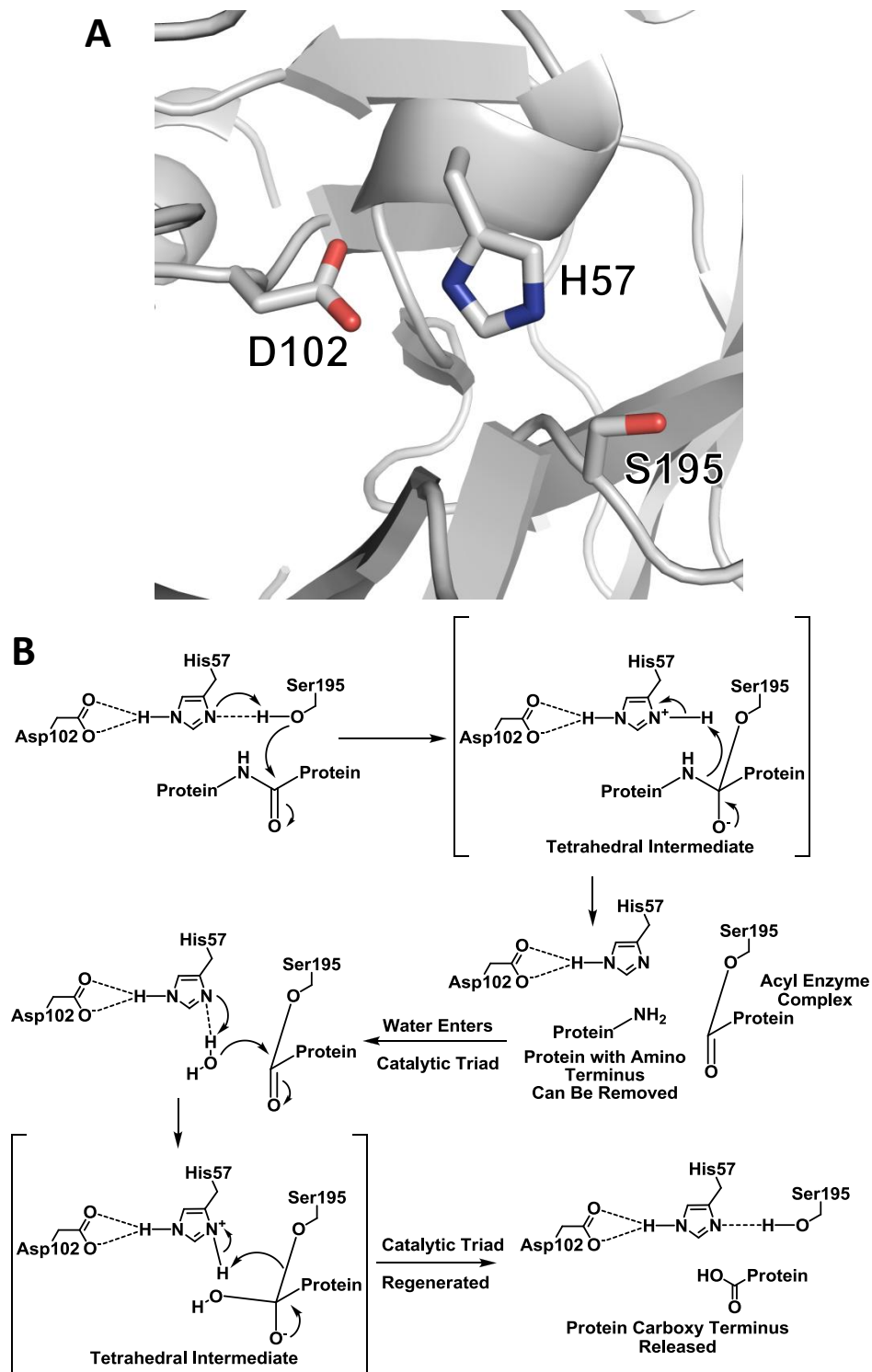


**Figure 4.** Serine Protease Catalysis (A) Catalytic triad as observed in thrombin consisting of Ser195, His57 and Asp102. (B) Mechanism of catalytic-triad mediated peptide bond cleavage in serine proteases.

### *Active Site Structure*

Like other proteases, the active site of thrombin can be represented by the Schechter and Berger nomenclature (Figure 5A).<sup>35</sup> According to this nomenclature, the active site of a protease is composed of subsites (S), wherein the sites on the enzyme which bind the substrate outwards from the site of cleavage towards the amino-terminus of the substrate are numbered S1, S2, S3,...Sn; while the sites on the enzyme which bind the substrate outwards from the site of cleavage towards the carboxy-terminus of the substrate are numbered S1', S2', S3',....Sn'. Thrombin contains an acidic Asp189 residue at the bottom of the S1 pocket, which further classifies it into the trypsin family of serine proteases (Figure 5C). However, unlike trypsin, thrombin is highly selective in cleaving between Arg/Lys-Gly bonds. In fact, thrombin is selectively able to cleave two specific Arg-Gly bonds out of 181 Arg/Lys-Xaa possible bonds on fibrinogen to produce fibrin.<sup>36</sup> The thrombin S1 pocket can possibly accommodate more bulkier P1 groups than trypsin.<sup>37</sup> Above the S1 pocket is a Trp215 residue, which forms a hydrophobic base for the S2 and S4 binding pockets (Figure 5C). The active site of thrombin forms a particularly deep cleft due to the insertion 60-loop above and the  $\gamma$ -loop (also called the autolysis loop) below. The 60-loop helps form the S2 and S4 sites, while the  $\gamma$ -loop forms the S' side (Figure 5B). These loops help enhance thrombin specificity for substrates.<sup>38</sup>



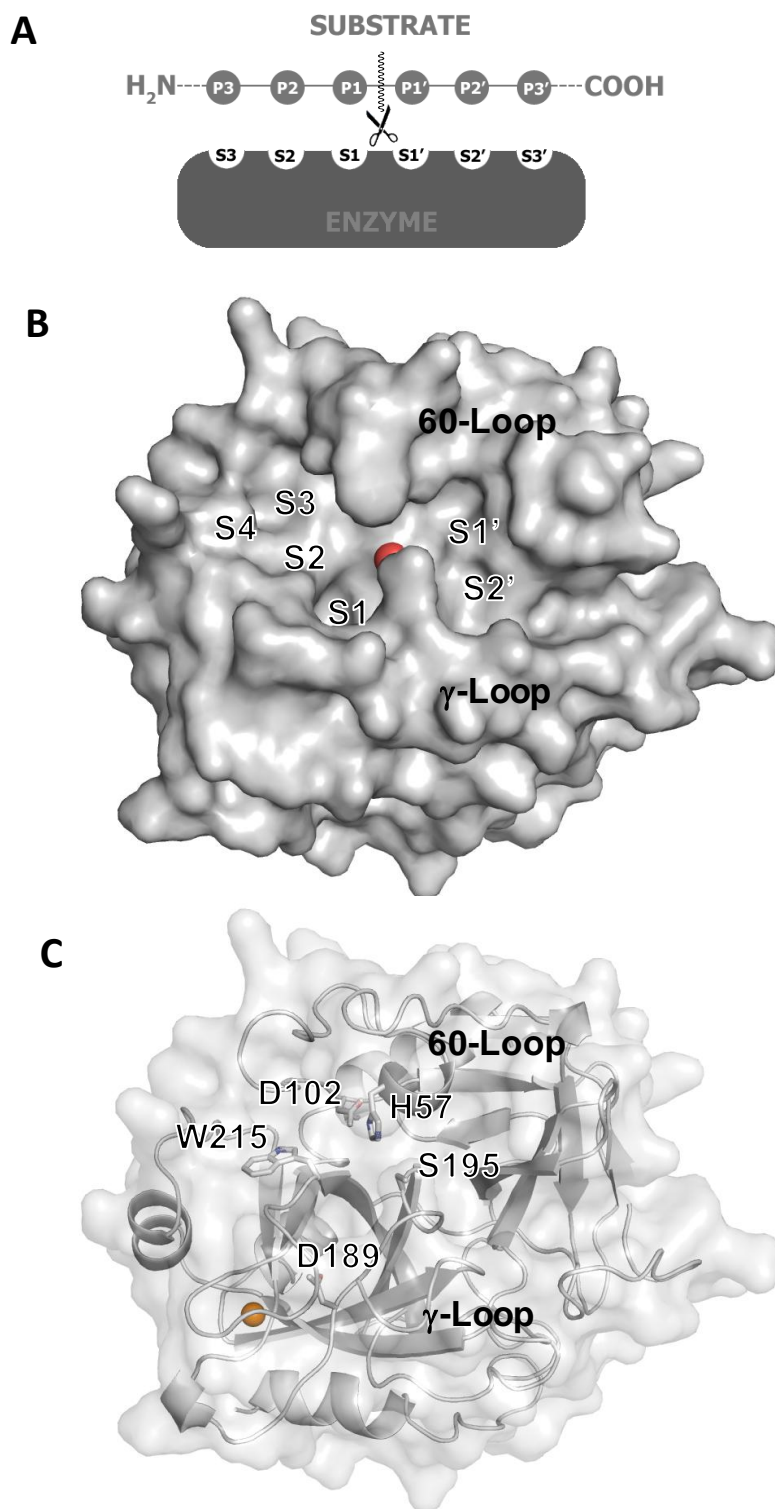


**Figure 5.** The active site of thrombin. (A) A structural depiction of the Schechter and Berger nomenclature of serine protease active site pockets (depicted as S3, S2, S1, S1', S2' and S3' on

*the enzyme) in relation to the protein substrate residues (depicted as P3, P2, P1, P1', P2' and P3'). (B) A surface model of thrombin showing the different pockets of the active site with the Ser195 of the catalytic triad in red. (C) The underlying chain structure and the defining amino acid residues of the corresponding active site pockets.*

### *The Sodium Binding Site*

Located approximately 15 Å from the catalytic triad is a Na<sup>+</sup> binding site formed by three antiparallel β-strands of the B-chain (Met180-Tyr184a, Lys224-Tyr228, and Val213-Gly219) and diagonally crossed by the Glu188-192 strand (Figure 6). The binding of sodium at this site is highly selective over other monovalent cations like K<sup>+</sup>, Li<sup>+</sup> or even Rb<sup>+</sup>. This Na<sup>+</sup> is coordinated to the main chain oxygens of Arg221a, Lys224 and four conserved water molecules. The binding of Na<sup>+</sup> forms a water mediated hydrogen bond with the Asp189 residue, which forms the base of the S1 pocket and forms a charge-relay system with the catalytic triad. This binding therefore, shifts thrombin from a “slow” to “fast” form. In fact, the binding of other ions like K<sup>+</sup> in place of Na<sup>+</sup>, shifts thrombin to an inactive or slow form.<sup>39</sup>

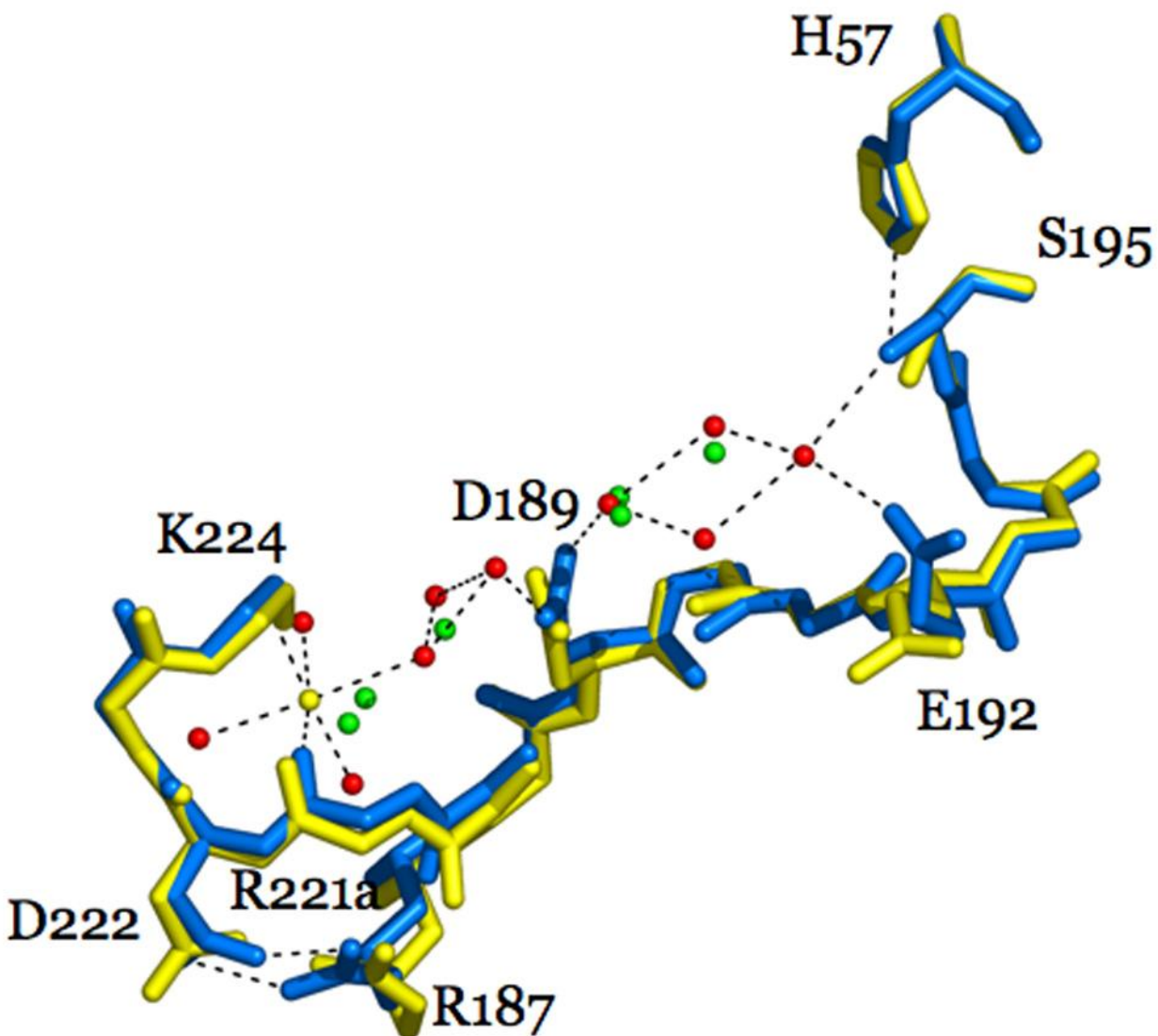


**Figure 6.** Structural difference due to sodium binding relays into the catalytic triad. An overlay of the fast sodium-bound form of thrombin (protein chain in blue, sodium as yellow ball, and waters as red balls) and the slow sodium-free form of thrombin (protein chain in yellow, waters as green balls) highlights the presence of a water mediated switch which links the sodium to the catalytic triad of thrombin. Image is taken from reference 40.<sup>40</sup>

### *Exosite 1*

Located approximately around 20 Å away from the active-site catalytic triad, there is a surface depression, which starts at the end of the P' site of the enzyme. This surface depression is mainly formed by insertion loops from 70-80 and is known as exosite 1 (Figure 7). Exosite 1 also encompasses some bordering residues from the 37 loop and Lys109, Lys110 residues. Exosite 1 is electropositive in nature due to the presence of Lys36, Lys70, Lys81, Lys107, Lys109, and Lys110; and Arg35, Arg67, Arg73, Arg75, Arg77A.<sup>32</sup> The base of the exosite 1 is however hydrophobic and is formed by the side chains of Tyr76 and Ile82. Exosite 1 is known to be crucial for fibrinogen activation by thrombin.<sup>32,41</sup> It is also known to interact with PARs,<sup>42</sup> fV,<sup>43</sup> fVIII,<sup>44</sup> fXI,<sup>45</sup> HCII,<sup>46</sup> hirudin,<sup>47</sup> and thrombomodulin.<sup>48</sup>

### *Exosite 2*

Exosite 2 is a large, highly electropositive area located near the C-terminus of the heavy chain of thrombin. As it binds heparin, this exosite is also known as the heparin binding exosite 2 and is roughly 200 Å<sup>2</sup> in area (Figure 8). The electropositive residues within exosite 2 include: Arg93, Arg97, Arg101, Arg126, Arg165, Lys169, Arg173, Arg175, Arg233, Lys235, Lys236 and Lys240.<sup>32,49</sup> As most of these residues do not have a compensatory acidic residues, exosite 2 presents a highly electropositive surface, which can attract anionic molecules such as heparin. In the zymogen form, the exosite 2 is covered by the F2 domain and is inaccessible in prothrombin, pre-thrombin-1 and meizothrombin forms.<sup>50,51</sup>

Besides heparin, exosite 2 is known to interact with platelet receptor GPIb $\alpha$ ,<sup>52</sup> prothrombin fragments 1.2,<sup>50</sup> chondroitin sulfate moiety of thrombomodulin,<sup>53</sup> and fVIII.<sup>44</sup> Some

exogenous ligands such as haemadin from *Haemadipsa sylvestris* leech is also known to interact with thrombin exosite 2.<sup>54</sup> Additionally, aptamers have been synthesized to interact with exosite 2 via their polyanionic nature.<sup>55,56</sup>

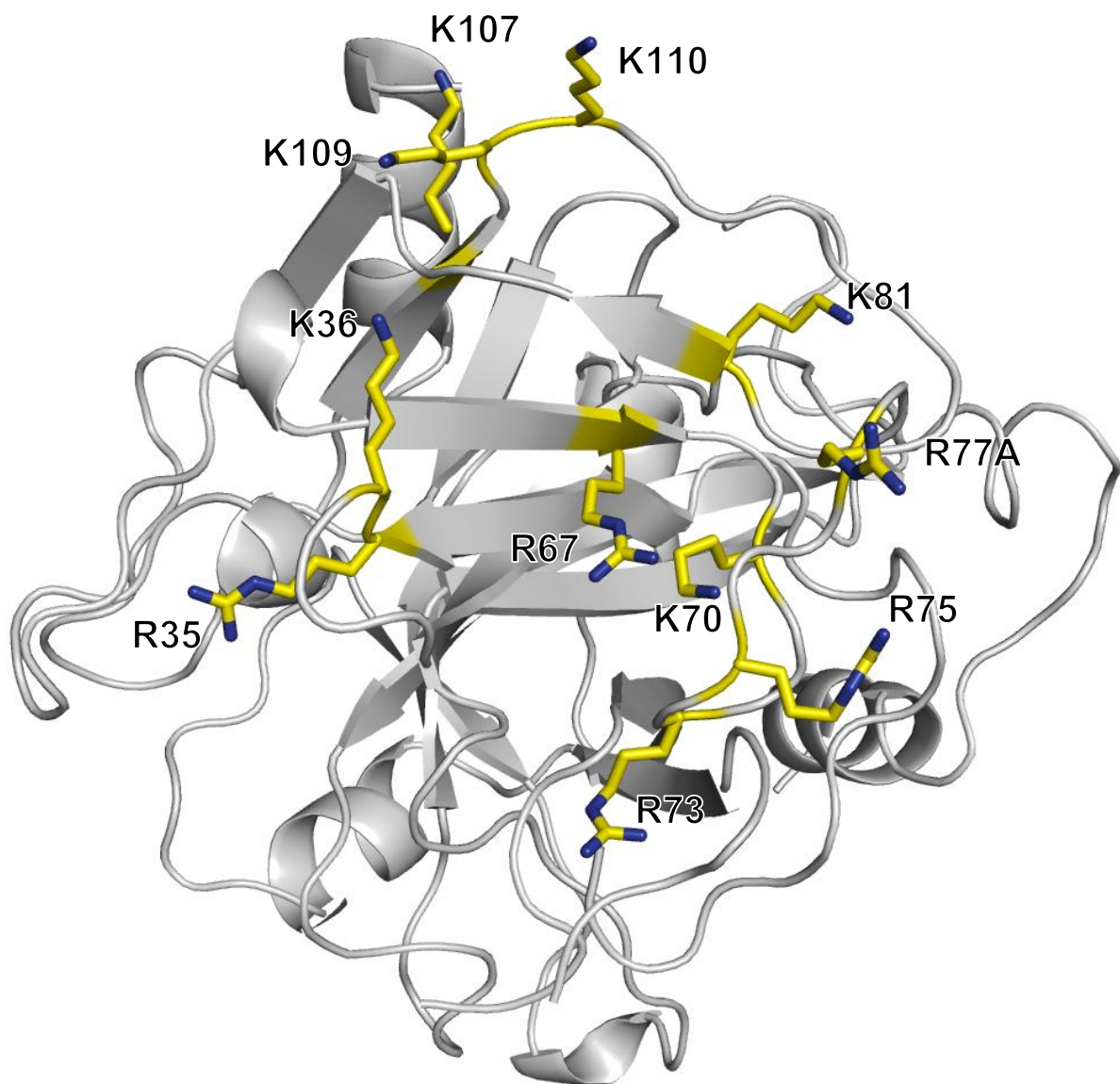


**Figure 7.** Structure of human thrombin showing all electropositive residues (arginines and lysines) present on the exosite 1 (in yellow).

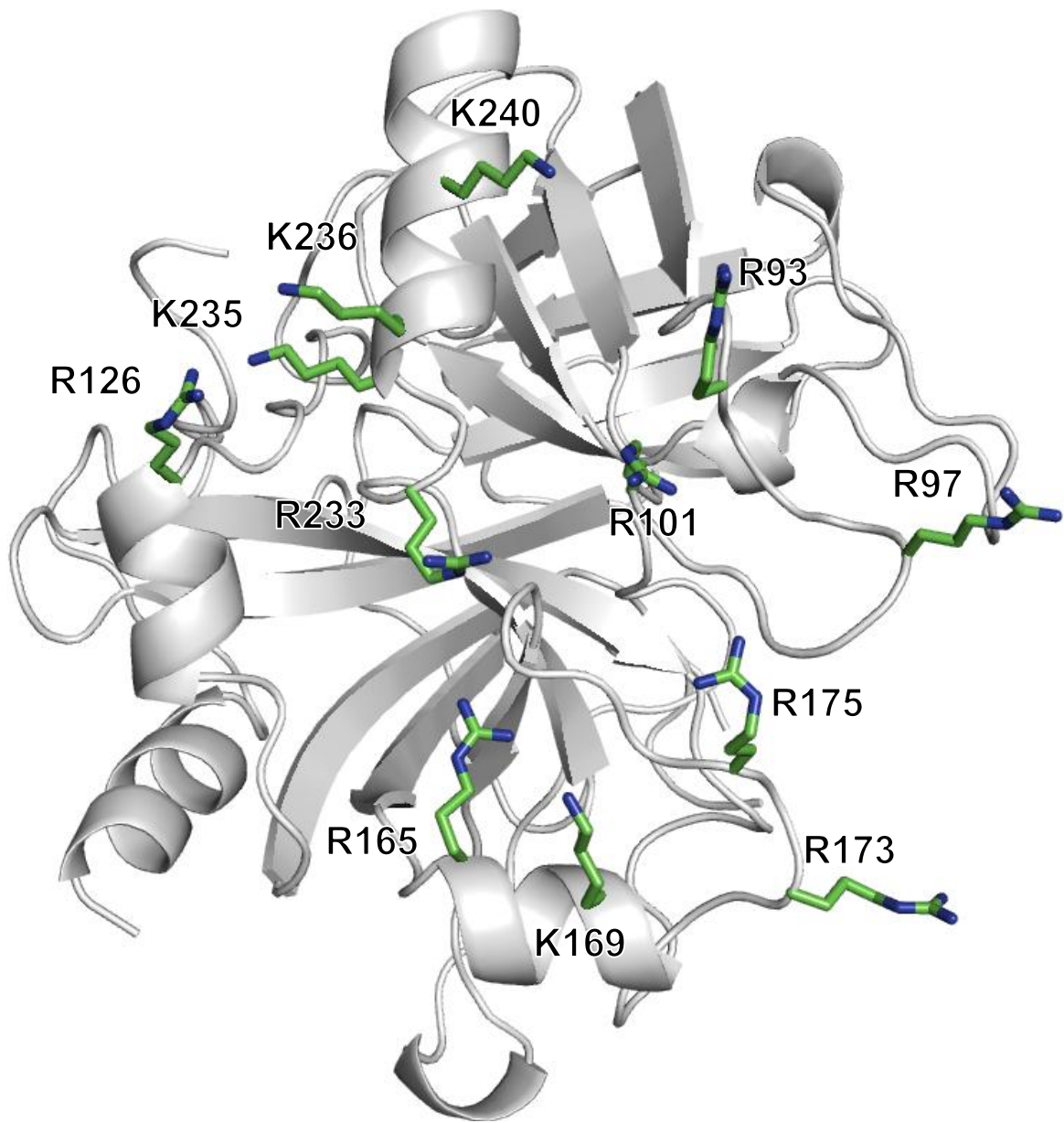


*Figure 8. Structure of human thrombin showing all electropositive residues (arginines and lysines) present on the exosite 2 (in green).*

## 1.5 Thrombin Allostery

Allostery by definition is the phenomenon where a ligand binding at a site away from the orthosteric/active site can affect the activity of the protein/enzyme. Thrombin is a highly plastic enzyme.<sup>57</sup> Its structural conformations and activity is highly regulated by the ligands it binds within the blood. The three aforementioned sites, i.e., the sodium binding site, and the exosites 1 and 2, present extended surfaces away from the active site via which ligand binding can demonstrate allosterism.

### *1.5.1. Sodium Binding Site and Thrombin Allostery*

Binding of  $\text{Na}^+$  ions to thrombin has been shown to increase thrombin activity for well over thirty years.<sup>58</sup> However, since the lack of  $\text{Na}^+$  did not completely abolish activity, it was concluded that  $\text{Na}^+$  is a positive allosteric effector of thrombin rather than a cofactor. Instead,  $\text{Na}^+$  binding to thrombin has been shown to shift the enzyme from “slow” or low-activity form, to a “fast” or high-activity form towards substrate hydrolysis.<sup>40</sup> Moreover, it has also been shown that the substrate specificity of these two forms of thrombin is widely different. The slow-form of thrombin has been shown to be a stronger anticoagulant enzyme with greater activation of protein C by binding to thrombomodulin and lack of activity against fibrinogen, PAR-1 and other procoagulant factors. On the other hand, the fast  $\text{Na}^+$ -bound form of thrombin demonstrates higher procoagulant activity as a result of greater proteolytic activity towards fibrinogen, PAR-1 and other procoagulant factors.<sup>59,60</sup> A structural link has been established between the  $\text{Na}^+$ -binding site and the catalytic triad which shows that a hydrogen bond network links the  $\text{Na}^+$  ion to the Asp189 of the active site.<sup>61</sup> Such an interaction could possibly account for the change in activity and substrate specificity. If  $\text{K}^+$  is replaced in place of  $\text{Na}^+$  in the buffer, the enzyme shifts

to a more inactive or slow form.<sup>39</sup> This demonstrates the selectivity for, and the fine tuning by  $\text{Na}^+$  at this site to maintain thrombin procoagulant activity and raises the possibility that this site could be a switch to shift between allosteric forms.

### *1.5.2. Exosite 1 and Thrombin Allostery*

Binding of different ligands to exosite 1 induces differential substrate specificity and activity within the active site. For example, thrombomodulin binding at exosite 1 changes thrombin substrate specificity from fibrinogen cleavage to protein C activation.<sup>62,63</sup> On the other hand, hirugen binding mildly alters (either increases or decreases) catalytic efficiency of thrombin towards an array of small chromogenic substrates and fibrinogen.<sup>64</sup> A PAR receptor fragment has been shown to resemble hirudin and alter thrombin specificity towards chromogenic substrates.<sup>65</sup> When bound to the exosite 1 of thrombin, PAR receptor fragments also show a collapsed conformational change within the active site via a network of polar interactions.<sup>66</sup> A 15-nucleotide DNA aptamer (also called HD1 or TBA<sub>15</sub>) was found to bind to thrombin exosite 1 causing inhibition of fibrinogen-clotting, platelet activation, and thrombomodulin-dependent protein C activation.<sup>67-69</sup> Several studies have also pointed towards an allosteric link between exosite 1, the  $\text{Na}^+$  binding site and the active site, suggesting a strong interplay among these sites.<sup>47,70,71</sup>

### *1.5.3. Exosite 2 and Thrombin Allostery*

Thrombin exosite 2 is more electropositive compared to exosite 1, and hence it is known to bind more anionic ligands like heparin. Although heparin binding does not induce allosteric modification of enzyme structure or function, it plays a vital role in a bridging mechanism for acceleration of inactivation by antithrombin III.<sup>49,72</sup> Binding of anionic proteins/peptides has



shown allosteric redirection or inhibition of the protease activity of thrombin. For example, the binding of the activation peptide fragment 1.2 (F12) from prothrombin to exosite 2 of thrombin results in the conversion of the enzyme to a zymogen like inactive state. The study also proposes a link between exosite 2 and the sodium binding site.<sup>73</sup> The fibrinogen  $\gamma'$  chain is also known to bind thrombin exosite 2 which results in inhibition of the proteolytic activity towards proteinaceous substrates, possibly resulting from perturbation of the Na<sup>+</sup> binding site, exosite 1 and the active site.<sup>74-76</sup> Another DNA aptamer (DNA 60-18[29] or HD22), that is 29-nucleotides in length was identified, which binds exosite 2 of thrombin and inhibits fibrin clot formation.<sup>77</sup>

On the flip-side, ecotin, an *E. coli* derived protein, decreases inhibition of thrombin by heparin/antithrombin, and produces a two-fold increase in thrombin catalysis of fibrinogen cleavage and inhibits thrombin-induced platelet aggregation via binding to exosite 2.<sup>78</sup> Platelet GPIIb $\alpha$  was also found to bind at exosite 2 and inhibit thrombin's fibrin formation ability as well as activity towards other coagulation proteins, but it activates thrombin towards PAR activation, thereby redirecting thrombin towards a pro-thrombotic role.<sup>79-82</sup> More recently, a novel sulfated pyranosic (1 $\rightarrow$ 3)- $\beta$ -L-arabinan (Ab1), which is obtained from the green seaweed *Codium vermilara* (Byrpsidales) was found to inhibit thrombin via direct and indirect mechanisms by binding to an allosteric site and inducing a conformational change.<sup>83</sup> However, more evidence needs to be presented to confirm that it does bind to exosite 2, since the authors have only performed molecular dynamic simulations to propose the binding at this site.

#### *1.5.4. Link between Allosteric Sites*

There exists some evidence that there is an allosteric network within thrombin, wherein ligand binding at either exosite would affect other allosteric sites such as the other exosite, the Na<sup>+</sup> binding site or the active site. We have seen several examples above which demonstrate a link between the exosites and the active site and the Na<sup>+</sup> binding site. It is therefore feasible that the two exosites could also be linked.

A study in 1997 was the first to demonstrate any kind of link between the two exosites.<sup>84</sup> A more recent study involving several exosite ligands such as, HD1, HD22,  $\gamma'$ -peptide, heparin,  $\gamma_A/\gamma_A$ -fibrin/fibrinogen, and prothrombin fragment 2 (FP12), has shown that there is long range, allosteric, bidirectional communication between the exosites 1 and 2 of thrombin.<sup>85</sup> A contradictory study involving mutagenesis gave some evidence that exosite 2 is an independent ligand binding site, but there is a link between the exosite 1 and the Na<sup>+</sup> binding site and the active site.<sup>62</sup> In comparison to the studies linking the two exosites using covalent fluorescent labels and surface-bound proteins in SPR, this study involved highly unnatural thrombin mutants with loops stabilized by engineered disulfide bonds within exosite 1 and the Na<sup>+</sup> binding site. Hence, interpretation of either of the results may be skewed due to experimental conditions, and care should be taken in not concluding possibilities or impossibilities about a link existing between the two exosites in a natural wild-type thrombin.

The occurrence of thrombin in such a vast variety of activity states due to various ligand binding, has led to a newer “ensemble view of thrombin allostery”, wherein thrombin can exist in various activation states in equilibrium and depending upon the ligands that bind to it a certain state may predominate over others.<sup>86</sup> Thus thrombin can be thought of as a “Swiss Army Knife”

within the coagulation cascade, which can be used and directed to a variety of utilities depending on the body's needs by various "hands" (or ligands). It also offers the development of newer ligands to redirect this knife into the safest possible direction and use it more for benefit than harm.

### **1.6 Sulfated Tyrosine Containing Proteins Involved in Hemostasis**

Tyrosine sulfates were first detected in 1984.<sup>87</sup> Yet even 30 years later, there is little known about the action of this post translational modification. From an evolutionary point of view, sulfation of tyrosines is a post translational modification, which is even found in plants. In humans (and mammals), sulfated tyrosine containing proteins are present mainly in the cardiovascular system, and especially in the blood.<sup>88</sup> However, little is known about the function of these groups within these proteins. Sulfated tyrosines are quickly gaining importance as a novel post translational modification, and people are realizing sulfated-tyrosine binding sites could possibly be targeted to obtain highly specific and allosteric drugs.

Tyrosine sulfation is carried out by tyrosylprotein sulfotransferase (TPST) enzyme. There are two isoforms of this enzyme, TPST-1 and TPST-2. Both TPST-1 and TPST-2 are found throughout the body at varying expression levels and use 3'-phosphoadenosine 5'-phosphosulfate (PAPS) as a sulfate donor (Figure 9).<sup>89,90</sup> It is of interest that the specificity of these enzymes to catalyze tyrosine sulfation is also different. Hence the expression of these enzymes seems to control important physiological outcomes. In fact, shear stress is known to play a role in the expression levels of these enzymes within endothelial cells, thereby further implicating the role of protein tyrosine sulfation in blood vessel pathologies.<sup>91</sup>

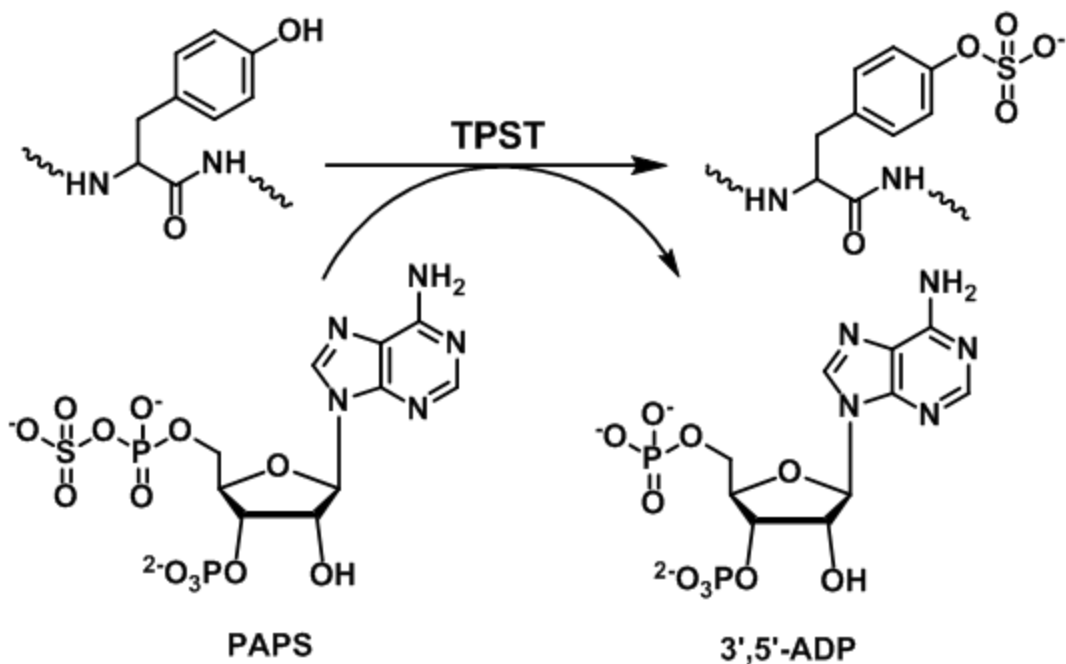


**Figure 9.** Tyrosine sulfation reaction as catalyzed by tyrosylprotein sulfotransferase (TPST) enzymes in the presence of 3'-phosphoadenosine 5'-phosphosulfate (PAPS).

Sulfated tyrosines are often located adjacent to negatively charged groups such as aspartates and glutamates. These sulfated tyrosine rich anionic peptides (STRAPs) are present in proteins that are essential for cell adhesion, immune response, and coagulation.<sup>88,90,92</sup> These STRAPs could provide selective interactions as there are no sequences in the literature, which were absolutely identical. This implies that these interactions are highly specific for certain characteristic features and mimicking them could provide a useful approach for drug design and development.

There are additional proteins found apart from those in the blood, which also contain sulfated tyrosines, such as gastrointestinal hormones (gastrin/CCK family), certain digestive enzymes, growth and developmental hormones and neuroendocrine peptides.<sup>88,90,92</sup> Yet no

STRAP is absolutely identical, further implying that mimicking STRAPs could provide useful therapies in not just hemostatic disorders but also inflammatory, neuronal, gastrointestinal and developmental disorders.

### **1.7 Structure and Functions of GPIb $\alpha$**

Glycoprotein Ib $\alpha$  (GPIb $\alpha$ ) is a 626 amino acid (Uniprot ID: P07359) long surface glycoprotein present on platelets. GPIb $\alpha$  exists as a complex along with GPIb $\beta$ , GPIX and GPV to form the GPIb-IX-V complex (Figure 10).<sup>93,94</sup> The long chain of GPIb $\alpha$  is split into 4 regions: N-terminal ligand binding domain (1-282), sialomucin core domain which acts as a linker, a transmembrane domain (506-526), and a cytoplasmic tail.

The N-terminal ligand binding domain is the business end of the protein that is extracellular and interacts with several ligands. It consists of an N-terminus capping sequence (1-35), seven tandem leucine rich repeats (LRR) (36-200) which are 24 amino acids in length, a C-terminal flanking sequence (201-268), which forms a knot due to two disulfide linkages, and finally ends in a sulfated tyrosine rich anionic peptide (STRAP) region (269-282) (Figure 10A).<sup>95,96</sup> The structure of the N-terminal domain is almost “hook-like” and is involved in adhesion as well as signaling functions. The following interactions mediate the majority of the functions of the N-terminus of GPIb $\alpha$  (Figure 10B):

1. Adhesion: Interaction with von Willebrand Factor (vWF), thrombospondin (TSP), P-selectin and integrin alpha M (ITGAM/ $\alpha$ M $\beta$ 2/MAC-1).
2. Procoagulant functions: Interaction with  $\alpha$ -thrombin, kininogen, factor XI and XII.
3. Signalling: via GPVI, ITGAM/MAC-1 and Fc $\gamma$ RIIa,

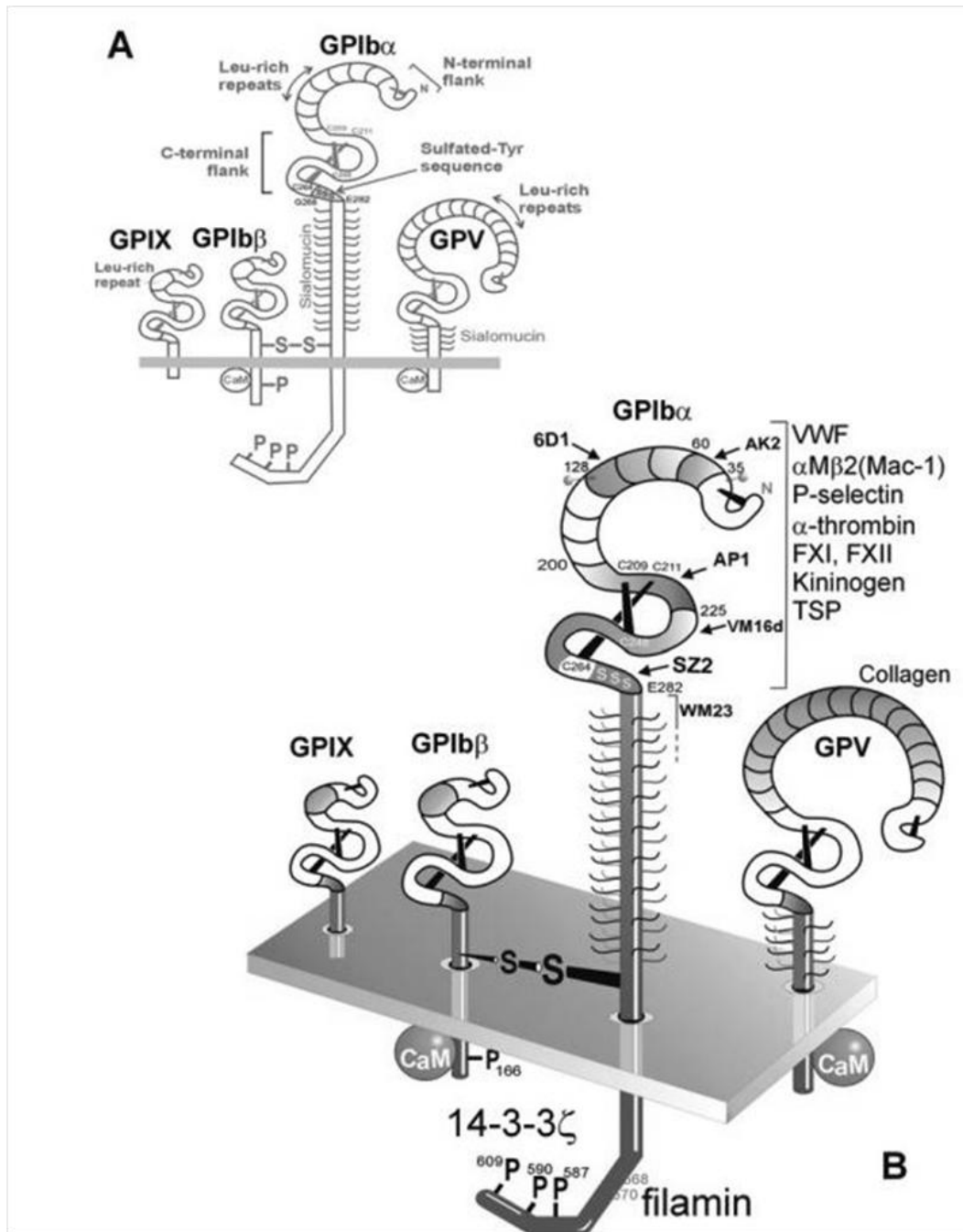


**Figure 10.** The GPIb-IX-V complex. (A) Cartoon representation of the GPIb-IX-V complex, showing the leucine-rich repeats, disulfide looped N- and C-terminal flanks, sulfated tyrosine containing sequences, and phosphorylation sites of the cytoplasmic tails.(B) Shows the functional binding sites of various ligands on the GPIb-IX-V complex. CaM : Calmodulin; FXI :

*factor XI; FXII : factor XII; TSP: Thrombospondin-1; VWF : von Willebrand factor. Image taken from reference 96.*<sup>96</sup>

The length of the sialomucin core of GPIb $\alpha$  appears to be an important factor in regulating the availability of the N-terminus sequence for ligand binding, thus making it devoid of steric hindrance from platelet surface molecules.<sup>97</sup> Hence the sequence is crucial for adhesion functions of platelets. The sialomucin chain is also recognized by cell wall proteins of bacteria such as *Streptococcus gordonii* to provide bacteria-platelet interaction.<sup>98</sup> However, other bacteria require the N-terminal region of the protein, or bridging mechanism between GPIb $\alpha$  and vWF for bacteria-platelet interactions.<sup>99-102</sup> The sialomucin core is also important for binding fVIIa, which might play a role in tissue factor-independent thrombin generation on activated platelet surface.<sup>103</sup>

The intracellular cytoplasmic tail contains a filamin and signaling protein 14-3-3 $\zeta$  binding region which are possibly involved in intracellular signaling.<sup>104,105</sup> The 14-3-3 $\zeta$  has been implicated in a toggle-switch mechanism which controls extracellular binding of vWF.<sup>106</sup> Filamin binding is believed to play roles in GPIb $\alpha$ -dependent adhesion, platelet shape and size, as well as raft localization of various receptors including the GPIb-IX-V complex.<sup>96</sup> However, the exact consequences of the interaction remain more or less a mystery.

Upon proteolytic digestion with Ca<sup>2+</sup> activated protease calpain, the extracellular terminal region sheds off to give the soluble form of GPIb $\alpha$ , known as glycofibrin, which is present at normal levels of 1-3  $\mu$ g/ml of blood.<sup>93,107,108</sup> Apart from these functions, there is also evidence to show that GPIb-IX complex could be a regulator of systemic inflammation via interaction with

$\alpha$ M $\beta$ 2 (MAC-1), and targeting this could prove promising as an anti-inflammatory and antithrombotic for sepsis and endotoxemia.<sup>109-111</sup>

## **1.8 Interaction between Thrombin and GPIIb $\alpha$ – Structure and Function**

The interaction between thrombin and GPIIb $\alpha$  has been highly studied in the last 30 years. Initial mutagenesis studies had localized thrombin binding sites on GPIIb $\alpha$  to the sulfated-tyrosine rich anionic peptide (STRAP) region of the protein.<sup>112</sup> On the other hand, until recently the binding site of GPIIb $\alpha$  on thrombin was heavily debated. It has been demonstrated in several instances that such interaction causes allosteric changes in thrombin activity and specificity.<sup>79,80</sup>

Earlier competitive studies with exosite 1 ligands such as hirudin, fibrinogen and thrombomodulin, showed that these ligands compete with GPIIb $\alpha$ -thrombin interaction.<sup>80,113</sup> Furthermore, synthetic anionic peptide of GPIIb $\alpha$  269-287 was earlier found to interact with thrombin exosite 1 and enhance catalytic efficiency of thrombin towards small chromogenic substrates.<sup>114</sup> However, such synthetic peptides were not revealed to have any sulfated tyrosines and there was no mention of sulfation step during their synthesis. In 2001, affinity studies on thrombin mutants revealed that GPIIb $\alpha$  binds to exosite 2 mainly involving residues: R93A (22-fold defect), R97A (8-fold defect), R101A (13-fold defect), R233A (29-fold defect), K236A (21-fold defect), K240A (5-fold defect), and for the triple mutant R233A/K236A/Q239A (31-fold defect), while the Q239A and R67A forms did not show any significant affinity change.<sup>115</sup> Additional mutational studies and competition studies with low molecular weight heparin further demonstrated involvement of exosite 2 and also that binding of GPIIb $\alpha$  to thrombin exosite 2 induced an allosteric change in the activity of thrombin.<sup>79</sup>



To further complicate the scenario, two separate groups released crystal structures in July 2003 having multiple thrombin molecules bound to GPIIb $\alpha$  (Figure 11).<sup>116,117</sup> In these crystal structures both exosite 1 and 2 binding to GPIIb $\alpha$  was demonstrated and multiple thrombin molecules were found to bind to GPIIb $\alpha$ . However, exosite 2-GPIIb $\alpha$  interface was more similar as compared to residues involved in the exosite 1-GPIIb $\alpha$  interface (Figure 11 and 12), suggesting that exosite 2 interaction was possibly tighter.<sup>118</sup> It was suggested that thrombin could possibly also act as an adhesion molecule between platelets due to the fact that multiple thrombin molecules could bind in different poses. Further modeling suggested that GPIIb $\alpha$ -thrombin interaction could be pH dependent and that binding to the STRAPs of GPIIb $\alpha$  is likely to precede the binding of the rest of the molecule to the LRR of GPIIb $\alpha$  in a loose manner.<sup>119</sup> However, two recent publications showed that GPIIb $\alpha$  binds to thrombin in 1:1 ratio in solution and that NMR studies have demonstrated that only exosite 2 is involved.<sup>52,120</sup> Furthermore, it was confirmed in all above studies that the STRAP of GPIIb $\alpha$  was essential for binding to thrombin.

**Celikel et al, Science** 301:218, 2003 (100K)      **Dumas et al, Science** 301:222, 2003 (1P8V)

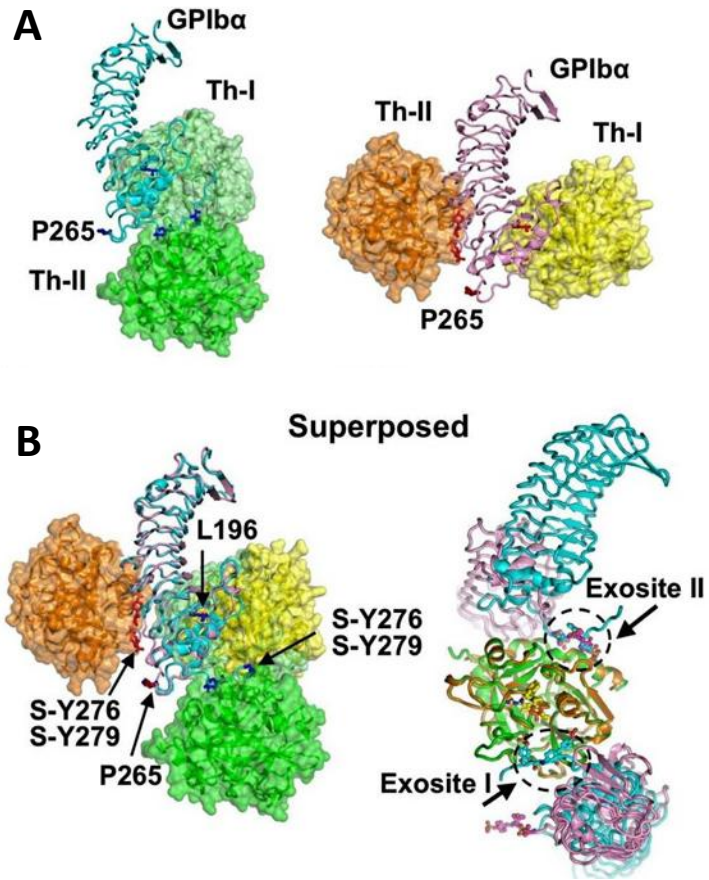


**Figure 11.** Comparison of two reported crystal structures of GPIIb/IIIa and thrombin. (A) Shows the individual crystal structures reported in PDB: 100K<sup>116</sup> and 1P8V.<sup>117</sup> (B) Shows the superimposed crystal structures showing that thrombin exosite-2 interacts in reproducible manner with the anionic peptide region of GPIIb/IIIa. Image adapted from reference 118.<sup>118</sup>

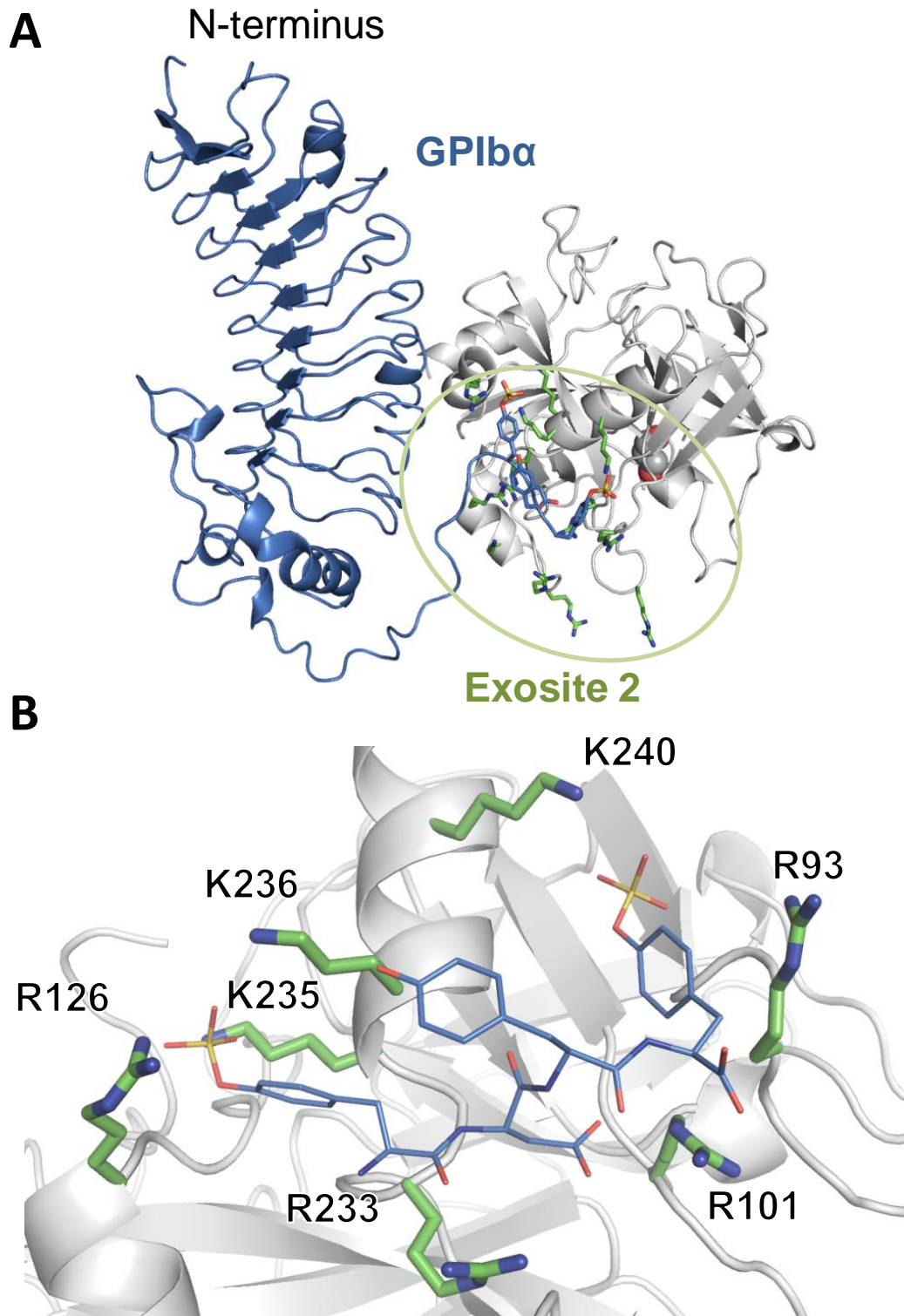


**Figure 12.** GPIb $\alpha$  interaction with thrombin exosite 2. (A) Interaction of STRAP found in GPIb $\alpha$  with exosite 2 of thrombin. (B) A closer look shows how STRAP interacts with R126, K235, K236, R233, R101, R93 and K240 of thrombin exosite 2.

The physiological consequences of binding of thrombin to GPIIb/IIIa are diverse. On one hand, binding of thrombin to GPIIb/IIIa can result in activation of platelets; a pro-thrombotic effect,<sup>121</sup> while on the other hand, GPIIb/IIIa binding to thrombin causes allosteric inhibition of thrombin's catalytic efficiency for fibrinogen cleavage, an anticoagulant effect.<sup>79,80</sup> Additionally, isolated STRAPs from GPIIb/IIIa (268-282) have been shown to bind to exosite 2 and allosterically inhibit thrombin-mediated activation of factor VIII.<sup>82</sup> Reviewing the two peptide studies above, it is possible that sulfated tyrosines could direct GPIIb/IIIa towards exosite 2 binding, while the non-sulfated forms could bind via exosite 1. Even hydrogen-deuterium exchange (HDX) studies show that exosite 2 binding of GPIIb/IIIa reduces HDX for sites distant from the binding interface suggesting long range conformational changes.<sup>120</sup>

Platelet activation by thrombin involves proteolytic and non-proteolytic mechanisms, and intact GPIIb/IIIa facilitates the platelet response to low but not high doses of thrombin.<sup>96</sup> GPIIb/IIIa acts as a cofactor for thrombin-dependent activation of PAR-1 as well as GPVI.<sup>81,122</sup> However, even active site blocked thrombin can activate platelets using GPIIb/IIIa when PAR-1 or GPIIb/IIIa is inhibited, suggesting alternate routes of thrombin-GPIIb/IIIa activation of platelets.<sup>123</sup> Such mechanisms can possibly explain why active site thrombin inhibitors and anti-platelet regimens do not completely abrogate thrombosis/restenosis in patients. Targeting the interface of the interaction could provide a more useful antithrombotic.

## 1.9 Structure and Function of Factor XIa – An Emerging Target for Prophylactic Anticoagulation

An ideal target for prophylactic anticoagulant therapy would be able to segregate hemostasis and thrombosis functions. Factor XIa (fXIa) is one such target that is believed to predominantly affect thrombus formation, rather than hemostasis. Although, the crystal structure of the entire apo-enzyme fXIa has not been resolved, there exists a crystal structure of the zymogen form of the enzyme fXI.<sup>124</sup> Additionally, there exist several crystal structures of the catalytic domains, which can help shed light on the structure of the apo-enzyme in its active conformation.

Structurally, factor XI is a unique 160kDa serine protease, which differs from vitamin-K dependent proteases in being a dimer of identical subunits (Figure 13A).<sup>125</sup> Each subunit consists of 4 apple domains (A1, A2, A3 and A4) composed of 90-91 amino acids at the N-terminus, and a trypsin-like catalytic domain (CD) at the C-terminus, which sits on top of the apple domains in a cup and saucer arrangement. The two subunits of fXI are held together by an interchain disulfide bond, Cys<sup>321</sup>-Cys<sup>321</sup>.<sup>124,126,127</sup> In the intrinsic pathway, factor XIIa (fXIIa) activates the zymogen factor XI (fXI) by catalyzing the cleavage of the peptide bond, Arg<sup>369</sup>-Ile<sup>370</sup> on each subunit. Following activation, the enzyme is believed to undergo a dramatic shape change leading to a reorientation of the structure such that the catalytic domains of the two subunits come closer together (Figure 13B).<sup>128</sup> Factor XIa has been shown to bind several biological macromolecules including high molecular weight kininogen,<sup>129</sup> thrombin,<sup>130</sup> heparin,<sup>131-134</sup> factor IX,<sup>135-137</sup> platelet glycoprotein Ib,<sup>138,139</sup> apolipoprotein E receptor 2<sup>140</sup> via allosteric sites (Figure 13C). Allosteric modulators similar to its protease counterpart thrombin could yield controlled anticoagulant therapy.

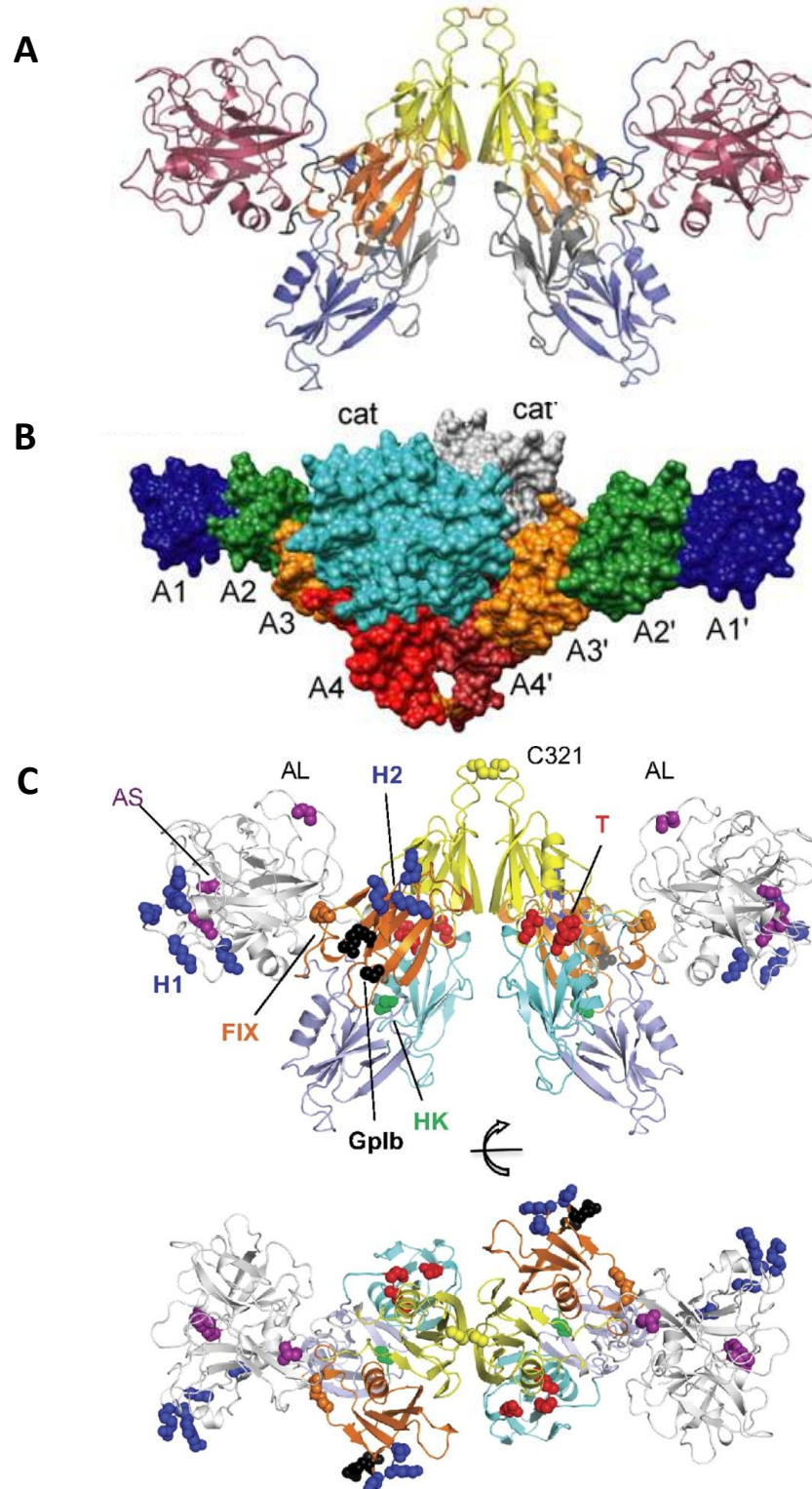


**Figure 13.** Structure of factor XI and XIa. (A) The topology of the factor XI dimer with catalytic domain colored in red, and the four apple domains (gray, blue, orange and yellow) arranged in a cup and saucer arrangement with the Cys321 disulfide bond linking the two sub-units.<sup>124</sup> (B) A

*factor XIa model created on the basis of small-angle x-ray scattering and electron microscopy data in which the two catalytic domains (cat and cat' in cyan and gray) come close to each other.<sup>128</sup> (C) The factor XI dimer from two perspectives rotated 90° highlighting the binding locations of different modulators of factor XI.<sup>126</sup> Sites for ligand binding are thrombin in red (T), high molecular weight kininogen in green (HK), GPIIb in black, heparin binding sites in blue (H1 and H2), factor IX in orange (FIX). In purple is shown the activation loop (AL) cleavage site (Arg360-Ile370) and the active site (AS) catalytic triad (Ser557, Asp462, and His413). Note: All images for this figure are taken directly from literature or corresponding supplementary information.*

Functionally, factor XIa activates factor IX (fIX), which in turn activates the downstream coagulation cascade. Thus, it ultimately contributes to the formation of a stable clot.<sup>141</sup> Apart from fXIIa, fXI can undergo autoactivation. More interestingly, it can be activated by thrombin generated in small amounts in the early stages of coagulation in a process that is independent of fXIIa.<sup>127,142</sup> In such a way, fXIa is responsible for rapidly regenerating thrombin which is essential for maintaining fibrin clot integrity, thus providing a positive feedback for coagulation.<sup>143</sup> fXIa also enhances activation of thrombin-activable fibrinolysis inhibitor (TAFI), which is known to make clots less sensitive to fibrinolysis.<sup>144</sup> Thus, targeting this upstream protease would leave the extrinsic and common pathways of the coagulation cascade intact, thereby preventing excessive bleeding.<sup>145</sup>

Several studies have confirmed fXIa is a useful target for development of prophylactic anticoagulant therapy:<sup>146</sup> for example, fXI-null mice, in comparison to wild type (WT) mice were clearly less susceptible to arterial and venous thrombosis when thrombosis was induced by

FeCl<sub>3</sub>,<sup>147</sup> or laser injury models.<sup>148</sup> This demonstrates that blocking fXIa could yield potential antithrombotic treatment. Additionally, fXI-deficient mice are healthy, thereby demonstrating that inhibition of the protease would result in safe anticoagulation.<sup>149</sup> Another study involving neutralizing antibodies against fXI have also demonstrated a reduction in thrombus formation in rabbits.<sup>150</sup> Even in humans, the natural deficiency of fXI (hemophilia C) (prominent in Ashkenazi Jews in Israel) results in a very benign bleeding phenotype compared to other hemophilia.<sup>151-154</sup> This provides strong support that fXIa inhibition could provide safe anticoagulant modality. Recent reports have also linked fXI with inflammation. Thus inhibition of fXIa could prove useful in its treatment as well.<sup>155-157</sup>

### **1.10 Current Thrombin, GPIIb/IIIa and Factor XIa Inhibitors**

The well accepted concept that inhibition of thrombin would result in efficacious anticoagulation to prevent several cardiovascular diseases has been around for more than 3 decades.<sup>158</sup> On the other hand, the concept of inhibition of GPIIb/IIIa to provide efficacious antithrombotic drugs is only surfacing recently.<sup>159</sup> This has been largely due to the fact that GPIIb/IIIa is a transmembrane protein, and technological limitations have limited the study of this target protein until recently.

Ever since heparin's discovery in 1916 by Jay Mclean, it has been a widely used antithrombotic drug.<sup>160</sup> Polymeric heparin which is a glycosaminoglycan, is the most anionic macromolecule found within the body and is highly decorated with carboxylic acid and sulfate groups (Figure 14).<sup>161</sup> It performs a number of interactions and is known to accelerate serpin-mediated inhibition of thrombin by: antithrombin, heparin cofactor II, protein C inhibitor and



protease nexin-1.<sup>162</sup> Yet full length heparin suffers from several drawbacks such as difficulty in dosing, bleeding complications and severe side effects such as heparin-induced thrombocytopenia (HIT).<sup>163</sup> Smaller versions of heparin such as low molecular weight heparin (LMWH) and heparin pentasaccharide (fondaparinux) seem to be safer. However, such smaller versions cannot participate in the bridging mechanism required to inhibit thrombin and therefore are only capable of inhibiting factor Xa.<sup>72</sup> As a consequence, subcutaneous LMWHs and fondaparinux take time to achieve anticoagulation and the therapeutic range is difficult to predict in order to treat arterial thrombosis.<sup>164</sup>

Another traditional anticoagulant, which has been used for more than 50 years is warfarin (Figure 14).<sup>165</sup> Mechanistically, warfarin acts as an inhibitor of vitamin K epoxide reductase enzyme, by antagonizing vitamin K. This enzyme is crucial for the generation of the  $\gamma$ -carboxyglutamic acid residues (GLA) which is an important post-translational modification in several proteases of the coagulation cascade including thrombin. The GLA domains of coagulation proteases help anchor them on cell surface membranes.<sup>166</sup> The advantage of warfarin as a therapy is its ease of synthesis and oral bioavailability. However, warfarin therapy suffers from several food-drug as well as drug-drug interactions and can cause severe bleeding side effects. Consequently, warfarin therapy requires constant monitoring due to unpredictable pharmacokinetics and inter-patient variability.<sup>167</sup>

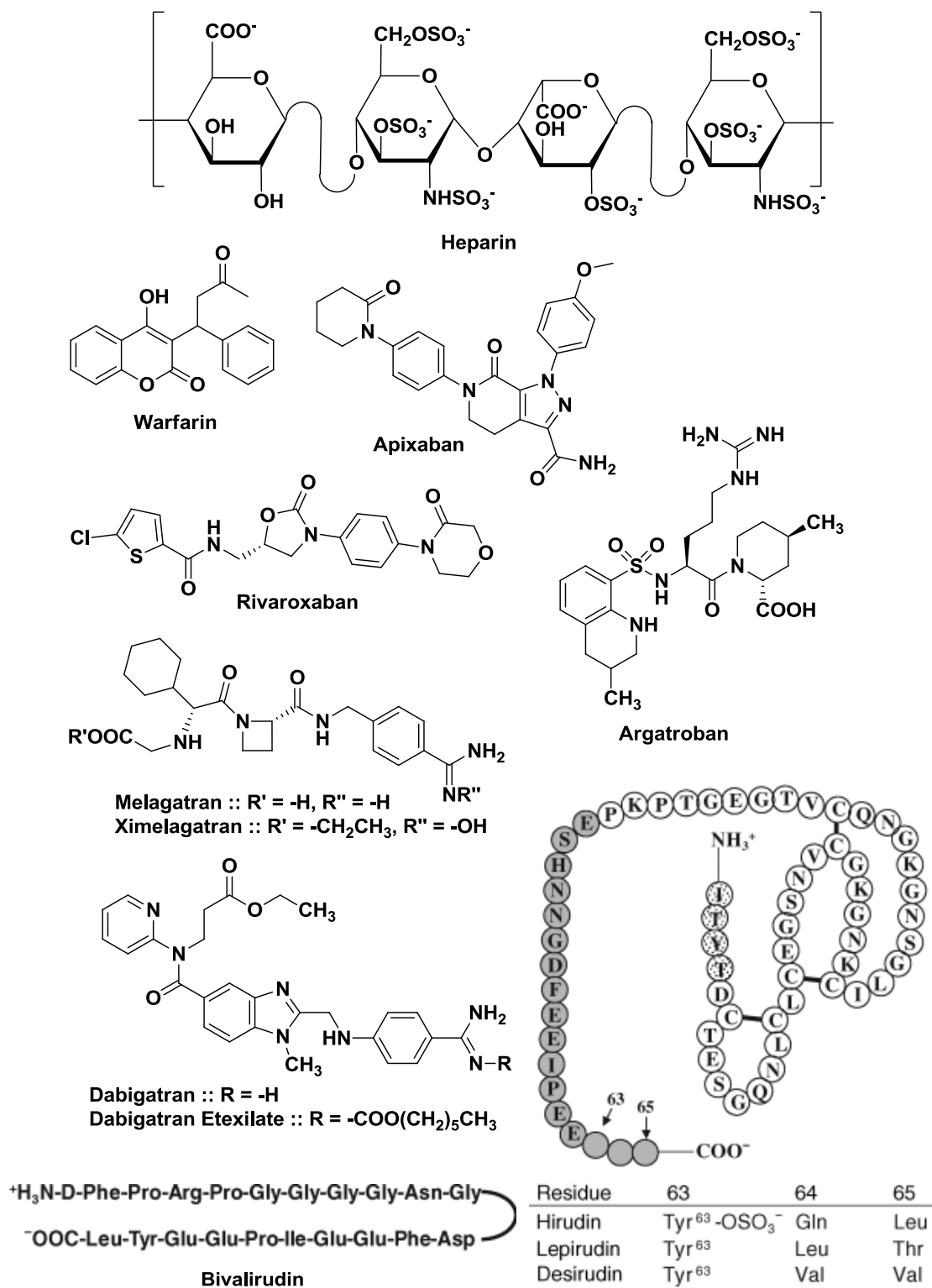


**Figure 14.** Structures of anticoagulants that have been introduced to the clinic including, heparin, warfarin, factor Xa inhibitors apixaban and rivaroxaban, thrombin inhibitors:

*argatroban, melagatran, ximelagatran, dabigatran and dabigatran etexilate, and the hirudin derivatives: hirudin, lepirudin, desirudin, and bivalirudin. The image of the hirudin derivatives is taken directly from reference 168.*<sup>168</sup>

Around two decades ago, a new class of peptide-based thrombin inhibitors was discovered from medicinal leeches, *Hirudo medicinalis*.<sup>169</sup> This peptide was called hirudin (Figure 14), and was found clinically useful in patients who suffer from heparin-induced thrombocytopenia. Hirudin inhibits thrombin by a dual binding site mechanism, where an anionic C-terminal binds to exosite 1 while the N-terminal interacts with the active site to abolish catalytic activity. This dual binding capability makes hirudin a highly specific inhibitor of thrombin ( $K_i = 20$  fM). Several derivatives of hirudin such as lepirudin, desirudin, bivalirudin were also developed and clinically used (Figure 14). Yet, being a peptide-based drug, these therapies suffered from quick proteolysis within the body and variation in clearance in patients with kidney disorders. These issues lead to dosing complications. Additionally, such molecules are difficult to produce on a large scale and are costly. Hence they can only be usefully as an alternative to UFH in patients with HIT.<sup>170</sup>

Several novel small molecule anticoagulants based on the active site inhibitors of thrombin and factor Xa have emerged in the market in the past decade (Figure 14). These include thrombin inhibitors such as argatroban, melagatran (and its prodrug ximelagatran), dabigatran (and its prodrug dabigatran etexilate); and factor Xa inhibitors like apixaban and rivaroxaban.<sup>171,172</sup> Out of these ximelagatran was taken off the shelf due to potential hepatotoxicity.<sup>173</sup> While these drugs have an improved safety profile of anticoagulant therapy,

they are still not completely devoid of bleeding complications.<sup>174</sup> This is understandable as these drugs target the active site of important coagulation proteases which results in complete knock-out of these enzyme activities. Alternatively allosteric inhibitors are gaining importance in order to modulate coagulation protease activity in a more fine-tuned manner, with possibly better safety profiles.<sup>3</sup>

In contrast to thrombin, no drug has reached the clinic which specifically targets platelet GPIIb/IIIa-protein interactions. However, targeting the platelet GPIIb/IIIa complex is thought to be a potential route for development of antithrombotic drug development.<sup>175</sup> Several antibodies, snake venom proteins, mutant thrombin molecules and peptides have been researched to bind to GPIIb/IIIa and inhibit its various physiological functions.<sup>175</sup> Such research has shown promise in in-vitro, ex-vivo and in-vivo animal models, that targeting GPIIb/IIIa can yield efficient antithrombotic without causing undue bleeding problems. However, only recently has there been any development of small molecules targeting specific protein-protein interactions involving GPIIb/IIIa, such as the GPIIb/IIIa-VWF interaction.<sup>176</sup> To date, heparin is the only clinically used drug which has been shown to prevent thrombin-mediated platelet aggregation and activation, by targeting exosite 2 of thrombin and preventing GPIIb/IIIa-thrombin interaction.<sup>177</sup>

Similarly, factor XIa also has no established clinically used drug. Yet there is significant data to support the hypothesis that targeting factor XIa would provide a useful prophylactic anticoagulant that would possibly have fewer anticoagulant side effects.<sup>145</sup>

## Chapter 2: Rationale

### 2.1. Background

The presence of thrombosis in several cardiovascular disorders stimulates an anticoagulant market which has grown to at least \$10 billion.<sup>3</sup> The anticoagulant market is dominated by the century old heparin and its derivatives. In the past decade, there has been an advent of novel active-site inhibitors of factor Xa and thrombin. Yet, there is not significant improvement of safety profiles of such drugs and long term side effects still remain questionable.

The active site of serine proteases is highly conserved among various enzymes within the body.<sup>34</sup> Due to this fact, targeting the active site specifically of a particular enzyme proves challenging and non-specific interactions could lead to long term toxicities. Such toxicity could possibly go unnoticed in short-term clinical trials. In comparison, allosteric sites on enzymes are relatively less conserved and offer a unique topographical identity, unlike active sites.<sup>97</sup> Furthermore, allosteric inhibition could possibly result in suppression of activity without complete blockage, resulting in safer anticoagulants with fewer bleeding complications. We have designed synthetic sulfated  $\beta$ -O4 lignin (SbO4L) as allosteric inhibitors of thrombin based on two elements (Figure 15):

1. Structural resemblance to chemoenzymatically synthesized lignins
2. Mechanistic resemblance to STRAP found in GPIIb $\alpha$

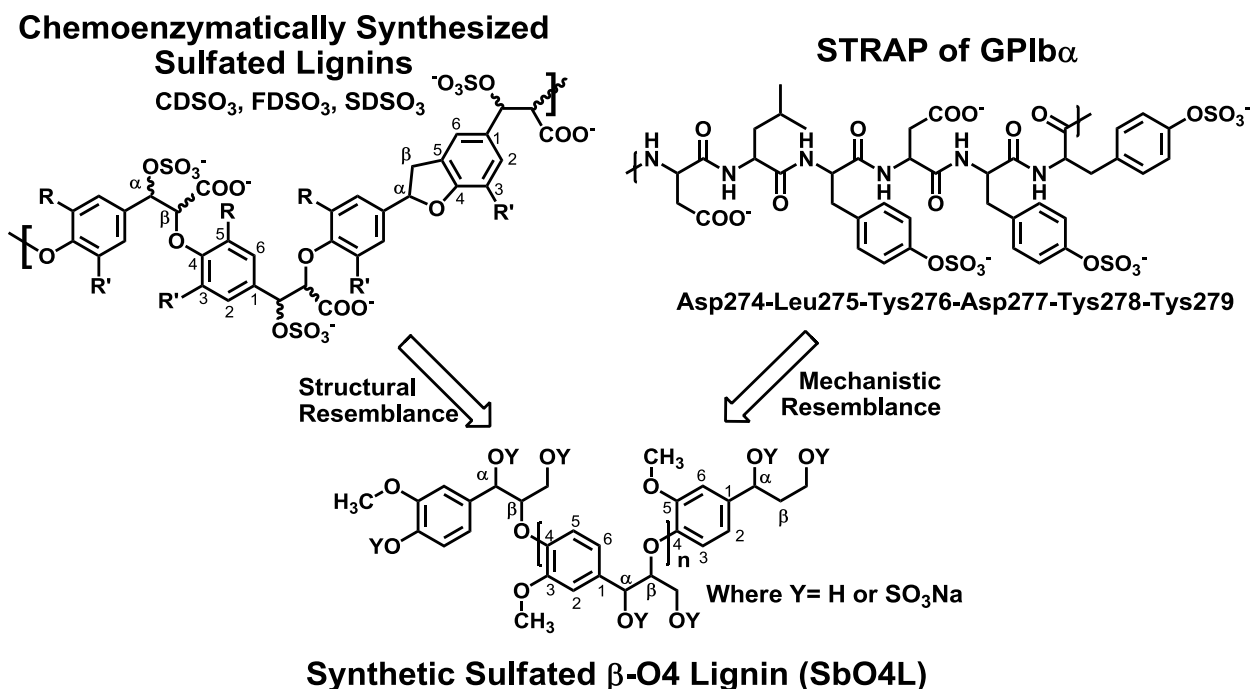


**Figure 15.** Rationale behind the creation of synthetic sulfated  $\beta$ -O4 lignin (SbO4L) polymer as a structural mimic of chemoenzymatically synthesized sulfated lignins ( $CDSO_3$ ,  $FDSO_3$ ,  $SDSO_3$ ) and mechanistic mimic of the STRAP of GPIb $\alpha$ .

## 2.2. Structural Resemblance to Direct Exosite 2 Binding Inhibitors

As seen earlier thrombin exosite 2 has been linked to modulation of active site function. Yet not all exosite 2 ligands induce a functional change in the catalytic activity of the enzyme. For example, heparin, which is the primary physiologic molecule that binds exosite 2 of thrombin, does not affect the catalytic efficiency alone, but acts as a cofactor for antithrombin III.<sup>72</sup> On the other hand, a number of physiologic ligands show modification of thrombin activity or specificity. Due to the presence of such an allosteric network, it is not impossible to fathom the probability of allosteric inhibitors of thrombin which target exosite 2 directly. In general, it is

observed that sulfated aromatic scaffolds like sulfated tyrosines are capable of inhibiting thrombin via exosite 2-mediated allosterism.

Overall, two pathways of research have emerged over the years to target thrombin exosite-2. One pathway involves the synthesis of DNA and RNA aptamers which inhibit thrombin by binding to exosite 2 of thrombin. Aptamers are small sequences of nucleic acids that are capable of binding a target protein or nucleic acid with high affinity.<sup>178</sup> Using SELEX (Systematic Evolution of Ligands by Exponential Enrichment), the first aptamer based thrombin inhibitors were obtained by Bock et al., which was a 15-mer (TBA-15).<sup>179</sup> This aptamer was found to bind at exosite 1 of thrombin.<sup>68</sup> However later, a 29-mer was identified (DNA 60-18) which binds at the heparin binding exosite 2 with 20 to 50-fold higher affinity compared to TBA-15.<sup>77</sup> The phosphate groups of the aptamers are capable of binding the electropositive residues on exosite 2 to enhance affinity, while the aromatic nature of the purines and pyrimidines can mimic the aromaticity of sulfated tyrosines to induce allosterism. Aptamer technology had gained a lot of popularity over a decade ago and had even reached Phase I clinical trials.<sup>3</sup> However, due to instability of the aptamers, the molecules have a short in vivo half-life (~2 min), requiring high doses of aptamers.<sup>180</sup> It is observed, that conformational stability of the aptamers is highly dependent on the cation it chelates.<sup>181</sup> Current research is on-going to improve aptamer stability. However, the aptamer technology remains elusive for therapeutic value and has greater potential in developing diagnostic biotechnologies in the form of nanosensors to detect levels of thrombin and other biomedical applications.<sup>181</sup>

The second approach was taken by our laboratory to mimic the sulfation patterns of heparin, while utilizing relatively hydrophobic aromatic lignins in order to induce inhibition of thrombin. The first generation lignins were synthesized utilizing chemoenzymatic methods in

order to form dehydropolymers (DHPs) of caffeic acid (CD), sinapic acid (SD) and ferulic acids (FD) using horse radish peroxidase enzyme.<sup>182</sup> Lignin synthesis via chemoenzymatic synthesis leads to heterogeneity in the intermonomeric linkages. Such synthesis yields predominantly  $\beta$ -O4 type linkage, followed by  $\beta$ 5 type linkage. These DHPs were then sulfated to give the respective sulfated lignins CDSO<sub>3</sub>, SDSO<sub>3</sub> and FDSO<sub>3</sub>. All sulfated lignins were found to be potent inhibitors of thrombin in nanomolar concentrations utilizing a direct allosteric mechanism which involves exosite 2.<sup>183</sup> Such lignins were also potent in ex vivo blood and plasma assays.<sup>184</sup> However, lack of homogeneity in intermonomeric linkage results in a mixture of diverse scaffolds, which was not specific for only thrombin inhibition, as it was found that these sulfated lignins were capable of inhibiting other heparin binding serine proteases found in the body such as plasmin, factor XIa, factor Xa, cathepsin G and human leukocyte elastase with relatively good potency in nM-range (Table 1).<sup>185,186</sup> The pursuit of identifying possible small molecule inhibitors from these parent lignins involved the exploration of selective synthesis of the  $\beta$ 5 type linkage in the synthesis of benzofuran monomers, dimers and trimers.<sup>187-189</sup> These studies revealed that exosite 2 of thrombin can be targeted using small molecules with low sulfation levels, and that there were different sub-pockets in exosite 2 which can possibly inhibit thrombin allosterically.

What was largely unexplored was the  $\beta$ -O4 type intermonomeric linkage, which is in fact, the most predominant linkage found in chemoenzymatically synthesized lignins. Hence the rationale exists that the development of a chemically synthesized, homogenous SbO<sub>4</sub>L lignin polymer would likely contain a more potent, and possibly a more selective derivative of the DHPs, which could inhibit thrombin via an exosite 2-driven allosterism.



**Table 1. Cross reactivity of chemoenzymatically synthesized lignins CDSO3, FDSO3 and SDSO3 against heparin binding serine proteases shows potent IC<sub>50</sub>.** <sup>185,186</sup>

<i>Proteases</i>	<i>CDSO3*</i>	<i>FDSO3*</i>	<i>SDSO3*</i>
<i>Cathepsin G</i>	232 ± 10	91 ± 7	105 ± 7
<i>Factor XIa</i>	22 ± 2	105 ± 11	176 ± 11
<i>HLE</i>	11 ± 2	9 ± 2	17 ± 1
<i>Factor Xa</i>	34 ± 5	74 ± 8	121 ± 26
<i>Plasmin</i>	240 ± 30	760 ± 20	1290 ± 60
<i>Thrombin</i>	18 ± 2	29 ± 2	94 ± 4

\*(all concentrations are in nM)

### 2.3. Mechanistic Resemblance Inspired from STRAP found in GPIb $\alpha$

As reviewed earlier (*Chapter 1: Introduction*), sulfated tyrosine rich anionic peptide (STRAP) region found in GPIb $\alpha$  is known to be crucial for the interaction between exosite 2 of thrombin and GPIb $\alpha$ . The physiological consequences of this interaction are both pro-thrombotic as well as anticoagulant. Thus, it would seem that nature has engineered a self check mechanism in order to control hemostatic and hemorrhaging factors utilizing this STRAP. By mimicking the STRAP using an aromatic sulfated scaffold like that found in SbO4L, we could possibly induce allosteric anticoagulant activity via inhibition of thrombin catalytic activity, while additionally obtaining a competitive antiplatelet activity by blocking the interaction of thrombin with platelet GPIb $\alpha$ . To date, no synthetic molecule has achieved this dual mechanism.

## 2.4. Questions to be answered

There are several questions which needed to be answered in a sequential and systematic manner. These are as follows:

1. Can we create a chemically synthesizable sulfated lignin with only  $\beta$ -O4 type intermonomeric linkage (SbO4L)?
2. Can such molecules induce allosteric inhibition of thrombin by binding to exosite 2?
3. Can such a molecule compete with GPIIb $\alpha$ ?
4. Will such a molecule be selective for thrombin compared to the parent sulfated lignins?
5. Will such a molecule resemble the STRAP of GPIIb $\alpha$  in its binding and allosterism mechanism?
6. Will the inhibition of thrombin translate to potent anticoagulation?
7. Will the competition with GPIIb $\alpha$  translate to potent anti-platelet effects?
8. Is the overall antithrombotic effect translatable to ex-vivo whole blood assays and in vivo in mice thrombosis assays?

These studies will not only help identify a new class of antithrombotics but also shed light on possible interplay between the coagulation and platelet aggregation/activation pathways of hemostasis. Additionally, such molecules will highlight the applicability of STRAP-mimetics to target important protein-protein interactions which could result in molecules with varying functions.

Since, the  $\beta$ -O4 type intermonomeric linkage showed greater selectivity for thrombin in our studies, we rationalized that small molecules of the  $\beta$ -5 type linkage such as the benzofuran dimers and trimers, could possibly be more potent inhibitors for other coagulation cascade proteins. In particular, factor XIa is gaining wide importance as a potential target for developing prophylactic anticoagulants that could prevent cardiovascular diseases (*as discussed in the Chapter 1: Introduction*). We therefore sought to screen and characterize the inhibition of a library of sulfated small molecules and in particular the sulfated benzofurans for factor XIa inhibition activity. We have attempted to address questions regarding its mechanism and plausible binding site via competition assays, recombinant proteins and molecular modeling.

## Chapter 3: Synthesis and Biochemical Analysis of Sulfated $\beta$ -O4 Lignin (SbO4L) Polymer

### 3.1 Introduction

Recently, our laboratory designed the first few examples of exclusively allosteric coagulation enzyme inhibitors. These include the sulfated LMW lignins and sulfated benzofurans.<sup>182-185,187,188,190</sup> Sulfated LMW lignins were originally designed to mimic the allosteric interaction of heparin with antithrombin, a key regulator of coagulation.<sup>182,191</sup> Yet, detailed studies pointed to direct inhibition of thrombin as the major mechanism of action.<sup>183,186,190</sup> Interestingly, these molecules were found to bind in the heparin-binding site of the enzyme and induce allosteric inhibition.<sup>183</sup> However, being chemo-enzymatically synthesized, these sulfated LMW lignins were polydisperse with respect to their inter monomer linkages, with various possibilities such as  $\beta$ -O4,  $\beta$ -5,  $\beta$ - $\beta$ , 5-5 and others.<sup>191</sup> As a result of this heterogeneity, they lacked selectivity and were capable of inhibiting serine proteases other than thrombin including factor Xa, factor XIa, human leucocyte elastase (HLE), plasmin, and cathepsin G (Table 1).<sup>186</sup> Hence, further anticoagulation studies were not pursued for these molecules.

We rationalized that a chemically synthesized molecule with greater homogeneity in the inter-monomeric linkage could possibly provide a more selective inhibitor. Further, such a molecule could possibly target exosite 2 in a manner similar to GPIIb/IIIa. In this work, we report on the development of a sulfated  $\beta$ -O4 lignin (SbO4L), a chemically synthesized lignin, which exhibits highly selective and potent inhibition of human thrombin and plasmin in comparison to

other serine proteases due to its homogeneity in its inter-monomeric linkages compared to parent lignins. Furthermore, SbO4L shows lower potency for thrombomodulin bound thrombin, indicating that it could be useful in directing thrombin to more anticoagulant state. SbO4L also inhibits thrombin in a mechanism which is independent of antithrombin III. It inhibits thrombin through an allosteric process by binding in exosite 2. Mutagenesis data suggests that SbO4L binds at a site similar to the GPIIb $\alpha$ -STRAP on the exosite 2 of thrombin. Additionally, SbO4L inhibition of thrombin is quantitatively and rapidly reversed by protamine. The work here demonstrates that small sulfated aromatic molecules could possibly be used to target the GPIIb $\alpha$ -STRAP binding site on the exosite 2 of thrombin for a novel mechanism of modulation of coagulation protease thrombin.

## **3.2 Experimental**

### *Materials*

Human plasma proteases, thrombin and factors Xa, IXa, XIa and VIIa, recombinant tissue factor (rTF), activated protein C, human protein C and human plasma antithrombin were from Haematologic Technologies (Essex Junction, VT). Cathepsin G, chymotrypsin, kallikrein, trypsin, pancreatic porcine elastase (PPE), protamine sulfate, recombinant human thrombomodulin, bovine serum albumin and argatroban monohydrate were obtained from Sigma Aldrich (St. Louis, MO). Recombinant glycoprotein Iba (GPIIb $\alpha$ ) was obtained from R&D Systems (Minneapolis, MN). Human leucocyte elastase (HLE) was from Elastin Products Company (Owensville, MO). Chromogenic substrates Spectrozyme TH, Spectrozyme FXa, Spectrozyme FIXa, Spectrozyme VIIa, Spectrozyme PCa, Spectrozyme PL, and Spectrozyme

CTY were obtained from Sekisui Diagnostics (Stamford, CT). Substrates N-succinyl-Ala-Ala-Pro-Phe-pNA, N-(methoxysuccinyl)-Ala-Ala-Pro-Val-pNA, and N-succinyl-Ala-Ala-Ala-pNA were obtained from Sigma Aldrich (St. Louis, MO) and S-2266, S-2222 and S-2366 were obtained from Diapharma (West Chester, OH). Stock solutions of proteins were prepared in 20 mM Tris-HCl buffer, pH 7.4, containing 100 mM NaCl, 2.5 mM CaCl<sub>2</sub>, and 0.1 % polyethylene glycol (PEG) 8000 (thrombin and factor XIa) or 20 mM sodium phosphate buffer, pH 7.4, containing 0.1 mM EDTA and 0.1% PEG8000 (factor Xa). Factor VIIa stock solutions of proteins were prepared in 25 mM HEPES buffer, pH 7.4, containing 100 mM NaCl and 5 mM CaCl<sub>2</sub>, while factor IXa stock solutions were prepared in 100 mM HEPES buffer, pH 8.0 containing 100 mM NaCl and 10 mM CaCl<sub>2</sub>. Porcine unfractionated heparin (MW 15000) was purchased from Sigma (St. Louis, MO). HirP, a Tyr63-sulfated hirudin-(54-65) peptide labeled with 5-(carboxy)fluorescein, i.e., [5F]-Hir[54-65](SO<sub>3</sub><sup>-</sup>), was a gift from the Bock laboratory at Vanderbilt University. Recombinant thrombin mutants were a gift from Dr. Alireza Rezaie (Saint Louis University, MO). All other chemicals were analytical reagent grade from either Sigma Aldrich (St. Louis, MO) or Fisher (Pittsburgh, PA) and used without further purification.

#### *Synthesis of SbO4L*

For synthetic scheme see Figure 16, Pg. 69.

**4-(tert-butyldimethylsilyloxy)-3-methoxybenzaldehyde (2):** In a 500ml round bottom flask add 20 g (1 eq) of vanillin (**1**) in 120 ml of dichloromethane. To this mixture add 45.8 ml (3 eq) of diisopropyl ethyl amine (DIPEA). Add 23.8 g (1.2 eq) of tert-butyldimethylsilane chloride (TBDMSCl). Stir overnight under nitrogen. Add 100 mL water to quench the reaction and dilute with 300 ml dichloromethane. Separate out the organic layer. Wash the aqueous layer with 500

ml x 2 dichloromethane. Collect the organic layer and dry with sodium sulfate, filter and evaporate using rotary evaporator. Perform a normal silica column by first washing with hexanes followed by a gradient elution up to 10% ethyl acetate (EtOAc) in hexanes to obtain pure compound **2** (35 g, yield = 99%).

<sup>1</sup>H-NMR (CDCl<sub>3</sub>): 9.85 (CHO) (s, 1 H), 7.39-7.40 (C2-H) (d, 1 H), 7.35-7.37 (C6-H) (m, 1 H), 6.95-6.97 (C5-H) (d, 1 H), 3.87 (-OCH<sub>3</sub>) (s, 3 H), 1.01 (TBDMS-t-butyl) (s, 9H), 0.19 (TBDMS-Me) (s, 6H).

<sup>13</sup>C-NMR (CDCl<sub>3</sub>): 190.95, 151.65, 151.35, 130.97, 126.17, 120.71, 110.18, 55.44, 25.59, 18.49, -4.56

***ethyl 3-(4-(tert-butyldimethylsilyloxy)-3-methoxyphenyl)-3-oxopropanoate (3)***: In a 500 ml round bottom flask, take 7.5 g of **2** and add a stir bar. To this add 250 ml dichloromethane. Flush nitrogen gas through the container and place on ice bath. Add 400 mg (0.05 eq) of niobium (V) chloride (NbCl<sub>5</sub>) as catalyst, which should be a fine, yellow colored powder. Seal the flask with a rubber stopper and parafilm or PTFE tape. Place a venting needle in the rubber stopper and slowly add 4.9 ml (1.4 eq) of ethyl diazoacetate solution (containing ≤ 15% dichloromethane) with care using a syringe. The reaction will effervesce vigorously for a few minutes with the release of nitrogen gas. Let the reaction mixture come to room temperature and stir for 3 hours. Monitor the reaction using TLC. Quench the reaction by adding 5 ml water and stir the flask open for 10 minutes. The solution will turn light yellow and a precipitate of NbCl<sub>5</sub> will be obtained. Filter the solution through a short pad of celite to remove the catalyst, and wash the celite pad with 2 x 200 ml dichloromethane. Add 100 ml water and extract the organic phase. Wash the aqueous layer with 2 x 200 ml dichloromethane. Collect the organic layer and dry over

sodium sulfate, filter and evaporate using rotary evaporator making sure that the temperature does not exceed 35°C. Remove any unreacted ethyl diazoacetate by evaporation on high vacuum overnight. The pure product **3** can be isolated using normal silica column with gradient elution up to 10% EtOAc in hexanes to give a pale-yellow to colorless oil (8.5 g, yield = 86%).

<sup>1</sup>H-NMR (CDCl<sub>3</sub>): 7.53 (C2-H) (d, 1 H), 7.44-7.46 (C6-H) (m, 1 H), 6.88-6.90 (C5-H) (d, 1 H), 4.19-4.25 (-OCH<sub>2</sub>CH<sub>3</sub>) (q, 2 H), 3.95 (α-CH<sub>2</sub>) (s, 2 H), 3.87 (-OCH<sub>3</sub>) (s, 3 H), 1.25-1.28 (-OCH<sub>2</sub>CH<sub>3</sub>) (t, 3 H), 1.01 (TBDMS-t-butyl) (s, 9H), 0.2 (TBDMS-Me) (s, 6H).

<sup>13</sup>C-NMR (CDCl<sub>3</sub>): 191.14, 167.73, 151.23, 150.70, 130.19, 123.16, 120.33, 111.41, 61.36, 55.47, 45.79, 25.59-25.70, 18.49, 14.08, -4.57.

**ethyl 3-(4-hydroxy-3-methoxyphenyl)-3-oxopropanoate (4)**: Take 6.3 g of **3** in a 250 ml round bottom flask and add 10 ml dimethylformamide (DMF) to it. Add 3.1 g (3 eq.) of potassium fluoride (KF) and catalytic quantity of acetic acid (0.01 ml). Stir the reaction vessel for 12 hours. Add 50 ml mildly-acidified water to quench the reaction. Extract the aqueous layer with 250 x 3 washes of ethyl acetate. Collect the organic extracts, dry over sodium sulfate and filter. Evaporate the filtrate using rotary evaporator. The product **4** is purified using normal silica column with step gradient elution up to 70% EtOAc in hexanes in 10% increments over two column volumes (3.98 g, yield = 94%).

<sup>1</sup>H-NMR (CDCl<sub>3</sub>): 7.55-7.56 (C2-H) (d, 1 H), 7.50-7.52 (C6-H) (m, 1 H), 6.95-6.98 (C5-H) (d, 1 H), 6.20 (-OH) (s, 1 H), 4.20-4.25 (-OCH<sub>2</sub>CH<sub>3</sub>) (q, 2 H), 3.96 (α-CH<sub>2</sub>) (s, 2 H), 3.95 (-OCH<sub>3</sub>) (s, 3 H), 1.25-1.29 (-OCH<sub>2</sub>CH<sub>3</sub>) (t, 3 H).

<sup>13</sup>C-NMR (CDCl<sub>3</sub>): 190.96, 167.74, 151.00, 146.80, 129.06, 124.17, 113.98, 110.11, 61.42, 56.09, 45.69, 14.08.



**ethyl 2-bromo-3-(4-hydroxy-3-methoxyphenyl)-3-oxo-propanoate (5):** In a 250 ml round bottom flask, take 1.2 g of compound 4. Place the flask on an ice bath and add 40 ml of dichloromethane and then 1.17g (1.05 eq) bromodimethylsulfonium bromide (BDMS) as a yellow powder. Stir the reaction mixture till it reaches room temperature (30 mins). Add 50 ml water and another 50 ml of dichloromethane. Separate the organic layer. Wash the aqueous layer with 3 x 50 ml dichloromethane. The collected organic layer is dried over sodium sulfate, filtered and evaporated using rotary evaporator taking care that the temperature does not exceed 35°C. The pure monomer **5** is obtained without any further purification (1.55g, yield = 97%).

<sup>1</sup>H-NMR (CDCl<sub>3</sub>): 7.58-7.60 (C2-H, C6-H) (m, 2 H) , 6.97-6.99 (C5-H) (d, 1 H), 6.23 (-OH) (s, 1 H), 5.65 (α-CHBr) (s, 1H), 4.27-4.33 (-OCH<sub>2</sub>CH<sub>3</sub>) (q, 2 H), 3.98 (-OCH<sub>3</sub>) (s, 3 H), 1.26-1.30 (-OCH<sub>2</sub>CH<sub>3</sub>) (t, 3 H).

<sup>13</sup>C-NMR (CDCl<sub>3</sub>): 186.64, 165.37, 151.51, 146.90, 126.14, 124.70, 114.12, 111.05, 63.23, 56.16, 46.20, 13.90.

**β-Keto-Ester Polymer (6):** In a flask containing the monomer **5** (0.97 g) (or other appropriate monomer) in anhydrous DMF (5 mL), anhydrous K<sub>2</sub>CO<sub>3</sub> (0.58 g) was added and stirred under nitrogen. After 24 h the reaction mixture was poured onto ice-water mixture (120 ml) and the pH adjusted to ~2.5 with 2M HCl. The precipitated polymer **6** was filtered, washed with water and lyophilized to remove moisture. (≈700 mg per reaction)

NMR characterization showed the following corresponding broad peaks for <sup>1</sup>H-NMR (DMSO-d<sub>6</sub>): 7.46-7.78 (C2-H and C5-H), 6.91-7.14 (Cβ-H), 6.52-6.66 (C6-H), 4.19-4.20 (-OCH<sub>2</sub>CH<sub>3</sub>), 3.79-3.81 (-OCH<sub>3</sub>), 1.12-1.22 (-OCH<sub>2</sub>CH<sub>3</sub>).

$^{13}\text{C}$ -NMR (DMSO- $d_6$ ) 188.53, 189.08 ( $\text{C}\alpha$ ), 165.81, 166.02 ( $\text{C}\gamma$ ), 153.16, 150.93, 149.48, 149.01, 147.64, 128.33, 125.51, 124.75, 123.73, 115.17, 114.08, 113.91, 113.09, 112.51, 112.30 (aromatic carbons), 78.54, 78.37 ( $\text{C}\beta$ ), 61.80, 61.67 (-OCH<sub>2</sub>CH<sub>3</sub>), 55.78, 55.58 (-OCH<sub>3</sub>), 13.77 (-OCH<sub>2</sub>CH<sub>3</sub>).

**Reduced Polymer (7):** 600 mg of solid **6** was suspended in methanol (10 ml) followed by careful addition of NaBH<sub>4</sub> (683 mg). The mixture was gradually heated to 50°C as it turned clear, and was stirred for 24 h. The solution was then neutralized with acetic acid and poured into 0.5M HCl (200 mL) to precipitate the reduced crude polymer **7**, which was isolated by filtration through sintered glass funnel, washed with water and lyophilized overnight. Dissolution and preferential precipitation using 1,4-dioxane and diethyl ether helped remove low molecular weight chains of the polymer and precipitate the high molecular weight chains. The precipitated pure reduced polymer **7** was filtered and dried using vacuum. ( $\approx$ 150 mg per reaction)

NMR characterization showed the following corresponding broad peaks for  $^1\text{H}$ -NMR (DMSO- $d_6$ ): 4.75 ( $\text{C}\alpha$ -H), 4.28 ( $\text{C}\beta$ -H), 3.20-3.71 ( $\text{C}\gamma$ -H and -OCH<sub>3</sub>), 7.02 ( $\text{C}2$ -H), 6.94 ( $\text{C}5$ -H), 6.85 ( $\text{C}6$ -H).

$^{13}\text{C}$ -NMR (DMSO- $d_6$ ): 70.8, 71.4 ( $\text{C}\alpha$ ), 83.6, 84.4 ( $\text{C}\beta$ ), 59.8, 59.9 ( $\text{C}\gamma$ ), 55.4 (-OCH<sub>3</sub>), 134.7-135.0 ( $\text{C}1$ ), 111.3-111.7 ( $\text{C}2$ ), 148.9 ( $\text{C}3$ ), 146.7-147.0 ( $\text{C}4$ ), 114.5-115.0 ( $\text{C}5$ ), 119.4-119.7 ( $\text{C}6$ ).

**SbO<sub>4</sub>L:** 50 mg of the reduced polymer **7**, so obtained was made to react with triethylamine-sulfur trioxide complex (600 mg) in anhydrous DMF (5 ml) at 65 °C for 24 h under reflux with nitrogen. Following the reaction, 30% (w/v) aqueous sodium acetate (35 ml) was added and the mixture stirred overnight to exchange the counter-ions of the sulfate groups. The solution was

then poured into ice-cold ethanol (100 ml) to precipitate crude **SbO4L**, which was filtered and washed twice with ice-cold ethanol (10 ml each) to remove any unreacted polymer. The recovered solid was desalted using FloatALyzer G2 (Spectrum Labs) dialysis tubes (MWCO 0.1-0.5 KDa) or using ultra-filtration membrane (Ultracel YM1, NMWL 1,000 Da) with a stirred cell under nitrogen at 30 psi (Millipore). Lyophilization of the retentate solution gave **SbO4L**. ( $\approx$ 100mg per reaction)

NMR characterization showed the following corresponding broad peaks for  $^1\text{H-NMR}$  (DMSO- $d_6$ ): 6.77 (aromatic protons), 3.47-4.27 ( $\text{C}\alpha\text{-H}$ ,  $\text{C}\beta\text{-H}$ ,  $\text{C}\gamma\text{-H}$ ,  $-\text{OCH}_3$ ).

Elemental Analysis of SbO4L was carried out by Atlantic Mircolabs (Norcross, GA). Anal. Calcd. for 22-mer SbO4L with 27 sulfate groups and associated with 24 waters is: C, 35.20; H, 3.85; S, 11.53. Found: C, 35.39; H, 4.15; S 11.54.

$^{13}\text{C-NMR}$  could not give sufficient signal even at high concentrations of the sample, possibly due to the presence of a wide variety of sulfation patterns and molecules of different chain lengths. Extensive characterization of SbO4L was therefore carried out using size exclusion chromatography and reversed-phase ion-pairing chromatography as described below.

#### *Size Exclusion Chromatography of SbO4L*

Size exclusion chromatography (SEC) was used to assess the molecular weight of the synthesized SbO4L. For SEC analysis the Asahipak GS320 HQ column (Shodex, New York, NY) was used with an isocratic flow rate of 0.7 mL/min of 0.1 N NaOH at pH 11.0. The wavelengths of 280nm were used to detect the eluted polymer. Polystyrene sulfonate (PSS)

standards were used for calibration purposes. The relationship between log of the molecular weight and the elution volume (V) of the standards was linear with a R<sup>2</sup> of 0.98. The chromatograms obtained were sliced into 1000 time periods providing the M<sub>R</sub> for each period and the corresponding intensity of absorbance (A) as the number of polymeric species with the particular M<sub>R</sub>. These values were then utilized to calculate the number average molecular weights (M<sub>N</sub>) and the weight average molecular weight (M<sub>W</sub>) and the polydispersity (P) using the following equations:

$$M_N = \frac{\sum A_i \times M_{Ri}}{\sum A_i} \quad (\text{Eq. 1})$$

$$M_W = \frac{\sum A_i \times M_{Ri}^2}{\sum A_i \times M_{Ri}} \quad (\text{Eq. 2})$$

$$P = \frac{M_W}{M_N} \quad (\text{Eq. 3})$$

The peak molecular weight (M<sub>P</sub>) was calculated from extrapolation in the equation obtained from the plot of log M<sub>W</sub> of PSS standards vs elution volume.

#### *Reversed-Phase Ion-Pairing (RPIP) UPLC-MS*

Three different batches of SbO<sub>4</sub>L synthesized were tested for similarity using a method of RPIP-UPLC-MS which was adapted from previous report.<sup>192</sup> Briefly, a Waters Acquity H-class UPLC system equipped with a PDA detector and a tandem quadrupole (TQD) mass spectrometer was used. A 1.7 μm BEH C18 column (2.1 mm X 150 mm) was used for fingerprinting, which required 5 μl injection of SbO<sub>4</sub>L (400 μg/mL) at 30 ± 2 °C and a solvent system composed of 10% v/v acetonitrile-water (solvent A) and 75% v/v acetonitrile-water (solvent B). Both solvents

contained n-hexylamine (25 mM) as an ion-pairing agent along with acid modifier formic acid (0.1%). Resolution of SbO4L was achieved using a linear gradient from 0% to 100% solvent B in 40 mins. Absorbance was monitored from 230-400 nm and the eluent was directly injected into the mass spectrometer. ESI-MS detection conditions utilized positive ion mode with capillary voltage of 4kV, cone voltage of 20 V, desolvation temperature of 350 °C and nitrogen gas flow rate of 650 L/h. Mass scans were collected in the range of 500-2048 m/z within 0.6 s to obtain the UPLC-MS fingerprints.

#### *Direct Inhibition of Enzymes of the Coagulation Cascade*

Inhibition of various coagulation cascade enzymes like thrombin, factors Xa, IXa, XIa and VIIa by SbO4L was characterized using chromogenic substrate hydrolysis assays, as described previously in literature.<sup>183,186</sup> Briefly, a 10 µl aqueous solution of SbO4L was diluted with 930 µl of an appropriate buffer in PEG20000-coated polystyrene cuvette. Plasmin, recombinant tissue factor – factor VIIa inhibition was studied in a 96-well microplate format, as described below in the section on heparin-binding serine proteases, except for measuring the activity over the full range of SbO4L concentrations. The buffers used in these experiments were as follows: 20 mM Tris-HCl buffer, pH 7.4, containing 100 mM NaCl, 2.5 mM CaCl<sub>2</sub> and 0.1 % PEG8000 for thrombin, factor Xa and factor XIa; 100 mM HEPES buffer, pH 8, containing 100 mM NaCl and 10 mM CaCl<sub>2</sub> for factor IXa; 25 mM HEPES buffer, pH 7.4, containing 100 mM NaCl and 5 mM CaCl<sub>2</sub> for factor VIIa and factor VIIa–tissue factor complex; and 50 mM Tris-HCl, 150 mM NaCl and 0.1% PEG8000, pH 7.4 for plasmin. This was followed by addition of a 10 µl solution of the protease (stock concentrations used: 600 nM thrombin, 108 nM factor Xa, 152 nM factor

XIa, 22.5  $\mu$ M factor IXa, 4  $\mu$ M factor VIIa). The enzyme and inhibitor were incubated at 37°C for 10 minutes. In case of fVIIa–tissue factor complex, 10 $\mu$ l of 1:1 mixture of 266 nM factor VIIa and 800 nM recombinant tissue factor was added as a complex. Following incubation, a 50  $\mu$ l (or 5  $\mu$ l in case of plasmin and recombinant tissue factor-VIIa assay) solution of chromogenic substrate was rapidly added and the residual enzyme activity was measured from the initial rate of increase in A405. The chromogenic substrates used were Spectrozyme TH (H-D-hexahydrotyrosol-Ala-Arg-p-nitroanilide), Spectrozyme FXa (methoxycarbonyl-D-cyclohexylglycyl-Gyl-Arg-p-nitroanilide), Spectrozyme FIXa (D-Leu-Phe-Gly-Arg-p-nitroanilide), Spectrozyme FVIIa (methanesulphonyl-D-cyclohexylalanyl-butyl-Arg-p-nitroanilide), Spectrozyme PL (H-D-norleucyl-hexahydrotyrosol-lysine-para-nitroanilide). Inhibition of factor XIa was studied using Spectrozyme FXa. Relative residual proteinase activity at each concentration was calculated using the activity measured under otherwise identical conditions, except for the absence of SbO4L. The IC<sub>50</sub> was calculated from the regression analysis using logistic equation 4.

$$Y = Y_0 + \frac{Y_M - Y_0}{1 + 10^{((\log[SbO4L]_0 - \log IC_{50}) \times HS)}} \quad (\text{Eq. 4})$$

In this equation Y is the fractional residual protease activity, i.e., the ratio of protease activity in the presence of inhibitor to that in its absence; Y<sub>M</sub> and Y<sub>0</sub> are the maximum and minimum fractional residual activities, respectively; IC<sub>50</sub> is the concentration of the inhibitor that results in 50% inhibition of enzyme activity; and HS is the Hill slope.

### *Inhibition of Other Heparin-Binding Serine Proteases*

Being highly sulfated, it is important to check if SbO4L can inhibit other proteases by mimicking heparin. The direct inhibition of other heparin binding serine proteases was tested against SbO4L using the chromogenic substrate hydrolysis assay (similar to above) using a 96-well microplate format with conditions adapted from previous literature.<sup>186</sup> Briefly, 5  $\mu$ l of SbO4L (1.62mg/ml) was diluted with 85  $\mu$ L of an appropriate buffer at either room temperature or 37°C followed by addition of 5  $\mu$ l of the protease solution and incubation for 5 min. The activity of the protease was assessed by addition of 5  $\mu$ l of chromogenic substrate and measuring the initial rate of increase in the absorbance at 405nm (<10% substrate consumption). The optimal assay conditions for the heparin-binding serine proteases were as follows: 50 mM Tris-HCl, 50 mM NaCl, pH 8.0, at room temperature for cathepsin G and Human Leukocyte Elastase (HLE); 20 mM Tris-HCl, 150 mM NaCl, 2 mM CaCl<sub>2</sub> and 0.1% PEG8000, pH 7.5, at 37°C for Porcine Pancreatic Elastase (PPE) and kallikrein; 50 mM Tris-HCl, 125 mM NaCl and 10 mM CaCl<sub>2</sub>, pH 8.0, at 37°C for activated protein C (APC); and 50 mM Tris-HCl, 150 mM NaCl and 0.1% PEG8000, pH 7.4, at 37°C for trypsin and chymotrypsin. The enzyme concentrations used in these experiments were 200 nM cathepsin G, 1  $\mu$ g/ml HLE, 0.005 U/ml kallikrein, 0.0125 U/ml PPE, 7 nM APC, 0.5  $\mu$ g/ml chymotrypsin and 0.145  $\mu$ g/ml trypsin. Chromogenic substrates used were 1 mM N-succinyl-Ala-Ala-Pro-Phe-pNA (cathepsin G); 100  $\mu$ M N-(methoxysuccinyl)-Ala-Ala-Pro-Val-pNA (HLE); 50  $\mu$ M H-D-Val-Leu-Arg-pNA (S-2266) (kallikrein), 100  $\mu$ M N-succinyl-Ala-Ala-Ala-pNA (PPE); 200  $\mu$ M H-d-( $\gamma$ -carboboxy)-Lys-Pro-Arg-pNA (Spectrozyme PCa) (APC); 160  $\mu$ M N-benzoyl-Ile-Glu(-OR)-Gly-Arg-pNA (S-2222) (trypsin) and 250  $\mu$ M H-D-Ala-Pro-Phe-pNA (Spectrozyme CTY) (chymotrypsin). The percent residual activity of the enzyme in the presence of the inhibitor with respect to control of no inhibitor was

calculated from the initial velocity of the enzyme measured as the increase in the absorbance at 405nm as a function of time. Each assay was performed in duplicate.

#### *Effect of SbO4L on Antithrombin III Inhibition*

SbO4L inhibition of thrombin in the presence and absence of antithrombin III (ATIII) was performed using a 96-well microplate assay that was adapted from previous reports.<sup>182</sup> Briefly, in 180  $\mu$ l of 20 mM Tris-HCl buffer, pH 7.4, containing 100 mM NaCl, 2.5 mM CaCl<sub>2</sub> and 0.1% PEG8000 a 5  $\mu$ l aqueous solution of SbO4L was added. This was followed by addition of 5  $\mu$ l of thrombin to give a final concentration of 6 nM and 5  $\mu$ l of antithrombin to give final concentration of 200 nM ATIII in each well. The mixture was incubated at 37°C for 10 min followed by addition of 5  $\mu$ l of 5 mM Spectrozyme TH. The residual enzyme activity was determined from the initial rate of increase in absorbance at 405 nm. The apparent IC<sub>50</sub> was calculated using logistic equation 4 along with other inhibition parameters such as Y<sub>M</sub>, Y<sub>0</sub> and HS.

#### *Inhibition of Activation of Protein C by Thrombin-Thrombomodulin Complex in the presence of SbO4L*

The protocol for measuring the activation of protein C by thrombin–thrombomodulin (TH-TM) complex was adapted to a 96-well format from the literature.<sup>193</sup> Briefly, in 70  $\mu$ l of 50 mM Tris-HCl buffer, pH 7.4, containing 100 mM NaCl, and 1 mM CaCl<sub>2</sub>, 5  $\mu$ l of SbO4L was added at concentrations ranging from 2.3 ng/ml to 2.3 mg/ml at 37°C, followed by addition of 5  $\mu$ l of



thrombin (240 nM) and 5  $\mu$ l of TM (400 nM). The mixture was incubated for 10 min and 5  $\mu$ l of protein C (10  $\mu$ M) added and incubated at 37°C for another 10 min. After this period, further generation of activated protein C (APC) was quenched by the addition of 5  $\mu$ l mixture of 10 mM EDTA and 16  $\mu$ M argatroban ( $\approx 20 \times K_i$ ). The APC generated was quantified from the initial rate of chromogenic substrate hydrolysis of 400  $\mu$ M S-2366. The percent activation of protein C was calculated from initial rate in the presence and absence of SbO4L and the apparent  $IC_{50}$  was calculated in a similar manner using equation 4.

#### *Variation of SbO4L Inhibition on Various Types of Thrombins*

In order to establish inter-species variability in the inhibitory potential of SbO4L and efficacy against thrombin degradation enzymes, chromogenic substrate hydrolysis assays were performed on human, mouse, bovine and gamma thrombin using a 96-well microplate format. Briefly, 5 $\mu$ L of either water or SbO4L at concentrations ranging from 2.3 ng/ml to 2.3 mg/ml was diluted with 185 $\mu$ L of 20mM Tris-HCl buffer, pH 7.4, containing 100mM NaCl, 2.5mM CaCl<sub>2</sub>, and 0.1% PEG 8000 in a 96-well polystyrene microplate at 37°C. To this was added 5 $\mu$ L of thrombin to give 6nM of the different thrombin in separate series. The solution was incubated for 10 minutes, following which 5 $\mu$ L of 5mM chromogenic substrate Spectrozyme TH was added. The residual activity of thrombin was determined by monitoring the initial rate of product formation at 405 nm wavelength. The percent residual activity and the  $IC_{50}$  was determined using logistic equation 4.

### *Fibrinogen Assay*

To test if SbO4L was active against physiologically relevant substrate fibrinogen, the following microplate assay was performed. Briefly, in 35  $\mu\text{L}$  of buffer (20mM TrisHCl, 100mM NaCl, 2.5mM  $\text{CaCl}_2$  0.1% PEG8000, pH 7.4), 10  $\mu\text{L}$  of thrombin (300nM) was added along with either 5 $\mu\text{L}$  of water as control or SbO4L at concentrations ranging from 2.3 $\mu\text{g}/\text{ml}$  to 5.6 mg/ml. The mixture was incubated for 10 minutes at 37°C, after which 10  $\mu\text{L}$  of this reaction was added to 140  $\mu\text{L}$  of 250 nM of fibrinogen. The formation of fibrin mesh was observed as absorbance at 600 nm for the first 100 seconds after initiation of the reaction. The slope was used to get the rate of enzyme activity towards fibrinogen cleaving activity. The percent residual activity and  $\text{IC}_{50}$  were calculated in a manner similar to that done for the peptide chromogenic substrate reactions using equation 4.

### *Michaelis Menten Kinetics*

To assess the nature of the inhibition of thrombin by SbO4L Michaelis-Menten kinetics experiments were performed in the presence of various concentrations of the inhibitor using previously reported protocols.<sup>183,188,189</sup> The initial rate of Spectrozyme TH hydrolysis by 3 nM thrombin was monitored from the linear increase in absorbance at 405 nm corresponding to less than 10% consumption of the substrate. The initial rate was measured as a function of substrate concentrations (0.6 to 20  $\mu\text{M}$ ) in the presence of a fixed concentration of SbO4L (0–2.3  $\mu\text{g}/\text{ml}$ ) in 20 mM Tris-HCl buffer, pH 7.4, containing 100 mM NaCl, 2.5 mM  $\text{CaCl}_2$  and 0.1 % PEG8000 at 25°C in a cuvette. Standard Michaelis-Menten equation was used to calculate  $K_M$  and  $V_{MAX}$  (Eq. 5).

$$v = \frac{V_{MAX}[S]}{K_M + [S]} \quad (\text{Eq. 5})$$

*Competition with Heparin, Hirugen Peptide and recombinant GPIIb*

SbO4L-dependent thrombin inhibition studies in the presence of competitors were performed as described earlier.<sup>183</sup> SbO4L (0–23 µg/ml) was incubated with either HirP (0 – 86 nM) or porcine UFH (0–100 µM) and thrombin (5 nM) in 20 mM Tris-HCl buffer, pH 7.4, containing 100 mM NaCl, 2.5 mM CaCl<sub>2</sub> and 0.1 % PEG 8000 at 25°C in PEG20000-coated polystyrene cuvettes for 10 minutes. For competition with GPIIb, SbO4L (0-1mg/ml) was incubated with GPIIb (0-458nM) and thrombin (6 nM) in 10mM HEPES buffer with 10mM Tris-HCl, pH 7.8 containing 100mM NaCl and 0.1% PEG 8000 in 96-well plate for 10 minutes. Following incubation, Spectrozyme TH (100 µM) was added and the initial rate of 405 nm absorbance change was measured. The dose-dependence of the fractional residual protease activity at each concentration of the competitor was fitted by equation 1 to calculate the  $IC_{50,app}$  of inhibition. The molecular weight of porcine UFH was assumed to be 15,000, while its affinity was measured earlier in the laboratory (15.6±3.1 µM).<sup>183</sup>

To quantify the degree of competition of SbO4L with its competitors, the Dixon-Webb relationship was used to calculate the apparent  $IC_{50,app}$  of the inhibitor in the presence of a competitor with known affinity ( $K_{competitor}$ ).<sup>183,190</sup> The equation is given as:

$$IC_{50,app.} = IC_{50,Obs.} \times \left[ 1 + \frac{[Competitor]}{K_{Competitor}} \right] \quad (\text{Eq. 6})$$

### *Mutagenesis Studies*

To localize the important residues for binding of SbO4L in the exosite 2 of thrombin, SbO4L inhibition of various thrombin mutants was performed. The  $IC_{50}$  of SbO4L against recombinant mutants of thrombin was measured using the chromogenic hydrolysis assay in a 96-well format. In general, SbO4L (0-2 mg/ml) was incubated with individual mutants of thrombin (6 nM) in a 20 mM Tris-HCl buffer containing 100 mM NaCl, 2.5 mM  $CaCl_2$ , 0.1% PEG 8000 at a pH 7.4 for 10 minutes. Following this, substrate Spectrozyme TH (100  $\mu$ M) was added to the reaction and the initial rate of increase in absorbance at 405nm was measured. The rate of initial hydrolysis was used to calculate residual thrombin activity, which was used to calculate the  $IC_{50}$  from equation 4.

### *Probing Allosteric Change in Active Site using Quenching*

Accessibility of the active site in the presence of SbO4L can be probed using a labeled enzyme and a collisional quencher.<sup>194</sup> 199  $\mu$ L of buffer containing 20 mM Tris HCl, 100mM NaCl, 2.5 mM  $CaCl_2$ , 0.1% PEG 8000 at pH 7.4 was taken in a quartz cuvette. To this was added 1  $\mu$ L of  $\beta$ FPR-Thrombin such that the final concentration of the enzyme was 170 nM. 3  $\mu$ L of either water or 3mg/mL SbO4L was added. The fluorescence intensity was monitored using a QM4 fluorometer (Photon Technology International, Birmingham, NJ) which was thermostated with a water bath at 25°C using excitation and emission wavelengths of 490 nm and 522 nm respectively, with slit-widths of 4nm each. The solutions were titrated with increasing concentrations of the quencher acrylamide (stock of 10 M with 1  $\mu$ L additions) and the fluorescence intensity monitored after each addition.

The ratio of the fluorescence without the quencher ( $F_0$ ) to the fluorescence in the presence of various concentrations of the quencher ( $F$ ) can be plotted against the quencher concentration ( $Q$ ) to yield a linear relationship which can fit the Stern-Volmer relationship<sup>194</sup>:

$$\frac{F_0}{F} = 1 + k_q\tau_0[Q] = 1 + K_{SV}[Q] \quad (\text{Eq. 7})$$

Where  $k_q$  is the bimolecular quenching constant,  $\tau_0$  is the fluorophore lifetime in the absence of the quencher and  $Q$  is the concentration of the quencher.  $K_{SV}$  in this case is the Stern-Volmer constant and is equal to  $k_q\tau_0$ .

#### *Quantitating Number of Ionic Interactions Involved by Salt Dependence Studies on Affinity*

To study the salt dependence of SbO4L interaction with thrombin, a fluorescence binding study was carried out using buffers having different concentrations of sodium chloride. Briefly, in 199  $\mu\text{L}$  of buffer containing 20 mM Tris HCl, 2.5 mM  $\text{CaCl}_2$ , 0.1% PEG 8000 at pH 7.4 containing various concentrations of NaCl (100-200 mM), 1  $\mu\text{L}$  of fFPR-Thrombin was added, to give a final concentration of 170 nM in the quartz cuvette. The experiments were performed using a QM4 fluorometer (Photon Technology International, Birmingham, NJ) which was thermostated with a water bath at 25°C. The mixture was then titrated with SbO4L and the decrease in fluorescence was monitored using excitation and emission wavelengths of 490 nm and 522 nm respectively, with slit widths of 4nm each. The decrease in fluorescence signal was fit to a quadratic equation to obtain the dissociation constant at various concentrations of salt:

$$\frac{\Delta F}{F_0} = \frac{\Delta F_{MAX}}{F_0} \left\{ \frac{[E]_0 + [SbO4L]_0 + K_D - \sqrt{([E]_0 + [SbO4L]_0 + K_D)^2 - 4[E]_0[SbO4L]_0}}{2[E]_0} \right\} \quad (\text{Eq. 8})$$

Where,  $\Delta F$  represents the change in fluorescence of fFPR-Thrombin at each addition of SbO4L from the initial fluorescence  $F_0$ .  $\Delta F_{MAX}$  represents the maximal change in fluorescence observed when the enzyme is saturated with the inhibitor.  $[E]_0$  is the enzyme concentration which is a constant for the experiment, while  $[SbO4L]_0$  is the concentration of the inhibitor during the titration.  $K_D$  is the dissociation constant of the complex.

The dissociation constant ( $K_D$ ) so obtained was further expressed as a linear function of the salt concentration according to the expression:

$$-\log K_D = A_0 + \Gamma_{salt} \log [salt] \quad (\text{Eq. 9})$$

The slope of the line yields  $\Gamma_{salt}$  which represents a thermodynamic measure of the effect of salt concentration on binding equilibria, which can be compared with other exosite binding ligands.

#### *Reversal of SbO4L Mediated Thrombin Inhibition by Protamine*

To test whether SbO4L inhibition of thrombin can be reversed by protamine, a solution of SbO4L (575 ng/ml) along with thrombin (6nM) in a 20 mM Tris-HCl buffer, pH 7.4, containing 100 mM NaCl, 2.5 mM CaCl<sub>2</sub> and 0.1% PEG8000 at 37°C was gradually titrated with protamine (4.9 ng/ml to 14.8 mg/ml) such that the final volume was 195  $\mu$ l. The solution was incubated for 10 minutes followed by addition of 5  $\mu$ l of Spectrozyme TH (5 mM) and the increase in absorbance at 405 nm observed. In the absence of protamine, SbO4L gave ~50% inhibition of thrombin at 37°C. Protamine alone did not affect the activity of thrombin as assessed by appropriate controls. The sigmoidal gain in thrombin activity could be fitted by the equation 4 to

obtain the effective concentration of protamine necessary to recover thrombin from SbO4L inhibition by 50%.

### 3.3 Results

#### *Synthesis of SbO4L*

The synthesis of SbO4L was accomplished using a 7-step synthetic protocol starting from commercially available vanillin (**1**). The key to the formation of the  $\beta$ -O4 lignin **7** is in the formation of reactive monomer **5**. The synthesis of monomer **5** was previously reported,<sup>195</sup> however, the strategy was not reproducible and often yielded lower yields than reported. This was largely due to the fact that the deprotection of the benzyl group involved palladium-catalyzed hydrogenation which also resulted in the reduction of the  $\alpha$ -keto to an alcohol. This resulted in lower overall yield. Additionally, the  $\beta$ -alcohol ester side product was rendered less reactive for bromination at the  $\alpha$ -position, and therefore could not be used further. As a result we developed a novel strategy for synthesis using TBDMS protection (Figure 16).

TBDMS protection of vanillin afforded compound **2** in almost quantitative yields at a large scale (>20 g). Synthesis of  $\beta$ -keto ester from aldehydes was reported earlier for vanillin derivatives with benzyl protecting group as a two step process using reactive reagents such as diethyl aluminium.<sup>195</sup> Alternatively, the paper also proposed the synthesis of beta-ketoester in a single step from acetovanillone using sodium hydride and ethyl carbonate. Such reactions could not work with TBDMS protection. Hence we adapted a milder method utilizing niobium (V)

chloride and ethyldiazoacetate.<sup>196</sup> The reaction had to be optimized for use with TBDMS protecting group with a reduction in temperature while addition of ethyldiazoacetate to prevent deprotection and other side reactions due to the heat generated from the reaction. This method produced the beta-ketoester **3** on a sufficiently large scale (>7 g) with good yield.

Deprotection of the TBDMS group was then performed using potassium fluoride with catalytic quantities of acetic acid to produce **4** in good yields and scale (> 3 g). Bromination was previously reported to have been performed using elemental bromine.<sup>195</sup> Use of elemental bromine requires special care as it is highly toxic. Furthermore, handling of the reagent and weighing can be difficult. As a result, one can often get higher orders of bromination or incomplete reactions. We therefore explored an alternative to synthesize the  $\alpha$ -bromo. Selective mono-bromination at the  $\alpha$ -position of the  $\beta$ -keto ester was performed with the use of bromodimethyl sulfonium bromide (BDMS) reagent.<sup>197</sup> BDMS reagent can be freshly prepared to yield a yellow powder which can be easily handled. This reaction was surprisingly very clean and the product **5** formed required no purification apart from simple aqueous work up. Since  $\alpha$ -bromo- $\beta$ -keto esters are reactive and susceptible to degradation, fresh monomer **5** was produced every time prior to polymerization.

Polymerization of **5** using  $K_2CO_3$  to form **6** and its subsequent reduction using  $NaBH_4$  to form the  $\beta$ -O4 lignin **7** was performed using methods previously described.<sup>198,199</sup> While the polymerization step gave good yields, reduction and subsequent purification to form **7** showed some loss of compound due to separation of lower molecular weight species from the polymer by precipitation. The NMR of the products obtained for these two steps matched well with the literature records.<sup>198,199</sup> A final step of sulfation was adapted from the sulfation methodologies used to create the chemoenzymatically synthesized lignins.<sup>182,183</sup> The  $\beta$ -O4 lignin polymer was



reacted with sulfating agent following which the counterion on the sulfated polymer was exchanged using sodium acetate resulting in a highly water soluble polymer which could be purified by precipitation (with ethanol) and dialysis/ultrafiltration to afford purified SbO<sub>4</sub>L. NMR characterization of SbO<sub>4</sub>L was challenging due to the fact that it was a heterogeneous mixture. Further characterization of SbO<sub>4</sub>L was carried out using size exclusion chromatography and reversed-phase ion-pairing chromatography, to establish reproducibility in the synthesis, as well as to determine length of the polymeric species.

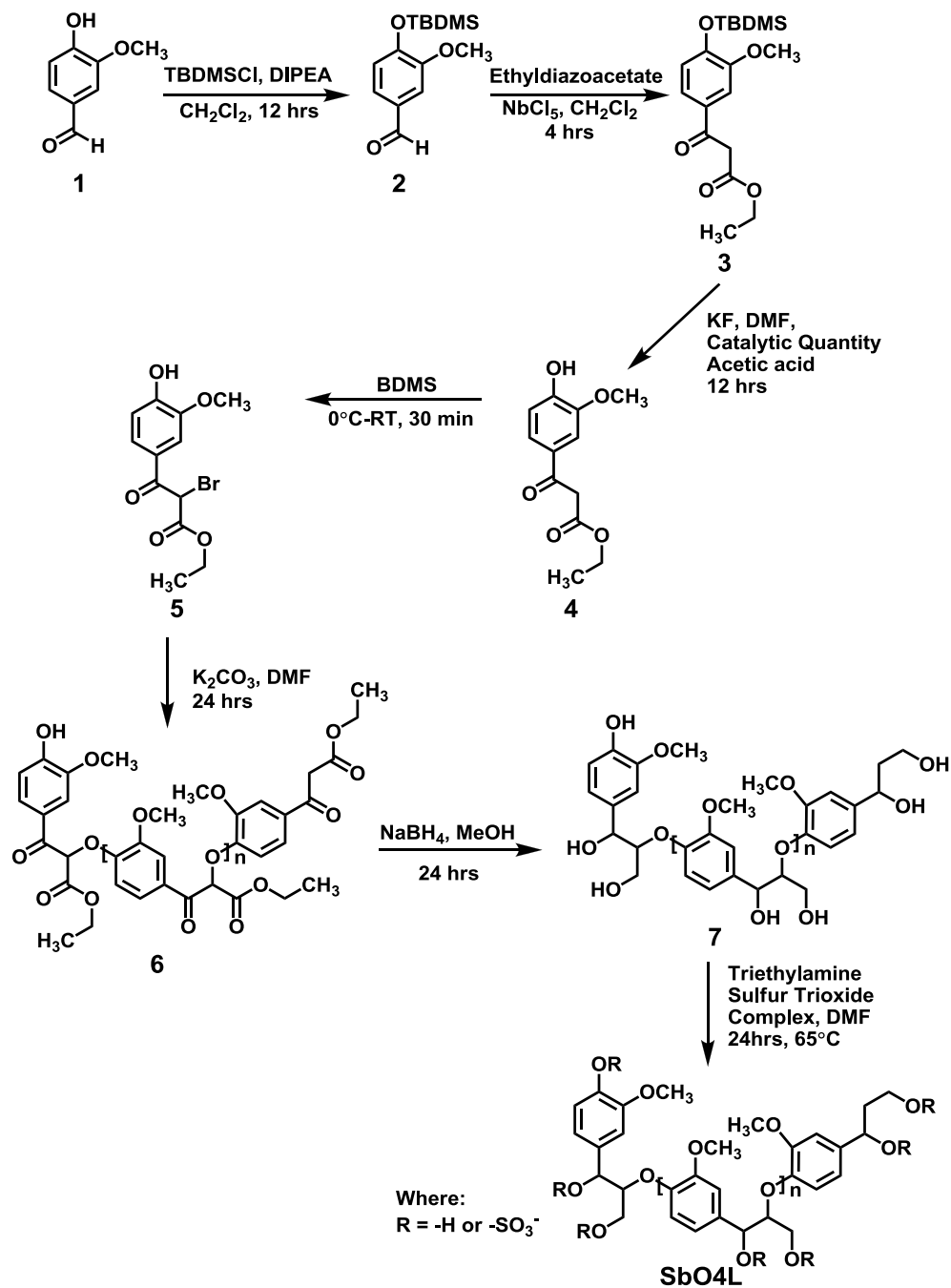


Figure 16. Synthetic scheme for production of SbO4L

### *SbO4L is a Sulfated Polymeric Species which can be Reproducibly Synthesized*

Characterizing sulfated polymers is extremely challenging.  $^1\text{H}$  and  $^{13}\text{C}$  NMR signals are relatively lower due to the lower relative abundance of these atoms within sulfated molecules as well as heterogeneity of molecules. Furthermore, SbO4L represents a polymeric mixture thus preventing the presentation of distinct peaks in these techniques. We characterized the final product of the synthesis of SbO4L using a combination of techniques such as size exclusion chromatography (SEC) HPLC, elemental analysis and reversed-phase ion pairing (RPIP) UPLC-MS.

The SEC chromatography is often used for the characterization of hydrophilic polymers. It gives an idea of the total size of the polymeric species. SbO4L elutes at 9.62 minutes which correlates to an elution volume of 6.74 ml in the method adopted (Figure 17A). A plot of log MW vs elution volume of known polystyrene sulfonate standards in the SEC method yields a straight line (Figure 17B) which can be used to extrapolate the molecular weight parameters of SbO4L. The aqueous SEC-HPLC profile of SbO4L indicated the number ( $M_N$ ), weight ( $M_W$ ) and peak ( $M_P$ ) average molecular weights of 9200, 12300, and 9100, respectively, which implied that on an average SbO4L chain is ~23 residues long. In comparison, an average UFH chain is 50 residues long. The SEC chromatograms also indicated that there were no peaks less than molecular weight of 1000 Da indicating that the purity of the polymeric species was greater than 98%. The polydispersity (P), of SbO4L was found to be 1.336, which is similar to that of UFH used in the clinic.<sup>200</sup> The sulfation density calculated on the basis of the difference in  $M_W$  between SbO4L and its unsulfated precursor was ~2 sulfate groups per monomer, which compares favorably with that of UFH and LMW heparins (~1.65 negative charges per monomer). However, calculation of sulfation using SEC can be exaggerated due to the

association of water molecules along with the sulfates. In combination, the uniform  $\beta$ -O4 linkage and the high sulfation density of SbO4L suggests a fairly uniform repeating structure in comparison to sulfated LMW lignins studied earlier.<sup>182</sup>

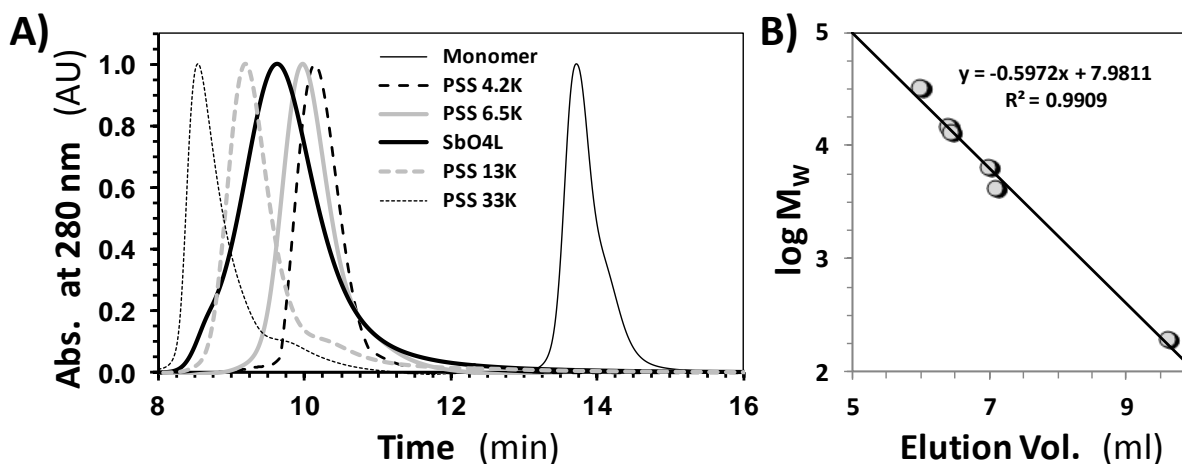


**Figure 17.** Characterizing molecular size of SbO4L. (A) SEC chromatograms for PSS standards, monomer ferrulic acid and SbO4L. (B) Plot of  $\log M_w$  vs elution volume of PSS standards yields a straight line which can be used to calculate the  $M_p$  of SbO4L.

Elemental analysis gives useful information about the total elemental composition of the molecule, and can be useful in determining purity as well as ratio of functional groups (such as sulfates) within a molecule. Elemental analysis indicates that the sulfation level is closer to 1.25 sulfate groups per monomer which is less than that of heparin and suggests that SbO4L may contain associated waters.

Further purity and reproducibility of synthesis was confirmed using reversed-phase ion pairing UPLC-MS and in vitro thrombin inhibition test for three different batches of synthesized polymer. The three batches of SbO4L demonstrated similar UPLC chromatograms in a

fingerprint like manner (Figure 18A), while showing identical  $IC_{50}$  for thrombin inhibition ( $0.20 \pm 0.04 \mu\text{g/ml}$ ) (Figure 18B).

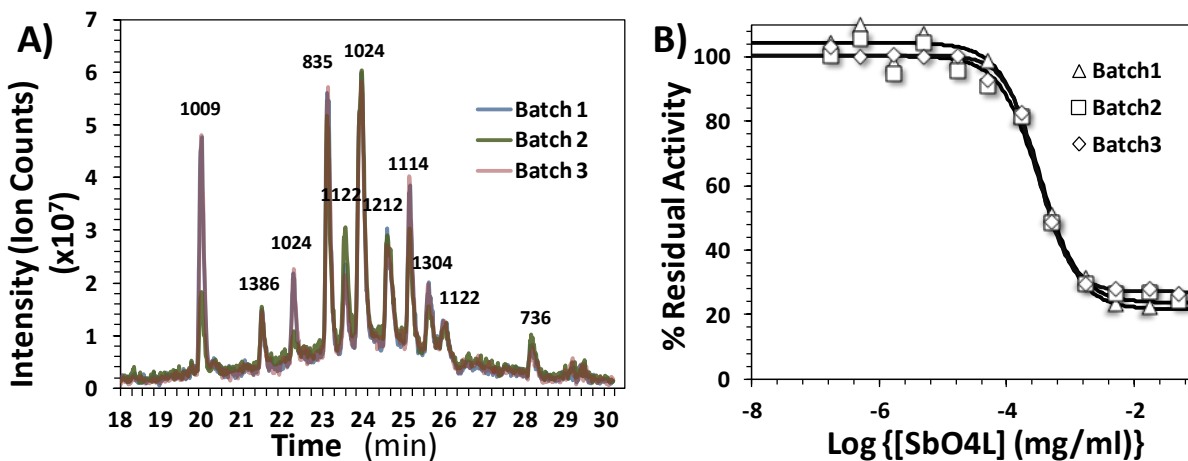


**Figure 18.** Comparison of three different batches of *SbO4L* using RPIP-UPLC-MS and Thrombin Inhibition. (A) Shows the total ion chromatogram (TIC) for the RPIP-UPLC-MS performed on three different batches of *SbO4L*. (B) Thrombin inhibition by three different batches of *SbO4L* shows identical decrease in residual activity of thrombin with an  $IC_{50}$  of  $0.20\mu\text{g/ml}$ .

*SbO4L* is a Selective and Potent Inhibitor of Thrombin and Plasmin among the Coagulation Enzymes.

To assess the selectivity of inhibition of *SbO4L* toward the different coagulation proteases, the inhibition of all relevant coagulation enzymes was studied using a chromogenic substrate assay in the presence of varying levels of *SbO4L*, using methods which have been adapted previously.<sup>148,151</sup> The decrease in residual protease activity as *SbO4L* was varied over 105-fold was fitted using the dose-response equation 4 to calculate the  $IC_{50}$ , hill slope (HS),

maximal ( $Y_M$ ) and minimal activity ( $Y_0$ ) parameters (Figure 19, Table 2). SbO4L inhibited human  $\alpha$ -thrombin with an  $IC_{50}$  of 0.17  $\mu\text{g/ml}$  ( $\sim 18$  nM), while fXa and fXIa were inhibited at 90–500  $\mu\text{g/ml}$  SbO4L ( $\sim 10$ –55  $\mu\text{M}$ ). In comparison, parent LMW lignins inhibited fXa with  $IC_{50}$  of 34–120 nM and fXIa with an  $IC_{50}$  of 22–176 nM (Table 1).<sup>186</sup> Finally, inhibition of FIXa was not noticeable at concentrations as high as 81  $\mu\text{g/ml}$  (8.7  $\mu\text{M}$ ), while fVIIa–recombinant tissue factor (rTF) complex was inhibited 50% at 9.4  $\mu\text{g/ml}$  (1  $\mu\text{M}$ ) SbO4L. The only coagulation protein that displayed inhibition close to thrombin was plasmin, with an  $IC_{50}$  of 0.38  $\mu\text{g/ml}$  ( $\sim 40$  nM). However, this is not surprising as the parent lignins were also found to inhibit plasmin in a potent, allosteric manner and there seems to be structural resemblance between the heparin binding sites of these proteins.<sup>185</sup> The results indicated that SbO4L inhibited human thrombin  $\sim 20$  – 2940-fold better than the closely related coagulation factors. This is a significant improvement in selectivity compared to parent chemoenzymatically synthesized lignins (Table 1). Also, most sulfated GAGs including UFH and fondaparinux do not inhibit these enzymes directly at concentrations as high as 100  $\mu\text{g/ml}$ .<sup>183</sup>

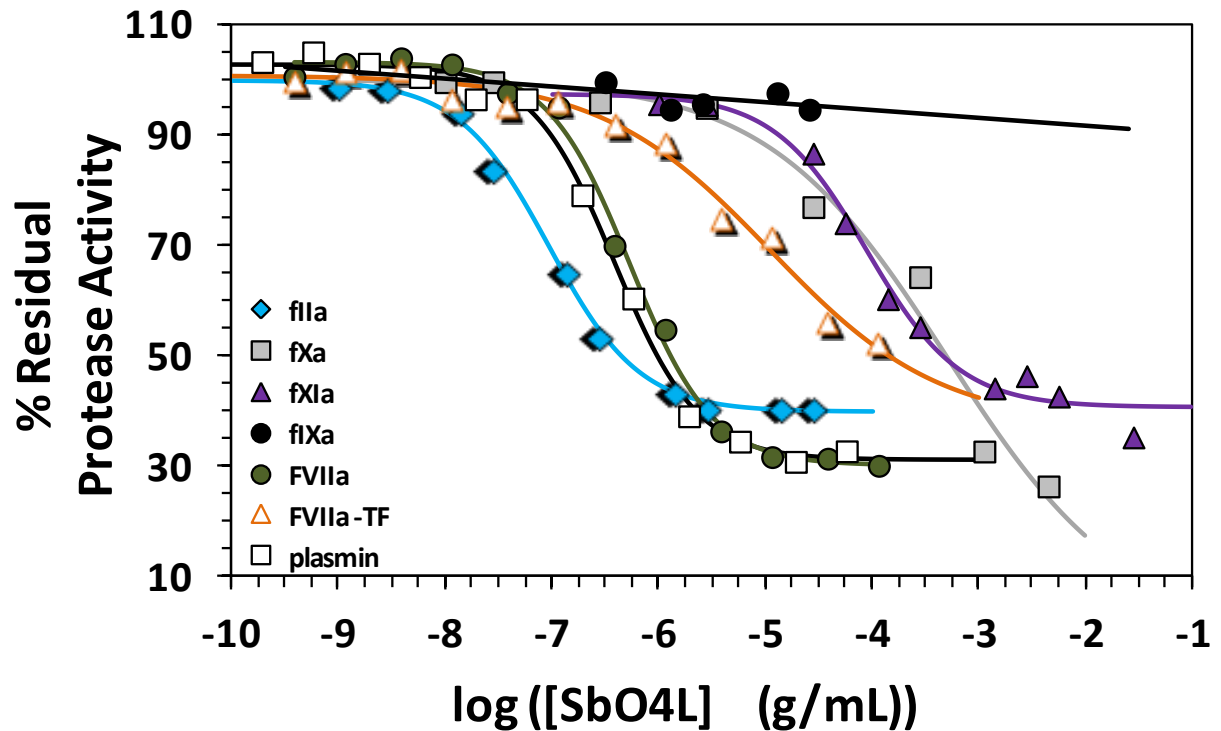


**Figure 19.** Direct inhibition of serine proteases of the coagulation cascade by SbO4L. The inhibition of factors IIa (thrombin, fIIa), Xa, XIa, IXa, VIIa, VIIa-tissue factor (TF) complex and plasmin by SbO4L was monitored using chromogenic substrate hydrolysis assay. The % residual activity of the enzymes was plotted against the log of the concentration to obtain a dose response curve which can be fitted to equation 4 to give the  $IC_{50}$ ,  $Y_M$ ,  $Y_0$  and HS parameters of inhibition.

**Table 2. Parameters for sulfated  $\beta$ -O4 lignin (SbO4L) inhibition of coagulation proteases. <sup>a</sup>**

Protease	$\log [IC_{50} \text{ (g/ml)}]$	$IC_{50} \text{ (}\mu\text{g/ml)}$	$Y_M$	$Y_0$	HS
Thrombin	$-6.8 \pm 0.1^b$	$0.17 \pm 0.01$	$99 \pm 1$	$29 \pm 1$	$1.6 \pm 0.1$
Factor Xa	$-3.3 \pm 0.6$	$500 \pm 300$	$100 \pm 4$	$\sim 1$	$0.5 \pm 0.2$
Factor IXa	NI <sup>c</sup>	NI	- <sup>d</sup>	-	-
Factor XIa	$-4.1 \pm 0.1$	$89 \pm 9$	$98 \pm 3$	$41 \pm 2$	$1.0 \pm 0.2$
Factor VIIa	$-6.3 \pm 0.1$	$0.54 \pm 0.05$	$103 \pm 3$	$31 \pm 3$	$1.1 \pm 0.1$
Factor VIIa – TF	$\sim -5.0^e$	$>11^e$	$100 \pm 2$	$\sim 38^e$	$\sim 0.5^e$
Plasmin	$-6.4 \pm 0.1$	$0.38 \pm 0.04$	$103 \pm 1$	$31 \pm 2$	$1.1 \pm 0.1$
Thrombin w/ AT <sup>f</sup>	$-6.7 \pm 0.1^b$	$0.20 \pm 0.01$	$64 \pm 1$	$6 \pm 1$	$1.9 \pm 0.4$
Thrombin/rTM – PC	$-5.4 \pm 0.1$	$4.20 \pm 0.08$	$98 \pm 2$	$3 \pm 5$	$0.96 \pm$

<sup>a</sup>The  $IC_{50}$ , HS,  $Y_M$ ,  $Y_0$  values were obtained following non-linear regression analysis of direct inhibition of the protease (see ‘Experimental Methods’ for details). <sup>b</sup>Errors represent  $\pm 1$  S. D. <sup>c</sup>No inhibition was observed up to concentrations as high as 81  $\mu\text{g/ml}$ . <sup>d</sup>Not applicable. <sup>e</sup>Estimated values. <sup>f</sup>In the presence of 200 nM AT. <sup>g</sup>Inhibition of activation of protein C by thrombin – thrombomodulin complex.

#### *SbO4L does not Inhibit Other Heparin Binding Serine Proteases*

To assess the selectivity against other heparin-binding serine proteases, we screened cathepsin G, human leukocyte elastase, kallikrein, porcine pancreatic elastase, activated protein C, plasmin, chymotrypsin, and trypsin, as studied earlier for sulfated LMW lignins.<sup>186</sup> Except for plasmin and factor VIIa, the activity of each protease remained relatively unaffected in the presence of 81  $\mu\text{g/ml}$  (8.7  $\mu\text{M}$ ) SbO4L (Figure 20) suggesting more than 475-fold selectivity. Factor VIIa inhibition by SbO4L does not exist in the physiologically relevant complex with tissue factor (TF), suggesting that SbO4L would be a selective inhibitor of plasmin and thrombin in the blood. Thus, SbO4L selectively inhibits human thrombin and plasmin among several



structurally similar and relevant trypsin-like proteases. This is a significant improvement in selectivity compared to parent LMW lignins which were also found to be potent inhibitors of cathepsin G (90-230 nM), HLE (9-17nM), and plasmin (240-1290nM) (Table 1).

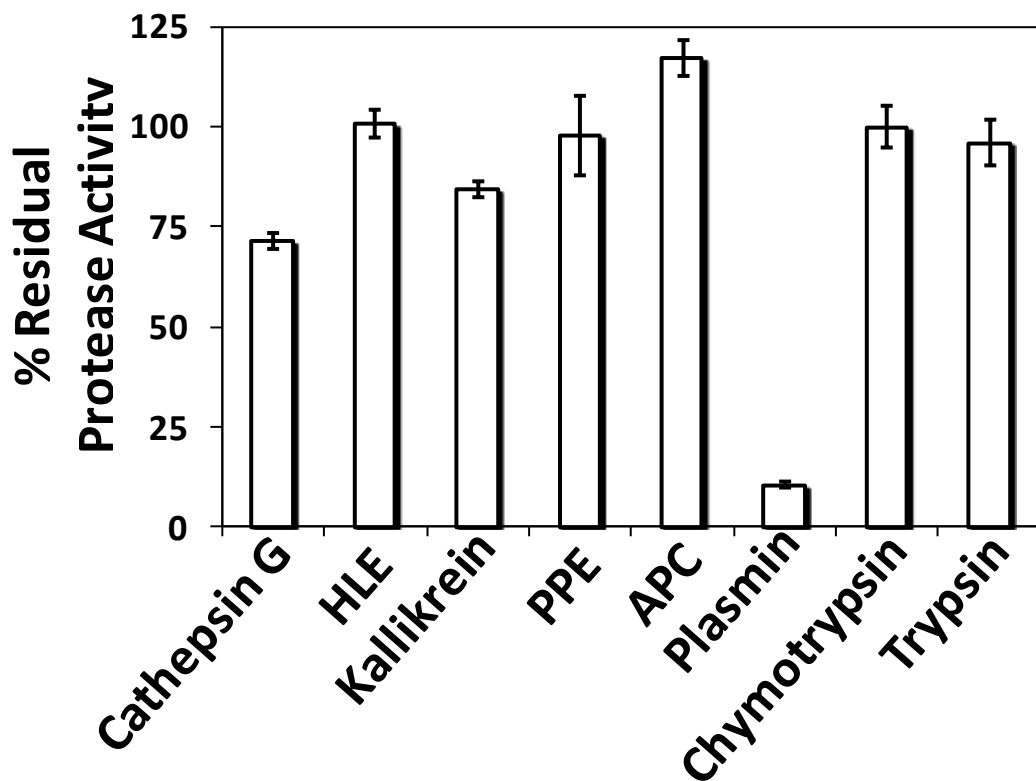


**Figure 20.** *SbO4L* inhibition of other heparin-binding serine proteases including cathepsin G, human leukocyte elastase (HLE), porcine pancreatic elastase (PPE), activated protein C (APC), plasmin, chymotrypsin and trypsin at a fixed 81  $\mu\text{g/ml}$  (8.7  $\mu\text{M}$ ) (~475-fold excess over the  $\text{IC}_{50}$  of thrombin inhibition).

### *Antithrombin III does not Potentiate SbO4L Mediated Thrombin Inhibition*

Polymeric heparin is a powerful antagonist of thrombin because of its ability to bind plasma antithrombin and bridge with thrombin.<sup>201</sup> In contrast, sulfated LMW lignins were found to bind the serpin with reasonable affinity, yet lose direct inhibition potential.<sup>191</sup> To assess the influence of antithrombin on SbO4L activity, direct inhibition of thrombin was studied in the presence of 200 nM serpin under otherwise identical conditions. A decrease in thrombin activity with increasing SbO4L levels was observed, which was identical to that measured in the absence of the serpin, except for the differences in maximal ( $Y_M$ ) and minimal ( $Y_0$ ) residual thrombin activities (Figure 21, Table 2). The  $Y_M$  and  $Y_0$  values decreased by 35% and 23%, respectively, due to the reaction of thrombin with antithrombin. However these changes did not affect SbO4L inhibition of thrombin ( $IC_{50} = 0.2$  and  $0.17 \mu\text{g/ml}$  with and without antithrombin, respectively (Table 2)). The result implies that antithrombin does not retard or stimulate SbO4L's inhibitory activity. This is a significant point of difference from the parent sulfated LMW lignins, for which the serpin-mediated pathway was found to be a competing side reaction.<sup>191</sup> The results highlight an interesting structural aspect that a specific scaffold, i.e., the  $\beta$ -O4-linked scaffold, of the many possible in sulfated LMW lignins does not appear to bind the serpin with high affinity, which improves mechanistic selectivity.

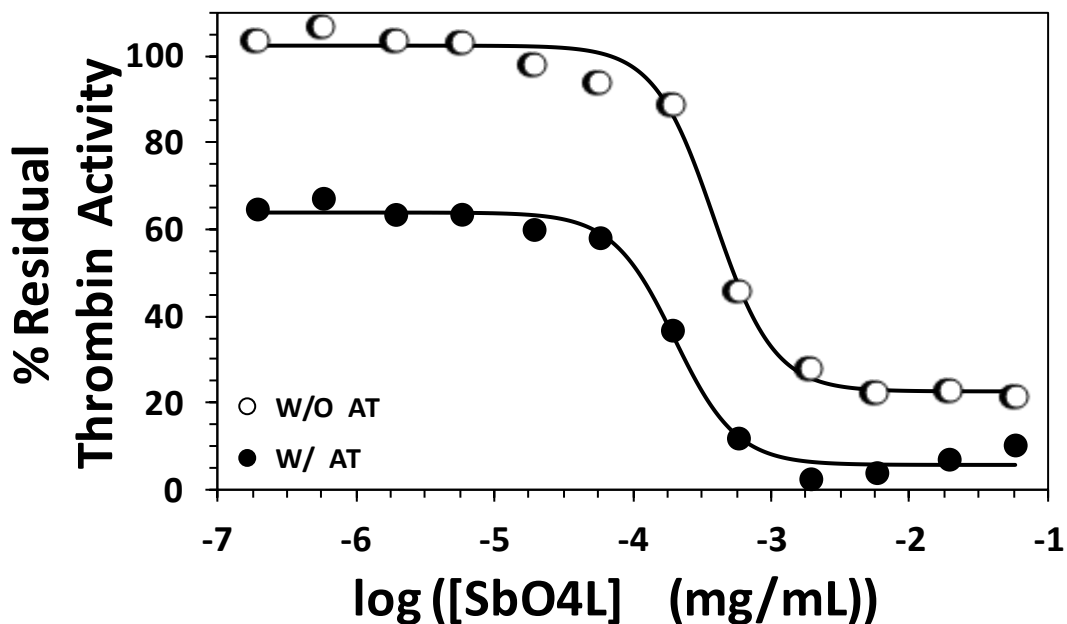


**Figure 21.** Effect of antithrombin III on SbO4L inhibition of thrombin. Inhibition of thrombin in the presence of antithrombin III (w/ AT) with SbO4L (●) was compared to SbO4L alone (○). A decrease in  $Y_M$  and  $Y_0$  was observed due to direct inhibition of thrombin with antithrombin III. However, no change in  $IC_{50}$  was observed.

*SbO4L Inhibits Thrombomodulin-Bound Thrombin Less Potently*

Thrombin’s procoagulant activity is highly regulated by cell surface thrombomodulin (TM), which transforms it into an anticoagulant protease with specificity for protein C.<sup>15,202</sup> To assess whether TM binding to thrombin alters the activity of SbO4L, we studied the efficacy of protein C activation. The level of proteolytically active protein C formed by thrombin–TM complex can be measured spectrometrically through hydrolysis of S-2366<sup>193</sup> following suppression of thrombin’s native proteolytic activity using argatroban ( $\sim 20 \times K_i$ )<sup>203</sup> as its specific inhibitor. Measurement of APC levels in the presence of varying SbO4L levels led to a sigmoidal

profile on a semi-log plot (Figure 22) suggesting that SbO4L inhibited the protein C activation potential of thrombin–TM complex. The  $IC_{50}$  was measured to be 4.2  $\mu\text{g}/\text{ml}$  (Table 2), which was ~20-fold higher than that measured for SbO4L inhibiting the procoagulant activity of thrombin alone. The efficacy of inhibition of protein C activation was found to be nearly 100% (Table 2), which is higher than that for thrombin alone (~70%, Table 2). Although the higher efficacy may appear to imply that the procoagulation potential of SbO4L is higher than the anticoagulant potential, protein C activation is inhibited at 20-times the concentration of thrombin inhibition. Thus, the results indicate that SbO4L is a selective inhibitor of the procoagulant form of thrombin compared to the anticoagulant form of it.

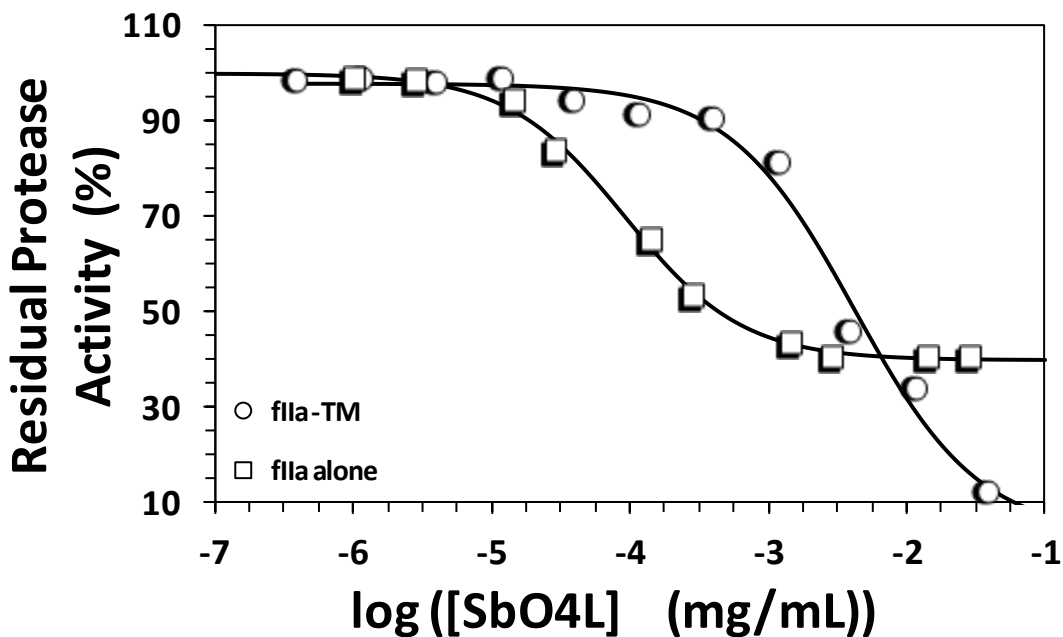


*Figure 22. SbO4L inhibition of thrombin-thrombomodulin complex. Inhibition of protein C activation potential of thrombomodulin-bound thrombin by SbO4L (○) in comparison to thrombin proteolytic activity (□). A shift in the dose response curve to the right by almost 1-log*

unit shows a change in the potency of almost 20-fold. This is a clear sign that SbO4L can inhibit free thrombin with greater potency than thrombomodulin-bound thrombin.

#### *SbO4L Inhibits Different Types of Thrombin in Equivalent Manner*

Small structural differences exist between thrombin structures between different species and the degradation products of thrombin. Therefore there is a need to establish SbO4L potency against thrombin from different species and  $\gamma$ -thrombin. In order to assess variation of inhibition of SbO4L versus different types of thrombin, we screened SbO4L against mouse (murine), cow (bovine) thrombin and  $\gamma$ -thrombin (Figure 23). It was found that SbO4L shows little or no inter-species variation of thrombin inhibition with an  $IC_{50}$  of  $0.17 \pm 0.03 \mu\text{g/ml}$ . However, SbO4L does show a slight decrease in potency against  $\gamma$ -thrombin with an  $IC_{50}$  of  $0.34 \pm 0.03 \mu\text{g/ml}$ .

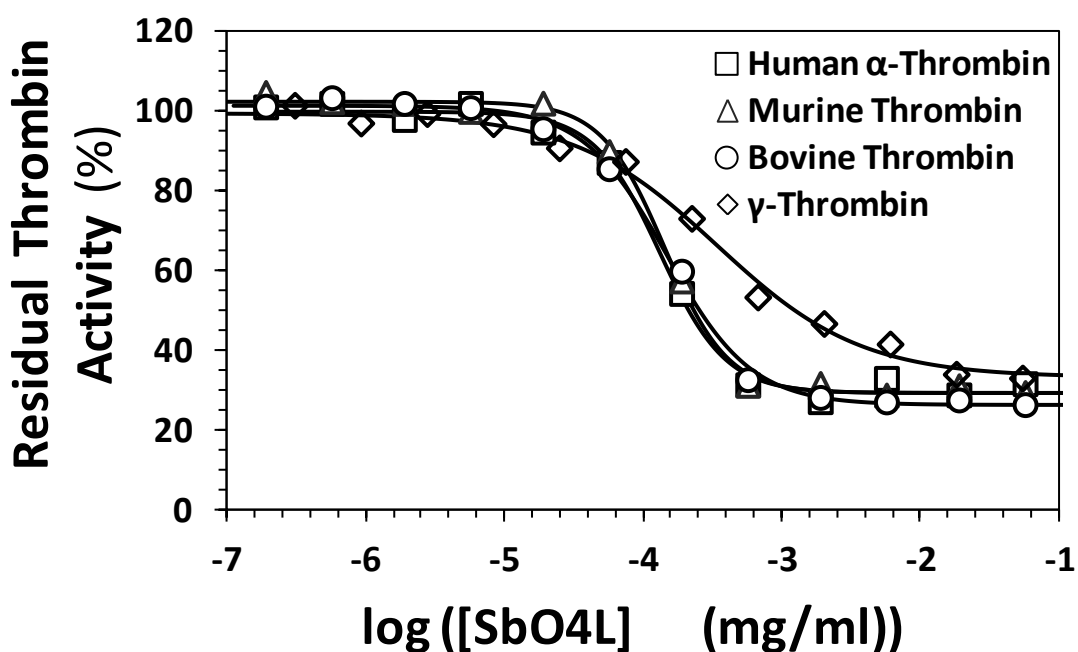


**Figure 23.** Inhibition of different types of thrombin by SbO4L. A comparison of the activity of SbO4L against human  $\alpha$ -thrombin ( $\square$ ), murine thrombin ( $\Delta$ ), bovine thrombin ( $\circ$ ) and human  $\gamma$ -

thrombin ( $\diamond$ ) was performed. It was observed that SbO4L inhibited the different species of thrombin with equal potency ( $IC_{50} = 0.17 \mu\text{g/ml}$ ), while inhibiting  $\gamma$ -thrombin with 2-fold less potent  $IC_{50}$  of  $0.34 \mu\text{g/ml}$ .

#### *SbO4L Shows Similar Potency Against Thrombin for Fibrinogen Substrate*

Since all ex vivo and in vivo experiments will be close to physiological conditions, we thought it would be useful to assess SbO4L inhibition of thrombin using physiologically relevant fibrinogen as the substrate. The assay monitors the change in absorbance due to formation of fibrin mesh in the presence of SbO4L which is compared to a reaction without the inhibitor to obtain the residual activity. A plot of the residual activity as a function of the concentration gives a curve similar to those observed with chromogenic substrates and can be fitted to equation 4 (Figure 24). The  $IC_{50}$  for SbO4L with fibrinogen at  $0.19 \pm 0.09 \mu\text{g/ml}$  thus obtained was similar to the  $IC_{50}$  with chromogenic substrate at  $0.17 \pm 0.01 \mu\text{g/ml}$ .

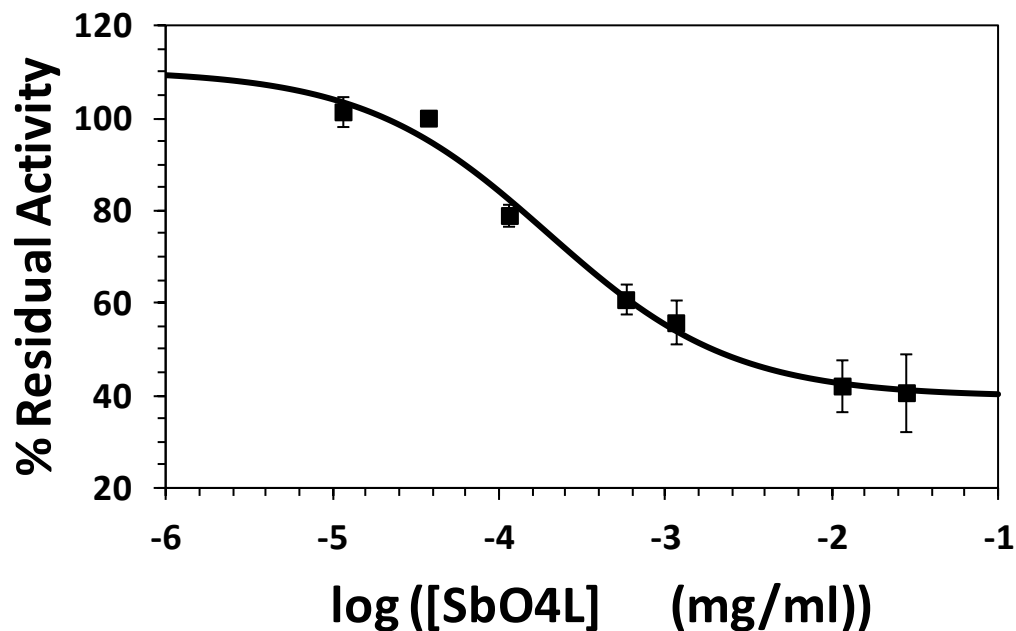


**Figure 24.** Shows the inhibition of thrombin mediated conversion of fibrinogen to fibrin by SbO4L.

*SbO4L is a Non-Competitive Inhibitor of Thrombin*

To understand the basis of thrombin inhibition, we measured the kinetics of Spectrozyme TH hydrolysis at pH 7.4 in the presence of SbO4L. Plots of the initial rates versus substrate concentration were hyperbolic, as expected (Figure 25). As the concentration of SbO4L was increased from 11.5 ng/ml to 2.3  $\mu\text{g/ml}$ , maximal velocity of hydrolysis,  $V_{MAX}$ , decreased in a dose dependant manner (Table 3). Fitting the data using the standard Michaelis-Menten equation gave an essentially invariant  $K_{M,app}$  of 1.5  $\mu\text{M}$  (Table 3). This suggests that SbO4L does not affect small molecule chromogenic substrate binding to the active site of thrombin. The  $V_{MAX}$  decreased from 27.5 to 7.4 mAbsU/min (Figure 25) corresponding to a decrease of more than 70%. Thus, SbO4L appears to not sterically hinder the interaction of thrombin substrate, but brings about changes in the active site that reduce the catalytic rate. This implies that SbO4L is a non-competitive, allosteric inhibitor of human thrombin.

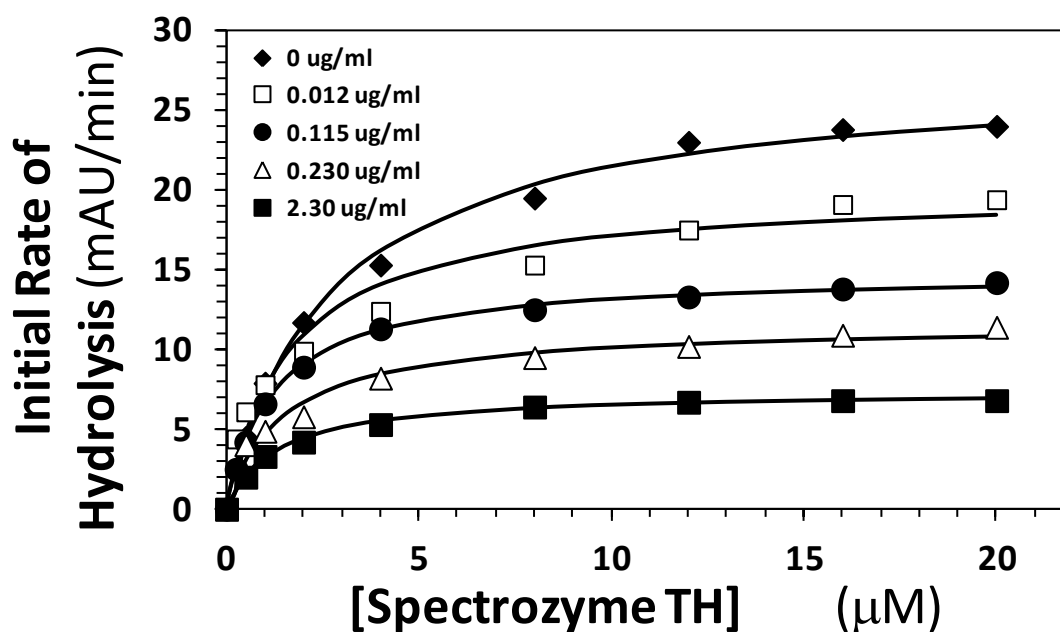


**Figure 25.** Michaelis-Menten kinetics of Spectrozyme TH hydrolysis by thrombin in the presence of SbO4L. The initial rate of hydrolysis at various substrate concentrations was measured in a

pH 7.4 buffer as described in 'Experimental Procedures'. The concentrations of SbO4L were 0 (◆), 0.012 (□), 0.115 (●), 0.230 (Δ) and 2.3 μg/ml (■). Solid lines represent non-linear fits to the data using the standard Michaelis-Menten equation.

**Table 3. The Michaelis-Menten Kinetic Parameters of SbO4L Inhibition of Thrombin**

<i>[SbO4L]</i> (μg/ml)	<i>K<sub>M</sub></i> (μM)	<i>V<sub>MAX</sub></i> (mAbsU/min)
0	1.6 ± 0.2	27.5 ± 0.7
0.0115	1.7 ± 0.3	20.0 ± 0.1
0.115	1.3 ± 0.1	14.8 ± 0.1
0.230	1.5 ± 0.3	11.7 ± 0.5
2.3	1.4 ± 0.1	7.4 ± 0.1

*SbO4L does not Compete with Exosite 1 Ligand Hirugen Peptide, but Competes with Exosite 2 Ligands Heparin and GPIIb*

To assess whether SbO4L engages one or both exosites of thrombin, competitive inhibition studies were performed using prototypical ligands, hirugen (exosite 1) and heparin (exosite 2). HirP, a hirudin-based dodecapeptide that binds avidly to exosite 1 ( $K_D = 28$  nM),<sup>204</sup> did not affect the apparent  $IC_{50}$  of thrombin inhibition by SbO4L at concentrations nearly 3.1 times higher than the affinity (Figure 26, Table 4). This implies that the SbO4L does not engage exosite 1 of thrombin. When the thrombin inhibition was studied in the presence of both SbO4L and UFH ( $K_D = 15.6$  μM,  $M_W = 15,000$ )<sup>183</sup>, the  $IC_{50}$  increased from 0.2 to 1.25 μg/ml (Figure



27A, Table 4), which paralleled that predicted by the Dixon-Webb relationship for ideal competitive behavior (Figure 27B). This implied that SbO4L competes with UFH for binding to human thrombin, which suggests interaction with residues in or near exosite 2. To further understand SbO4L allostery, we decided to utilize recombinant GPIIb $\alpha$  ( $K_i = 100$  nM)<sup>80</sup>, which is known to bind exosite 2 of thrombin.<sup>52</sup> Although GPIIb $\alpha$  inhibits thrombin-mediated fibrinogen to fibrin conversion, it does not affect thrombin's hydrolysis of small peptides.<sup>80</sup> As the concentration of GPIIb $\alpha$  increases from 0 to 458 nM, the  $IC_{50}$  of SbO4L inhibition of thrombin increased from 0.17 to 1.15  $\mu$ g/ml, which paralleled the predicted values assuming ideal competition (Figure 28A and 28B). Thus, SbO4L competes with GPIIb $\alpha$  for binding to thrombin. This implies that exosite 2 residues that are important for both UFH and GPIIb $\alpha$  are likely to be important for binding to SbO4L.

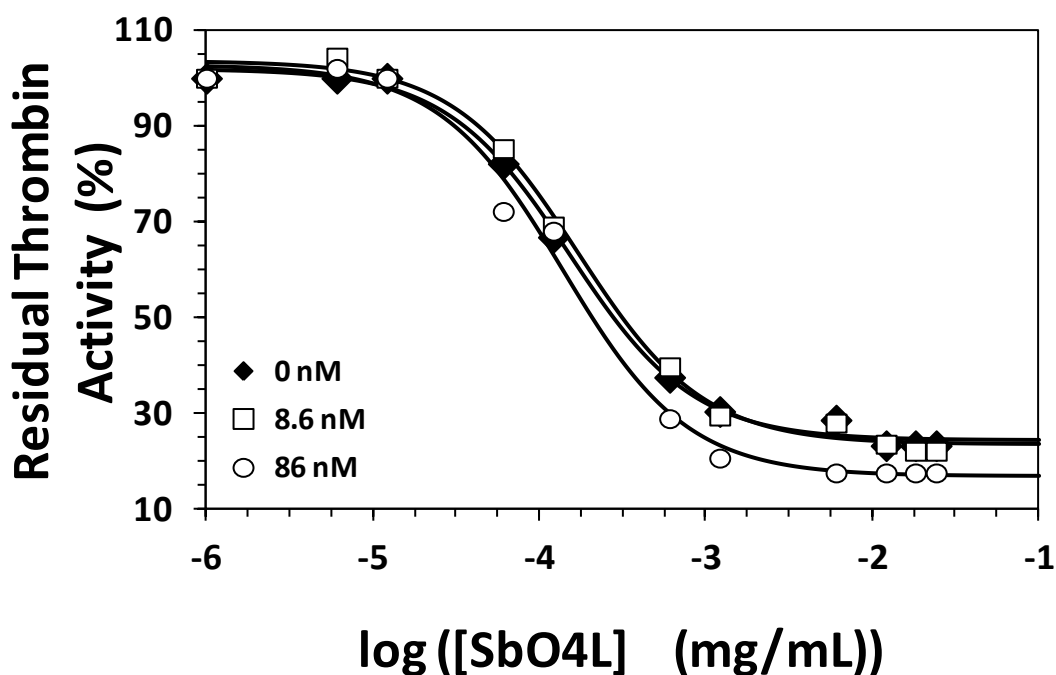


**Figure 26.** Effect of exosite-1 binding competitor hirudin-based peptide (HirP) on the inhibition of thrombin by SbO4L. The inhibition of human  $\alpha$ -thrombin was studied through Spectrozyme

TH hydrolysis assay at pH 7.4 in the presence of fixed concentrations of the competitor HirP.  
 Solid lines represent dose-response curves formed by fitting the data points to equation 4.

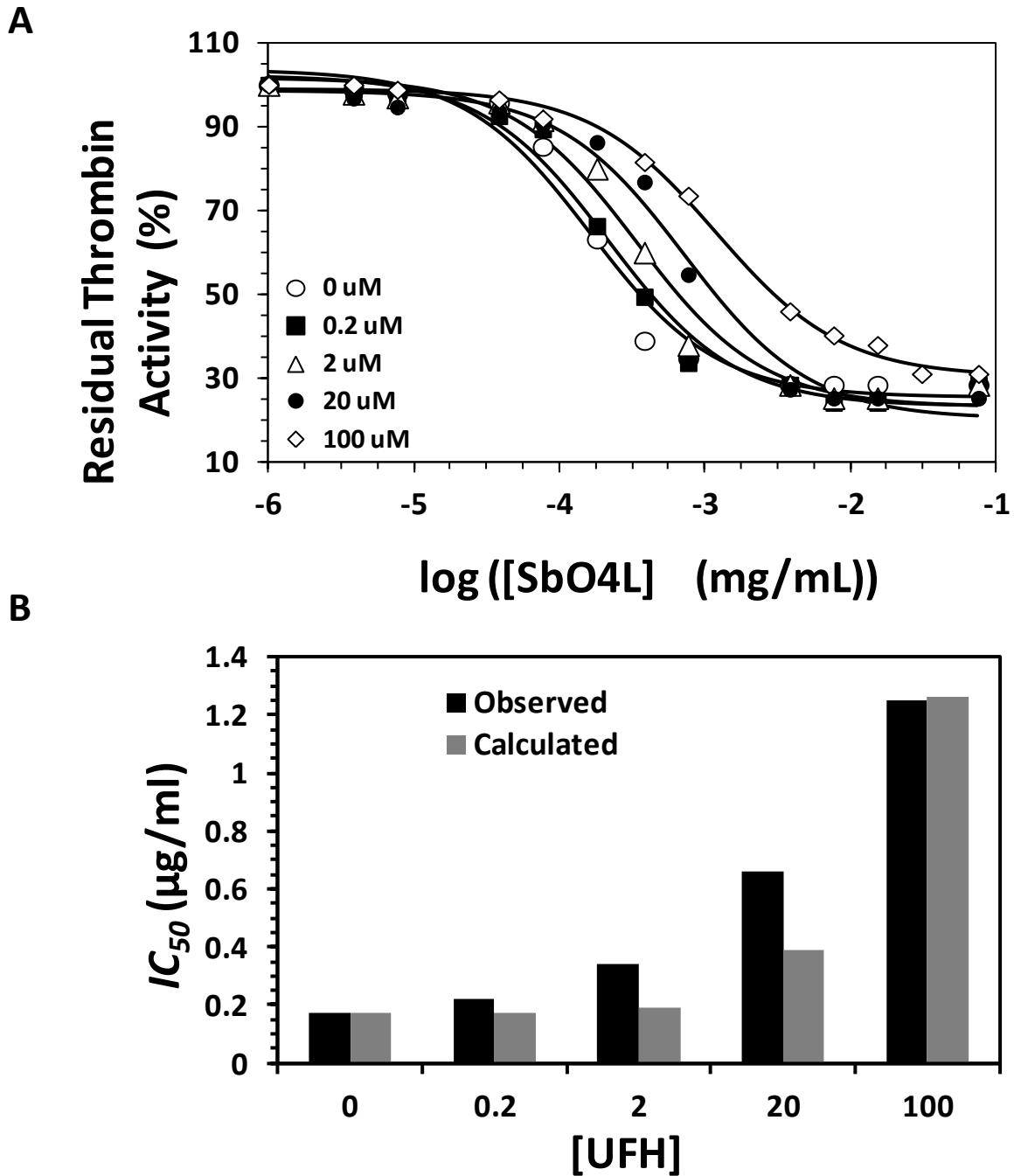


**Figure 27.** Effect of exosite-2 binding competitor unfractionated heparin (UFH) on the inhibition of thrombin by SbO4L. (A) The inhibition of human  $\alpha$ -thrombin was studied through

*Spectrozyme TH hydrolysis assay at pH 7.4 in the presence of fixed concentrations of the competitor porcine UFH. Solid lines represent dose-response curves formed by fitting the data points to equation 4 to yield the  $IC_{50}$  at various concentrations of the competitor. (B) Analysis of ideality of competition between SbO4L and porcine UFH. A comparison between the observed  $IC_{50}$  (in black) and those calculated using the Dixon-Webb relationship (Eq. 6) (in grey) at different concentrations of UFH (0-100  $\mu$ M) demonstrates that porcine UFH competes effectively against SbO4L thereby causing an increase in  $IC_{50}$  which is comparable to the predicted  $IC_{50}$  for ideal competition.*

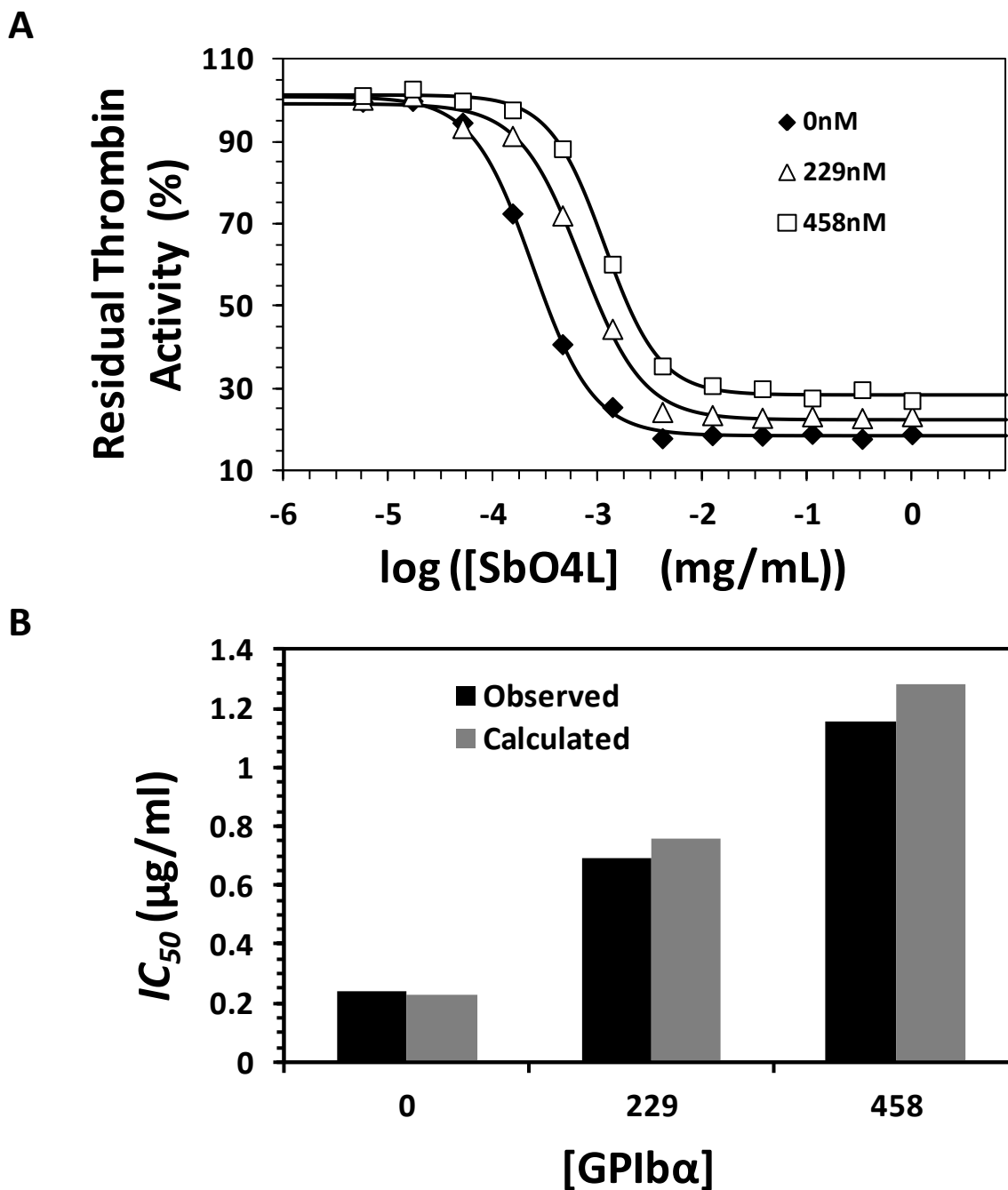


**Figure 28.** Effect of exosite-2 binding ligand GPIb $\alpha$  on the inhibition of thrombin by SbO4L. (A) The inhibition of human  $\alpha$ -thrombin was studied through Spectrozyme TH hydrolysis assay at pH 7.4 in the presence of fixed concentrations of the competitor GPIb $\alpha$ . Solid lines represent dose-response curves formed by fitting the data points to equation 4 to yield the IC<sub>50</sub> at various

concentrations of the competitor. (B) Analysis of ideality of competition between SbO4L and GPIba. A comparison between the observed  $IC_{50}$  (in black) and those calculated using the Dixon-Webb relationship (Eq. 6) (in grey) at different concentrations of GPIba (0, 229 and 458 nM) demonstrates that GPIba competes effectively against SbO4L thereby causing an increase in  $IC_{50}$  which is comparable to the predicted  $IC_{50}$  for ideal competition.

**Table 4. Inhibition parameters of human  $\alpha$ -thrombin by SbO4L in the presence of exosite 1 (HirP) and exosite 2 (UFH and GPIba) ligands.**

	$IC_{50}$	$Y_M$	$Y_0$	HS
<b>[HirP] nM</b>				
0	$0.15 \pm 0.01^b$	$102 \pm 14$	$24 \pm 1$	$1.2 \pm 0.1$
8.6	$0.17 \pm 0.02$	$103 \pm 2$	$23 \pm 1$	$1.2 \pm 0.1$
86	$0.14 \pm 0.02$	$102 \pm 3$	$17 \pm 2$	$1.2 \pm 0.2$
<b>[UFH] <math>\mu</math>M</b>				
0.2	$0.22 \pm 0.01$	$99 \pm 1$	$26 \pm 1$	$1.6 \pm 0.1$
2.0	$0.34 \pm 0.02$	$98 \pm 1$	$26 \pm 1$	$1.8 \pm 0.1$
20	$0.66 \pm 0.05$	$96 \pm 1$	$24 \pm 1$	$1.6 \pm 0.2$
100	$1.25 \pm 0.14$	$100 \pm 1$	$28 \pm 2$	$0.9 \pm 0.1$
<b>[GPIba] nM</b>				
0	$0.23 \pm 0.01$	$101 \pm 2$	$18 \pm 1$	$1.5 \pm 0.1$
229	$0.69 \pm 0.05$	$99 \pm 1$	$22 \pm 1$	$1.5 \pm 0.1$
458	$1.15 \pm 0.05$	$101 \pm 2$	$28 \pm 1$	$1.6 \pm 0.1$

<sup>a</sup>The  $IC_{50}$ , HS,  $Y_M$ ,  $Y_0$  values were obtained following non-linear regression analysis of direct inhibition of human  $\alpha$ -thrombin. <sup>b</sup>Errors represent  $\pm 1$  S. E.

*SbO4L Mediates Thrombin Inhibition via Binding to Arg233, Lys235 and Lys236 residues on Exosite 2.*

To pinpoint the exosite 2 residues that interact with SbO4L, we studied 11 recombinant thrombins containing substitution of basic residues with alanine. These single- or multi-site thrombin mutants have been shown earlier to possess fully functional catalytic machinery.<sup>190,205</sup> Alanine replacement at either Arg126, Arg165, Lys169, Arg173, Arg175, or Lys240 showed minimal change (0.9 – 2.1-fold) in SbO4L inhibitory potential as compared to their wild-type recombinant reference (Figure 29A, Table 5). Likewise, a triple mutant containing Arg93,101,107Ala did not affect the IC<sub>50</sub>. However, single-site alanine substitution at Arg233, Lys235, and Lys236 positions was found to have 8 – 9-fold increase in IC<sub>50</sub> as compared that for the wild-type thrombin indicating that each of these residues are important for SbO4L-mediated inhibition of thrombin (Figure 29A and 29B, Table 5). Interestingly, these residues are also known to be crucial for interaction with heparin<sup>206</sup> and GPIIb<sup>52,116,117</sup>.

**Table 5. Inhibition parameters of SbO4L for different thrombin exosite 2 mutants in comparison to wild type recombinant protein.**

<b>Thrombin Enzyme</b>	<b><math>IC_{50}</math> (<math>\mu\text{g/ml}</math>)<sup>a</sup></b>	<b><math>Y_M</math></b>	<b><math>Y_0</math></b>	<b>HS</b>
WT	$0.34 \pm 0.03^b$	$102 \pm 3$	$14 \pm 1$	$1.5 \pm 0.2$
Triple Mutant	$0.52 \pm 0.07$	$101 \pm 3$	$32 \pm 2$	$1.4 \pm 0.3$
R126A	$0.67 \pm 0.04$	$101 \pm 1$	$18 \pm 1$	$1.3 \pm 0.1$
R165A	$0.41 \pm 0.06$	$100 \pm 3$	$33 \pm 2$	$1.3 \pm 0.2$
K169A	$0.55 \pm 0.02$	$101 \pm 1$	$15 \pm 1$	$1.6 \pm 0.1$
R173A	$0.32 \pm 0.04$	$103 \pm 2$	$35 \pm 1$	$1.2 \pm 0.1$
R175A	$0.66 \pm 0.03$	$102 \pm 1$	$25 \pm 1$	$1.2 \pm 0.1$
R233A	$3.2 \pm 0.1$	$99 \pm 1$	$16 \pm 1$	$1.4 \pm 0.1$
K235A	$2.8 \pm 0.2$	$100 \pm 1$	$17 \pm 1$	$1.4 \pm 0.1$
K236A	$2.8 \pm 0.2$	$97 \pm 1$	$16 \pm 1$	$1.3 \pm 0.1$
K240A	$0.73 \pm 0.02$	$99 \pm 1$	$22 \pm 1$	$1.5 \pm 0.1$

<sup>a</sup>The  $IC_{50}$ , HS,  $Y_M$ ,  $Y_0$  values were obtained following non-linear regression analysis of direct inhibition of human  $\alpha$ -thrombin. <sup>b</sup>Errors represent  $\pm 1$  S. E.

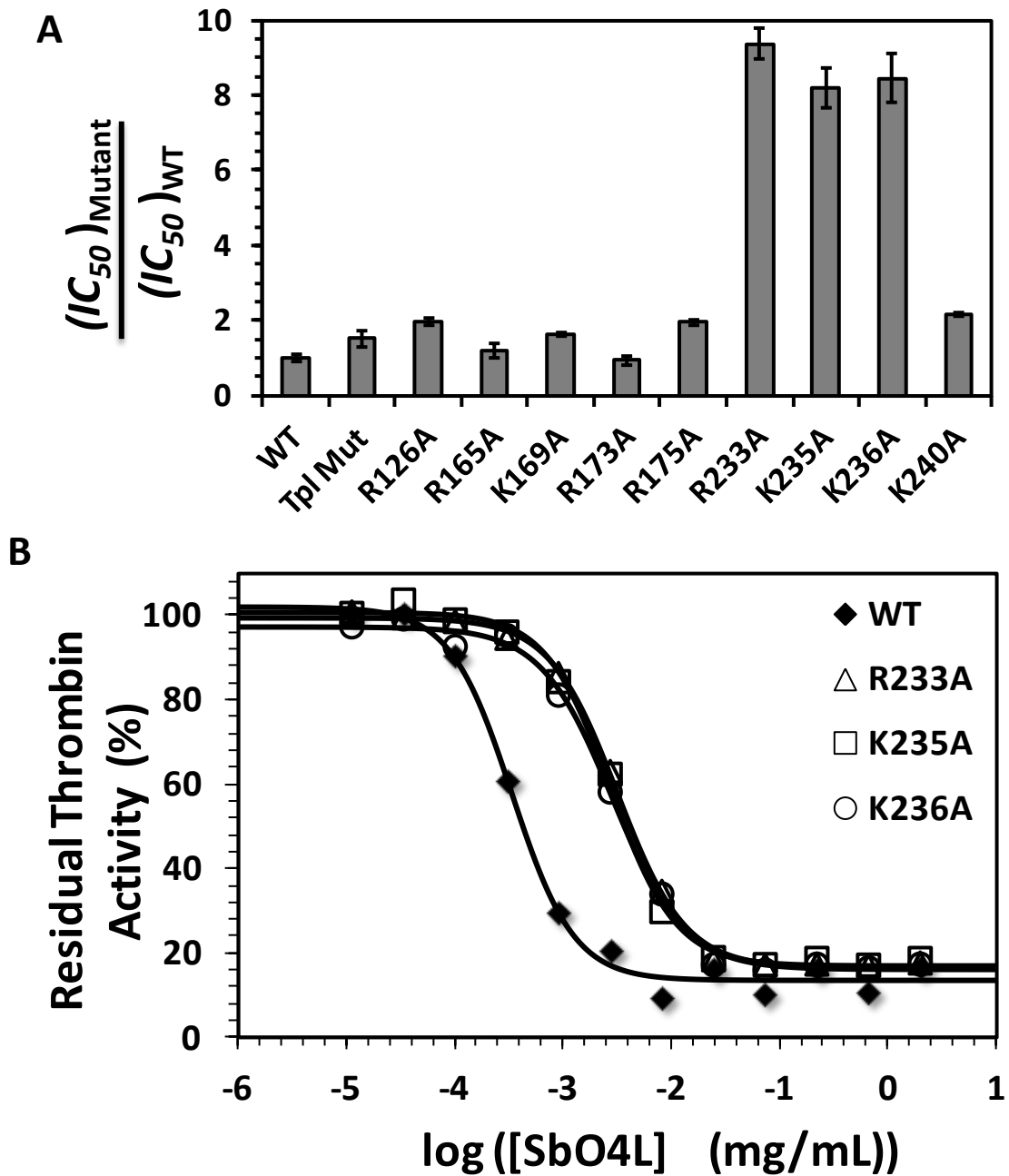


**Figure 29.** Effect of SbO<sub>4</sub>L on Thrombin Mutants (A) Shows a comparison of SbO<sub>4</sub>L inhibition of mutant vs wild type (WT) for the different thrombin mutants which included a triple mutant (Tpl Mut) R93,97,101A, R126A, R165A, K169A, R173A, R175A, R233A, K235A, K236A and K240A. (B) Shows the representative dose response curves for SbO<sub>4</sub>L inhibition for recombinant thrombin mutants R233A, K235A and K236A in comparison to wild type (WT) thrombin.



### *SbO4L Causes Allosteric Change in Active Site that restricts Quenching by Acrylamide*

To check accessibility of the active site upon SbO4L binding, quenching studies were carried out on  $\beta$ FPR-Thrombin using the collisional quencher- acrylamide. Collisional quenching occurs when the fluorophore comes in contact with the quenching agent in the excited state. If the binding of SbO4L causes a dramatic conformation change within the active site, the active site fluorescein of  $\beta$ FPR-Thrombin would be less accessible to quenching by the collisional quencher acrylamide. We observed that SbO4L bound  $\beta$ FPR-Thrombin was more resistant to collisional quenching compared to  $\beta$ FPR-Thrombin alone (Figure 30A). Upon treating the data thus obtained in the Stern-Volmer relationship we noticed that the Stern-Volmer relationship fitted well with a linear relationship (Figure 30B), indicating one type of fluorophore present both with and without inhibitor. The quenching constant ( $K_{SV}$ ) obtained from the slope, was almost 80% lower in the presence of SbO4L, suggesting that the conformational change induced restricts the accessibility of the quenching agent by a great extent. This is a clear indication of a dramatic change in the active site conformation due to SbO4L binding to thrombin.

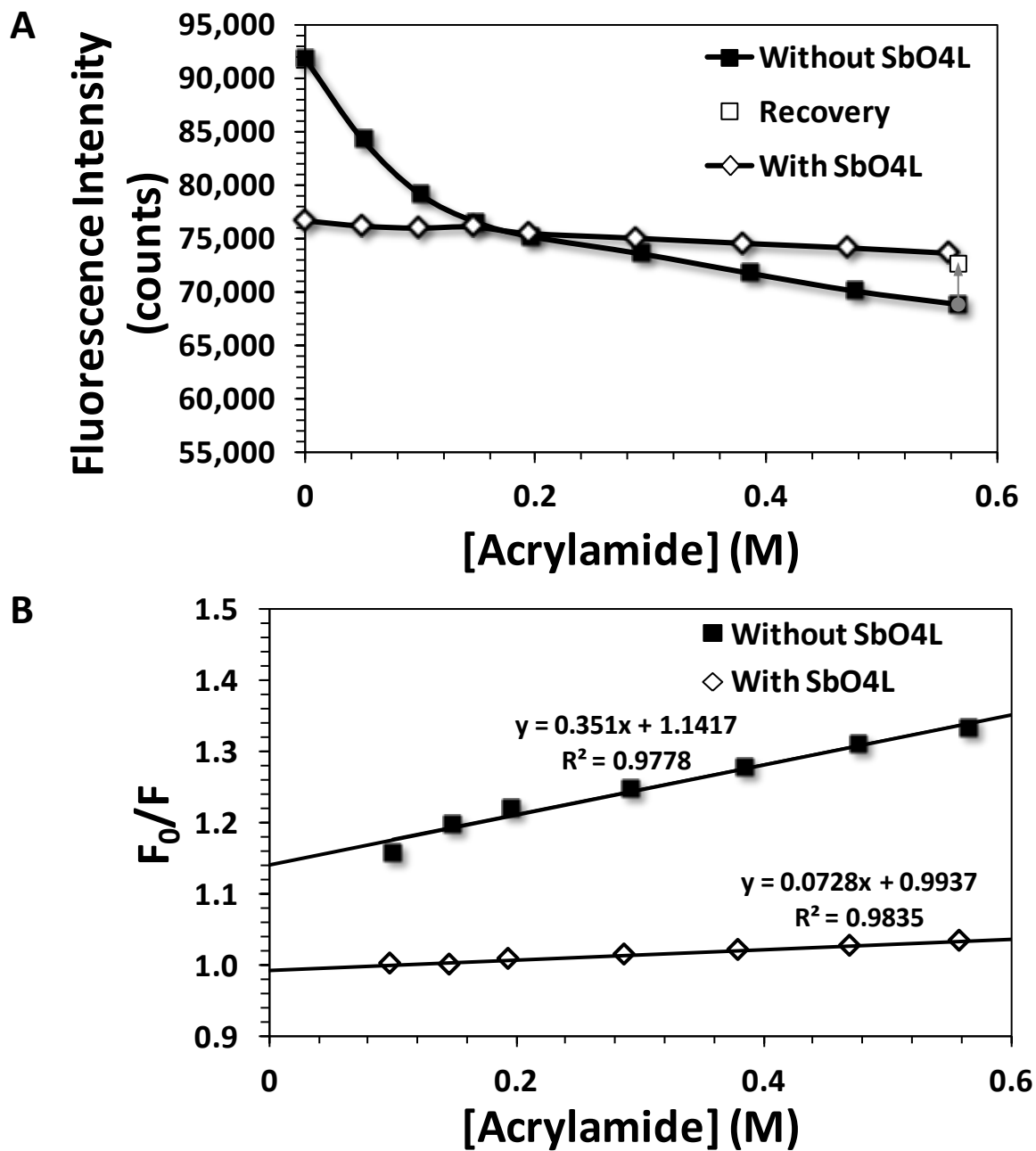


**Figure 30.** Active site fluorescence quenching in presence of SbO<sub>4</sub>L (A) The fluorescence intensity of fFPR-Thrombin was monitored with and without SbO<sub>4</sub>L at various concentrations of collisional quencher acrylamide. It was observed that the enzyme active site fluorescein was more susceptible to quenching in the absence of SbO<sub>4</sub>L compared to in its presence. Further, there was a recovery of fluorescence (shown in grey arrow) when SbO<sub>4</sub>L was added to the

*enzyme alone after addition of final concentration of acrylamide. (B) Stern-Volmer plots further showed that there was approximately 80% reduction in the quenching constant in the presence of SbO4L suggesting that the fluorophore was less accessible for quenching.*

#### *SbO4L binds Exosite 2 with Approximately Five Ionic Interactions*

Exosite 2 binding ligands are in general highly ionic in nature. To learn about the ionic contributions of SbO4L while binding to thrombin we performed salt dependence binding affinity studies. The affinity was measured by monitoring the change in fluorescence of active-site labeled  $\beta$ FPR-Thrombin in titrations with SbO4L. It was observed that as the concentration of salt increased, the binding affinity of SbO4L for thrombin decreased (Figure 31A, Table 6). A plot of the log of the dissociation constant as a function of log of the salt concentration yielded a straight line (Figure 31B) with a  $R^2$  of 0.98, whose slope gave the  $\Gamma_{\text{salt}}$  value of -5.0 (Equation 9). This is comparable to other exosite 2 binding ligands such as reported values of GPIIb $\alpha$  and Heparin (Table 7).  $\Gamma_{\text{salt}}$  values can roughly indicate that there are 5 ionic interactions occurring between SbO4L and thrombin. This combined with the sulfation level of approximately 1-2 sulfates per monomer indicates that the active binding portion of SbO4L could be limited to a simple dimeric-pentameric lignin molecule.

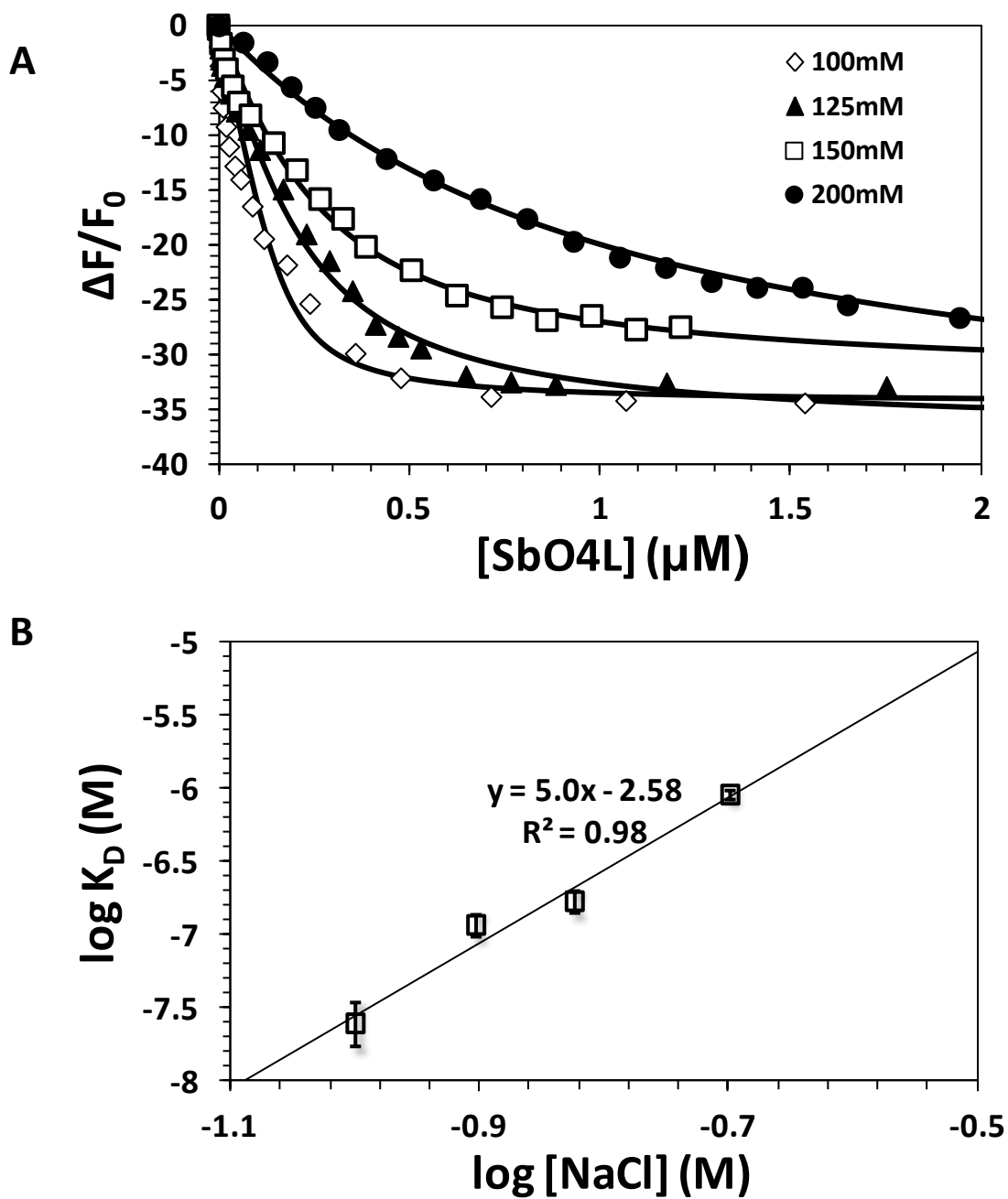


**Figure 31.** Effect of salt on SbO4L binding to thrombin. (A) Decrease in fluorescence intensity was observed as fFPR-Thrombin was titrated with SbO4L at various concentrations of sodium chloride. The change in fluorescence calculated as a ratio to the initial fluorescence was plotted against the concentration of SbO4L and fitted to the quadratic equation to obtain the

dissociation constant under the various conditions. (B) A linear relationship of  $\log K_D$  vs  $\log [NaCl]$  for SbO4L interaction with thrombin yields an  $R^2$  of 0.98. The slope of the line provides information on the  $\Gamma_{salt}$  which indicates that there are approximately 5 ionic interactions involved between SbO4L and thrombin.

**Table 6. Dissociation Constant of SbO4L at various concentrations of NaCl. The 100mM  $K_D$  is comparable to the  $IC_{50}$  obtained as the  $IC_{50}$  experiment is performed at similar salt concentration.**

<i>NaCl (mM)</i>	<i>K<sub>D</sub> (μM)</i>
100	0.02 ± 0.01
125	0.12 ± 0.02
150	0.17 ± 0.03
200	0.89 ± 0.06

**Table 7. A comparison of the  $\Gamma_{salt}$  values of SbO4L to various thrombin binding ligands from literature. It can be seen that SbO4L shows comparable salt interactions to exosite 2 binding ligands as compared to exosite 1 binding ligands.**

<i>Ligand</i>	<i><math>\Gamma_{salt}</math> (NaCl)</i>
<i>Hirugen</i>	-1.06 ± 0.02 <sup>207</sup>
<i>Thrombomodulin ± Chondroitin Sulfate</i>	-4.8 ± 0.6 <sup>207</sup>
<i>Thrombomodulin – Chondroitin Sulfate</i>	-2.2 ± 0.4 <sup>207</sup>
<i>Glycocalicin (Soluble GPIIb)</i>	-4.2 ± 0.2 <sup>79</sup>
	-4.6 ± 0.4 <sup>208</sup>
<i>Heparin</i>	-4.8 ± 0.6 <sup>209</sup>
<i>SbO4L</i>	-5.0 ± 0.2

### *Thrombin Inhibition by SbO4L can be Reversed by Protamine*

A major advantage of heparin therapy is its amenability to protamine-based reversal. It is also one of the reasons why fondaparinux continues to suffer because its iatrogenic bleeding is difficult to reverse rapidly. To test whether SbO4L inhibition of thrombin can be reversed, we studied the recovery of thrombin activity following successive introduction of protamine. Figure 32 shows the thrombin recovery profile with varying levels of protamine after achieving 50% inhibition with SbO4L. The protamine-mediated recovery profile essentially mirrors the SbO4L-induced inhibition profile. More importantly, the level of recovery is quantitative at high enough protamine concentrations. Further, the recovery was instantaneous as no extended incubation was necessary to observe reversal. The concentration of protamine necessary to recover 50% thrombin activity, i.e.,  $RC_{50}$ , could be calculated using an equation similar to the logistic equation 4 used for inhibition studies and found to be  $\sim 0.1 \mu\text{g/ml}$ , a concentration equivalent to the  $IC_{50}$  for SbO4L inhibition of thrombin.

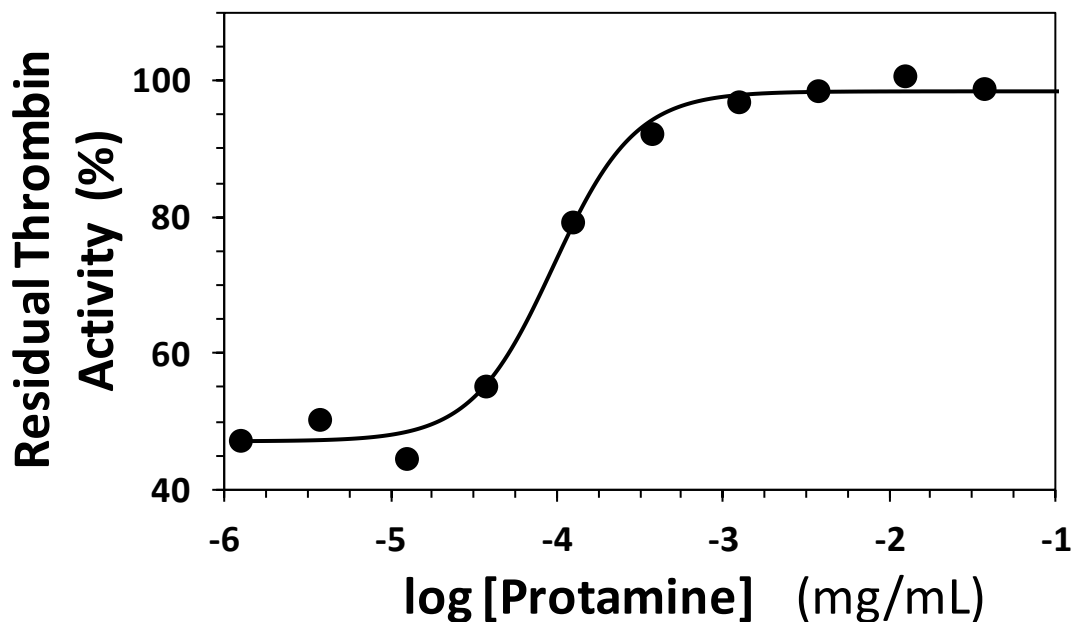


**Figure 32.** Protamine-mediated reversal of SbO4L inhibition of thrombin. Recovery of thrombin activity at varying levels of protamine following 50% inhibition by SbO4L was measured through the Spectrozyme TH hydrolysis assay at pH 7.4. Solid line represents non-linear fit of the data by a logistic function similar to equation 4 to obtain the  $RC_{50}$ , the concentration of protamine necessary to recover 50% thrombin activity.

### 3.4 Discussion

Current anticoagulation therapy largely involves heparin, heparin derivatives and vitamin K antagonists. While being inexpensive, such therapies suffer from complications such as bleeding and heparin-induced thrombocytopenia arising due to their non-selectivity in activity.<sup>210</sup> Alternative small molecule inhibitors of coagulation enzymes such as dabigatran against thrombin and rivaroxaban against factor Xa have also been proposed for therapy. But such treatments still have bleeding complications and safety concerns over long term use and are

expensive in comparison to heparins.<sup>211,212</sup> The ideal anticoagulant when compared to these would therefore have to be highly selective, with little or no side-effects, while also being inexpensive.

Thrombin, being a central enzyme in the coagulation cascade, would seem to be an ideal target for preventing coagulation. Yet due to its plastic nature, active site inhibitors of the enzyme have been unable to protect the haemostatic system from bleeding risks, and therapies targeting thrombin require frequent monitoring. On the other hand, targeting thrombin's allosteric exosites in a manner similar to nature could potentially lead to a better anticoagulant for clinical purposes.<sup>213</sup>

The design for a homogenous direct thrombin inhibitor which acts on thrombin via allosteric mechanisms has originated in the form of sulfated low molecular weight lignins.<sup>183</sup> Originally, such sulfated lignins were designed to mimic heparin.<sup>182</sup> However, heparin is devoid of any direct inhibition of thrombin, i.e. it requires antithrombin to inhibit thrombin. In contrast these sulfated lignins were found to inhibit thrombin by targeting exosite 2 without any need of serpin.<sup>183</sup> Hence the mechanism of such parent lignins was unique and not comparable to any natural ligand. Additionally, such chemoenzymatically synthesized lignins were complex heterogeneous mixtures with respect to their inter-monomeric linkages. As a result, these polymers were not selective for a single enzyme and were found to be active against a number of other heparin binding serine proteases (Table 1).<sup>185,186</sup> The predominant inter monomeric linkage found in such lignins is generally  $\beta$ -O4 type. Thus the idea arose that a chemically synthesized homogenous lignin polymer with the  $\beta$ -O4 type inter-monomeric linkage would possibly be more selective and potent as a thrombin inhibitor. The synthesis of such a molecule could further provide insight into the novelty of the mechanism.



We synthesized SbO4L using simple 7-step protocol with readily available and inexpensive starting materials. The  $\beta$ -O4 lignin polymer can be synthesized easily in two steps from the monomer **5**. To generate sufficient quantities of SbO4L for all studies, the key intermediate **5** was produced in larger quantities using a new 4-step, mild synthetic route which can be utilized in the future for creating modifications.<sup>196,197</sup> Polymerization of monomer **5** followed by reduction gave purified  $\beta$ -O4 lignin using methods described before.<sup>198,199</sup> Ultimately, the sulfation of the lignin so synthesized yielded SbO4L. The SbO4L so produced was characterized utilizing elemental analysis and SEC, while batch-to-batch reproducibility of the synthesis to produce biosimilars was established using RPIP-UPLC-MS fingerprinting and thrombin inhibition assay. Overall, the synthetic procedure yielded highly reproducibly active SbO4L which can be scaled up for the most part.

SbO4L was found to inhibit thrombin and plasmin with high potency and selectivity over other serine proteases. Such selectivity is remarkable when compared to previous chemoenzymatically synthesized lignins (Table 1). While inhibition of plasmin may seem to thwart the anticoagulant potential of SbO4L, free plasmin is not normally present in blood and is often neutralized by  $\alpha$ 2-antiplasmin and  $\alpha$ 2-macroglobulin, which ensures buildup of plasmin for antifibrinolytic activity takes several hours.<sup>214,215</sup> As a result the antifibrinolytic effect of SbO4L may not be observed if it successfully prevents clot formation in the first place. Moreover, SbO4L might be capable of providing better prophylactic anticoagulation by preventing the fibrinolysis of already formed clots, thereby preventing bleeding but simultaneously preventing new clot formation. Clinically, this dual mechanism of anticoagulation and plasmin inhibition by SbO4L could prove useful in disseminated intravascular coagulation (DIC) which can be caused by sepsis, surgery or trauma, cancer and complications during pregnancy or childbirth.<sup>185,216,217</sup>

DIC manifests when there is widespread clotting due to thrombin mediated coagulation and paradoxical bleeding due to plasmin mediated fibrinolysis.

Mechanistically SbO4L was found to inhibit thrombin without the help of antithrombin III. While addition of antithrombin III does not result in an increased potency, it does increase the efficacy (indicated by the decrease in  $Y_M$  and  $Y_0$  values) of SbO4L mediated thrombin inhibition. These results suggest an independent mechanism of SbO4L and antithrombin against thrombin. In comparison parent LMW lignins showed increased potency in the presence of antithrombin III.<sup>191</sup> Thus SbO4L is mechanistically more selective than parent lignins.

Since thrombin plays vital anticoagulant functions by binding to thrombomodulin, we investigated if SbO4L abrogates such antithrombotic action by testing it against thrombomodulin thrombin complex for physiological substrate activated protein C. Our results indicated clearly that SbO4L is a more potent inhibitor of free thrombin compared to the anticoagulant form of thrombin. Thus SbO4L could be used to shift the population of thrombin in the blood from a net procoagulant state to thrombomodulin bound anticoagulant state. Furthermore, combining SbO4L with thrombomodulin as a therapy for DIC could prove very useful in management of the coagulopathy.

SbO4L inhibits a variety of types of thrombin from different species as well as thrombin degradation products in an equipotent manner. This is important because significant structural differences exist between different types of thrombin among species and thrombin degradation products. For example, in place of Asp222 in the sodium binding site, murine thrombin has a Lys222 which results in a charge reversal substitution in the Na<sup>+</sup> binding loop.<sup>218</sup> This allows the N $\zeta$  atom of the Lys222 of murine thrombin to mimic the positive charge of the Na<sup>+</sup> and mimic the cation, thereby locking the enzyme in a “fast-form” which is also believed to be the

procoagulant form. SbO4L's equipotent inhibition of murine thrombin is a sign that the molecule is capable of inhibiting the fast-form of thrombin. This is also important from a translational point of view to show that SbO4L based inhibition can possibly be tested in mouse thrombosis models. Bovine thrombin on the other hand shows differences in the Tyr-Pro-Pro-Trp segment of the 60-loop, Glu-192 and catalytic residues His57 and Ser195.<sup>219</sup> SbO4L inhibition of bovine thrombin further confirms that the molecule possibly binds at the more conserved exosite 2 rather than the structurally different active site when compared to human thrombin. Human  $\gamma$ -thrombin is a degradation product of human  $\alpha$ -thrombin in which the exosite 1 is disordered.<sup>220</sup> As a result of this  $\gamma$ -thrombin has a disrupted capability for cleaving physiological substrate fibrinogen to form a clot.<sup>221</sup> SbO4L shows potent inhibition of  $\gamma$ -thrombin, albeit with 2-fold lower activity. This was important from future translational research in establishing SbO4L antiplatelet activity. SbO4L was also found to inhibit thrombin while using fibrinogen as a substrate with comparable potency to the chromogenic substrates. This is fundamental for development of any anticoagulant to ultimately be useful with physiologically relevant substrates.

The mechanism by which SbO4L inhibits thrombin was deduced by an amalgamation of Michaelis-Menten kinetics, competition and mutagenesis studies. Michaelis-Menten kinetics data showed that SbO4L inhibition is non-competitive with chromogenic substrate and is therefore binding at an allosteric site – away from the active site of the enzyme. Binding of SbO4L was found to induce allosteric change in the active site conformation as was confirmed using collisional quenching.

Competition with known exosite 2 ligands unfractionated heparin (UFH) and GPIIb $\alpha$  and exosite 1 ligand hirugen peptide further help locate SbO4L binding at exosite 2 of thrombin.

Using specific single and triple mutants of exosite 2 basic residues, it was concluded that SbO4L requires Arg233, Lys235 and Lys236 of thrombin exosite 2 for binding. These residues are known to be vital for the interaction of sulfated tyrosine-rich anionic peptide (STRAP) of GPIIb $\alpha$ , a platelet surface glycoprotein, with thrombin.<sup>79,115-118</sup> Structurally this STRAP resembles the aromatic-sulfate strategy observed in SbO4L and hence it can be imagined that the binding sites of the two molecules are overlapping. Mechanistically, it is known that GPIIb $\alpha$  can inhibit thrombin's fibrin formation activity via binding to exosite II, which is comparable to SbO4L.<sup>79,80</sup> However, this site of thrombin has never been explored previously from a potential drug-targeting perspective.

Characterizing the binding nature of SbO4L to thrombin, using a salt dependant study of binding affinity helped in identifying that the nature of the interactions has a high ionic component similar to other known exosite 2 ligands (Table 8). This study indicated that approximately 5 sulfate groups were involved in the binding of SbO4L to thrombin. This result when taken together with the elemental and size exclusion chromatography data, suggests that the actual pharmacophore moiety of SbO4L may be a simple dimeric-pentameric lignin molecule.

Lastly, we have demonstrated the possibility of reversing SbO4L activity using FDA approved protamine in an in vitro assay. From a therapeutic point of view, these results suggest that an antidote for SbO4L is already present in the market. Hence establishing safety windows should be easier knowing that the antidote is at hand.

Overall, we have shown a significant step forward from parent LMW lignins in terms of homogeneity, ease and reproducibility of synthesis, potency and selectivity with the development of SbO4L. Furthermore, we have been able to compare the mechanism of SbO4L with an

endogenous ligand in the form of GPIb $\alpha$ . Our in vitro studies have helped us identify a potential pathway to develop smaller and more homogenous molecules to target the GPIb $\alpha$  site by mimicking SbO4L. However, further validation of targeting this site was required in higher order assays such as in plasma, whole blood and even in vivo.

## Chapter 4: Advanced Level Characterization of Antithrombotic Potential of SbO4L

### 4.1 Introduction

Annually, more than 100 publications present data on thrombin inhibitors, yet only a small percentage of the publications involve new chemistry.<sup>3</sup> The majority of small molecules out of these target the active site of thrombin. This trend is gradually changing as allosteric inhibitors are gaining more importance. Targeting the active site results in complete knockout of the enzyme and hence results in complicated clinical outcomes. As a result there is a large amount of research being performed on determining the efficacy, pharmacology, toxicology and clinical outcomes of thrombin inhibitors.

SbO4L, a completely synthetic sulfated  $\beta$ -O4 lignin, was found to be a potent and selective inhibitor of thrombin when tested in vitro. We established that the mechanism involved in SbO4L mediated anticoagulation was unique in that it mimicked the platelet receptor GPIb $\alpha$ . Similar to GPIb $\alpha$ , SbO4L is known to reduce the catalytic efficiency of thrombin towards fibrinogen cleavage by binding to exosite 2 of thrombin.<sup>79</sup> Competition and mutagenesis data highlighted the fact that the binding site was identical to the GPIb $\alpha$ -STRAP. Physiologically thrombin binding to GPIb $\alpha$  is vital for procoagulant platelet aggregation and activation functions.<sup>81,222</sup>

For any new mechanism of anticoagulation to be clinically relevant, it has to translate well from in vitro assays to ex vivo and finally to in vivo tests. Therefore, it is vital for us to

establish that targeting the GPIIb/IIIa site on thrombin by SbO4L could yield a potentially useful antithrombotic, which is effective even in vivo. Additionally, we reasoned that the fact that SbO4L could compete and mimic GPIIb/IIIa for binding to thrombin may result in dual pharmacological actions in ex vivo and in vivo systems. We hypothesized that SbO4L could possibly act as antithrombotic using a dual mechanism, wherein, (a) it could provide an allosteric direct inhibition of thrombin to produce anticoagulant activity; and (b) it could compete with GPIIb/IIIa from binding to thrombin and thereby producing antiplatelet activity as well (Figure 33).

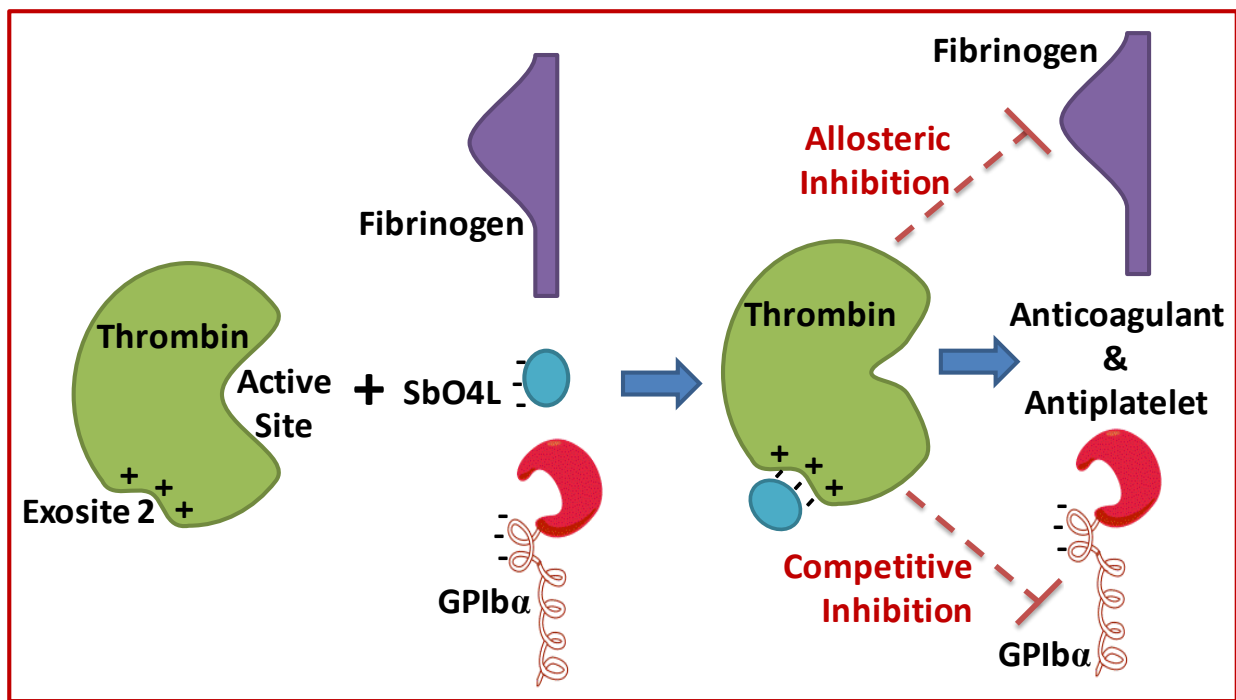


**Figure 33.** Dual mechanism of antithrombotic action by SbO4L in advanced assays. Thrombin is capable of cleaving fibrinogen using its active site, and binding to GPIIb/IIIa using its exosite 2. Binding of GPIIb/IIIa to exosite 2 causes an allosteric change within the active site. SbO4L binding to thrombin at exosite 2 in a manner similar to GPIIb/IIIa could possibly induce allosteric inhibition of thrombin towards catalytic conversion of fibrinogen resulting in anticoagulant activity, while

*also providing a competitive inhibition of thrombin binding to GPIIb/IIIa resulting in antiplatelet activity.*

To verify if our hypothesis of dual mechanism holds true in complex systems, we first tested the anticoagulant and antiplatelet activities separately in plasma and platelet rich plasma using APTT/PT assays and platelet aggregation/activation assays respectively. We then sought to investigate the properties of this dual mechanism in tandem by using whole blood with Hemostatic Analysis System and Thromboelastography tests. Finally we tested if SbO<sub>4</sub>L could provide sufficient antithrombotic effect in vivo in several mouse thrombosis models.

## **4.2 Experimental Procedures**

### *Materials*

Pooled normal human plasma for coagulation assays was purchased from Valley Biomedical (Winchester, VA). Activated partial thromboplastin time (APTT) reagent containing ellagic acid, thromboplastin-D and 25 mM CaCl<sub>2</sub> were obtained from Fisher Diagnostics (Middletown, VA). Thromboelastograph® Coagulation Analyzer 5000 (TEG®), disposable cups and pins, and 200 mM stock CaCl<sub>2</sub> were obtained from Haemoscope Corporation (Niles, IL). All other chemicals were analytical reagent grade from either Sigma Chemicals (St. Louis, MO) or Fisher (Pittsburgh, PA) and used without further purification.



### *Plasma APTT/PT Assay*

Clotting times were determined in a standard 1-stage recalcification assay with a BBL Fibrosystem fibrometer (Becton-Dickinson, Sparks, MD), as reported previously.<sup>183,184</sup> For prothrombin time (PT) assays, 10  $\mu$ l of SbO4L (or a reference agent) was mixed with 90  $\mu$ l of citrated human plasma, incubated for 30 s at 37°C, followed by the addition of 200  $\mu$ l of pre-warmed thromboplastin. For activated partial thromboplastin time (APTT) assays, 10  $\mu$ l of SbO4L solution was mixed with 90  $\mu$ l citrated human plasma and 100  $\mu$ l 0.2% ellagic acid. Clotting was initiated by adding 100  $\mu$ l of 25 mM CaCl<sub>2</sub>. Each experiment was performed in duplicate. The averaged data was plotted and a quadratic trend line was used to calculate the concentration of SbO4L that doubles the clotting time (2×APTT or 2×PT).

### *Effect of Serum Albumin on the Inhibition Efficacy of SbO4L*

The effect of serum albumin on SbO4L inhibition of thrombin was tested by assessing residual thrombin activity in 20 mM Tris-HCl, 100 mM NaCl, 2.5 mM CaCl<sub>2</sub>, 0.1% PEG 8000, pH 7.4, containing BSA at four different concentrations (0, 1, 2.5 and 10 mg/ml). Briefly, 5  $\mu$ l of 2.3 mg/ml SbO4L was incubated with 185  $\mu$ l of each of these buffers in a 96-well plate at 37°C in duplicate. To this was added 5  $\mu$ l of 240 nM thrombin, incubated for 10 minutes and 5  $\mu$ l of 5 mM Spectrozyme TH added to measure the residual active thrombin.

### *Preparation of Platelet Rich and Platelet Poor Plasma*

Whole human blood was collected from healthy volunteers and used to prepare platelet rich plasma (PRP) by spinning at 70 x g for 10 minutes and platelet poor plasma (PPP) by spinning at 900 x g for 10 minutes. The platelet count in the PRP was adjusted to 220,000 platelets / ml using the PPP and the material was used within 4 hours of withdrawal.

### *Platelet Aggregation Assay*

The effects of SbO<sub>4</sub>L on  $\gamma$ -thrombin induced platelet aggregation were studied using the Chrono-log Model 700 Optical Lumi-Aggregometer (Chrono-Log Corporation, Havertown, PA). Briefly, 250  $\mu$ l of PRP was incubated with SbO<sub>4</sub>L (0-535  $\mu$ g/ml) for 3 minutes at 37°C. Aggregation was initiated by using either 152nM or 76nM of  $\gamma$ -thrombin. Aggregation was monitored using the optical settings of the aggregometer for at least 6 minutes.

### *ATP Secretion Assay*

The effects of SbO<sub>4</sub>L on  $\alpha$ -thrombin mediated ATP secretion were studied using the Chrono-log Model 700 Optical Lumi-Aggregometer (Chrono-Log Corporation, Havertown, PA) following manufacturers protocol with slight modification. Briefly 450  $\mu$ l of PRP was incubated with 50 $\mu$ l of CHRONO-LUME reagent containing Luciferase enzyme and 0-5 $\mu$ l SbO<sub>4</sub>L (0-248  $\mu$ g/ml final concentration in the cuvette) for 3 minutes at 37°C. One unit of CHRONO-PAR thrombin ( $\alpha$ -thrombin) was added to the solution and the luminescence was monitored for at least 6 minutes.

An ATP standard of 2 nmoles was run separately in similar conditions to standardize the luminescence and obtain quantitative results of the amount of ATP released in each run.

#### *Haemostatic Analysis System*

Analysis of platelet function and clot structure was performed using the HASTM from Hemodyne, Inc., Richmond, VA, as reported earlier.<sup>184</sup> A mixture of 700  $\mu$ l of citrated whole blood and 10  $\mu$ l SbO4L (or water as control) was co-incubated at room temperature for 5 minutes and then placed in a disposable cup. To initiate clotting, 50  $\mu$ l of 150 mM CaCl<sub>2</sub> was added. As the clotting proceeds, platelets attach to surfaces generating tension within the fibrin meshwork from which platelet contractile force (PCF) and clot elastic modulus (CEM) parameters are obtained in an automated manner.

#### *Thromboelastography TEG<sup>®</sup> Analysis of Clot Formation*

TEG<sup>®</sup> assays were performed as reported earlier.<sup>184</sup> Briefly, the assays were initiated by transferring 20  $\mu$ l of 200 mM CaCl<sub>2</sub> into the Haemoscope<sup>™</sup> disposable cup, oscillating through 4°45' angle at 0.1 Hz, followed by the addition of a mixture of 340  $\mu$ l of sodium citrated whole blood containing 10  $\mu$ l SbO4L or water (control) at 37°C. This recalcification initiates clot formation in the TEG<sup>®</sup> coagulation analyzer, which operates until all data collection (R, K,  $\alpha$  and MA) is computed in an automated manner.

### *In Vivo FeCl<sub>3</sub> Carotid Artery Thrombosis Model*

Procedures involving mice were approved by the Institutional Animal Care and Use Committee of Vanderbilt University and have been previously reported.<sup>223,224</sup> Wild type C57Bl/6 mice were anesthetized with 50 mg/kg IP pentobarbital. SbO<sub>4</sub>L (0, 100, 300, 500 or 1000 µg in 100 µl phosphate buffered saline) was infused into the right internal jugular vein. Five minutes after infusion, the right common carotid artery was exposed and fitted with a Doppler flow probe (Model 0.5 VB, Transonic System, Ithaca, NY). Thrombus formation was induced by applying two 1 x 1.5 mm filter papers (GB003, Schleicher & Schuell, Keene, NH) saturated with FeCl<sub>3</sub> (3.5% solution) to opposite sides of the artery for three min. After washing the site of injury with PBS, flow was monitored for 30 min. Mice were sacrificed by pentobarbital overdose after conclusion of the experiment, while under anesthesia.

### *In Vivo Rose-Bengal Laser Thrombosis Model*

In vivo testing using Rose Bengal thrombosis model was adapted from previously reported literature.<sup>224</sup> C57Bl/6 mice were anesthetized as above and 500 µg of SbO<sub>4</sub>L in 100 µl phosphate buffered saline was infused into the right internal jugular vein. Five minutes after infusion, Rose Bengal (75mg/kg) was infused through the internal jugular vein, and the carotid artery was illuminated with a 1.5 mW 540 nm laser (Melles Griot, Carlsbad, CA) positioned 6 cm from the artery. Flow was monitored for 120 min. Mice were sacrificed by pentobarbital overdose after conclusion of the experiment, while under anesthesia.

### *Tail Bleeding Time*

Tail bleeding assays offer a measure of hemostasis in the presence of SbO4L. To perform the tail bleeding assay, the mice are anesthetized as mentioned above, following which the animal is placed on a 37 °C heating pad. 100 µl SbO4L is then injected into a lateral vein using a 1 ml tuberculin syringe fitted with a 27-gauge needle. The tail is trasected with a scalpel just above the tip. The bleeding tail is immersed in a centrifuge tube filled with PBS and kept at 37 °C. The animal is observed for up to 1000 seconds and the time required to cease the bleeding is noted. Mice are sacrificed prior to recovering from bleeding.

## **4.3 Results**

### *SbO4L Prolongs Clot Formation in Plasma APTT/PT Assays*

Prothrombin (PT) and activated partial thromboplastin times (APTT) are traditional measures of the anticoagulation state of human plasma. Figure 34 shows the variation in plasma PT and APTT in the presence of SbO4L. A significant concentration-dependent prolongation of clotting times was observed suggesting good anticoagulation potential. A 2-fold increase in PT required 68 µg/ml of SbO4L, corresponding to 7.5 µM, which is significantly lower than that needed for a generic LMWH (142 µg/ml, 31.6 µM) and a clinically used LMWH (enoxaparin, 339 µg/ml or 75 µM).<sup>184</sup> Likewise, a two-fold increase in APTT required 20 µg/ml (2.2 µM) of SbO4L, which compares favorably with a concentration of 5.9 µg/ml (1.3 µM) for generic LMWH in inducing plasma anticoagulation.

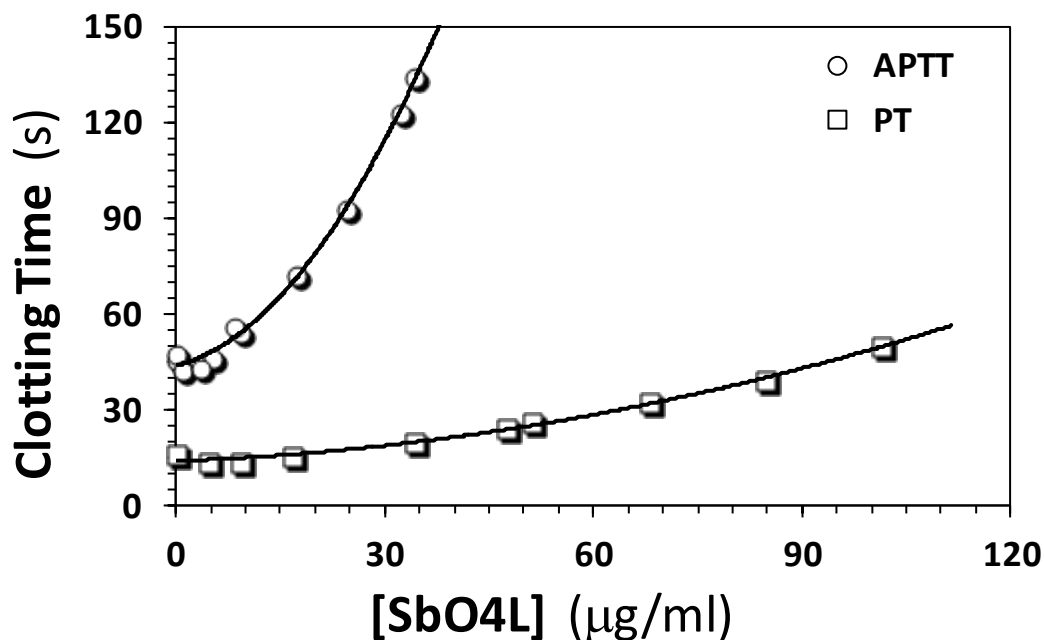


**Figure 34.** Prolongation of clotting time as a function of *SbO4L* concentration in either the prothrombin time (PT) or the activated partial thromboplastin time (APTT) assay. The solid lines are trend lines, and not exponential fits.

#### *SbO4L Inhibition of Thrombin is Abrogated in the Presence of Albumin*

Despite this high potency (comparable to enoxaparin), *SbO4L* displays a loss of ~100–340-fold in potency in human plasma from that in *in vitro* enzyme systems. To assess the basis for this difference, we studied the effect of serum albumin on the effectiveness of *SbO4L*. Figure 35 shows the change in relative thrombin activity in the presence of fixed concentration of *SbO4L* and varying concentrations of bovine serum albumin (BSA), a surrogate for its human counterpart. In the absence of BSA, thrombin’s hydrolytic activity was 22% ( $[SbO4L] = 0.42 \mu\text{g/ml}$ ), which was found to increase to 56, 59 and 72% in the presence of 1, 2.5 and 10 mg/dl BSA, respectively. This suggests that the presence of BSA results in a significant drop in inhibitor potency probably arising from non-specific sequestering of *SbO4L*. Interestingly, a

maximal thrombin activity of ~75% is reached suggesting that some SbO4L remains free, and therefore inhibitory, at high enough plasma albumin concentration.

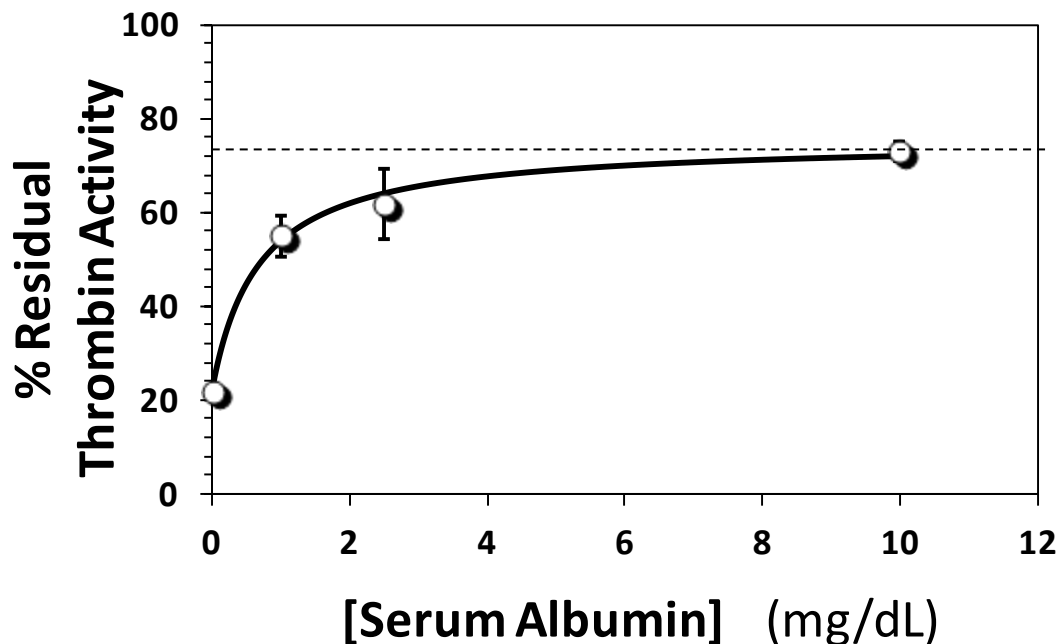


*Figure 35. The effect of serum albumin on the thrombin inhibition potential of SbO4L. Solid line to the data represents a rectangular hyperbolic fit to the data to derive the maximal thrombin activity at limiting concentrations of BSA. The dotted line represents the maximal thrombin activity. See text for details.*

#### *SbO4L Potently Inhibits Platelet Aggregation in Platelet Rich Plasma (PRP)*

The idea that targeting GPIIb/IIIa could also be utilized to prevent platelet aggregation and activation for antithrombotic potential has been around.<sup>159</sup> Since SbO4L binds to identical binding site as GPIIb/IIIa and competes with it, we tested the effects our molecule had on thrombin mediated platelet aggregation. An optical method to monitor platelet aggregation was used which

employs an increase in transmittance of platelet rich plasma (PRP) as a signal for aggregation under high shear. The use of  $\gamma$ -thrombin was done so as to monitor purely platelet aggregation activity without interference by fibrin mesh formation (Figure 36).<sup>123</sup> Two different test concentrations of  $\gamma$ -thrombin were used as the trigger and it was noticed that as the concentration of the activating thrombin was lowered from 152 nM and 76 nM (Figure 37A and 37B respectively), the amount of SbO4L required to prevent platelet aggregation was also reduced from 321  $\mu\text{g/ml}$  to 105  $\mu\text{g/ml}$ . Furthermore at all doses of SbO4L, a unique platelet response was observed in which the platelets would initiate aggregation no matter how high the concentration of SbO4L, but after reaching its peak aggregation would start showing a reduced transmittance(Figure 37C). This could be a result of change of shape of the platelets or disaggregation.

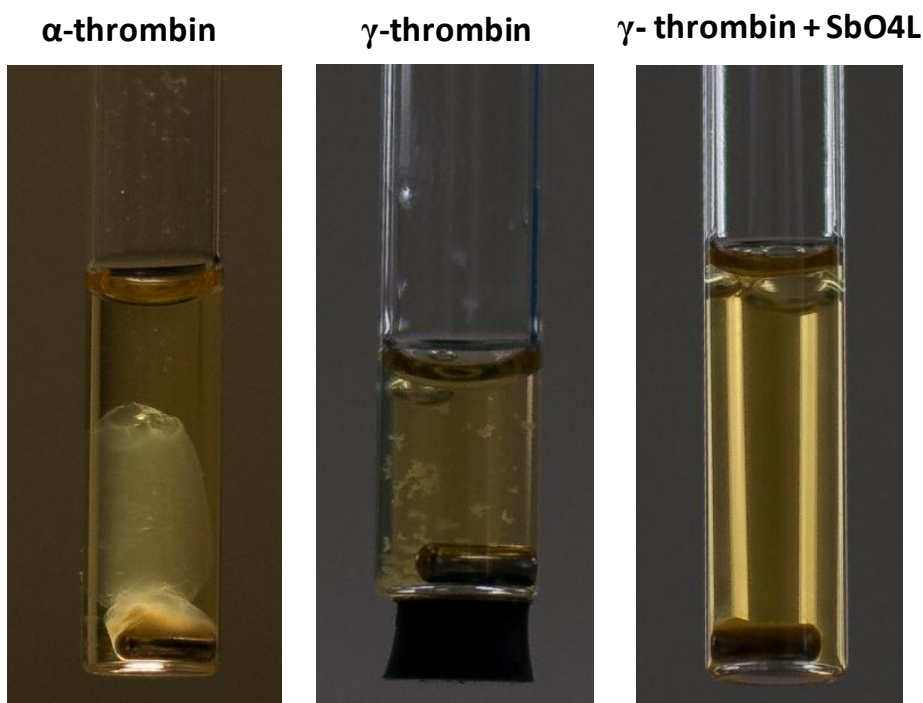


**Figure 36.** A comparison of  $\alpha$ -thrombin and  $\gamma$ -thrombin as platelet aggregation initiators.  $\alpha$ -thrombin causes the formation of a fibrin mesh which traps the platelet aggregates. In comparison,  $\gamma$ -thrombin creates aggregates without any formation of fibrin network. The last



image shows that in the presence of SbO4L,  $\gamma$ -thrombin is incapable of forming platelet aggregates.

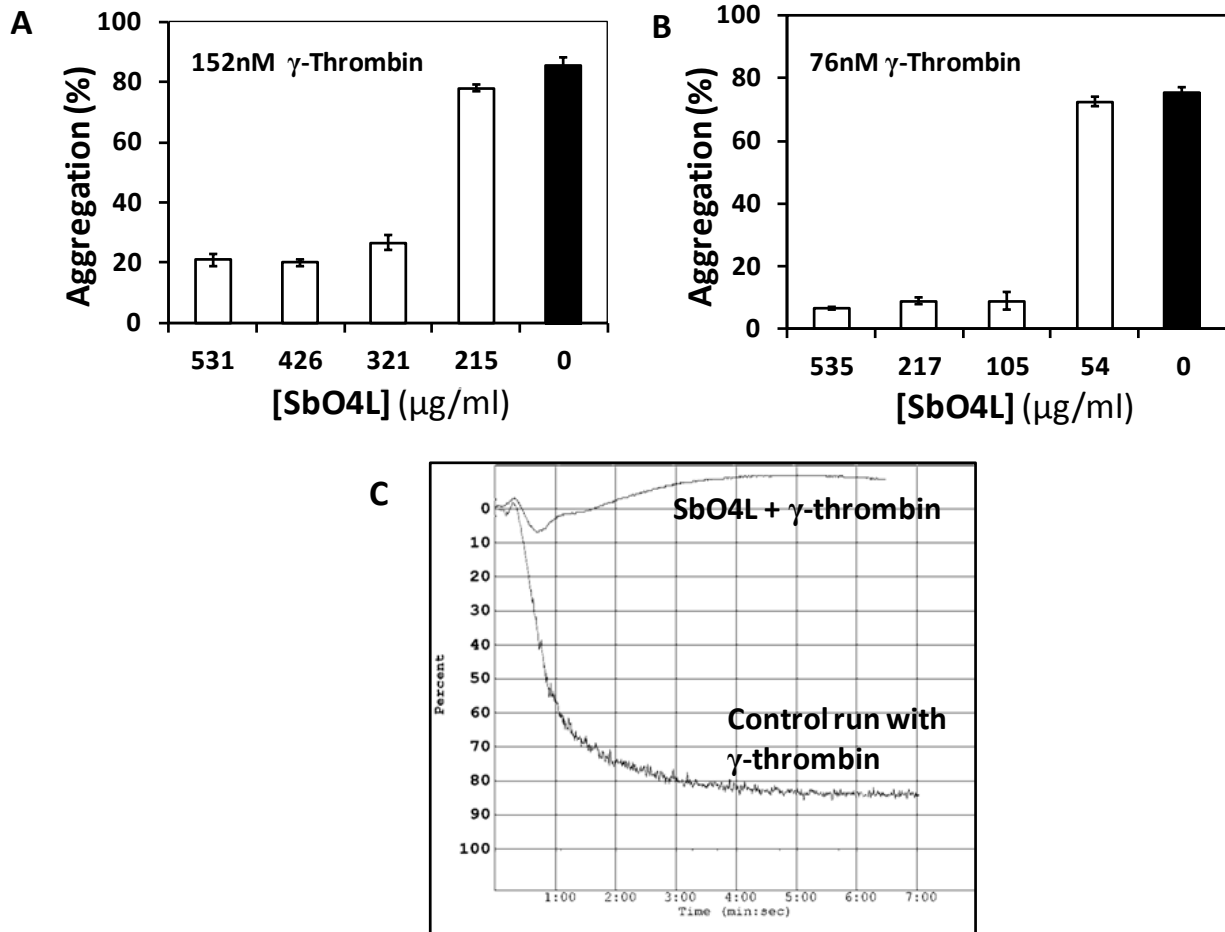


**Figure 37.** Variation in level of platelet aggregation as a function of the concentration of SbO4L. Platelet aggregation was measured in the presence of varying concentrations of SbO4L using either 152 nM (A) or 76 nM (B)  $\gamma$ -thrombin as the trigger. Representative traces (C) of human platelet rich plasma (PRP) aggregation induced by 76 nM  $\gamma$ -thrombin in the presence or absence of 217  $\mu\text{g/mL}$  SbO4L. Aggregation was monitored by following time dependence of transmittance at 620 nm following addition of  $\gamma$ -thrombin.

*SbO4L Potently Prevents ATP Secretion by Platelets in PRP*

To assess platelet activation, ATP secretion was monitored using luminescence method of monitoring ATP release by using luciferase enzyme under high shear. Use of  $\alpha$ -thrombin was possible in this assay due to the fact that fluorescence detections were independent of fibrin formation. It was observed that 248  $\mu\text{g/ml}$  of SbO4L potently inhibited ATP release by 85% when 1 unit of  $\alpha$ -thrombin was used to trigger platelet activation (Figure 38), and a dose dependant increase in ATP release was observed with decrease in SbO4L.

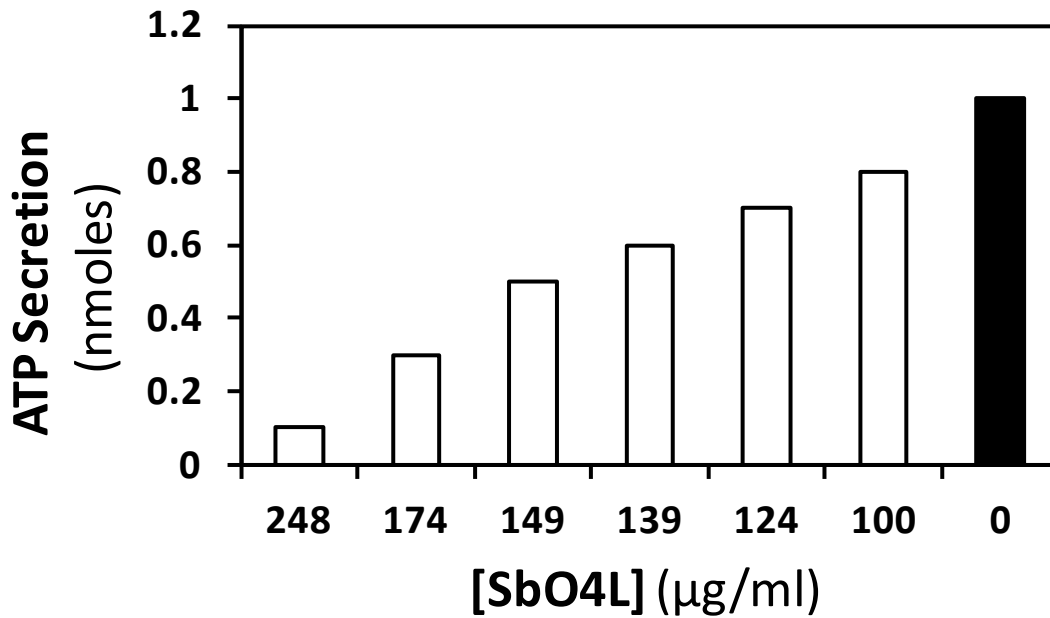


**Figure 38.** Reduction in the level of ATP released by platelets in the presence of varying levels of SbO4L. ATP release by platelets was monitored using luminescence in the presence of luciferase enzyme.

*SbO4L Inhibits Platelet Prothrombotic Function in Whole Blood when Analyzed using Hemostasis Analysis System (HAS)*

To further assess the whole blood anticoagulant potential of SbO4L, we utilized HAS™, which evaluates platelet contribution to clot formation (Figure 39).<sup>184</sup> This technique evaluates clot structure through the measurement of clot elastic modulus (CEM), which is the ratio of stress induced by platelets to strain arising from the change in clot thickness. The technique also provides information on contractile forces between platelets, i.e., the platelet contractile force (PCF), that adhere to surfaces and restrict relative movement of two cups. PCF depends on the platelet number, their metabolic status, presence of thrombin inhibitors and degree of GPIIb/IIIa exposure.<sup>225</sup> On the other hand, CEM depends on the clot micro-structure, fibrinogen concentration, and thrombin formation rate. It has been suggested that PCF and CEM changes can be correlated with susceptibility to bleeding and/or thrombotic tendency.

SbO4L affects PCF and CEM in a dose-dependent manner (Table 8). As the concentration of SbO4L increases from 0 to 74 µg/ml, the PCF and CEM decrease from 8.0 to 0.7 kDynes and 18.3 to 0.6 kDynes/cm<sup>2</sup>, respectively (Figure 39A and 39B, Table 8). When comparisons are made with enoxaparin, strikingly similar results are observed except for the range of concentration used for the clinically used anticoagulant. Whereas PCF value of 0.7 was achieved at 74 µg/ml (8.1 µM) for SbO4L, it was achieved at 2.0 µg/ml (444 nM) for enoxaparin suggesting a ~37-fold better potency for the latter on weight basis and ~18-fold better potency on molar basis. These results further confirm that SbO4L mediated targeting of the GPIIb site of thrombin exosite II could be useful in creating future antithrombotics.

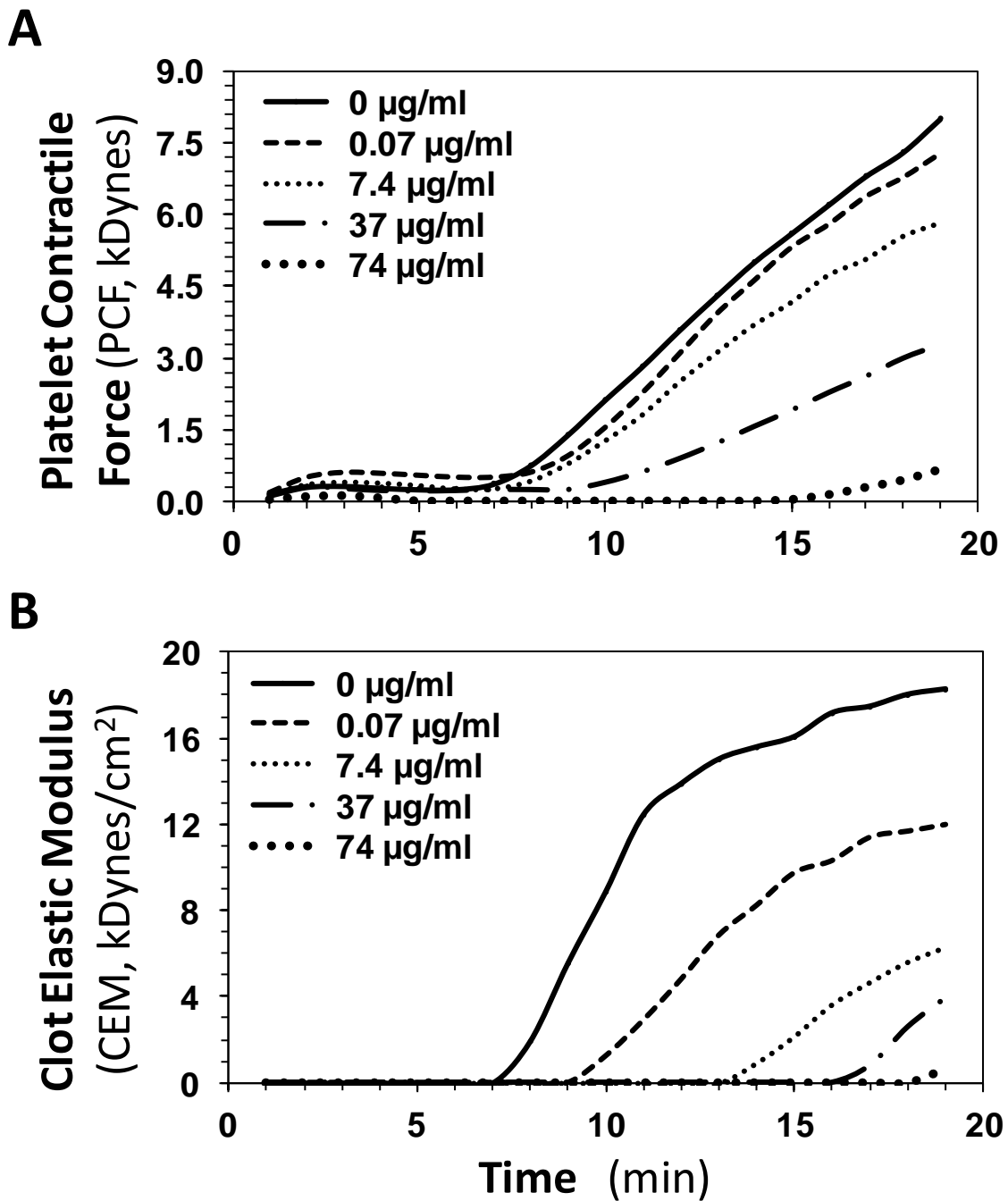


*Figure 39. Comparison of the effect of SbO<sub>4</sub>L on platelet function in whole blood using hemostasis analysis system (HAS<sup>TM</sup>). (A) and (B) show the change in platelet contractile force (PCF) and clot elastic modulus (CEM), respectively, with time at various fixed concentrations of SbO<sub>4</sub>L (0–74 µg/ml).*

**Table 8. Hemostasis Analysis System Parameters for SbO4L Anticoagulation in Comparison to Enoxaparin.**

	<i>Hemostasis Analysis</i> *			
	<i>[Conc]</i> ( $\mu\text{g/ml}$ )	<i>TOT</i> * ( <i>min</i> )	<i>PCF</i> * ( <i>kDynes</i> )	<i>CEM</i> * ( <i>kDynes/cm<sup>2</sup></i> )
<b>SbO4L</b>	0	6.3	8.0	18.3
	0.07	5.1	7.3	12.0
	7.4	6.6	5.8	6.3
	37	11.3	3.3	3.9
	74	13.6	0.7	0.6
<b>Enoxaparin</b>	0	3.6	7.6	21.6
	0.7	5.2	5.3	15.1
	1.0	9.1	3.6	12.7
	1.6	11.0	2.8	8.5
	2.0	12.5	0.9	2.9

\*Analysis was performed using Hemostasis Analysis System (HAS) on human whole blood as described in 'Experimental Procedures'. Parameters deduced from this analysis included TOT (thrombin onset time), PCF (platelet contractile force) and CEM (clot elastic modulus).

*SbO4L Inhibits Thrombus Formation in Whole Blood when Analyzed using Thromboelastography (TEG)*

To evaluate SbO4L as an anticoagulant in whole blood, we employed TEG<sup>®</sup>, which is quite often used to monitor anticoagulation therapy with LMWH.<sup>184</sup> TEG<sup>®</sup> assesses the nature of physical forces within a clot, which are dramatically affected by the presence of an anticoagulant in blood. In a nutshell, the clot formation in TEG<sup>®</sup> is recorded as a force transduced on a pin at the center of a blood-containing cup. Several parameters are evaluated from this force measurement including maximum amplitude (MA), the shear elastic modulus (G), the reaction

time (R) and the angle  $\alpha$ . MA and G are measures of clot stiffness, while R and  $\alpha$  are measures of the rate of clotting. Figure 40 shows the output obtained from the instrument.

Table 9 shows the change in R,  $\alpha$ , MA and G parameters as a function of the concentration of SbO4L. Briefly, as the concentration of SbO4L increases from 0 to 152  $\mu\text{g/ml}$ , R increases from 7.7 to 25.9 min, while  $\alpha$  decreases from  $56^\circ$  for normal blood to  $22^\circ$  indicating that the kinetics of fibrin polymerization and network formation is significantly depressed by the presence of SbO4L. Enoxaparin behaves in a similar manner, except that its effective concentrations range from 1–5  $\mu\text{g/ml}$ . Likewise, SbO4L reduces MA and G in a manner similar to enoxaparin (Table 10), except for the  $\sim 30$ -fold better potency of the latter ( $\sim 15$ -fold molar basis).

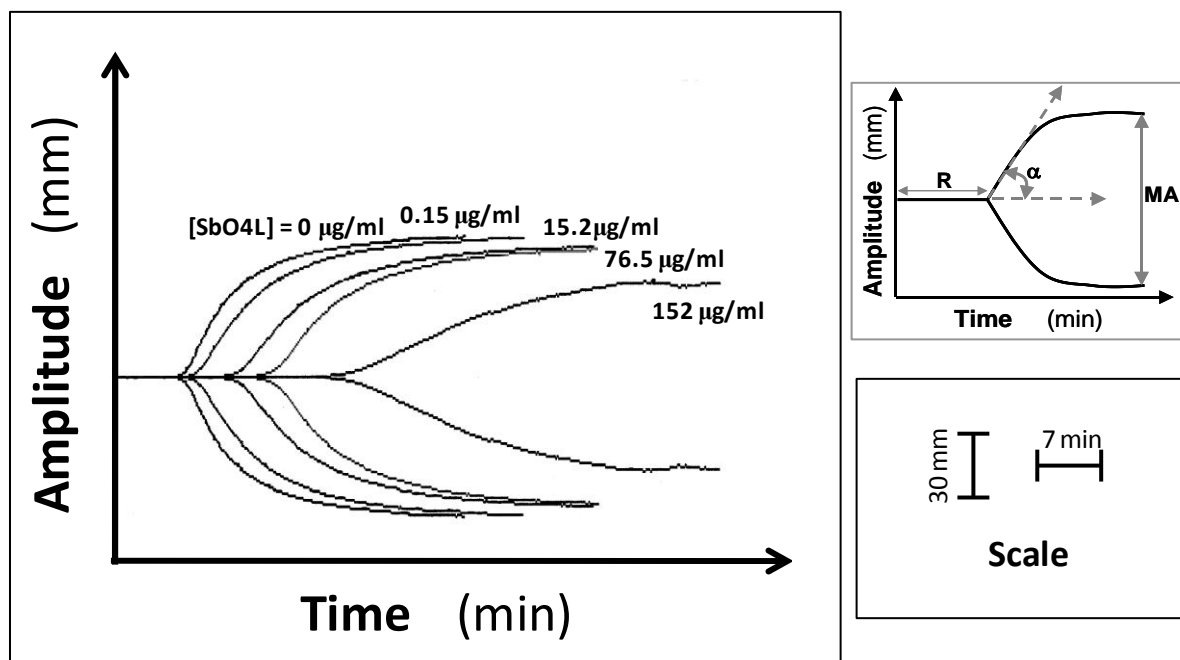


**Figure 40.** Effect of SbO4L on whole blood hemostasis using Thromboelastography (TEG). Insert on the right shows different parameters obtained from TEG study. SbO4L shows a dose

dependant change in clotting parameters MA, R,  $\alpha$  and G, with a doubling in clot initiation time (R) at 76.5  $\mu\text{g/ml}$ .

**Table 9. Thromboelastography Parameters for SbO4L Anticoagulation in Comparison to Enoxaparin**

	<i>Thromboelastography</i> <sup>*</sup>				
	[Conc] ( $\mu\text{g/ml}$ )	R <sup>*</sup> (min)	$\alpha$ <sup>*</sup> (degs)	MA <sup>*</sup> (mm)	G <sup>*</sup> (kDynes/cm <sup>2</sup> )
<b>SbO4L</b>	0	7.7	56.0	61.0	7821
	0.15	8.9	50.5	50.5	7658
	15.2	13.2	42.5	57.0	6628
	76.5	16.9	43.0	55.5	6236
	152	25.9	22.0	41.5	3547
<b>Enoxaparin</b>	0	7.0	59.0	56.5	6457
	1.35	8.0	49.0	51.0	5204
	2.7	11.5	43.0	47.0	4434
	3.4	14.0	41.0	46.0	4260
	4.5	17.0	31.5	42.0	3621

*\*Analysis was performed using thromboelastography (TEG) on human whole blood as described in 'Experimental Procedures'. Parameters deduced from this analysis included R (time to clot initiation),  $\alpha$  (angle), MA (maximum amplitude) and G (shear elastic modulus).*

*SbO4L shows potent Antithrombotic Action in FeCl<sub>3</sub> Thrombosis Model, Rose Bengal Laser Injury Model and Tail-Bleeding Time In Vivo in Mice*

The antithrombotic effect of SbO4L was tested in two well-characterized arterial thrombosis models following procedures previously reported.<sup>223,224</sup> Exposure of the carotid

artery of wild type mice to a 3.5% solution of FeCl<sub>3</sub> results in formation of an occlusive platelet-rich thrombus within 15 minute (Figure 41A). SbO<sub>4</sub>L prevented occlusion of the arteries of some mice at doses of 250 or 500 µg, with all mice protected from vessel occlusion at a dose of 1000 µg (Figure 41A and 41B). FeCl<sub>3</sub> is thought to produce a severe injury accompanied by desquamation of vascular endothelium.

The effects of a 500 µg dose of SbO<sub>4</sub>L were also tested in a model in which vessel injury is produced by exposure to laser light after infusion of the dye Rose Bengal. The carotid artery is surgically made accessible and the laser light is shined upon it. The laser light converts the dye to free radicals, which result in vessel occlusion with a platelet-rich thrombus in  $44.7 \pm 6.5$  minutes in vehicle treated controls. Occlusion occurred in  $76 \pm 21.3$  minutes in animals treated with 500 µg SbO<sub>4</sub>L.

The effective dose of SbO<sub>4</sub>L that prevented thrombosis in the FeCl<sub>3</sub> model (1000 µg), also caused a marked prolongation of the tail bleeding time, from ~110 s to > 1000 s. The total blood loss was also higher from 50 µl to 120 µl.

*Note- This work was performed by the Dr. David Gailani Laboratory (Vanderbilt University Medical Center, Nashville, TN)*



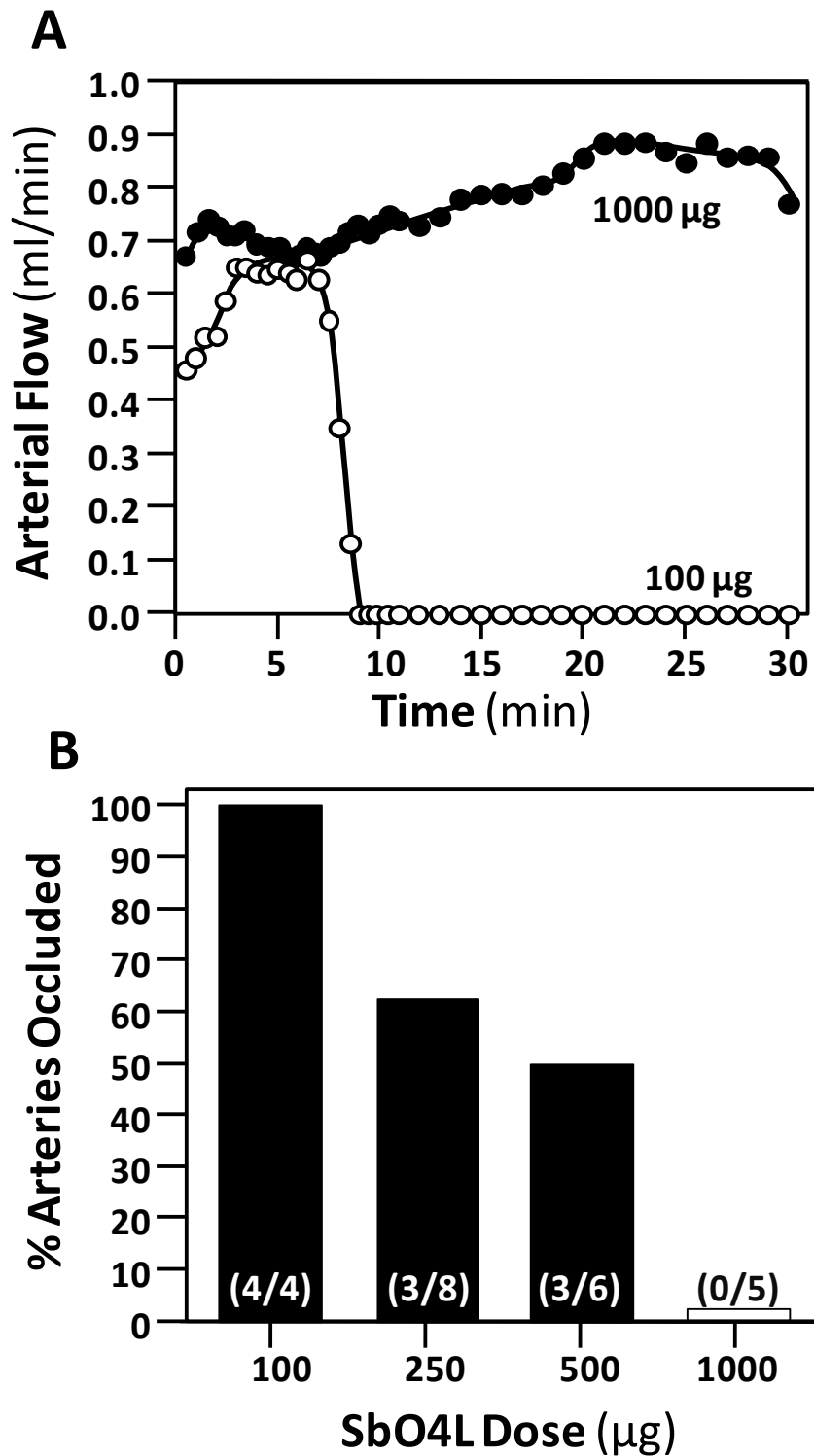


*Figure 41. In vivo anticoagulant effect of SbO4L as observed in C57BL/6 mice. (A) Measurement of arterial blood flow using Doppler flow probe, as a representation of the*

*formation of occlusive platelet-rich thrombus in the carotid artery of mice with the application of 3.5% FeCl<sub>3</sub> with a prior injection of either 100 or 1000 µg of SbO<sub>4</sub>L. (B) Dose-dependent decrease in arterial clot formation in a study with 4-8 C57BL/6 mice shows that SbO<sub>4</sub>L is most effective at a dose of 1000 µg.*

#### **4.4 Discussion**

In order to test if the in vitro efficacy holds true ex vivo and in vivo, we put SbO<sub>4</sub>L through an array of assays in ascending order of complexity. Furthermore, such assays helped in characterizing the dual mechanism of antithrombosis demonstrated by SbO<sub>4</sub>L, which is truly unique in comparison to any known molecule.

First, to test the anticoagulant activity, SbO<sub>4</sub>L was tested in classical APTT and PT assays which are standard assays often used to test anticoagulant drugs.<sup>226,227</sup> SbO<sub>4</sub>L was found to double the clotting times in both the assays 20 and 68 µg/ml concentrations, which was comparable to clinically approved LMWH Enoxaparin. More importantly since there is only a 3-fold difference between 2xAPTT and 2xPT values, suggesting that in advanced systems, SbO<sub>4</sub>L is possibly inhibiting the common pathway of coagulation involving thrombin alone, with little side reaction more with the intrinsic pathway. These results agree well with the screening information obtained from the in vitro tests. Interestingly, prolonging the APTT rather than PT might be vital to prevent thrombosis and thromboembolism.<sup>228</sup> Hence SbO<sub>4</sub>L selectivity of effect on APTT over PT might be a boon to the molecule's safety profile.

When the quantitative numbers of the APTT and PT are compared to the in vitro results, there is a remarkable drop in activity (~ 100 fold). The most likely explanation is that SbO<sub>4</sub>L

binds to albumin in the plasma. Albumin is the most abundant carrier protein present within the blood and is known to bind almost all drugs. We successfully demonstrated that SbO4L's in vitro inhibition of thrombin is in fact lowered by the presence of serum albumin. The most interesting fact was that even at high concentrations of serum albumin, SbO4L retained some thrombin inhibitory potential. Thus it is possible that albumin binding of SbO4L might reduce the efficacy but not completely eliminate it. Additionally, this binding might extend the duration of SbO4L action as albumin binding may prove a useful reservoir for SbO4L.

To test our second hypothesis that SbO4L could possibly inhibit thrombin-mediated platelet aggregation and activation by competing with GPIb $\alpha$ , we performed extensive platelet aggregation and activation studies in platelet rich plasma (PRP). Platelet aggregation studied by light transmission and activation studied by ATP secretion using luminescence are well standardized tests used to test antiplatelet agents.<sup>229,230</sup> We found that SbO4L was a good antiplatelet agent at low concentrations. These results when taken together with the competition data, support the fact that SbO4L's competition with GPIb $\alpha$  could potentially abrogate thrombin-mediated platelet aggregation. When given in vivo, it is highly probable that both mechanisms, i.e., anticoagulation and antiplatelet, play a role. Further, our studies showed that the amount of SbO4L required to thwart the platelet aggregation was related to the amount of the triggering agent used. This could be an important observation, which might affect dosing regimens in future studies.

SbO4L was then tested in whole blood using HAS and TEG. Whole blood is a system in which both coagulation and platelets play a role. While the HAS system tests the platelet functions more closely, TEG is useful to look at the coagulation parameters. Both systems are often used to monitor and test anticoagulant and antiplatelet therapy clinically.<sup>229-231</sup> In both, the

HAS and TEG studies, SbO4L showed good potency comparable to the concentrations used in the plasma and PRP assays. Furthermore, in both assays SbO4L's potency was comparable to clinically used enoxaparin, suggesting that SbO4L's antithrombotic potential could be useful.

The ultimate test to check for SbO4L's efficacy was performed using two in vivo arterial thrombosis models. The FeCl<sub>3</sub> mouse arterial thrombosis model has been used since 1944 to stimulate thrombosis, and is widely used to test the efficacy of anticoagulant and antiplatelet therapies.<sup>232</sup> SbO4L was found to be effective at dose of 1 mg i.v. bolus and showed a dose dependant efficacy. However, the FeCl<sub>3</sub> induced thrombosis is a severe injury cause by an "outside-in" mechanism on the vessel walls, which is unlike what is observed in pathological clotting.<sup>233</sup> We therefore also analyzed the efficacy of SbO4L using laser induced arterial thrombosis model which is physiologically more similar to what is observed in thrombotic disorders where the clotting occurs without damage to the vessel wall. We found SbO4L effective at doses of even 500 µg i.v. which is comparable to all the ex vivo data that we have obtained.

To assess the effect of SbO4L on hemostatic function, we tested the effect of the molecule on the tail bleeding time in mice. The effective dose of SbO4L in the FeCl<sub>3</sub> model (1000 µg) did show a prolonged tail-bleeding time and total blood loss compared to controls. However, this is not surprising given the molecule's dual mechanism of action. It is known that patients suffering from Bernard Soulier syndrome, who show defective expression of GPIb-IX-V complex, demonstrate such phenotype as well.<sup>234</sup> Furthermore, bleeding models only provide information about hemostasis in response to specific type of injury, and will not necessarily reflect the propensity to bleed, especially when the injury involves other body parts. Additionally, it is possible that the bleeding issues could be arising from the fact that SbO4L is

still a mixture and possibly has off-site effects elsewhere. Therefore, future smaller, homogenous derivatives of SbO<sub>4</sub>L would need to be tested in more in vitro, ex vivo and animal models in order to establish efficacy, safety and bleeding risks.

Overall, we have established that ex vivo and in vivo, SbO<sub>4</sub>L can act via a dual mechanism of anticoagulation and antiplatelet action. Furthermore, such activity gives SbO<sub>4</sub>L antithrombotic potential similar to LMWH which is clinically used. Thus targeting the GPIIb/IIIa site with more homogenous small molecules may prove to be a useful means of producing newer antithrombotic drugs, but may require some more testing to establish safety with respect to bleeding.

## Chapter 5: Identifying Novel Lignin Based Inhibitors and Mechanisms for Factor XIa

### 5.1 Introduction

As discussed in chapter 1, factor XIa (fXIa) is emerging as a useful target for prophylactic treatments of hyper-thrombotic states.<sup>145</sup> It is believed that developing novel inhibitors of factor XIa could possibly prevent thrombosis, while not causing bleeding side effects. Furthermore, an allosteric inhibitor of factor XIa could possibly fine tune this control further.

It has been reported that the allosteric inhibition of fXIa can be brought about by large molecules with highly charged polyanions such as dextran sulfate, heparin, hypersulfated heparin, sulfated pentagalloyl glucoside (SPGG) and sulfated quinazolin-4(3H)-ones (QAOs).<sup>192,194,235</sup> Although a number of active site inhibitors have been reported, there has been only one report on allosteric small-molecule inhibitors (<1000 Da) of fXIa.<sup>235</sup> These are the sulfated QAOs, that demonstrated a maximum potency of only 52  $\mu$ M. This leaves room for more potent small-molecule allosteric inhibitors for fXIa to be discovered. The sulfated QAOs were found to bind near the heparin binding site (HBS). Sulfated QAOs are expected to display poor bioavailability owing to their large size and high charge density. Finally, no inhibitor of factor XIa has been approved for use as anticoagulant in the clinic.

Chemo-enzymatically synthesized LMW lignins were found to be potent inhibitors of factor XIa with  $IC_{50}$  ranging from 22-176 nM (Table 1). Such lignins presented diversity in their

inter-monomeric, linkage which resulted in lack of selectivity and were found to be potent inhibitors of other serine proteases as well. Hence, it was necessary to fish-out structural components from these mixtures with selective activity for specific target serine proteases. Interestingly, the chemically synthesized SbO4L, which has only the  $\beta$ -O4 type inter-monomeric linkage was found not to be a potent inhibitor of factor XIa ( $IC_{50} = 89 \mu\text{g/ml}$  or  $9.6 \mu\text{M}$ ). This suggested that it is possible that some other scaffold within the chemoenzymatic LMW lignins was more potent towards factor XIa (Figure 42).

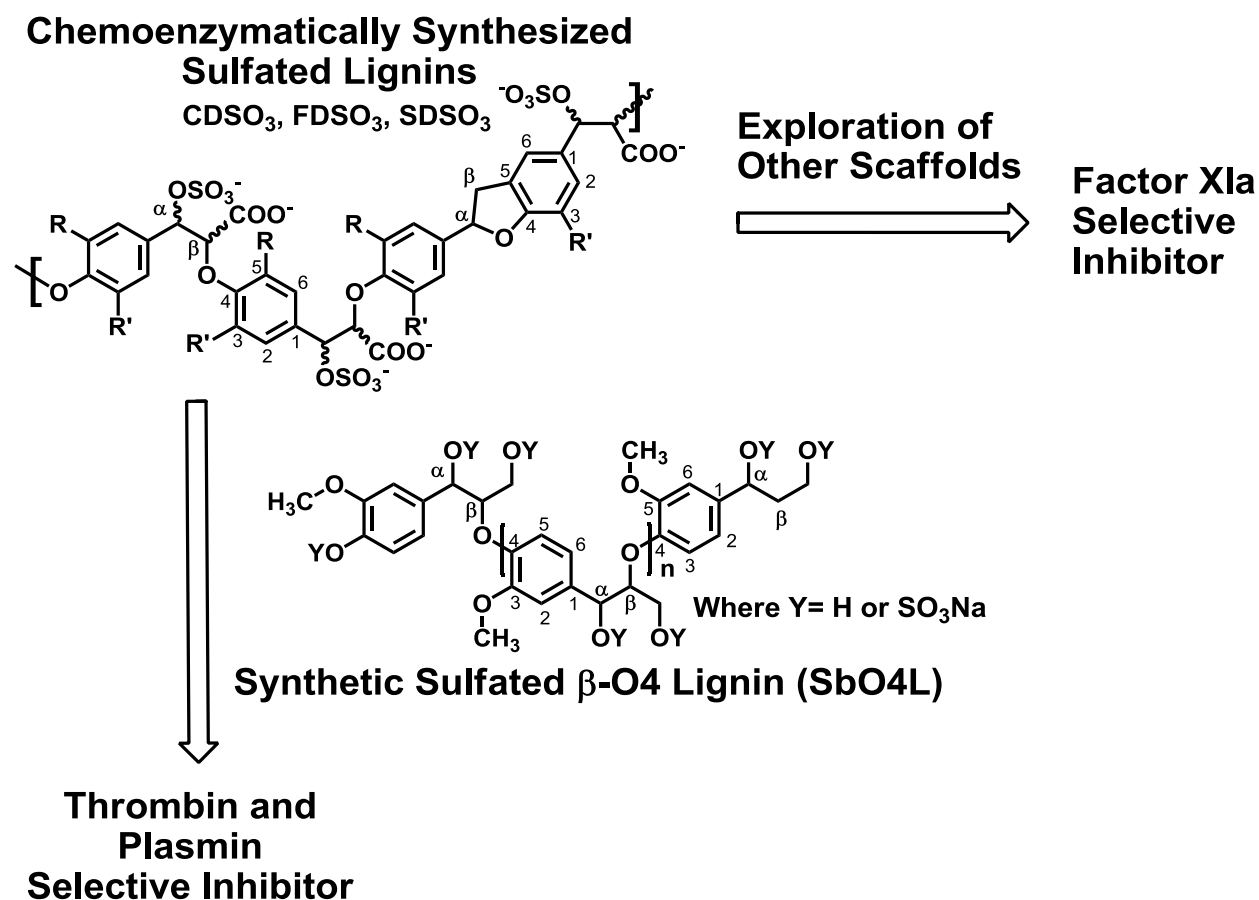


**Figure 42.** Rationale for screening sulfated small molecule library to identify factor XIa selective inhibitor. Synthetic SbO4L, which was designed from chemo-enzymatic lignins provided selective thrombin and plasmin inhibition. Therefore, it could be possible that other scaffolds

*from the parent lignins have high selectivity for other enzymes for which the chemo-enzymatic lignins showed good potency. One such enzyme of interest is factor XIa. We therefore wanted to explore possibilities for finding a factor XIa selective inhibitor through library screening of sulfated small molecules enriched in the  $\beta$ -5 type linkage mimetics in the form of the benzofuran molecules.*

In order to find such a selective inhibitor lead molecule, the Desai Lab decided to screen a library of sulfated aromatic small molecules that have been previously synthesized in our laboratory. A library of 65 molecules (Figure 43) was tested based on various scaffolds including sulfated flavonoids,<sup>236-240</sup> sulfated tetrahydro-isoquinoline,<sup>241-243</sup> sulfated quinazolinone,<sup>235</sup> sulfated benzofurans,<sup>187-189</sup> and other sulfated small molecules.<sup>242,244</sup> As a group, the library consisted of at least 12 different scaffolds allowing for a diverse range of structures to be profiled. In particular, this library was enriched in the benzofuran scaffold, which is expected to mimic the  $\beta$ -5 type linkage found in lignins and therefore explore the possibility of finding new lignin based inhibitors of factor XIa.<sup>187-189</sup> Our initial screen, followed by defined inhibition profiles identified a number of benzofuran dimers and trimers with potent inhibition of factor XIa (Table 10). In particular, molecule **24** showed highest potency at sub-micromolar concentrations ( $IC_{50} = 0.82 \mu M$ ) and was 8-fold more selective for factor XIa over thrombin ( $IC_{50} = 5.8 \mu M$ ).<sup>189</sup>



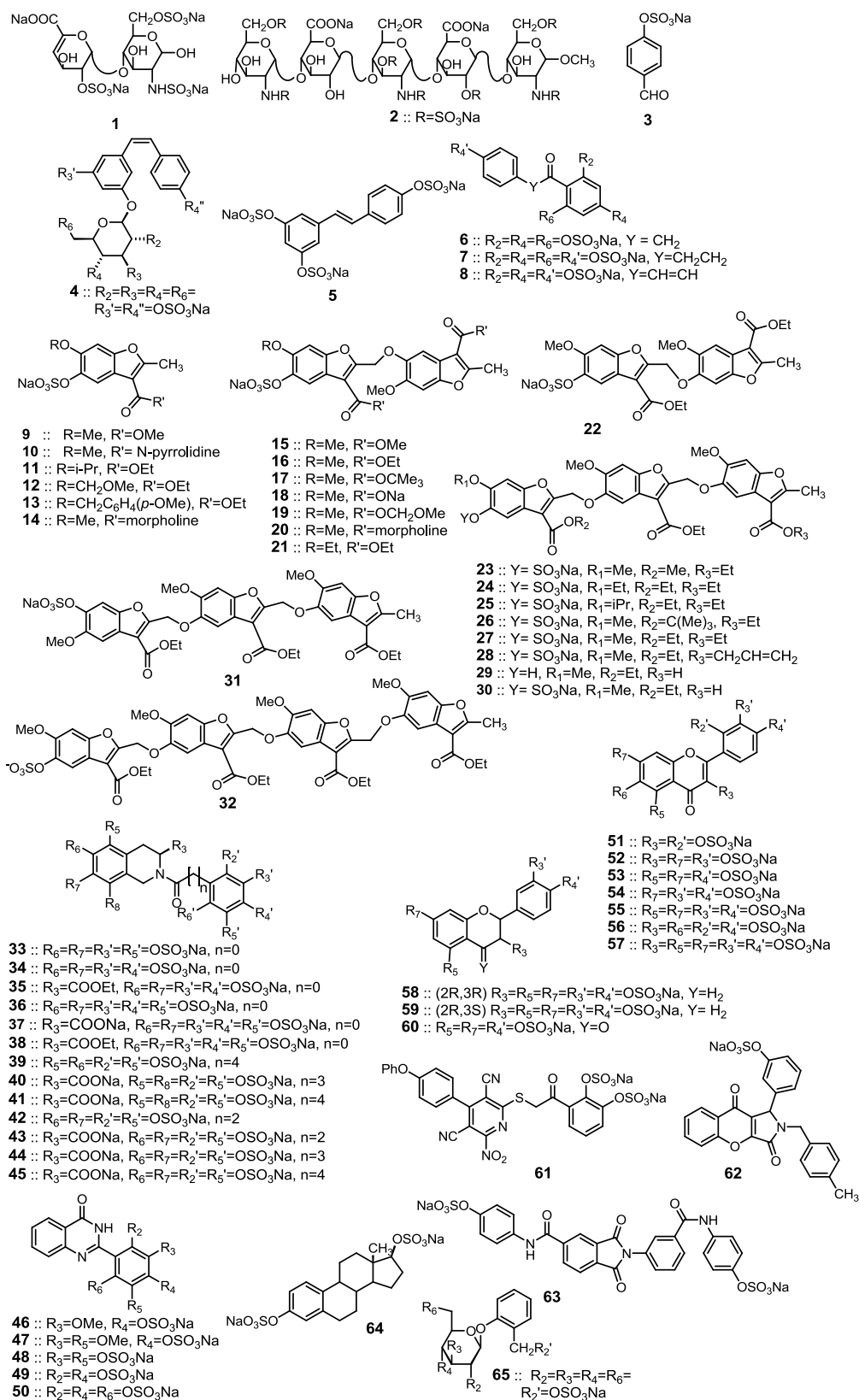


Figure 43. Library of sulfated small molecules (SSMs).

**Table 10. Inhibition Parameters of Sulfated Small Molecules (SSMs) against factor XIa.**

<i>SSM No.</i>	<i>IC<sub>50</sub> (μM)*</i>	<i>Y<sub>M</sub>*</i>	<i>Y<sub>0</sub>*</i>	<i>HS*</i>
<b>15</b>	9.7 ± 0.3	102±2	4±4	6.9±1.2
<b>21</b>	7.5 ± 0.6	95±3	0±2	1.9±0.3
<b>23</b>	14.9 ± 0.3	94±1	7±1	5.2±0.4
<b>24</b>	0.82 ± 0.02	99±2	0±1	3.8±0.3
<b>25</b>	47.2 ± 0.9	99±2	3±2	6.6±0.8
<b>27</b>	6.4 ± 0.1	99±2	2±1	11.7±1.5
<b>28</b>	29.9 ± 0.8	103±2	10±2	6.4±0.9
<b>29</b>	384 ± 38	98±4	0±1	1.9±0.4
<b>30</b>	29.9 ± 0.5	100±2	3±2	6.9±0.7
<b>32</b>	99 ± 13	101±5	0±1	1.3±0.2
<b>61</b>	109 ± 2	96±1	0±1	6.2±0.5
<b>63</b>	122 ± 3	98±2	0±1	6.0±0.9

\* Error bars represent ± 1 S.E.

\*\*Work reported in Argade, M; MS Thesis, Titled: *Discovery and biophysical characterization of allosteric inhibitors of factor XIa (FXIa)*. (2012).

The affinity for **24** was found to be similar to the  $IC_{50}$  with a  $K_D$  of  $1.2 \pm 0.3 \mu\text{M}$  (*data not shown*). Michaelis-Menten kinetics data indicated that **24** inhibits factor XIa by binding away from the active site (Figure 44A). To localize the binding site of **24** on factor XIa, we tried competition with heparin. We expected there to be good competition with heparin due to the fact that **24** is a derivative of chemoenzymatic lignins, which are known to bind at heparin binding site of factor XIa, and the fact that it is sulfated. However, to our surprise we found no direct

competition of **24** with heparin (Figure 44B). To date, no allosteric factor XIa inhibitor was developed which was incapable of competing with heparin. This fact led us to believe that compound **24** and its congeners were possibly binding at a novel site, and inducing factor XIa inhibition by a truly unique mechanism.

*Note- The screening, inhibition and allostery was determined with the help of a fellow graduate student Ms. Malaika D. Argade and have been reported earlier in her master's thesis. Title: Discovery and biophysical characterization of allosteric inhibitors of factor XIa (FXIa). (2012).*

We therefore pursued the identification of the binding site utilizing molecular modeling. We confirmed these results by explaining the activities of congeners of **24** and characterizing the inhibition of **24** with the catalytic domain alone. Lastly, we tested if the binding of **24** to factor XIa could possibly convert the enzyme back into a zymogen-like conformation.

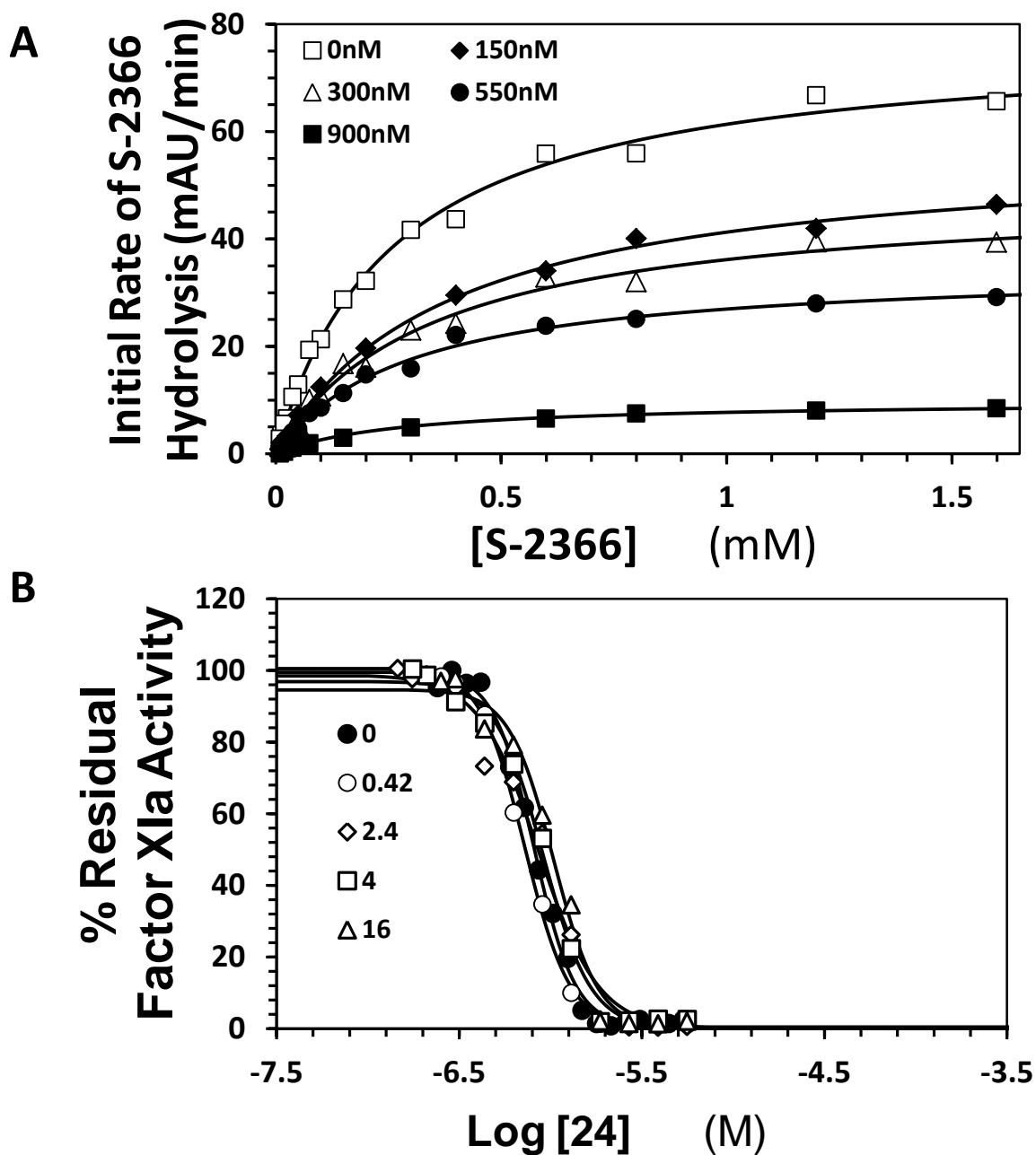


**Figure 44.** Compound 24 inhibits factor XIa by allosteric mechanism. (A) Michaelis-Menten Kinetics of substrate S-2366 hydrolysis in the presence of inhibitor 24 from 0-900 nM. A clear change in  $V_{MAX}$  from  $77.4 \pm 1.7$  to  $9.8 \pm 0.5$  was observed, with relatively no change in  $K_M$  ( $0.32 \pm 0.06$  mM), which is characteristic of non-competitive inhibition. (B) Competition of inhibition of factor XIa by 24 in the presence of varying concentrations of porcine UFH from 0-16  $\mu$ M. It

can be seen that there is essentially no change in  $IC_{50}$  even in the presence of 16  $\mu\text{M}$  UFH, which indicates that **24** inhibits factor XIa allosterically at a site away from the heparin binding site.

## 5.2 Experimental Procedures

### *Materials*

The recombinant catalytic domain and wild-type full length factor XIa were gifts from Dr. Alireza Rezaie (Saint Louis University, MO). Dansyl-EGR labeled factor XIa (*d*EGR-fXIa) was obtained from Haematologic Technologies (Essex Junction, VT). All other chemicals were analytical reagent grade from either Sigma Chemicals (St. Louis, MO) or Fisher (Pittsburgh, PA) and used without further purification.

### *fXIa Structure Model Generation*

Since no crystal structure exists for the activated form of factor XIa, a model for the complete fXIa was created by replacing the inactive catalytic domain of the zymogen form (PDB id: 2f83) with the activated catalytic domain crystal structure available (PDB id: 1zom) using Pymol.<sup>245</sup> Further, hydrogens were added to the chimera protein and minimized keeping all heavy atoms as aggregates using Tripos Sybyl-X v.2.1 [[www.tripos.com/sybyl](http://www.tripos.com/sybyl)].

### *Docking of Compound 24*

An in silico localization of the possible binding sites for compound **24** was performed using simple docking protocols. Briefly, the most active compound, **24**, was modeled in SybylX 2.1 [www.tripos.com/sybyl] and docked into the structure of the chimera at 8 sites. These sites were defined as being within 24 Å around residues Lys8, Arg136, Gln153, Lys252, Lys325, Lys357, Asn566, and Arg584 as shown in Figure 45A. For each site, 1000 genetic algorithm runs were employed without allowing early termination. Automatic cavity detection was permitted. Docked poses were scored using GOLDScore and only the top two poses were retained. Triplicate docking runs were employed to ensure the docked poses were reproducible giving us a total of 6 docked poses per site. No constraints were employed because this was an exploratory docking simulation. Average RMSD across the docked poses was ascertained using in-house code utilizing the Openeye OEChem toolkit.<sup>246</sup>

### *Inhibition of Catalytic Domain of Factor XIa*

The inhibition of molecule **24** was tested against the catalytic domain of factor XIa alone using a microplate assay similar to the one described above. Briefly, in each well 85 µL of buffer (0.05M Tris, 0.15M NaCl, 0.1% PEG-8000, 0.02% Tween-80 at pH=7.4) was taken, to which was added 5 µL of enzyme fXIa (final concentration of 0.765 nM in each well). Serial dilutions of the inhibitor stock with decrements of 2/3<sup>rd</sup> were incubated with the enzyme by addition of 5 µL of stock inhibitor solutions. The mixture was then incubated for 10 minutes and throughout the experiment the temperature was maintained at 37°C. After incubation, 5 µL of substrate S-2366 (final concentration of 330 µM) was added to each well and the initial velocities of the reaction were determined by measuring the absorbance of p-nitroaniline at 405nm released due to

substrate cleavage by fXIa. The initial rate of substrate hydrolysis was treated using equation 4 and a nonlinear curve fitting was performed to give the IC<sub>50</sub> values.

#### *Effect on Protein Anisotropy in Presence of 24 using Perrin Plot*

Monitoring protein anisotropy at variable temperatures or viscosities can demonstrate change in the hydrodynamic radius of the protein. Briefly, in a 96-well microplate, 33  $\mu$ l of water along with 5  $\mu$ l of tris-HCl buffer (to give final concentrations of 50mM tris-HCl and 150mM NaCl pH=7.4) was added. To this, 20  $\mu$ l of dansyl-EGR labelled factor XIa (*dEGR-fXIa*) was added (final concentration of enzyme was 0.81 $\mu$ M) along with 2  $\mu$ l of either solvent or 1mM of compound **24**. The wells were read using the FlexStation III, (Molecular Devices, Sunnyvale, CA) polarization module. The excitation and emission wavelengths were set at 340 nm and 530 nm, respectively. The plate was incubated at various temperatures ranging from 22-40°C for 10 minutes before reading the plate for the parallel ( $I_{\parallel}$ ) and perpendicular ( $I_{\perp}$ ) intensities of fluorescent light. The average of 13 readings was taken and the anisotropy ( $r$ ) calculated using the classical equation.<sup>247</sup>

$$r = \frac{I_{\parallel} - I_{\perp}}{I_{\parallel} + 2I_{\perp}} \quad (\text{Eq. 10})$$

The viscosity ( $\eta$ ) of the solution at various temperatures (T) was obtained using a calculator based on previous literature.<sup>248,249</sup> A plot of the reciprocal of anisotropy ( $1/r$ ) versus the  $T/\eta$  yields a straight line which fits the Perrin equation<sup>247</sup>:

$$\frac{1}{r} = \frac{1}{r_0} + \frac{\tau RT}{Vr_0\eta} \quad (\text{Eq. 11})$$

where,  $r_0$  is the fundamental anisotropy of the fluorophore in the absence of diffusion,  $\tau$  is the fluorescence lifetime of the fluorophore,  $R$  is the gas constant,  $V$  is the hydrodynamic volume of

the protein to which the fluorophore is attached,  $T$  is the temperature and  $\eta$  is the viscosity of the solution. When fit to the equation of a straight line  $y = mx + c$ , where  $y = 1/r$ ,  $c = 1/r_0$  and  $m = \tau RT/Vr_0$ . The ratio of the slopes of the lines corrected for the  $r_0$ , give the ratio of the hydrodynamic volumes in the presence and absence of the inhibitor.

### 5.3 Results

#### *Preparation of a Knowledge-Based Model for Full-Length Factor XIa*

Molecular modeling has been used previously to predict binding mode of benzofuran oligomers to thrombin exosite 2.<sup>189</sup> We therefore hypothesized that similar docking studies could be used to identify the binding site of **24** within factor XIa. However, docking studies require the existence of a crystal structure of the target protein. To date, there is no complete crystal structure of full length factor XIa with its four apple domains. The crystal structures of full-length zymogen form of factor XIa, i.e. factor XI,<sup>124</sup> and the catalytic domain of factor XIa<sup>250</sup> are available. This gave us an opportunity to create a model chimera full length factor XIa by simple replacement of the inactive catalytic domain of the zymogen with the active structure (Figure 45A). Such a model would be physiologically relevant as the protein would be presented in its zymogen-like inactive state.

#### *Docking Suggests Probable Binding Pose for Benzofuran Trimers*

The binding site of benzofuran trimers on fXIa is, as of yet, unknown. We conducted computational studies to predict the same. Eight areas on the protein surface displayed a relatively higher positive charge density, and were stochastically nominated as possible binding sites for **24**. The residue approximately at the center of the positively charged patch was



identified (Figure 45A) and all residues within **24** Å around of it were defined as the binding site. This covered practically the entire protein surface, ensuring exhaustive exploration during identification of possible binding sites. The small molecule was then docked into all 8 sites exhaustively. Any sites where **24** could interact reproducibly would be a plausible binding site.

Five out of 6 docked poses of **24** displayed a very low RMSD (1.6 Å) near Lys252 displayed a very low RMSD (Figure 45B). Moreover, this reproducible pose rationalized the observed SAR of the benzofuran trimers quite well (Figure 45B, C and D). The lone sulfate of the trimers present on ring A is required for activity because it forms strong interactions with Lys255. *Note-* although the docking center was Lys252, the molecule seemed to localize near Lys255 near it. When this sulfate is removed in compounds **29**, this vital interaction cannot be formed, resulting in  $\approx 400$  fold loss of activity ( $IC_{50} = 384 \mu\text{M}$ ). The 6-ethoxy position of the benzofuran A of the trimer occupies a shallow hydrophobic pocket, where an ethyl group displayed optimal van der Waal's interactions. While a methyl group was tolerated here (as in compound **23** with  $IC_{50} = 14.9 \mu\text{M}$  and **27** with  $IC_{50} = 6.4 \mu\text{M}$ ), an isopropyl group displayed reduced activity because of steric hindrance, as observed in compounds **25** ( $IC_{50} = 47\mu\text{M}$ ). Finally, a negative charge density at the 3-position of the benzofuran C on the trimer, as present in compounds **29** and **30**, was not tolerated because the hydrophobic nature of the binding pocket and the presence of Glu567 near the trimer.

Interestingly, this binding site is on the A3 domain of fXIa, which is also known to possess a heparin-binding site (HBS).<sup>131,132</sup> Even though compound **24** is sulfated, it binds adjacent to the HBS, which explains why we did not observe competitive binding with heparin. While heparin does cause some inhibition of factor XIa activity ( $\sim 30\%$  with an  $IC_{50} \sim 220\text{nM}$ ), it cannot completely inhibit the enzyme compared to **24**, indicating that the site of **24** is unique in

its mechanism and away from the heparin binding site. The strong correlation with experimentally observed SAR and biophysical studies constitutes conclusive evidence that we have successfully identified the binding site for these benzofuran trimers on fXIa.

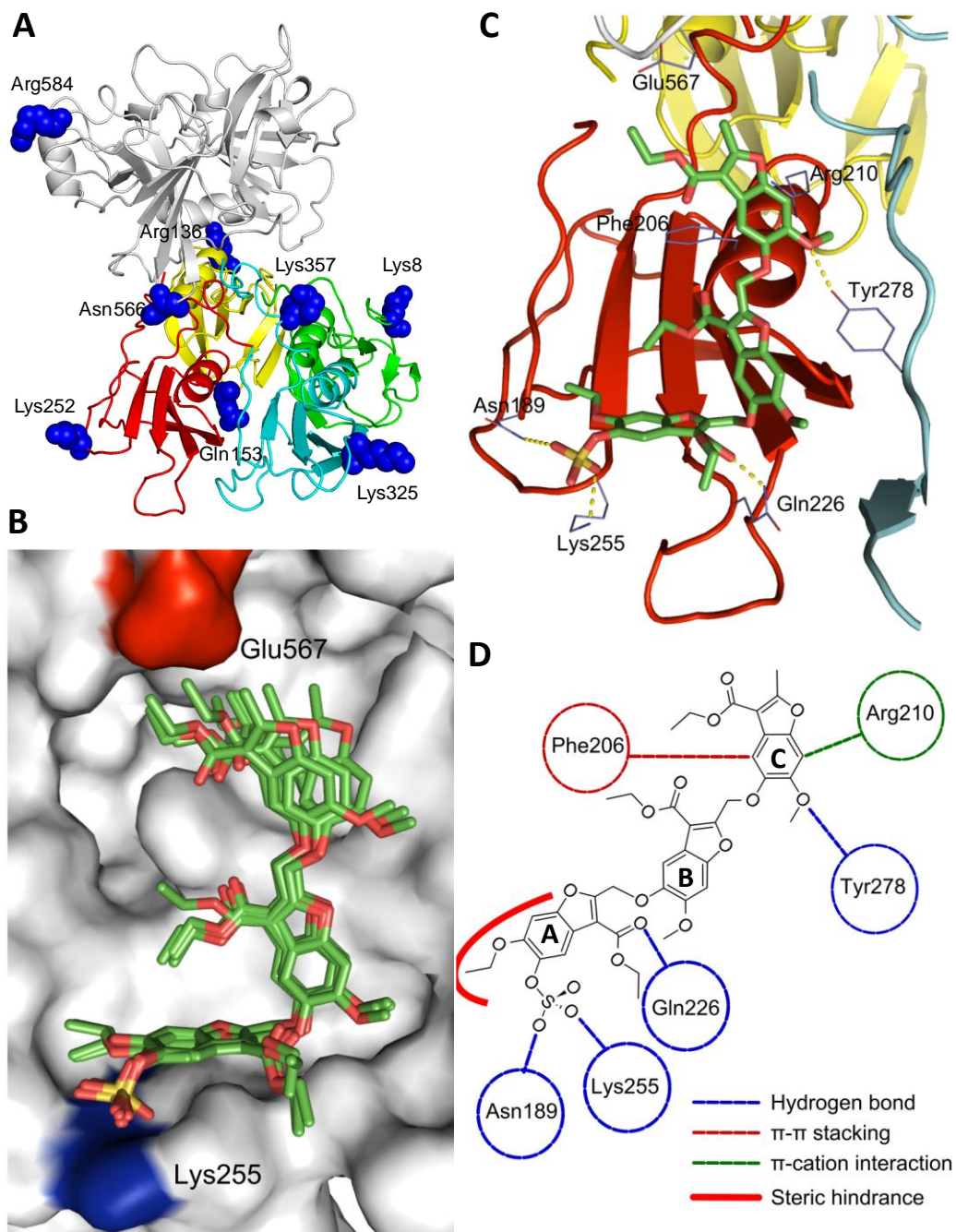


**Figure 45.** Modeling studies for inhibitor 24. (A) A chimera model was created using the catalytic domain crystal structure (PDB i.d.: 1zom) and the heavy chain from the zymogen

crystal structure (PDB i.d.: 2f83). Compound **24** was docked into 8 loci around residues Lys8, Arg136, Arg184, Lys252, Lys325, Lys357, Asn566, and Arg584,, shown as blue spheres. (B) The structure docked reproducibly at a site located near residue Lys252, as witnessed by a low RMSD between the docked poses. (C) Surface features of the site where **24** docked reproducibly, shows that the sulfate group of **24** interacts well with Lys255. (D) A cartoon representation the best docked pose of **24** near Lys252 with the interactions highlighted with the binding pocket and the benzofurans A, B and C. The panels C and D explains the SAR observed. Lys255 interacts favorably with the sulfate group of **24** – removing the latter eradicates activity. Ethyl groups at 6-ethoxy position of benzofuran A of the benzofuran trimers are ideal for van der Waal's contacts with the protein, producing optimum activity. Methyl groups are also tolerated here because they are smaller, but isopropyl groups reduce activity because the trimers can no longer fit. Presence of a carboxylate at 3-position of benzofuran C of the trimers is not tolerated due to the presence of a hydrophobic pocket and two acidic residues (Glu202 and Glu227) which repel the compounds with acidic functionality here.

#### *Inhibition of Factor XIa by **24** is Apple-Domain Driven*

In order to check if the inhibition of factor XIa by **24** is apple domain driven, we tested **24** against the catalytic domain of factor XIa (fXIa-CD) (Figure 46). It was observed that the IC<sub>50</sub> of **24** against fXIa was  $1.2 \pm 0.2 \mu\text{M}$ , while that for fXIa-CD was  $49 \pm 2 \mu\text{M}$ , indicating that without the heavy chain of fXIa there is almost a 40-fold reduction in potency.

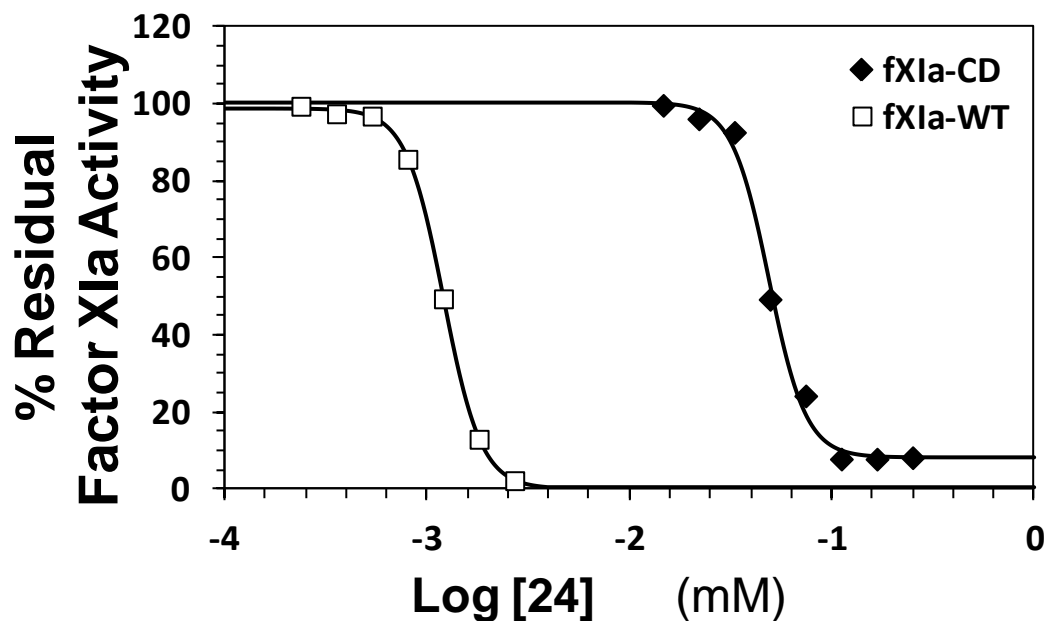


**Figure 46.** Loss in inhibition potency of **24** upon removal of the Apple domains containing the putative site of binding. Inhibitor **24** shows a 40-fold higher  $IC_{50}$  against the catalytic domain of factor XIa ( $\blacklozenge$ , fXIa-CD) in comparison to that against the wild-type fXIa ( $\square$ ).

#### *Inhibition of Factor XIa by **24** Causes a Dramatic Conformational Change in Protein Structure*

As the temperature increases, the rotational correlation time ( $\theta$ ) of the protein decreases due to increased motion. This causes a decrease in anisotropy. The rotational correlation time of the protein is direct function of the hydrodynamic volume of the protein.<sup>247</sup> However, to monitor such changes, the fluorescence lifetime ( $\tau$ ) of the fluorophore must be comparable to the rotational correlation time of the protein.<sup>251</sup> Hence, we used dansyl labeled factor XIa, as dansyl has a relatively long fluorescence lifetime.<sup>252</sup> We used a Perrin plot (Figure 47) in order to identify any dramatic changes in the hydrodynamic volume of the protein due to inhibitor

binding. When fit to the Perrin equation, dEGR-factor XIa gave a best fit line having an equation:

$$y = 10.61 \times 10^{-6} x + 4.05 \quad (R^2 = 0.988),$$

while in the presence of the inhibitor the equation changed to:

$$y = 7.50 \times 10^{-6} x + 4.46 \quad (R^2 = 0.979).$$

The reciprocal of the intercept would yield fundamental anisotropy of the fluorophore in the absence of diffusion (i.e.  $c=1/r_0$ ). This means that in ideal conditions the intercept should have identical values. However, in practice, fluorophores display segmental motions, which are independent of overall diffusion when bound to proteins.<sup>247</sup> Binding of the inhibitor has been shown to cause conformational changes within the active site which could affect such segmental motions and hence there is a small variation between the intercepts of the two plots. When the  $r_0$  is corrected for within the slope of the line, the ratio of the slopes would yield the ratio of the hydrodynamic volumes as all other values are constant under the conditions of the experiment:

$$\frac{\left(\frac{m}{c}\right)_{dEGR-fXIa}}{\left(\frac{m}{c}\right)_{dEGR-fXIa+24}} = \frac{V_{dEGR-fXIa+24}}{V_{dEGR-fXIa}} \quad (\text{Eq. 12})$$

The ratio of the corrected slopes ( $m/c$ ) is  $1.55 \pm 0.06$  suggesting that when **24** binds to fXIa, it causes a  $55 \pm 6\%$  increase in the hydrodynamic volume of the protein. Such an increase would be indicative of a dramatic conformational change within the protein.

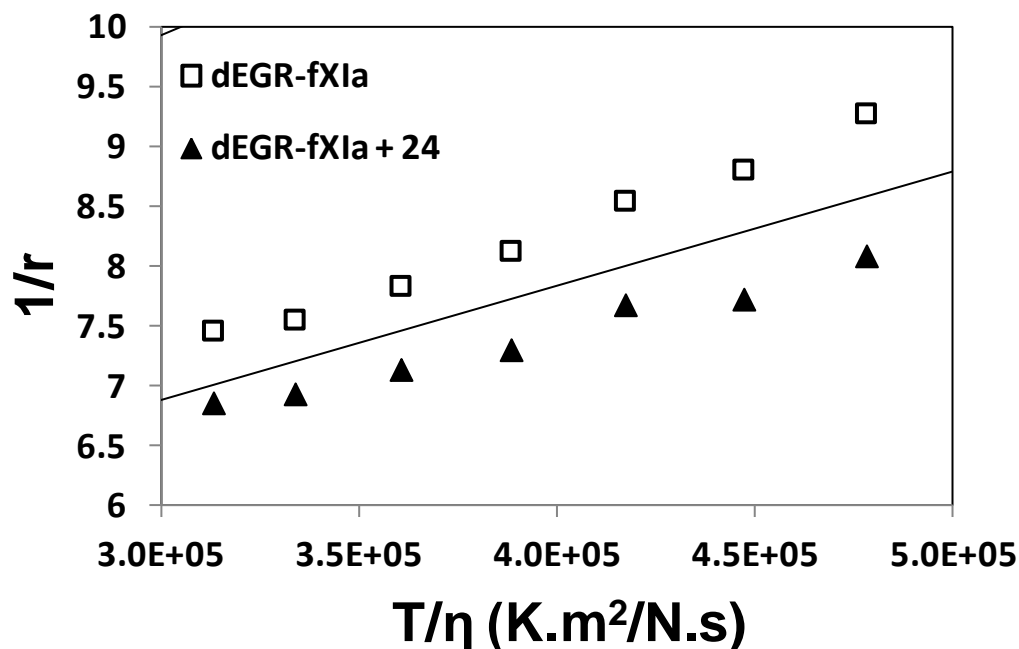


**Figure 47.** Binding of **24** to factor XIa induces a large conformational change. A Perrin-plot for dansylated factor XIa (dEGR-fXIa) in the absence ( $\square$ ) and presence ( $\blacktriangle$ ) of **24** showing a significant difference in slope indicating considerably different hydrodynamic volumes of factor XIa alone and in complex with **24**.

## 5.4 Discussion

Development of inhibitors targeting upstream processes of the coagulation cascade is gradually gaining speed in order to obtain drugs with fewer side-effects.<sup>140</sup> Active site inhibitors of factor XIa have been synthesized recently (within the last 10 years) but often are either irreversible by forming a covalent bond with Ser195 or have a strongly basic group to identify the Asp189 in the S1 pocket of serine proteases.<sup>250,253-258</sup> Both these methods of inhibition lead to lack of selectivity as these features are present on most, if not all, serine proteases.

Previously synthesized QAOs offered a novel pathway of discovering small-molecule allosteric inhibition of factor XIa by targeting hydrophobic domains adjacent to heparin-binding sites.<sup>235</sup> They do so by initial coulombic attraction of anionic parts of the ligand (sulfate groups) to the cationic heparin binding site of fXIa, followed by formation of a tight lock with an adjacent hydrophobic patch. Although the potency of these molecules was relatively low, with the lowest  $IC_{50}$  of only 52 $\mu$ M, the study provided impetus to search for a more potent allosteric inhibitor using similar rationale of coulombic-attraction followed by inhibition using sulfated small molecule.

Chemo-enzymatically synthesized LMW lignins were found to be potent inhibitors of factor XIa (Table 1). Yet they suffered from lack of selectivity due to their heterogeneity in their intermonomeric linkage. Furthermore, SbO4L was found to not have factor XIa inhibitory potential, suggesting that the lignin factor XIa inhibitory activity possibly arose from other scaffolds than the  $\beta$ -O4 type lignins.

Our library screen of 65 SSMs took upon the challenge of finding smaller or more potent analogs, which could possibly inhibit fXIa via allosteric mechanisms. We have successfully identified at least 8 molecules (Table 10) with an  $IC_{50}$  lower (greater potency) than previously reported QAOs against fXIa. Furthermore, the predominant class of inhibitors was identified as the benzofuran dimers and trimers, which are close mimics of the  $\beta$ -5 type linkage found in lignins.<sup>188</sup> The most potent trimer **24** was 50-fold more active than the most active QAO. Trimer **24** was shown to be an allosteric inhibitor of factor XIa, but was surprisingly not competitive with heparin. We therefore needed to identify the plausible binding site for **24**, which might explain mechanism and help in the development of future inhibitors.

To explore the possible binding sites for **24** an exhaustive docking search involving 8 sites on a chimera factor XIa model was performed. The search revealed a unique binding site within the A3 domain of factor XIa which satisfied the SAR observed experimentally. Additionally it was confirmed that the heavy chain of factor XIa is required for optimal inhibition by **24**, suggesting that a high affinity binding site is located within the apple domains.

The A3 domain has been known to be a key domain for factor XIa activity towards factor IX activation.<sup>137,259</sup> It has also been suggested that Arg184 within the A3 domain sits within a pocket of the catalytic domain within the zymogen, forming hydrogen bond interactions with Ser268, Asp488, and Asn566. Upon activation, there is a dramatic change in the catalytic domain which could release the Arg184 from this cavity and allow it to interact with factor IX. Thus Arg184 acts as a switch that holds factor XI (zymogen) in an inactive conformation in the zymogen form. Binding to the proposed binding site of **24** could possibly restrict the movement of the catalytic domain and force the enzyme into an inactive conformation wherein the “switch” is in the off-position by restoring Arg184 into the cavity of the catalytic domain, thereby shutting down the catalytic activity of factor XIa.

We also demonstrated that binding of **24** to factor XIa would cause a dramatic increase in the hydrodynamic volume of the protein, which is indicative of large conformational changes in the overall quaternary structure of factor XIa. It is known that the zymogen form of the enzyme is proportionately larger in size compared to the activated form,<sup>128</sup> suggesting that binding of **24** may convert the enzyme back into a conformationally inactive zymogen-like shape.

Our current results highlight the fact that there is a site in the A3 domain of factor XIa which can be targeted using small aromatic lignin-like molecules with relatively fewer sulfate



groups to produce potent, allosteric inhibition of factor XIa. Such allosteric inhibition brings about large conformation change within the protein structure possibly reverting the enzyme into an inactive zymogen-like conformation. Further structural analysis, mutagenesis studies and functional bioassays should be performed to confirm the utility of targeting such a site.

## **Literature Cited**

1. Tortora, G. J.; Derrickson, B. *Principles of anatomy & physiology*. 13th ed.; Wiley: Hoboken, NJ, 2012.
2. Marder, V. J. *Hemostasis and thrombosis : basic principles and clinical practice*. 6th ed.; Wolters Kluwer/Lippincott Williams & Wilkins Health: Philadelphia, 2013.
3. Mehta, A. Y.; Jin, Y.; Desai, U. R. An update on recent patents on thrombin inhibitors (2010 - 2013). *Expert Opin Ther Pat* **2014**, *24*, 47-67.
4. Konigsberg, W.; Kirchhofer, D.; Riederer, M. A.; Nemerson, Y. The TF:VIIa complex: clinical significance, structure-function relationships and its role in signaling and metastasis. *Thromb. Haemost.* **2001**, *86*, 757-771.
5. Mackman, N.; Tilley, R. E.; Key, N. S. Role of the extrinsic pathway of blood coagulation in hemostasis and thrombosis. *Arterioscler. Thromb. Vasc. Biol.* **2007**, *27*, 1687-1693.
6. Stassen, J. M.; Arnout, J.; Deckmyn, H. The hemostatic system. *Curr. Med. Chem.* **2004**, *11*, 2245-2260.
7. Woodruff, R. S.; Sullenger, B.; Becker, R. C. The many faces of the contact pathway and their role in thrombosis. *J. Thromb. Thrombolysis* **2011**, *32*, 9-20.
8. Gailani, D.; Renne, T. Intrinsic pathway of coagulation and arterial thrombosis. *Arterioscler. Thromb. Vasc. Biol.* **2007**, *27*, 2507-2513.
9. Greenberg, C. S.; Miraglia, C. C.; Rickles, F. R.; Shuman, M. A. Cleavage of blood coagulation factor XIII and fibrinogen by thrombin during in vitro clotting. *J. Clin. Invest.* **1985**, *75*, 1463-1470.
10. Ozge-Anwar, A. H.; Connell, G. E.; Mustard, J. F. The activation of factor 8 by thrombin. *Blood* **1965**, *26*, 500-509.

11. Monkovic, D. D.; Tracy, P. B. Activation of human factor V by factor Xa and thrombin. *Biochemistry (Mosc)*. **1990**, *29*, 1118-1128.
12. Oliver, J. A.; Monroe, D. M.; Roberts, H. R.; Hoffman, M. Thrombin activates factor XI on activated platelets in the absence of factor XII. *Arterioscler. Thromb. Vasc. Biol.* **1999**, *19*, 170-177.
13. De Candia, E. Mechanisms of platelet activation by thrombin: a short history. *Thromb. Res.* **2012**, *129*, 250-256.
14. Esmon, C. T.; Esmon, N. L.; Harris, K. W. Complex formation between thrombin and thrombomodulin inhibits both thrombin-catalyzed fibrin formation and factor V activation. *J. Biol. Chem.* **1982**, *257*, 7944-7947.
15. Rezaie, A. R. Regulation of the protein C anticoagulant and antiinflammatory pathways. *Curr. Med. Chem.* **2010**, *17*, 2059-2069.
16. Rau, J. C.; Beaulieu, L. M.; Huntington, J. A.; Church, F. C. Serpins in thrombosis, hemostasis and fibrinolysis. *J Thromb Haemost* **2007**, *5 Suppl 1*, 102-115.
17. Kluft, C. The fibrinolytic system and thrombotic tendency. *Pathophysiol Haemost Thromb* **2003**, *33*, 425-429.
18. Patel, S. R.; Hartwig, J. H.; Italiano, J. E., Jr. The biogenesis of platelets from megakaryocyte proplatelets. *J. Clin. Invest.* **2005**, *115*, 3348-3354.
19. Machlus, K. R.; Italiano, J. E., Jr. The incredible journey: From megakaryocyte development to platelet formation. *J. Cell Biol.* **2013**, *201*, 785-796.
20. White, J. G. Platelet Structure. In *Platelets*, 2nd ed.; Michelson, A. D., Ed. Academic Press - Elsevier: Waltham, MA, 2007; pp 45-74.

21. Udan, R. S.; Culver, J. C.; Dickinson, M. E. Understanding vascular development. *Wiley Interdiscip Rev Dev Biol* **2013**, *2*, 327-346.
22. Chen, J.; Lopez, J. A. Interactions of platelets with subendothelium and endothelium. *Microcirculation* **2005**, *12*, 235-246.
23. Rendu, F.; Brohard-Bohn, B. The platelet release reaction: granules' constituents, secretion and functions. *Platelets* **2001**, *12*, 261-273.
24. Monroe, D. M.; Hoffman, M.; Roberts, H. R. Platelets and thrombin generation. *Arterioscler. Thromb. Vasc. Biol.* **2002**, *22*, 1381-1389.
25. Hartwig, J. H. The Platelet Cytoskeleton. In *Platelets*, 2nd ed.; Michelson, A. D., Ed. Elsevier: Oxford, UK, 2007; pp 75-97.
26. Kauskot, A.; Hoylaerts, M. F. Platelet Receptors. In *Antiplatelet Agents*, Gresele, P.; Born, G. V. R.; Patrono, C.; Page, C. P., Eds. Handbook of Experimental Pharmacology 210; Springer-Verlag: Berlin, Heidelberg, 2012; pp 23-57.
27. Clemetson, K. J.; Clemetson, J. M. Platelet Receptors. In *Platelets*, 3rd ed.; Michelson, A. D., Ed. Academic Press - Elsevier: Waltham, MA, 2013; pp 169-194.
28. Nesheim, M. E.; Mann, K. G. The kinetics and cofactor dependence of the two cleavages involved in prothrombin activation. *J. Biol. Chem.* **1983**, *258*, 5386-5391.
29. Mann, K. G.; Elion, J.; Butkowski, R. J.; Downing, M.; Nesheim, M. E. Prothrombin. *Methods Enzymol.* **1981**, *80 Pt C*, 286-302.
30. Butkowski, R. J.; Elion, J.; Downing, M. R.; Mann, K. G. Primary structure of human prothrombin 2 and alpha-thrombin. *J. Biol. Chem.* **1977**, *252*, 4942-4957.
31. Walz, D. A.; Hewett-Emmett, D.; Seegers, W. H. Amino acid sequence of human prothrombin fragments 1 and 2. *Proc. Natl. Acad. Sci. U. S. A.* **1977**, *74*, 1969-1972.

32. Bode, W.; Turk, D.; Karshikov, A. The refined 1.9-A X-ray crystal structure of D-Phe-Pro-Arg chloromethylketone-inhibited human alpha-thrombin: structure analysis, overall structure, electrostatic properties, detailed active-site geometry, and structure-function relationships. *Protein Sci.* **1992**, *1*, 426-471.
33. Davie, E. W.; Kulman, J. D. An overview of the structure and function of thrombin. *Semin. Thromb. Hemost.* **2006**, *32 Suppl 1*, 3-15.
34. Hedstrom, L. Serine protease mechanism and specificity. *Chem. Rev.* **2002**, *102*, 4501-4524.
35. Schechter, I.; Berger, A. On the size of the active site in proteases. I. Papain. *Biochem. Biophys. Res. Commun.* **1967**, *27*, 157-162.
36. Blomback, B.; Blomback, M.; Hessel, B.; Iwanaga, S. Structure of N-terminal fragments of fibrinogen and specificity of thrombin. *Nature* **1967**, *215*, 1445-1448.
37. Chen, Z.; Li, Y.; Mulichak, A. M.; Lewis, S. D.; Shafer, J. A. Crystal structure of human alpha-thrombin complexed with hirugen and p-amidinophenylpyruvate at 1.6 A resolution. *Arch. Biochem. Biophys.* **1995**, *322*, 198-203.
38. Chang, J. Y. Thrombin specificity. Requirement for apolar amino acids adjacent to the thrombin cleavage site of polypeptide substrate. *Eur. J. Biochem.* **1985**, *151*, 217-224.
39. Carrell, C. J.; Bush, L. A.; Mathews, F. S.; Di Cera, E. High resolution crystal structures of free thrombin in the presence of K(+) reveal the molecular basis of monovalent cation selectivity and an inactive slow form. *Biophys. Chem.* **2006**, *121*, 177-184.
40. Di Cera, E. Thrombin. *Mol. Aspects Med.* **2008**, *29*, 203-254.

41. Naski, M. C.; Fenton, J. W., 2nd; Maraganore, J. M.; Olson, S. T.; Shafer, J. A. The COOH-terminal domain of hirudin. An exosite-directed competitive inhibitor of the action of alpha-thrombin on fibrinogen. *J. Biol. Chem.* **1990**, *265*, 13484-13489.
42. Ayala, Y. M.; Cantwell, A. M.; Rose, T.; Bush, L. A.; Arosio, D.; Di Cera, E. Molecular mapping of thrombin-receptor interactions. *Proteins* **2001**, *45*, 107-116.
43. Dharmawardana, K. R.; Olson, S. T.; Bock, P. E. Role of regulatory exosite I in binding of thrombin to human factor V, factor Va, factor Va subunits, and activation fragments. *J. Biol. Chem.* **1999**, *274*, 18635-18643.
44. Esmon, C. T.; Lollar, P. Involvement of thrombin anion-binding exosites 1 and 2 in the activation of factor V and factor VIII. *J. Biol. Chem.* **1996**, *271*, 13882-13887.
45. Yun, T. H.; Baglia, F. A.; Myles, T.; Navaneetham, D.; Lopez, J. A.; Walsh, P. N.; Leung, L. L. Thrombin activation of factor XI on activated platelets requires the interaction of factor XI and platelet glycoprotein Ib alpha with thrombin anion-binding exosites I and II, respectively. *J. Biol. Chem.* **2003**, *278*, 48112-48119.
46. Fortenberry, Y. M.; Whinna, H. C.; Gentry, H. R.; Myles, T.; Leung, L. L.; Church, F. C. Molecular mapping of the thrombin-heparin cofactor II complex. *J. Biol. Chem.* **2004**, *279*, 43237-43244.
47. Mengwasser, K. E.; Bush, L. A.; Shih, P.; Cantwell, A. M.; Di Cera, E. Hirudin binding reveals key determinants of thrombin allostery. *J. Biol. Chem.* **2005**, *280*, 26997-27003.
48. Hall, S. W.; Nagashima, M.; Zhao, L.; Morser, J.; Leung, L. L. Thrombin interacts with thrombomodulin, protein C, and thrombin-activatable fibrinolysis inhibitor via specific and distinct domains. *J. Biol. Chem.* **1999**, *274*, 25510-25516.

49. Li, W.; Johnson, D. J.; Esmon, C. T.; Huntington, J. A. Structure of the antithrombin-thrombin-heparin ternary complex reveals the antithrombotic mechanism of heparin. *Nat Struct Mol Biol* **2004**, *11*, 857-862.
50. Arni, R. K.; Padmanabhan, K.; Padmanabhan, K. P.; Wu, T. P.; Tulinsky, A. Structure of the non-covalent complex of prothrombin kringle 2 with PPACK-thrombin. *Chem. Phys. Lipids* **1994**, *67-68*, 59-66.
51. Bock, P. E.; Panizzi, P.; Verhamme, I. M. Exosites in the substrate specificity of blood coagulation reactions. *J Thromb Haemost* **2007**, *5 Suppl 1*, 81-94.
52. Lechtenberg, B. C.; Freund, S. M.; Huntington, J. A. GpIbalpha Interacts Exclusively with Exosite II of Thrombin. *J. Mol. Biol.* **2014**, *426*, 881-893.
53. Liu, L. W.; Rezaie, A. R.; Carson, C. W.; Esmon, N. L.; Esmon, C. T. Occupancy of anion binding exosite 2 on thrombin determines Ca<sup>2+</sup> dependence of protein C activation. *J. Biol. Chem.* **1994**, *269*, 11807-11812.
54. Richardson, J. L.; Kroger, B.; Hoeffken, W.; Sadler, J. E.; Pereira, P.; Huber, R.; Bode, W.; Fuentes-Prior, P. Crystal structure of the human alpha-thrombin-haemadin complex: an exosite II-binding inhibitor. *EMBO J.* **2000**, *19*, 5650-5660.
55. Jeter, M. L.; Ly, L. V.; Fortenberry, Y. M.; Whinna, H. C.; White, R. R.; Rusconi, C. P.; Sullenger, B. A.; Church, F. C. RNA aptamer to thrombin binds anion-binding exosite-2 and alters protease inhibition by heparin-binding serpins. *FEBS Lett.* **2004**, *568*, 10-14.
56. Russo Krauss, I.; Pica, A.; Merlino, A.; Mazzarella, L.; Sica, F. Duplex-quadruplex motifs in a peculiar structural organization cooperatively contribute to thrombin binding of a DNA aptamer. *Acta Crystallogr D Biol Crystallogr* **2013**, *69*, 2403-2411.
57. Huntington, J. A. Thrombin plasticity. *Biochim. Biophys. Acta* **2012**, *1824*, 246-252.



58. Orthner, C. L.; Kosow, D. P. Evidence that human alpha-thrombin is a monovalent cation-activated enzyme. *Arch. Biochem. Biophys.* **1980**, *202*, 63-75.
59. Di Cera, E. Thrombin as procoagulant and anticoagulant. *J Thromb Haemost* **2007**, *5 Suppl 1*, 196-202.
60. Dang, O. D.; Vindigni, A.; Di Cera, E. An allosteric switch controls the procoagulant and anticoagulant activities of thrombin. *Proc. Natl. Acad. Sci. U. S. A.* **1995**, *92*, 5977-5981.
61. Pineda, A. O.; Carrell, C. J.; Bush, L. A.; Prasad, S.; Caccia, S.; Chen, Z. W.; Mathews, F. S.; Di Cera, E. Molecular dissection of Na<sup>+</sup> binding to thrombin. *J. Biol. Chem.* **2004**, *279*, 31842-31853.
62. Qureshi, S. H.; Yang, L.; Manithody, C.; Iakhiaev, A. V.; Rezaie, A. R. Mutagenesis studies toward understanding allostery in thrombin. *Biochemistry (Mosc)*. **2009**, *48*, 8261-8270.
63. Ye, J.; Liu, L. W.; Esmon, C. T.; Johnson, A. E. The fifth and sixth growth factor-like domains of thrombomodulin bind to the anion-binding exosite of thrombin and alter its specificity. *J. Biol. Chem.* **1992**, *267*, 11023-11028.
64. Hortin, G. L.; Trimpe, B. L. Allosteric changes in thrombin's activity produced by peptides corresponding to segments of natural inhibitors and substrates. *J. Biol. Chem.* **1991**, *266*, 6866-6871.
65. Liu, L. W.; Vu, T. K.; Esmon, C. T.; Coughlin, S. R. The region of the thrombin receptor resembling hirudin binds to thrombin and alters enzyme specificity. *J. Biol. Chem.* **1991**, *266*, 16977-16980.
66. Gandhi, P. S.; Chen, Z.; Mathews, F. S.; Di Cera, E. Structural identification of the pathway of long-range communication in an allosteric enzyme. *Proc. Natl. Acad. Sci. U. S. A.* **2008**, *105*, 1832-1837.

67. Paborsky, L. R.; McCurdy, S. N.; Griffin, L. C.; Toole, J. J.; Leung, L. L. The single-stranded DNA aptamer-binding site of human thrombin. *J. Biol. Chem.* **1993**, *268*, 20808-20811.
68. Wu, Q.; Tsiang, M.; Sadler, J. E. Localization of the single-stranded DNA binding site in the thrombin anion-binding exosite. *J. Biol. Chem.* **1992**, *267*, 24408-24412.
69. Pica, A.; Russo Krauss, I.; Merlino, A.; Nagatoishi, S.; Sugimoto, N.; Sica, F. Dissecting the contribution of thrombin exosite I in the recognition of thrombin binding aptamer. *FEBS J* **2013**, *280*, 6581-6588.
70. Lai, M. T.; Di Cera, E.; Shafer, J. A. Kinetic pathway for the slow to fast transition of thrombin. Evidence of linked ligand binding at structurally distinct domains. *J. Biol. Chem.* **1997**, *272*, 30275-30282.
71. Lechtenberg, B. C.; Johnson, D. J.; Freund, S. M.; Huntington, J. A. NMR resonance assignments of thrombin reveal the conformational and dynamic effects of ligation. *Proc. Natl. Acad. Sci. U. S. A.* **2010**, *107*, 14087-14092.
72. Olson, S. T.; Swanson, R.; Raub-Segall, E.; Bedsted, T.; Sadri, M.; Petitou, M.; Herault, J. P.; Herbert, J. M.; Bjork, I. Accelerating ability of synthetic oligosaccharides on antithrombin inhibition of proteinases of the clotting and fibrinolytic systems. Comparison with heparin and low-molecular-weight heparin. *Thromb. Haemost.* **2004**, *92*, 929-939.
73. Kamath, P.; Huntington, J. A.; Krishnaswamy, S. Ligand binding shuttles thrombin along a continuum of zymogen- and proteinase-like states. *J. Biol. Chem.* **2010**, *285*, 28651-28658.
74. Lovely, R. S.; Boshkov, L. K.; Marzec, U. M.; Hanson, S. R.; Farrell, D. H. Fibrinogen gamma' chain carboxy terminal peptide selectively inhibits the intrinsic coagulation pathway. *Br. J. Haematol.* **2007**, *139*, 494-503.

75. Pineda, A. O.; Chen, Z. W.; Marino, F.; Mathews, F. S.; Mosesson, M. W.; Di Cera, E. Crystal structure of thrombin in complex with fibrinogen gamma' peptide. *Biophys. Chem.* **2007**, *125*, 556-559.
76. Sabo, T. M.; Farrell, D. H.; Maurer, M. C. Conformational analysis of gamma' peptide (410-427) interactions with thrombin anion binding exosite II. *Biochemistry (Mosc)*. **2006**, *45*, 7434-7445.
77. Tasset, D. M.; Kubik, M. F.; Steiner, W. Oligonucleotide inhibitors of human thrombin that bind distinct epitopes. *J. Mol. Biol.* **1997**, *272*, 688-698.
78. Castro, H. C.; Monteiro, R. Q.; Assafim, M.; Loureiro, N. I.; Craik, C.; Zingali, R. B. Ectoin modulates thrombin activity through exosite-2 interactions. *Int. J. Biochem. Cell Biol.* **2006**, *38*, 1893-1900.
79. Li, C. Q.; Vindigni, A.; Sadler, J. E.; Wardell, M. R. Platelet glycoprotein Ib alpha binds to thrombin anion-binding exosite II inducing allosteric changes in the activity of thrombin. *The Journal of biological chemistry* **2001**, *276*, 6161-6168.
80. Jandrot-Perrus, M.; Clemetson, K. J.; Huisse, M. G.; Guillin, M. C. Thrombin interaction with platelet glycoprotein Ib: effect of glyocalicin on thrombin specificity. *Blood* **1992**, *80*, 2781-2786.
81. De Candia, E.; Hall, S. W.; Rutella, S.; Landolfi, R.; Andrews, R. K.; De Cristofaro, R. Binding of thrombin to glycoprotein Ib accelerates the hydrolysis of Par-1 on intact platelets. *J. Biol. Chem.* **2001**, *276*, 4692-4698.
82. De Cristofaro, R.; De Filippis, V. Interaction of the 268-282 region of glycoprotein Ibalpha with the heparin-binding site of thrombin inhibits the enzyme activation of factor VIII. *Biochem. J.* **2003**, *373*, 593-601.

83. Fernandez, P. V.; Quintana, I.; Cerezo, A. S.; Caramelo, J. J.; Pol-Fachin, L.; Verli, H.; Estevez, J. M.; Ciancia, M. Anticoagulant activity of a unique sulfated pyranosic (1->3)-beta-L-arabinan through direct interaction with thrombin. *J. Biol. Chem.* **2013**, *288*, 223-233.
84. Fredenburgh, J. C.; Stafford, A. R.; Weitz, J. I. Evidence for allosteric linkage between exosites 1 and 2 of thrombin. *J. Biol. Chem.* **1997**, *272*, 25493-25499.
85. Petretera, N. S.; Stafford, A. R.; Leslie, B. A.; Kretz, C. A.; Fredenburgh, J. C.; Weitz, J. I. Long range communication between exosites 1 and 2 modulates thrombin function. *J. Biol. Chem.* **2009**, *284*, 25620-25629.
86. Lechtenberg, B. C.; Freund, S. M.; Huntington, J. A. An ensemble view of thrombin allostery. *Biol. Chem.* **2012**, *393*, 889-898.
87. Huttner, W. B. Determination and occurrence of tyrosine O-sulfate in proteins. *Methods Enzymol.* **1984**, *107*, 200-223.
88. Sasaki, N. Current status and future prospects for research on tyrosine sulfation. *Curr Pharm Biotechnol* **2012**, *13*, 2632-2641.
89. Mishiro, E.; Sakakibara, Y.; Liu, M. C.; Suiko, M. Differential enzymatic characteristics and tissue-specific expression of human TPST-1 and TPST-2. *J Biochem* **2006**, *140*, 731-737.
90. Moore, K. L. The biology and enzymology of protein tyrosine O-sulfation. *J. Biol. Chem.* **2003**, *278*, 24243-24246.
91. Goettsch, S.; Goettsch, W.; Morawietz, H.; Bayer, P. Shear stress mediates tyrosylprotein sulfotransferase isoform shift in human endothelial cells. *Biochem. Biophys. Res. Commun.* **2002**, *294*, 541-546.
92. Kehoe, J. W.; Bertozzi, C. R. Tyrosine sulfation: a modulator of extracellular protein-protein interactions. *Chem. Biol.* **2000**, *7*, R57-61.

93. Berndt, M. C.; Gregory, C.; Kabral, A.; Zola, H.; Fournier, D.; Castaldi, P. A. Purification and preliminary characterization of the glycoprotein Ib complex in the human platelet membrane. *Eur. J. Biochem.* **1985**, *151*, 637-649.
94. Li, C. Q.; Dong, J. F.; Lanza, F.; Sanan, D. A.; Sae-Tung, G.; Lopez, J. A. Expression of platelet glycoprotein (GP) V in heterologous cells and evidence for its association with GP Ib alpha in forming a GP Ib-IX-V complex on the cell surface. *J. Biol. Chem.* **1995**, *270*, 16302-16307.
95. Lopez, J. A.; Dong, J. F. Structure and function of the glycoprotein Ib-IX-V complex. *Curr. Opin. Hematol.* **1997**, *4*, 323-329.
96. Andrews, R. K.; Berndt, M. C. The GPIb-IX-V Complex. In *Platelets*, 3rd ed.; Michelson, A. D., Ed. Academic Press - Elsevier: Waltham, MA, 2013; pp 169-194.
97. Li, C. Q.; Dong, J. F.; Lopez, J. A. The mucin-like macroglycopeptide region of glycoprotein Ibalpha is required for cell adhesion to immobilized von Willebrand factor (VWF) under flow but not for static VWF binding. *Thromb. Haemost.* **2002**, *88*, 673-677.
98. Bensing, B. A.; Lopez, J. A.; Sullam, P. M. The *Streptococcus gordonii* surface proteins GspB and Hsa mediate binding to sialylated carbohydrate epitopes on the platelet membrane glycoprotein Ibalpha. *Infect. Immun.* **2004**, *72*, 6528-6537.
99. Kerrigan, S. W.; Douglas, I.; Wray, A.; Heath, J.; Byrne, M. F.; Fitzgerald, D.; Cox, D. A role for glycoprotein Ib in *Streptococcus sanguis*-induced platelet aggregation. *Blood* **2002**, *100*, 509-516.
100. McNicol, A.; Eyer, E.; Jackson, E. C.; Israels, S. J. A role for von Willebrand factor in *Streptococcus sanguis*-induced platelet activation. *Thromb. Haemost.* **2007**, *98*, 1382-1384.

101. Pawar, P.; Shin, P. K.; Mousa, S. A.; Ross, J. M.; Konstantopoulos, K. Fluid shear regulates the kinetics and receptor specificity of *Staphylococcus aureus* binding to activated platelets. *J. Immunol.* **2004**, *173*, 1258-1265.
102. Fitzgerald, J. R.; Foster, T. J.; Cox, D. The interaction of bacterial pathogens with platelets. *Nat Rev Microbiol* **2006**, *4*, 445-457.
103. Weeterings, C.; de Groot, P. G.; Adelmeijer, J.; Lisman, T. The glycoprotein Ib-IX-V complex contributes to tissue factor-independent thrombin generation by recombinant factor VIIa on the activated platelet surface. *Blood* **2008**, *112*, 3227-3233.
104. Cranmer, S. L.; Pikovski, I.; Mangin, P.; Thompson, P. E.; Domagala, T.; Frazzetto, M.; Salem, H. H.; Jackson, S. P. Identification of a unique filamin A binding region within the cytoplasmic domain of glycoprotein Ibalpha. *Biochem. J.* **2005**, *387*, 849-858.
105. Feng, S.; Christodoulides, N.; Resendiz, J. C.; Berndt, M. C.; Kroll, M. H. Cytoplasmic domains of GpIbalpha and GpIbbeta regulate 14-3-3zeta binding to GpIb/IX/V. *Blood* **2000**, *95*, 551-557.
106. Dai, K.; Bodnar, R.; Berndt, M. C.; Du, X. A critical role for 14-3-3zeta protein in regulating the VWF binding function of platelet glycoprotein Ib-IX and its therapeutic implications. *Blood* **2005**, *106*, 1975-1981.
107. Clemetson, K. J.; Naim, H. Y.; Luscher, E. F. Relationship between glyocalicin and glycoprotein Ib of human platelets. *Proc. Natl. Acad. Sci. U. S. A.* **1981**, *78*, 2712-2716.
108. Coller, B. S.; Kalomiris, E.; Steinberg, M.; Scudder, L. E. Evidence that glyocalicin circulates in normal plasma. *J. Clin. Invest.* **1984**, *73*, 794-799.
109. Corken, A.; Russell, S.; Dent, J.; Post, S. R.; Ware, J. Platelet Glycoprotein Ib-IX as a Regulator of Systemic Inflammation. *Arterioscler. Thromb. Vasc. Biol.* **2014**.

110. Yin, H.; Stojanovic-Terpo, A.; Xu, W.; Corken, A.; Zakharov, A.; Qian, F.; Pavlovic, S.; Krbanjevic, A.; Lyubimov, A. V.; Wang, Z. J.; Ware, J.; Du, X. Role for platelet glycoprotein Ib-IX and effects of its inhibition in endotoxemia-induced thrombosis, thrombocytopenia, and mortality. *Arterioscler. Thromb. Vasc. Biol.* **2013**, *33*, 2529-2537.
111. Simon, D. I. Inflammation and vascular injury: basic discovery to drug development. *Circ J* **2012**, *76*, 1811-1818.
112. Marchese, P.; Murata, M.; Mazzucato, M.; Pradella, P.; De Marco, L.; Ware, J.; Ruggeri, Z. M. Identification of three tyrosine residues of glycoprotein Ib alpha with distinct roles in von Willebrand factor and alpha-thrombin binding. *J. Biol. Chem.* **1995**, *270*, 9571-9578.
113. Jandrot-Perrus, M.; Bouton, M. C.; Lanza, F.; Guillin, M. C. Thrombin interaction with platelet membrane glycoprotein Ib. *Semin. Thromb. Hemost.* **1996**, *22*, 151-156.
114. Bouton, M. C.; Thurieau, C.; Guillin, M. C.; Jandrot-Perrus, M. Characteristics of the interaction between thrombin exosite 1 and the sequence 269-287 [correction of 269-297] of platelet glycoprotein Ibalpha. *Thromb. Haemost.* **1998**, *80*, 310-315.
115. De Cristofaro, R.; De Candia, E.; Landolfi, R.; Rutella, S.; Hall, S. W. Structural and functional mapping of the thrombin domain involved in the binding to the platelet glycoprotein Ib. *Biochemistry (Mosc)*. **2001**, *40*, 13268-13273.
116. Celikel, R.; McClintock, R. A.; Roberts, J. R.; Mendolicchio, G. L.; Ware, J.; Varughese, K. I.; Ruggeri, Z. M. Modulation of alpha-thrombin function by distinct interactions with platelet glycoprotein Ibalpha. *Science* **2003**, *301*, 218-221.
117. Dumas, J. J.; Kumar, R.; Seehra, J.; Somers, W. S.; Mosyak, L. Crystal structure of the GpIbalpha-thrombin complex essential for platelet aggregation. *Science* **2003**, *301*, 222-226.

118. Ruggeri, Z. M.; Zarpellon, A.; Roberts, J. R.; Mc Clintock, R. A.; Jing, H.; Mendolicchio, G. L. Unravelling the mechanism and significance of thrombin binding to platelet glycoprotein Ib. *Thromb. Haemost.* **2010**, *104*, 894-902.
119. Kobe, B.; Guncar, G.; Buchholz, R.; Huber, T.; Maco, B. The many faces of platelet glycoprotein Ibalpha--thrombin interaction. *Curr Protein Pept Sci* **2009**, *10*, 551-558.
120. Sabo, T. M.; Maurer, M. C. Biophysical investigation of GpIbalpha binding to thrombin anion binding exosite II. *Biochemistry (Mosc)*. **2009**, *48*, 7110-7122.
121. Sidhu, P.; Sutherland, S. B.; Ganguly, P. Interaction of thrombin with mammalian platelets. *Am. J. Physiol.* **1979**, *237*, H353-358.
122. Ramakrishnan, V.; DeGuzman, F.; Bao, M.; Hall, S. W.; Leung, L. L.; Phillips, D. R. A thrombin receptor function for platelet glycoprotein Ib-IX unmasked by cleavage of glycoprotein V. *Proc. Natl. Acad. Sci. U. S. A.* **2001**, *98*, 1823-1828.
123. Soslau, G.; Class, R.; Morgan, D. A.; Foster, C.; Lord, S. T.; Marchese, P.; Ruggeri, Z. M. Unique pathway of thrombin-induced platelet aggregation mediated by glycoprotein Ib. *J. Biol. Chem.* **2001**, *276*, 21173-21183.
124. Papagrigroriou, E.; McEwan, P. A.; Walsh, P. N.; Emsley, J. Crystal structure of the factor XI zymogen reveals a pathway for transactivation. *Nat Struct Mol Biol* **2006**, *13*, 557-558.
125. Wu, W.; Sinha, D.; Shikov, S.; Yip, C. K.; Walz, T.; Billings, P. C.; Lear, J. D.; Walsh, P. N. Factor XI homodimer structure is essential for normal proteolytic activation by factor XIIa, thrombin, and factor XIa. *J. Biol. Chem.* **2008**, *283*, 18655-18664.
126. Emsley, J.; McEwan, P. A.; Gailani, D. Structure and function of factor XI. *Blood* **2010**, *115*, 2569-2577.



127. Geng, Y.; Verhamme, I. M.; Smith, S. B.; Sun, M. F.; Matafonov, A.; Cheng, Q.; Smith, S. A.; Morrissey, J. H.; Gailani, D. The dimeric structure of factor XI and zymogen activation. *Blood* **2013**, *121*, 3962-3969.
128. Samuel, D.; Cheng, H.; Riley, P. W.; Canutescu, A. A.; Nagaswami, C.; Weisel, J. W.; Bu, Z.; Walsh, P. N.; Roder, H. Solution structure of the A4 domain of factor XI sheds light on the mechanism of zymogen activation. *Proc. Natl. Acad. Sci. U. S. A.* **2007**, *104*, 15693-15698.
129. Renne, T.; Gailani, D.; Meijers, J. C.; Muller-Esterl, W. Characterization of the H-kininogen-binding site on factor XI: a comparison of factor XI and plasma prekallikrein. *J. Biol. Chem.* **2002**, *277*, 4892-4899.
130. Baglia, F. A.; Walsh, P. N. A binding site for thrombin in the apple 1 domain of factor XI. *J. Biol. Chem.* **1996**, *271*, 3652-3658.
131. Ho, D. H.; Badellino, K.; Baglia, F. A.; Walsh, P. N. A binding site for heparin in the apple 3 domain of factor XI. *J. Biol. Chem.* **1998**, *273*, 16382-16390.
132. Zhao, M.; Abdel-Razek, T.; Sun, M. F.; Gailani, D. Characterization of a heparin binding site on the heavy chain of factor XI. *J. Biol. Chem.* **1998**, *273*, 31153-31159.
133. Badellino, K. O.; Walsh, P. N. Localization of a heparin binding site in the catalytic domain of factor XIa. *Biochemistry (Mosc)*. **2001**, *40*, 7569-7580.
134. Yang, L.; Sun, M. F.; Gailani, D.; Rezaie, A. R. Characterization of a heparin-binding site on the catalytic domain of factor XIa: mechanism of heparin acceleration of factor XIa inhibition by the serpins antithrombin and C1-inhibitor. *Biochemistry (Mosc)*. **2009**, *48*, 1517-1524.
135. Sun, Y.; Gailani, D. Identification of a factor IX binding site on the third apple domain of activated factor XI. *J. Biol. Chem.* **1996**, *271*, 29023-29028.

136. Sun, M. F.; Zhao, M.; Gailani, D. Identification of amino acids in the factor XI apple 3 domain required for activation of factor IX. *J. Biol. Chem.* **1999**, *274*, 36373-36378.
137. Geng, Y.; Verhamme, I. M.; Messer, A.; Sun, M. F.; Smith, S. B.; Bajaj, S. P.; Gailani, D. A sequential mechanism for exosite-mediated factor IX activation by factor XIa. *J. Biol. Chem.* **2012**, *287*, 38200-38209.
138. Baglia, F. A.; Gailani, D.; Lopez, J. A.; Walsh, P. N. Identification of a binding site for glycoprotein Ibalpha in the Apple 3 domain of factor XI. *J. Biol. Chem.* **2004**, *279*, 45470-45476.
139. Miller, T. N.; Sinha, D.; Baird, T. R.; Walsh, P. N. A catalytic domain exosite (Cys527-Cys542) in factor XIa mediates binding to a site on activated platelets. *Biochemistry (Mosc)*. **2007**, *46*, 14450-14460.
140. White-Adams, T. C.; Berny, M. A.; Tucker, E. I.; Gertz, J. M.; Gailani, D.; Urbanus, R. T.; de Groot, P. G.; Gruber, A.; McCarty, O. J. Identification of coagulation factor XI as a ligand for platelet apolipoprotein E receptor 2 (ApoER2). *Arterioscler. Thromb. Vasc. Biol.* **2009**, *29*, 1602-1607.
141. Gailani, D. Activation of factor IX by factor XIa. *Trends Cardiovasc. Med.* **2000**, *10*, 198-204.
142. Baglia, F. A.; Walsh, P. N. Thrombin-mediated feedback activation of factor XI on the activated platelet surface is preferred over contact activation by factor XIIa or factor XIa. *J. Biol. Chem.* **2000**, *275*, 20514-20519.
143. von dem Borne, P. A.; Meijers, J. C.; Bouma, B. N. Feedback activation of factor XI by thrombin in plasma results in additional formation of thrombin that protects fibrin clots from fibrinolysis. *Blood* **1995**, *86*, 3035-3042.

144. Von dem Borne, P. A.; Bajzar, L.; Meijers, J. C.; Nesheim, M. E.; Bouma, B. N. Thrombin-mediated activation of factor XI results in a thrombin-activatable fibrinolysis inhibitor-dependent inhibition of fibrinolysis. *J. Clin. Invest.* **1997**, *99*, 2323-2327.
145. Schumacher, W. A.; Luetzgen, J. M.; Quan, M. L.; Seiffert, D. A. Inhibition of factor XIa as a new approach to anticoagulation. *Arterioscler. Thromb. Vasc. Biol.* **2010**, *30*, 388-392.
146. Renne, T.; Oschatz, C.; Seifert, S.; Muller, F.; Antovic, J.; Karlman, M.; Benz, P. M. Factor XI deficiency in animal models. *J Thromb Haemost* **2009**, *7 Suppl 1*, 79-83.
147. Rosen, E. D.; Gailani, D.; Castellino, F. J. FXI is essential for thrombus formation following FeCl<sub>3</sub>-induced injury of the carotid artery in the mouse. *Thromb. Haemost.* **2002**, *87*, 774-776.
148. Furie, B.; Furie, B. C. In vivo thrombus formation. *J Thromb Haemost* **2007**, *5 Suppl 1*, 12-17.
149. Gailani, D.; Lasky, N. M.; Broze, G. J., Jr. A murine model of factor XI deficiency. *Blood Coagul. Fibrinolysis* **1997**, *8*, 134-144.
150. Yamashita, A.; Nishihira, K.; Kitazawa, T.; Yoshihashi, K.; Soeda, T.; Esaki, K.; Imamura, T.; Hattori, K.; Asada, Y. Factor XI contributes to thrombus propagation on injured neointima of the rabbit iliac artery. *J Thromb Haemost* **2006**, *4*, 1496-1501.
151. Seligsohn, U. Factor XI deficiency in humans. *J Thromb Haemost* **2009**, *7 Suppl 1*, 84-87.
152. Gomez, K.; Bolton-Maggs, P. Factor XI deficiency. *Haemophilia* **2008**, *14*, 1183-1189.
153. Asakai, R.; Chung, D. W.; Davie, E. W.; Seligsohn, U. Factor XI deficiency in Ashkenazi Jews in Israel. *N. Engl. J. Med.* **1991**, *325*, 153-158.

154. Duga, S.; Salomon, O. Factor XI Deficiency. *Semin. Thromb. Hemost.* **2009**, *35*, 416-425.
155. Luo, D.; Szaba, F. M.; Kummer, L. W.; Johnson, L. L.; Tucker, E. I.; Gruber, A.; Gailani, D.; Smiley, S. T. Factor XI-deficient mice display reduced inflammation, coagulopathy, and bacterial growth during listeriosis. *Infect. Immun.* **2012**, *80*, 91-99.
156. Tucker, E. I.; Verbout, N. G.; Leung, P. Y.; Hurst, S.; McCarty, O. J.; Gailani, D.; Gruber, A. Inhibition of factor XI activation attenuates inflammation and coagulopathy while improving the survival of mouse polymicrobial sepsis. *Blood* **2012**, *119*, 4762-4768.
157. Jankowski, M.; Undas, A.; Kaczmarek, P.; Butenas, S. Activated factor XI and tissue factor in chronic obstructive pulmonary disease: links with inflammation and thrombin generation. *Thromb. Res.* **2011**, *127*, 242-246.
158. Markwardt, F. Synthetic, low molecular thrombin inhibitors. A new concept of anticoagulants? *Haemostasis* **1974**, *3*, 185-202.
159. Vanhoorelbeke, K.; Ulrichs, H.; Van de Walle, G.; Fontayne, A.; Deckmyn, H. Inhibition of platelet glycoprotein Ib and its antithrombotic potential. *Curr. Pharm. Des.* **2007**, *13*, 2684-2697.
160. McLean, J. The discovery of heparin. *Circulation* **1959**, *19*, 75-78.
161. Capila, I.; Linhardt, R. J. Heparin-protein interactions. *Angew. Chem. Int. Ed. Engl.* **2002**, *41*, 391-412.
162. Huntington, J. A. Thrombin inhibition by the serpins. *J Thromb Haemost* **2013**, *11 Suppl 1*, 254-264.
163. Denas, G.; Pengo, V. Current anticoagulant safety. *Expert Opin Drug Saf* **2012**, *11*, 401-413.

164. Canales, J. F.; Ferguson, J. J. Low-molecular-weight heparins : mechanisms, trials, and role in contemporary interventional medicine. *Am J Cardiovasc Drugs* **2008**, *8*, 15-25.
165. Francis, C. W. Warfarin: an historical perspective. *Hematology Am Soc Hematol Educ Program* **2008**, 251.
166. Bandyopadhyay, P. K. Vitamin K-dependent gamma-glutamylcarboxylation: an ancient posttranslational modification. *Vitam. Horm.* **2008**, *78*, 157-184.
167. Ansell, J.; Hirsh, J.; Hylek, E.; Jacobson, A.; Crowther, M.; Palareti, G. Pharmacology and management of the vitamin K antagonists: American College of Chest Physicians Evidence-Based Clinical Practice Guidelines (8th Edition). *Chest* **2008**, *133*, 160S-198S.
168. Henry, B. L.; Desai, U. R. Anticoagulants. In *Burger's Medicinal Chemistry, Drug Discovery and Development.*, 7th ed.; Abraham, D. J.; Rotella, D. P., Eds. John Wiley: Hoboken, NJ, 2010; Vol. 4, pp 365-408.
169. Cheng-Lai, A. Cardiovascular drug highlight: hirudin. *Heart Dis* **1999**, *1*, 41-49.
170. Gladwell, T. D. Bivalirudin: a direct thrombin inhibitor. *Clin. Ther.* **2002**, *24*, 38-58.
171. Di Nisio, M.; Middeldorp, S.; Buller, H. R. Direct thrombin inhibitors. *N. Engl. J. Med.* **2005**, *353*, 1028-1040.
172. Akwaa, F.; Spyropoulos, A. C. Novel oral anticoagulants: a review of the literature and considerations in special clinical situations. *Hosp Pract (1995)* **2013**, *41*, 8-18.
173. Mohapatra, R.; Tran, M.; Gore, J. M.; Spencer, F. A. A review of the oral direct thrombin inhibitor ximelagatran: not yet the end of the warfarin era. *Am. Heart J.* **2005**, *150*, 19-26.
174. Majeed, A.; Schulman, S. Bleeding and antidotes in new oral anticoagulants. *Best Pract Res Clin Haematol* **2013**, *26*, 191-202.

175. Clemetson, K. J.; Clemetson, J. M. Platelet GPIb complex as a target for anti-thrombotic drug development. *Thromb. Haemost.* **2008**, *99*, 473-479.
176. Broos, K.; Trekels, M.; Jose, R. A.; Demeulemeester, J.; Vandebulcke, A.; Vandeputte, N.; Venken, T.; Egle, B.; De Borggraeve, W. M.; Deckmyn, H.; De Maeyer, M. Identification of a small molecule that modulates platelet glycoprotein Ib-von Willebrand factor interaction. *J. Biol. Chem.* **2012**, *287*, 9461-9472.
177. De Candia, E.; De Cristofaro, R.; Landolfi, R. Thrombin-induced platelet activation is inhibited by high- and low-molecular-weight heparin. *Circulation* **1999**, *99*, 3308-3314.
178. Musumeci, D.; Montesarchio, D. Polyvalent nucleic acid aptamers and modulation of their activity: a focus on the thrombin binding aptamer. *Pharmacol. Ther.* **2012**, *136*, 202-215.
179. Bock, L. C.; Griffin, L. C.; Latham, J. A.; Vermaas, E. H.; Toole, J. J. Selection of single-stranded DNA molecules that bind and inhibit human thrombin. *Nature* **1992**, *355*, 564-566.
180. Griffin, L. C.; Tidmarsh, G. F.; Bock, L. C.; Toole, J. J.; Leung, L. L. In vivo anticoagulant properties of a novel nucleotide-based thrombin inhibitor and demonstration of regional anticoagulation in extracorporeal circuits. *Blood* **1993**, *81*, 3271-3276.
181. Avino, A.; Fabrega, C.; Tintore, M.; Eritja, R. Thrombin binding aptamer, more than a simple aptamer: chemically modified derivatives and biomedical applications. *Curr. Pharm. Des.* **2012**, *18*, 2036-2047.
182. Monien, B. H.; Henry, B. L.; Raghuraman, A.; Hindle, M.; Desai, U. R. Novel chemo-enzymatic oligomers of cinnamic acids as direct and indirect inhibitors of coagulation proteinases. *Bioorg. Med. Chem.* **2006**, *14*, 7988-7998.

183. Henry, B. L.; Monien, B. H.; Bock, P. E.; Desai, U. R. A novel allosteric pathway of thrombin inhibition: Exosite II mediated potent inhibition of thrombin by chemo-enzymatic, sulfated dehydropolymers of 4-hydroxycinnamic acids. *J. Biol. Chem.* **2007**, *282*, 31891-31899.
184. Henry, B. L.; Thakkar, J. N.; Martin, E. J.; Brophy, D. F.; Desai, U. R. Characterization of the plasma and blood anticoagulant potential of structurally and mechanistically novel oligomers of 4-hydroxycinnamic acids. *Blood Coagul. Fibrinolysis* **2009**, *20*, 27-34.
185. Henry, B. L.; Abdel Aziz, M.; Zhou, Q.; Desai, U. R. Sulfated, low-molecular-weight lignins are potent inhibitors of plasmin, in addition to thrombin and factor Xa: Novel opportunity for controlling complex pathologies. *Thromb. Haemost.* **2010**, *103*, 507-515.
186. Henry, B. L.; Thakkar, J. N.; Liang, A.; Desai, U. R. Sulfated, low molecular weight lignins inhibit a select group of heparin-binding serine proteases. *Biochem. Biophys. Res. Commun.* **2012**, *417*, 382-386.
187. Verghese, J.; Liang, A.; Sidhu, P. P.; Hindle, M.; Zhou, Q.; Desai, U. R. First steps in the direction of synthetic, allosteric, direct inhibitors of thrombin and factor Xa. *Bioorg. Med. Chem. Lett.* **2009**, *19*, 4126-4129.
188. Sidhu, P. S.; Liang, A.; Mehta, A. Y.; Abdel Aziz, M. H.; Zhou, Q.; Desai, U. R. Rational design of potent, small, synthetic allosteric inhibitors of thrombin. *J. Med. Chem.* **2011**, *54*, 5522-5531.
189. Sidhu, P. S.; Abdel Aziz, M. H.; Sarkar, A.; Mehta, A. Y.; Zhou, Q.; Desai, U. R. Designing allosteric regulators of thrombin. Exosite 2 features multiple subsites that can be targeted by sulfated small molecules for inducing inhibition. *J. Med. Chem.* **2013**, *56*, 5059-5070.

190. Abdel Aziz, M. H.; Mosier, P. D.; Desai, U. R. Identification of the site of binding of sulfated, low molecular weight lignins on thrombin. *Biochem. Biophys. Res. Commun.* **2011**, *413*, 348-352.
191. Henry, B. L.; Connell, J.; Liang, A.; Krishnasamy, C.; Desai, U. R. Interaction of antithrombin with sulfated, low molecular weight lignins: opportunities for potent, selective modulation of antithrombin function. *J. Biol. Chem.* **2009**, *284*, 20897-20908.
192. Al-Horani, R. A.; Ponnusamy, P.; Mehta, A. Y.; Gailani, D.; Desai, U. R. Sulfated pentagalloylglucoside is a potent, allosteric, and selective inhibitor of factor XIa. *J. Med. Chem.* **2013**, *56*, 867-878.
193. Slungaard, A.; Key, N. S. Platelet factor 4 stimulates thrombomodulin protein C-activating cofactor activity. A structure-function analysis. *J. Biol. Chem.* **1994**, *269*, 25549-25556.
194. Sinha, D.; Badellino, K. O.; Marcinkiewicz, M.; Walsh, P. N. Allosteric modification of factor XIa functional activity upon binding to polyanions. *Biochemistry (Mosc)*. **2004**, *43*, 7593-7600.
195. Kishimoto, T.; Uraki, Y.; Ubukata, M. Synthesis of bromoacetophenone derivatives as starting monomers for beta-O-4 type artificial lignin polymers. *Journal of Wood Chemistry and Technology* **2008**, *28*, 97-105.
196. Yadav, J. S.; Reddy, B. V. S.; Eeshwaraiah, B.; Reddy, P. N. Niobium(V) chloride-catalyzed C-H insertion reactions of alpha-diazoesters: synthesis of beta-keto esters. *Tetrahedron* **2005**, *61*, 875-878.



197. Khan, A. T.; Ali, M. A.; Goswami, P.; Choudhury, L. H. A mild and regioselective method for alpha-bromination of beta-keto esters and 1,3-diketones using bromodimethylsulfonium bromide (BDMS). *J. Org. Chem.* **2006**, *71*, 8961-8963.
198. Kishimoto, T.; Uraki, Y.; Ubukata, M. Synthesis of beta-O-4-type artificial lignin polymers and their analysis by NMR spectroscopy. *Org Biomol Chem* **2008**, *6*, 2982-2987.
199. Kishimoto, T.; Uraki, Y.; Ubukata, M. Chemical synthesis of beta-O-4 type artificial lignin. *Org Biomol Chem* **2006**, *4*, 1343-1347.
200. Zhang, F.; Yang, B.; Ly, M.; Solakyildirim, K.; Xiao, Z.; Wang, Z.; Beaudet, J. M.; Torelli, A. Y.; Dordick, J. S.; Linhardt, R. J. Structural characterization of heparins from different commercial sources. *Anal Bioanal Chem* **2011**, *401*, 2793-2803.
201. Desai, U. R. New antithrombin-based anticoagulants. *Med. Res. Rev.* **2004**, *24*, 151-181.
202. Anastasiou, G.; Gialeraki, A.; Merkouri, E.; Politou, M.; Travlou, A. Thrombomodulin as a regulator of the anticoagulant pathway: implication in the development of thrombosis. *Blood Coagul. Fibrinolysis* **2012**, *23*, 1-10.
203. Warkentin, T. E.; Greinacher, A.; Craven, S.; Dewar, L.; Sheppard, J. A.; Ofose, F. A. Differences in the clinically effective molar concentrations of four direct thrombin inhibitors explain their variable prothrombin time prolongation. *Thromb. Haemost.* **2005**, *94*, 958-964.
204. Verhamme, I. M.; Olson, S. T.; Tollefsen, D. M.; Bock, P. E. Binding of exosite ligands to human thrombin. Re-evaluation of allosteric linkage between thrombin exosites I and II. *J. Biol. Chem.* **2002**, *277*, 6788-6798.
205. Yang, L.; Rezaie, A. R. Calcium-binding sites of the thrombin-thrombomodulin-protein C complex: possible implications for the effect of platelet factor 4 on the activation of vitamin K-dependent coagulation factors. *Thromb. Haemost.* **2007**, *97*, 899-906.

206. Carter, W. J.; Cama, E.; Huntington, J. A. Crystal structure of thrombin bound to heparin. *J. Biol. Chem.* **2005**, *280*, 2745-2749.
207. Vindigni, A.; White, C. E.; Komives, E. A.; Di Cera, E. Energetics of thrombin-thrombomodulin interaction. *Biochemistry (Mosc)*. **1997**, *36*, 6674-6681.
208. De Cristofaro, R.; De Candia, E.; Rutella, S.; Weitz, J. I. The Asp(272)-Glu(282) region of platelet glycoprotein I $\alpha$  interacts with the heparin-binding site of alpha-thrombin and protects the enzyme from the heparin-catalyzed inhibition by antithrombin III. *J. Biol. Chem.* **2000**, *275*, 3887-3895.
209. Olson, S. T.; Halvorson, H. R.; Bjork, I. Quantitative characterization of the thrombin-heparin interaction. Discrimination between specific and nonspecific binding models. *J. Biol. Chem.* **1991**, *266*, 6342-6352.
210. Henry B L; Desai U R. Anticoagulants. In *Burger's Medicinal Chemistry, Drug Discovery and Development*, 7th ed.; Abraham D J; Rotella D P, Eds. John Wiley: Hoboken, NJ, 2010; pp 365-408.
211. Eriksson, B. I.; Dahl, O. E.; Huo, M. H.; Kurth, A. A.; Hantel, S.; Hermansson, K.; Schnee, J. M.; Friedman, R. J. Oral dabigatran versus enoxaparin for thromboprophylaxis after primary total hip arthroplasty (RE-NOVATE II\*). A randomised, double-blind, non-inferiority trial. *Thrombosis and haemostasis* **2011**, *105*, 721-729.
212. Alexander, D.; Jeremias, A. Rivaroxaban in the contemporary treatment of acute coronary syndromes. *Expert Opin Investig Drugs* **2011**, *20*, 849-857.
213. Di Cera, E.; Page, M. J.; Bah, A.; Bush-Pelc, L. A.; Garvey, L. C. Thrombin allostery. *Phys Chem Chem Phys* **2007**, *9*, 1291-1306.

214. Banbula, A.; Zimmerman, T. P.; Novokhatny, V. V. Blood inhibitory capacity toward exogenous plasmin. *Blood Coagul. Fibrinolysis* **2007**, *18*, 241-246.
215. Smith, A. A.; Jacobson, L. J.; Miller, B. I.; Hathaway, W. E.; Manco-Johnson, M. J. A new euglobulin clot lysis assay for global fibrinolysis. *Thromb. Res.* **2003**, *112*, 329-337.
216. Hunt, B. J. Bleeding and coagulopathies in critical care. *N. Engl. J. Med.* **2014**, *370*, 847-859.
217. Hossain, N.; Paidas, M. J. Disseminated intravascular coagulation. *Semin. Perinatol.* **2013**, *37*, 257-266.
218. Marino, F.; Chen, Z. W.; Ergenekan, C. E.; Bush-Pelc, L. A.; Mathews, F. S.; Di Cera, E. Structural basis of Na<sup>+</sup> activation mimicry in murine thrombin. *J. Biol. Chem.* **2007**, *282*, 16355-16361.
219. Malkowski, M. G.; Martin, P. D.; Guzik, J. C.; Edwards, B. F. The co-crystal structure of unliganded bovine alpha-thrombin and prethrombin-2: movement of the Tyr-Pro-Pro-Trp segment and active site residues upon ligand binding. *Protein Sci.* **1997**, *6*, 1438-1448.
220. Rydel, T. J.; Yin, M.; Padmanabhan, K. P.; Blankenship, D. T.; Cardin, A. D.; Correa, P. E.; Fenton, J. W., 2nd; Tulinsky, A. Crystallographic structure of human gamma-thrombin. *J. Biol. Chem.* **1994**, *269*, 22000-22006.
221. Lewis, S. D.; Lorand, L.; Fenton, J. W., 2nd; Shafer, J. A. Catalytic competence of human alpha- and gamma-thrombin in the activation of fibrinogen and factor XIII. *Biochemistry (Mosc.)* **1987**, *26*, 7597-7603.
222. Adam, F.; Guillin, M. C.; Jandrot-Perrus, M. Glycoprotein Ib-mediated platelet activation. A signalling pathway triggered by thrombin. *Eur. J. Biochem.* **2003**, *270*, 2959-2970.

223. Wang, X.; Cheng, Q.; Xu, L.; Feuerstein, G. Z.; Hsu, M. Y.; Smith, P. L.; Seiffert, D. A.; Schumacher, W. A.; Ogletree, M. L.; Gailani, D. Effects of factor IX or factor XI deficiency on ferric chloride-induced carotid artery occlusion in mice. *J Thromb Haemost* **2005**, *3*, 695-702.
224. Cheng, Q.; Tucker, E. I.; Pine, M. S.; Sisler, I.; Matafonov, A.; Sun, M. F.; White-Adams, T. C.; Smith, S. A.; Hanson, S. R.; McCarty, O. J.; Renne, T.; Gruber, A.; Gailani, D. A role for factor XIIa-mediated factor XI activation in thrombus formation in vivo. *Blood* **2010**, *116*, 3981-3989.
225. Carr, M. E. Development of platelet contractile force as a research and clinical measure of platelet function. *Cell Biochem. Biophys.* **2003**, *38*, 55-78.
226. Favaloro, E. J.; Lippi, G.; Koutts, J. Laboratory testing of anticoagulants: the present and the future. *Pathology* **2011**, *43*, 682-692.
227. Favaloro, E. J.; Lippi, G. The new oral anticoagulants and the future of haemostasis laboratory testing. *Biochem Med (Zagreb)* **2012**, *22*, 329-341.
228. Korte, W.; Clarke, S.; Lefkowitz, J. B. Short activated partial thromboplastin times are related to increased thrombin generation and an increased risk for thromboembolism. *Am. J. Clin. Pathol.* **2000**, *113*, 123-127.
229. Mylotte, D.; Foley, D.; Kenny, D. Platelet function testing: methods of assessment and clinical utility. *Cardiovasc Hematol Agents Med Chem* **2011**, *9*, 14-24.
230. Tan, K. T.; Lip, G. Y. The assessment of platelet activation in antiplatelet drug development. *Curr. Med. Chem.* **2005**, *12*, 3117-3125.
231. Bowry, R.; Fraser, S.; Archeval-Lao, J. M.; Parker, S. A.; Cai, C.; Rahbar, M. H.; Grotta, J. C. Thrombelastography detects the anticoagulant effect of rivaroxaban in patients with stroke. *Stroke* **2014**, *45*, 880-883.

232. Westrick, R. J.; Winn, M. E.; Eitzman, D. T. Murine models of vascular thrombosis (Eitzman series). *Arterioscler. Thromb. Vasc. Biol.* **2007**, *27*, 2079-2093.
233. Day, S. M.; Reeve, J. L.; Myers, D. D.; Fay, W. P. Murine thrombosis models. *Thromb. Haemost.* **2004**, *92*, 486-494.
234. Andrews, R. K.; Berndt, M. C. Bernard-Soulier syndrome: an update. *Semin. Thromb. Hemost.* **2013**, *39*, 656-662.
235. Karuturi, R.; Al-Horani, R. A.; Mehta, S. C.; Gailani, D.; Desai, U. R. Discovery of allosteric modulators of factor XIa by targeting hydrophobic domains adjacent to its heparin-binding site. *J. Med. Chem.* **2013**, *56*, 2415-2428.
236. Gunnarsson, G. T.; Desai, U. R. Interaction of designed sulfated flavanoids with antithrombin: lessons on the design of organic activators. *J. Med. Chem.* **2002**, *45*, 4460-4470.
237. Gunnarsson, G. T.; Desai, U. R. Designing small, nonsugar activators of antithrombin using hydrophobic interaction analyses. *J. Med. Chem.* **2002**, *45*, 1233-1243.
238. Gunnarsson, G. T.; Desai, U. R. Exploring new non-sugar sulfated molecules as activators of antithrombin. *Bioorg. Med. Chem. Lett.* **2003**, *13*, 679-683.
239. Raman, K.; Karuturi, R.; Swarup, V. P.; Desai, U. R.; Kuberan, B. Discovery of novel sulfonated small molecules that inhibit vascular tube formation. *Bioorg. Med. Chem. Lett.* **2012**, *22*, 4467-4470.
240. Gunnarsson, G. T.; Riaz, M.; Adams, J.; Desai, U. R. Synthesis of per-sulfated flavonoids using 2,2,2-trichloro ethyl protecting group and their factor Xa inhibition potential. *Bioorg. Med. Chem.* **2005**, *13*, 1783-1789.

241. Raghuraman, A.; Liang, A.; Krishnasamy, C.; Lauck, T.; Gunnarsson, G. T.; Desai, U. R. On designing non-saccharide, allosteric activators of antithrombin. *Eur J Med Chem* **2009**, *44*, 2626-2631.
242. Raghuraman, A.; Riaz, M.; Hindle, M.; Desai, U. R. Rapid and efficient microwave-assisted synthesis of highly sulfated organic scaffolds. *Tetrahedron Lett.* **2007**, *48*, 6754-6758.
243. Al-Horani, R. A.; Liang, A.; Desai, U. R. Designing nonsaccharide, allosteric activators of antithrombin for accelerated inhibition of factor Xa. *J. Med. Chem.* **2011**, *54*, 6125-6138.
244. Sidhu, P. S.; Mosier, P. D.; Zhou, Q.; Desai, U. R. On scaffold hopping: challenges in the discovery of sulfated small molecules as mimetics of glycosaminoglycans. *Bioorg. Med. Chem. Lett.* **2013**, *23*, 355-359.
245. *The PyMOL Molecular Graphics System, Version 1.5.0.4 Schrödinger, LLC.*
246. *OEChem, version 1.7.7, OpenEye Scientific Software, Inc., Santa Fe, NM, USA, [www.eyesopen.com](http://www.eyesopen.com), 2014.*
247. Lakowicz, J. R. Principles of Fluorescence Spectroscopy. In 3rd ed.; Springer: New York, 2006.
248. Cheng, N. S. Formula for the viscosity of a glycerol-water mixture. *Industrial & Engineering Chemistry Research* **2008**, *47*, 3285-3288.
249. Westbrook, C. Calculate density and viscosity of glycerol/water mixtures. [http://www.met.reading.ac.uk/~sws04cdw/viscosity\\_calc.html](http://www.met.reading.ac.uk/~sws04cdw/viscosity_calc.html) (Last Accessed: March 23, 2014).
250. Lin, J.; Deng, H.; Jin, L.; Pandey, P.; Quinn, J.; Cantin, S.; Rynkiewicz, M. J.; Gorga, J. C.; Bibbins, F.; Celatka, C. A.; Nagafuji, P.; Bannister, T. D.; Meyers, H. V.; Babine, R. E.; Hayward, N. J.; Weaver, D.; Benjamin, H.; Stassen, F.; Abdel-Meguid, S. S.; Strickler, J. E.

Design, synthesis, and biological evaluation of peptidomimetic inhibitors of factor XIa as novel anticoagulants. *J. Med. Chem.* **2006**, *49*, 7781-7791.

251. Flecha, F. L. G.; Levi, V. Determination of the molecular size of BSA by fluorescence anisotropy. *Biochemistry and Molecular Biology Education* **2003**, *31*, 319-322.

252. Grabowski, J. J.; Bertozzi, C. R.; Jacobsen, J. R.; Jain, A.; Marzluff, E. M.; Suh, A. Y. Fluorescence probes in biochemistry: an examination of the non-fluorescent behavior of dansylamide by photoacoustic calorimetry. *Anal. Biochem.* **1992**, *207*, 214-226.

253. Wong, P. C.; Crain, E. J.; Watson, C. A.; Schumacher, W. A. A small-molecule factor XIa inhibitor produces antithrombotic efficacy with minimal bleeding time prolongation in rabbits. *J. Thromb. Thrombolysis* **2011**, *32*, 129-137.

254. Deng, H.; Bannister, T. D.; Jin, L.; Babine, R. E.; Quinn, J.; Nagafuji, P.; Celatka, C. A.; Lin, J.; Lazarova, T. I.; Rynkiewicz, M. J.; Bibbins, F.; Pandey, P.; Gorga, J.; Meyers, H. V.; Abdel-Meguid, S. S.; Strickler, J. E. Synthesis, SAR exploration, and X-ray crystal structures of factor XIa inhibitors containing an alpha-ketothiazole arginine. *Bioorg. Med. Chem. Lett.* **2006**, *16*, 3049-3054.

255. Lazarova, T. I.; Jin, L.; Rynkiewicz, M.; Gorga, J. C.; Bibbins, F.; Meyers, H. V.; Babine, R.; Strickler, J. Synthesis and in vitro biological evaluation of aryl boronic acids as potential inhibitors of factor XIa. *Bioorg. Med. Chem. Lett.* **2006**, *16*, 5022-5027.

256. Schumacher, W. A.; Seiler, S. E.; Steinbacher, T. E.; Stewart, A. B.; Bostwick, J. S.; Hartl, K. S.; Liu, E. C.; Ogletree, M. L. Antithrombotic and hemostatic effects of a small molecule factor XIa inhibitor in rats. *Eur. J. Pharmacol.* **2007**, *570*, 167-174.

257. Buchanan, M. S.; Carroll, A. R.; Wessling, D.; Jobling, M.; Avery, V. M.; Davis, R. A.; Feng, Y.; Xue, Y.; Oster, L.; Fex, T.; Deinum, J.; Hooper, J. N.; Quinn, R. J. Clavatadine A, a

natural product with selective recognition and irreversible inhibition of factor XIa. *J. Med. Chem.* **2008**, *51*, 3583-3587.

258. Hanessian, S.; Larsson, A.; Fex, T.; Knecht, W.; Blomberg, N. Design and synthesis of macrocyclic indoles targeting blood coagulation cascade Factor XIa. *Bioorg. Med. Chem. Lett.* **2010**, *20*, 6925-6928.

259. Geng, Y.; Verhamme, I. M.; Sun, M. F.; Bajaj, S. P.; Emsley, J.; Gailani, D. Analysis of the factor XI variant Arg184Gly suggests a structural basis for factor IX binding to factor XIa. *J Thromb Haemost* **2013**, *11*, 1374-1384.



## Appendix A. Abbreviations

$^{13}\text{C}$	Carbon
$^1\text{H}$	Proton
APTT	Activated partial thromboplastin time
BDMS	bromo dimethyl sulfonium bromide
BSA	Bovine serum albumin
CD	Catalytic domain
$d\text{EGR-fXIa}$	Dansyl-EGR labeled active site factor XIa
DHP	Dehydropolymer
f	Factor
$f\text{FPR-Thrombin}$	Active site fluorescein labeled thrombin
GAG	Glycosaminoglycan
$\text{GPIb}\alpha$	Platelet glycoprotein Ib $\alpha$
HAS	Hemostasis Analysis System

HBS	heparin binding site
HirP	A Tyr63-sulfated hirudin peptide with fluorescein, i.e., [5F]-Hir[54-65](SO <sub>3</sub> -),
HIT	Heparin-induced thrombocytopenia
HLE	Human leukocyte elastase
HMWK	High molecular weight kininogen
LMWH	low molecular weight heparin (enoxaparin)
LRR	Leucine rich repeats
NMR	Nuclear Magnetic Resonance
PAR	Protease activated receptor
PK	Pre-kallikrein
PPE	Porcine pancreatic elastase
PPP	platelet poor plasma
PRP	Platelet rich plasma
PT	Prothrombin time
QAOs	Sulfated quinazolin-4(3H)-ones
RPIP-UPLC-MS	Reversed-phase ion-pairing ultraperformance liquid chromatography mass spectrometry

SbO4L	Sulfated $\beta$ -O4 Lignin
SEC	Size exclusion chromatography
SPGG	Sulfated pentagalloyl glucoside
SPR	Surface plasmon resonance
SSM	Sulfated small molecule
STRAP	Sulfated tyrosine rich anionic peptide
TBDMS	tert-butyl dimethyl silane
TEG	Thromboelastography
TF	Tissue Factor
TH	Thrombin
TM	Thrombomodulin
tPA	Tissue plasminogen activator
TPST	tyrosylprotein sulfotransferase

## **Vita**

Akul Mehta was born on June 13, 1985 in Mumbai, India. Akul graduated from Jambhaji Narsee School in 2001 and Mithibai College in 2003. Following which, Akul joined Mumbai Educational Trust (MET) Institute of Pharmacy, in which he received his Bachelor of Pharmacy (B. Pharm.) with distinction, from University of Mumbai in 2007. Akul worked to develop PharmaXChange.info- a website to help students of pharmacy and pharmaceutical sciences in 2007. He obtained admission into the PhD program in the Department of Medicinal Chemistry, at Virginia Commonwealth University in the USA in 2008. Akul has since then been inducted into the three honor societies. These include the Phi Kappa Phi, Alpha Epsilon Lambda and the Rho Chi honor societies. He is also a member of the American Society of Hematology and the American Association for Advancement of Science. Akul has obtained the Thesis/Dissertation Assistantship from the Graduate School at VCU (Spring 2014). His poster presentations have been acknowledged in the 2012 School of Pharmacy, Research and Career Day (Runner-Up) and the 2014 Inter-PEG Meeting (Best Poster). Akul has won the Departmental J. Doyle Smith award (2014). Akul is also a contributor on three invention disclosures and has 8 publications with his name. He is also a co-author of a book chapter, "Cardiovascular Agents", in "The Chemistry of Drugs for Nurse Anesthetists" (2<sup>nd</sup> Ed.).